EXAMINING THE REGULATION OF ADIPOCYTOKINE EXPRESSION DURING CHRONIC INSULIN RESISTANCE

by

EDITH ELIZABETH HAYDEN

(Under the Direction of Lance Wells)

ABSTRACT

Type II diabetes, characterized by hyperglycemia and hyperinsulinemia, results in many costly and debilitating patient complications. A broad range of tissues respond to insulin and help to mediate its effects. In particular, adipose tissue secretes proteins known as adipocytokines, which play an important role in whole body energy homeostasis and have been implicated in the pathogenesis of diabetes. Increased flux through the hexosamine biosynthetic pathway and the corresponding increase in intracellular glycosylation of proteins via O-GlcNAc is sufficient to induce insulin resistance (IR) in multiple systems. Previously, our group used shotgun proteomics to identify rodent adipocytokines whose levels are modulated upon the induction of IR by indirectly and directly modulating O-GlcNAc levels. Since adipocytokines levels are regulated primarily at the level of transcription and O-GlcNAc alters the function of many transcription factors, we hypothesized that elevated O-GlcNAc levels on key transcription factors are modulating adipocytokine expression. Here, we show that upon the elevation of O-GlcNAc levels and the induction of IR in mature 3T3-F442a adipocytes, the transcript levels of multiple adipocytokines, as measured by quantitative RT-PCR, reflect the modulation observed at the protein level. We have gone on to validate the adipocytokine transcript levels in mouse

models of diabetes. Using inguinal fat pads from the *db/db* mouse model and the diet-induced obesity mouse model, we have confirmed that the adipocytokines regulated by O-GlcNAc modulation in cell culture are likewise modulated in the whole animal upon a shift to IR. We find that Sp1 is a common cis-acting element on the promoters of co-regulated genes. Sp1 O-GlcNAc modification increases during IR. As measured by chromatin immunoprecipitation, Sp1 and O-GlcNAc modified proteins are enriched on the LPL and SPARC promoters during insulin resistance. These data lead us to the conclusion that adipocytokine expression is modulated by global O-GlcNAc levels and potentially by Sp1. We go on to characterize the primary human adipocyte secretome in order to identify more adipocytokines whose expression is modulated by O-GlcNAc and find that many of the rodent adipocytokines are likewise regulated by O-GlcNAc levels in *homo sapiens*.

INDEX WORDS: O-GlcNAc, insulin resistance, adipocytes, adipokines, adipocytokines

EXAMINING THE REGULATION OF ADIPOCYTOKINE EXPRESSION DURING CHRONIC INSULIN RESISTANCE

by

EDITH ELIZABETH HAYDEN

BS, Saint Vincent College, 2006

A Dissertation Submitted to the Graduate Faculty of The University of Georgia in Partial Fulfillment of the Requirements for the Degree

DOCTOR OF PHILOSOPHY

ATHENS, GEORGIA

2012

EXAMING THE REGULATION OF ADIPOCYTOKINE EXPRESSION DURING CHRONIC INSULIN RESISTANCE

by

EDITH ELIZABETH HAYDEN

Major Professor:	Lance Wells
Committee:	Stephen Dalton
	Shaying Zhao
	Ruth Harris

Electronic Version Approved:

Maureen Grasso
Dean of the Graduate School
The University of Georgia
August 2012

DEDICATION

I would like to dedicate this work to my life partner, Paul, and my friends and family. Thank you for your patience and support.

ACKNOWLEDGEMENTS

Many people have helped to guide me through my time in graduate school. I would like to thank the members of of the Wells' lab past and present for their helpful discussions and support. Special thanks goes to Lance Wells for helping me so much with my science and professional development and for dealing with my frequent stress-induced tantrums. My committee members, Steve, Ruth, and Shaying, have continually given me helpful advice. Thank you also to the many members of BCMB department and the CCRC who have helped me over the years, especially Alison Nairn and Mitche de la Rosa. For technical advice about sonication, thank you to James Chappell and Kenneth Lyon. Thank you to Bingqiang Liu for assistance with bioinformatics. Thank you to Ruth Harris for kindly providing us with mouse tissues and helping us to develop a diet-induced insulin resistant mouse model. Thank you to Dorothy Hausman for helping us to collect and culture primary adipocytes. I would also like to extend thanks to the administrative staff of the BCMB department and the CCRC. Finally, thank you to my friends, family, and pets whom have continuously provided love and support.

TABLE OF CONTENTS

Page

LIST OF TABLES

Page

LIST OF FIGURES

Page

CHAPTER 1

INSULIN RESISTANCE, ADIPOCYTOKINES, AND O-GLCNAC

Insulin Resistance

Type 2 diabetes mellitus (T2DM) is characterized by both hyperinsulemia and hyperglycemia, which results from a combination of whole-body insulin resistance and pancreatic beta-cell dysfunction that leads to insulin insufficiency [1]. Evidence suggests that T2DM develops from a combination of genetic and environmental factors, but the relative contribution of each is unclear [2]. Several genome wide association studies have identified around 50 susceptibility loci for T2DM although their predictive values tend to be low due to the polygenic and heterogeneous nature of T2DM [3]. Studies to identify the biological significance of these loci will hopefully reveal novel therapeutic targets. Already these studies have shown that variants for reduced beta-cell function tend to be more predictive of T2DM than those for reduced insulin sensitivity [4, 5]. The increasing prevalence of obesity, more than 10% of adults world-wide in 2008, is associated with the increasing prevalence of T2DM. The increased availability of energy-dense foods along with the decreased levels of physical activity are implicated in the rise in obesity rates [6-8]. T2DM is associated with a wide range of costly complications such as blindness, kidney failure, stroke, and cardiovascular disease [9]. The abundance of complications reflects the number of interrelated systems involved in T2DM pathogenesis [10, 11]. Insulin resistance affects insulin responsive tissues such as the liver, pancreatic β-cells, and peripheral tissues (including skeletal muscle and adipocytes).

Insulin is normally secreted from the pancreatic β-cells in response to increased glucose flux and acts to modulate the energy homeostasis of the body mainly by, 1) inhibiting gluconeogenesis in the liver [12], 2) promoting glucose uptake and glycogen synthesis in the skeletal muscle and liver [13], 3) inhibiting lipolysis and promoting lipogenesis and glucose uptake in adipocytes [14], and 4) altering the secretion of adipocytokines from adipose tissue. Tissues that become insulin resistant fail to activate the appropriate energy storing pathways and inactivate energy releasing pathways leading to hyperglycemia and hyperlipidemia [1, 15].

White Adipose Tissue and Adipocytokines

White adipose tissue (WAT) plays an important role in the maintenance of energy homeostasis. Upon insulin stimulation, the inducible glucose transporter-4 (GLUT-4) translocates to the cell surface to initiate plasma glucose uptake. Adipose tissue specific GLUT4 knockout mice demonstrate whole-body insulin resistance. However, skeletal muscle glucose uptake returns to normal when measured *ex vivo*, suggesting that secreted factors from adipose tissue contribute to the whole-body insulin resistance [16] In addition, the whole-body insulin resistance of muscle specific GLUT4 knockout mice can be reversed by crossing them with adipose tissue specific GLUT4 overexpressing transgenic mice, which supports the theory that WAT is not only a passive energy storage depot but also functions as an endocrine organ [17] . Further gene expression analysis of adipose tissue specific GLUT 4 knockout mice identified retinol-binding protein 4 (Rbp4) as the main secreted factor responsible for inducing whole-body insulin resistance in these mice [18]. WAT expresses and secretes multiple adipocytokines that act in autocrine, paracrine, and endocrine manners. The term adipocytokines is sometimes a misnomer, as not all secreted proteins from adipose tissue are cytokines. In this text, we refer to the secretome of adipose tissue as adipocytokines or adipokines. Several of adipocytokines have

been shown to alter the insulin sensitivity of other organs and convey information about the energy homeostasis of the system [19].

The expression and secretion of most adipocytokines studied has been shown to be modulated mainly by hormonal, cytokine, and/or nutrient signals, as highlighted by the observation that adipocytokine levels are altered with increasing fat mass [20]. Increased fat mass is a result of adipocyte hypertrophy and hyperplasia. Mature adipocytes differentiate from preadipocytes in response to paracrine and endocrine signals. It has been proposed that during obesity there are a higher proportion of large adipocytes, which tend to have altered cellular homeostasis and secretory profiles [21, 22]. The extensive remodeling required for the expansion of fat pads during obesity can generate an inflammatory response due to limited angiogenesis, localized hypoxia, adipocyte necrosis, increased fibrosis, altered cytokine secretion, and M1-stage macrophage and other immune cell infiltration [20-25]. The crosstalk between and relative contribution of each of the multiple cell types that comprise white adipose tissue during obesity and their contribution to the development of insulin resistance is an area of active investigation [26]. Adequate fat mass homeostasis is important for the maintenance of whole-body insulin sensitivity, as demonstrated by the propensity of both obesity and lipoatrophy to result in insulin resistance [27]. The ability of adipocytes to respond to nutrient flux and alter their metabolism and secretion profiles allows their function as energy homeostasis sensors and regulators. Because of this, the dysregulation of adipocytokine secretion and signaling likely plays a major role in the development of obesity, insulin resistance, and T2DM [28-30]. To illustrate the role of adipocytokines in energy homeostasis, I will briefly highlight three of the many known adipocytokines.

Leptin

Leptin, the prototypic adipocytokine, is the product of the *ob* gene, which was cloned by Freidman's group in 1994 [31]. *ob/ob* mice, which are leptin deficient, are severely obese and diabetic. Leptin has diverse functions, including regulating energy metabolism, bone metabolism, reproduction, behavior, and immunity. It is secreted from adipocytes in proportion to adipocyte mass and nutritional status. Fasting lowers leptin levels, which acts as a starvation signal. During obesity, circulating leptin levels are high; however, the body fails to respond to leptin to reduce energy intake and increase energy expenditure [32, 33].

Leptin signals through the leptin receptors of which there are various isoforms. OB-Rb is the long form and is expressed in most tissues but the highest levels in the brain. OB-Ra, Rc, Rd, and Re are widely expressed. Ob-Re is the only short isoform that lacks the cytoplasmic domain. The long cytoplasmic tail of OB-Rb signals through the Janus kinase (JAK) – signal transducer and activator of transcription (STAT) pathway [34]. OB-Rb is highly expressed in the arcuate nucleus, dorsomedial, ventromedial, and ventral premamillary hypothalamic nuclei of the hypothalamus although it is also expressed at lower levels in many other areas of the brain. The specific leptin responsive neurons and their effects on the body have been explored using central injection of leptin into very specific brain sites and by making highly specific genetic mouse models [33]. Leptin suppresses orexigenic peptides neuropeptide Y (NPY) and agouti-related protein (AgRP) and activates anorectic peptides α-melanocyte-stimulating hormone (αMSH), produced by proopiomelanocortin (POMC) neurons, and cocaine and amphetamine regulated transcript (CART). αMSH is an agonist of the melanocortin-4 receptor (MC4R) and AgRP is an antagonist [33, 35]. Mutations in the MC4R are highly associated with human obesity [32]. Leptin exerts its effects using both the parasympathetic (ie. vagus nerve) and

sympathetic nervous system [33]. Increased outflow of the sympathetic nervous system leads to suppression of *de novo* lipogenesis and activation of lipolysis [33].

When leptin binds OB-Rb it activates JAK, a tyrosine kinase, which phosphorylates the cytoplasmic tail of the receptor leading to the recruitment and phosphorylation of STAT3. p-STAT3 dimerizes and translocates to the nucleus and regulates the transcription of target genes, including suppressor of cytokine signaling 3 (SOCS3). SOCS3 acts as a feedback regulator of leptin signaling and insulin signaling. Protein-tyrosine phosphatase-1B (PTP1B) also acts to negatively regulate insulin and leptin signaling. JAK phosphorylation also leads to the recruitment of SH2 domain-containing phosphatase-2 (SHP-2), which activates the extracellular signal regulated kinase (ERK) pathway. Leptin also activates the insulin receptor substrate-phosphatidylinositol-3-OH kinase (IRS-PI3K) pathway. PI3K activates phosphodiesterase-3B (PDE3B), which in turn lowers cAMP levels. In addition, leptin is reported to affect the mammalian target of rapamycin (mTOR) and AMP-activated protein kinase (AMPK) pathways [36].

Adiponectin

Adiponectin is secreted in large quantities from adipocytes. Circulating levels in humans are regularly 3-30ug/ml in serum even though the protein half-life is short (9 hours for the high molecular weight form). Adiponectin has an N-terminal signal sequence, a variable domain, a collagen-like domain, and a C-terminal globular domain. The actual effect of circulating adiponectin is dependent upon the relative concentration of its isoforms. Adiponectin oligomerizes as a trimer, two trimers, which is known as the low molecular weight form (LMW), or as six trimers, which is known as the high molecular weight form (HMW). The HMW form of adiponectin is more predicative of insulin sensitivity [37]. Unlike most other adipocytokines,

adiponectin expression is lower during the loss of insulin sensitivity and increase in fat mass. Adiponectin acts as an insulin sensitizer by increasing fatty acid oxidation in the liver and muscle, by increasing glucose uptake in muscle and adipose tissue, and by decreasing gluconeogenesis in the liver. Adiponectin binds to its receptors (AdipoR1 and AdipoR2) that initiate the downstream activation of AMPK [38]. Tumor necrosis factor (TNF) and adiponectin generally have opposing expression, which relates to their roles as pro- and anti-inflammatory modulators, respectively. Low adiponectin levels are associated with an increased risk of cardiovascular disease. Adiponectin is known as an anti-inflammatory adipocytokine in part because it inhibits NFκB, decreases the expression of vascular adhesion molecules, activates cyclooxygenase-2, increases endothelial nitric oxide production, and stimulates IL-10 expression[37-39].

Retinol binding protein 4

Retinol binding protein 4 (Rbp4) is an adipocytokine that is expressed in adipose tissue and liver. Its main function is to transport retinol from the liver to other tissues. Its mechanism of action with regard to obesity and insulin resistance is still unclear; however, its action may depend upon its activation of cytokine receptor stimulated by retinoic acid 6 (STRA6). STRA6 activates a JAK/STAT signaling cascade that can result in the activation of SOCS3. SOCS3 is a known negative regulator of insulin signaling [40]. Rbp4 single nucleotide polymorphisms (SNPs) have been associated with increased adipose tissue mass, insulin resistance, and predisposition for the development of diabetes [41]. Its circulating levels consistently correlate with fat mass in animal models; however, several clinical studies have reported conflicting results in humans. The differences in clinical trials may be due to various collection and testing methods, differences in age, race, and gender proportion, and the renal function of subjects.

Rbp4 expression is reported to be sexually dimorphic, possible due to its interrelation with iron metabolism. Its clearance from the circulation depends on renal function, because the kidneys are the main location of Rbp4 degradation [41]. Rbp4 levels are lower during acute inflammation, such as during active tuberculosis infection [42].

Several adipocytokines have been shown to be regulated at the level of transcription [43-47]. Interestingly, many of the transcription factors involved in adipogenesis also regulate adipocytokine transcription. Since the transcription of both adipogenic and adipocytokine genes is regulated in response to hormonal, cytokine, and nutrient signals, it is logical that adipogenic transcription factors also help to control adipocytokine transcription [48-57]. The transcription of two well-characterized adipocytokines, leptin and adiponectin, is regulated by glucose flux through the hexosamine biosynthetic pathway (HBP) [47, 58-60].

Hexosamine Biosynthetic Pathway

One possible way for cells to sense nutrient abundance and thereby alter their metabolism and gene expression is through the HBP (Figure 1.1). In 1991, Marshall *et al.* found that adipocytes required hyperglycemia, hyperinsulemia, and the amino acid glutamine to become insulin resistant. They knew the rate limiting enzyme of the HBP, glutamine: fructose-6-P aminotransferase (GFAT), utilizes glutamine to form glucosamine-6-P (GlcN-6-P) from frucose-6-P (Fruc-6-P). The end product of the pathway is uridine 5'-diphospho-N-acetylglucosamine (UDP-GlcNAc). UDP-GlcNAc can be converted into other nucleotide sugars or used as a nucleotide sugar donor for complex glycosylation or nucleocytosolic O-linked β-N-acetylglucosamine (O-GlcNAc) glycosylation. Experiments in adipocytes showed the inhibition of GFAT prevented the induction of insulin resistance, and the addition of glucosamine, which enters into the pathway after GFAT, could compensate for GFAT inhibition and was more potent

than glucose in inducing insulin resistance. They proposed the HBP could act as a nutrient flux sensor, since it utilizes 2-5% of intracellular glucose, and act to limit the amount of incoming glucose by inducing insulin resistance [61]. In addition to glucose, the levels of nucleotides, amino acids, and free fatty acids (FFAs) also alter flux through the HBP [62, 63]. UDP-GlcNAc acts as a feedback inhibitor of GFAT [47]. When insulin resistance is induced in adipocyte cell lines through the addition of glucose or glucosamine, a defect in insulin-regulated GLUT4 translocation to the cell membrane is observed [64-68]. Many studies have confirmed the correlation between increased HBP flux and the development of insulin resistance [47, 58-60, 69-73]. It bears mentioning that the high levels of glucosamine used in some early studies to increase HBP flux may also lead to ATP depletion [74].

Genetic mouse models helped to specifically investigate the effects of HBP flux without the potential far-reaching effects of increasing HBP flux using metabolites. Similarly to the GLUT4 knockout mice, transgenic mice that overexpress GFAT under the control of the GLUT4 promoter exhibit whole-body insulin resistance, moreover, muscle glucose uptake tested *ex vivo* is normal [58, 69, 70]. Adipocyte-specific GFAT transgenic mice also exhibit whole body insulin resistance, increased fat pad mass, as well as elevated leptin levels and lowered adiponectin levels [58]. The adipocytes from the adipocyte specific GFAT transgenic mice have greater glucose uptake and GLUT4 expression although their responsiveness to insulin is diminished. Both fatty acid synthesis and oxidation are elevated in the adipocytes suggesting that there is an underlying defect in fatty acid metabolism regulation [75]. Glucosamine treatment of 3T3-L1 adipocytes results in increased activation of AMP-activated protein kinase (AMPK) and increased fatty acid oxidation, which can be prevented using an inhibitor of GFAT [76]. SNPs in GFAT2 have been associated with T2DM in humans [77]. Knocking out

glucosamine-6-phosphate acetyltransferase (EMeg32), an enzyme following GFAT in the HBP, in mice is embryonic lethal. EMeg32 knockout mouse embryonic fibroblasts display low UDP-GlcNAc levels and lack of O-GlcNAc modification of proteins; however, complex glycosylation products are preserved [78]. The cellular changes leading to insulin resistance are extremely complex and although flux through the HBP has been shown to be sufficient to induce insulin resistance that is not to say that it is the only pathway that can lead to insulin resistance [63, 79].

O-GlcNAc

The end product of the HBP, UDP-GlcNAc, is the sugar donor for the enzyme O-GlcNAc transferase (OGT), which transfers the O-GlcNAc post-translational modification onto serine or threonine residues of nuclear and cytoplasmic proteins (Figure 1.2) [80, 81]. OGT is responsive to physiological levels of UDP-GlcNAc, so increased HBP flux results in globally elevated levels of the O-GlcNAc modification [82-84]. O-GlcNAc is more akin to phosphorylation than complex glycosylation in that it is not elongated, its cycling enzymes, OGT and O-GlcNAcase (OGA), are nucleocytoplasmic, it is dynamic and inducible, and it can regulate protein localization, stability, and molecular interactions. O-GlcNAc is often found on the same residues as known phosphorylation sites, suggesting reciprocity between the modifications in some cases, although the relationship is complex [85-93]. In a proteomic study, upon elevation of global O-GlcNAc levels, a similar number of phosphorylation sites were increased or decreased suggesting extensive interaction between the two modifications [94]. In addition, many kinases can be modified by O-GlcNAc, and both OGT and OGA are phosphorylated [95]. Notably, most of the proteins that form the proximal insulin pathway are O-GlcNAc modified, including the insulin receptor, IRS, PI3K, PDK-1, and Akt [96]. Increased HBP flux leads to AMPK

phosphorylation, which stimulates fatty acid oxidation. AMPK is O-GlcNAc modified and the degree of modification and activity of AMPK is modulated by HBP flux [76].

A recent example demonstrates the complexity of these interactions as well as a novel way to simulate O-GlcNAc modification. In the study, four sites of O-GlcNAc modification were mapped on Akt. Akt glycosylation was found to inhibit akt phosphorylation. Using threonine to tyrosine Akt mutants to simulate the bulky steric hindrance from O-GlcNAc, the authors found that glycosylation at Thr305 and Thr312 drastically lowered phosphorylation specifically at Thr308 in response to hormone stimulation by disrupting the interaction between Akt and phosphoinositide-dependent kinase 1 (PDK1). The mutants also displayed lower Akt activity *in vitro* and *in vivo* [97]. Future studies to elucidate the biological role of the akt glycosylation/phosphorylation dynamic during insulin resistance in adipocytes would help to solidify O-GlcNAc's role as a regulator of insulin signaling.

Increased hexosamine biosynthetic pathway flux has been shown to correlate with increased global O-GlcNAc levels in many cell culture and animal model systems [58, 71, 72, 98-101]. One study showed that increased HBP flux increases global O-GlcNAc levels in human skeletal muscle, but in general, whole-body studies in humans have been lacking [102]. It has been demonstrated by many groups, including our own, that in multiple systems the elevation of global O-GlcNAc levels is sufficient to induce insulin resistance [98, 103-105]. Correspondingly, global O-GlcNAc levels are increased in animal models of insulin resistance [102, 106-108].

All metazoans studied contain the O-GlcNAc modification. Mammals contain only one gene each for OGT and OGA. OGT is highly conserved from nematodes to humans. OGT has a varying number of N-terminal tetratricopeptide repeats (TPRs), depending on the species,

followed by a catalytic domain [83]. The TPRs are thought to target OGT to substrates [109]. Human OGT crystal structures have revealed that UDP-GlcNAc is bound before catalysis occurs [110]. Recently, it was discovered that OGT has the ability to modify and then cleave the cell-cycle regulator HCF-1 to generate the mature form, revealing a novel function for the enzyme [111]. OGT regulation is still being revealed and is bound to be highly complex, since unlike the hundreds of kinases that regulate phosphorylation, there is only one OGT [112].

Deletion of OGT, which is located on the X chromosome, is embryonic lethal in mammals but not in *Caenorhabditis elegans* [113, 114]. OGA and OGT null *C. elegans* have elevated levels of glycogen and trehalose and lowered levels of neutral lipid stores. The OGT null *C. elegans* display characteristics demonstrating increased insulin sensitivity whereas the OGA null *C. elegans* show resistance to the insulin-like signaling pathway, suggesting that O-GlcNAc levels also play an important role in the energy metabolism in the worm that parallels its function in mammals [114-117]. In *Drosophila*, OGT was found to be the previously known homeotic gene regulator, Super Sex Combs. Polycomb transcriptional repression was not maintained in OGT null flies [118]. Transgenic mice overexpressing OGT in peripheral tissues are hyperinsulemic and hyperleptinemic [104].

OGT contains a phosphatidylinositol 3,4,5-trisphosphate (PIP_3)-binding motif. Insulin signaling leads the activation of PI3K, which generates PIP_3. PIP_3 attracts proteins with a pleckstrin homology (PH) domain as well as OGT to the plasma membrane. It is thought that OGT acts to attenuate insulin signaling. Overexpression of a mutant OGT that does not bind PIP_3 does not lead to the impairment in insulin signaling seen when wild type OGT is overexpressed in the liver [100]. These experiments provide more evidence that O-GlcNAc acts as an intermediate between nutrient sensing and cellular signaling.

OGA has a two major isoforms. Both contain a hyaluronidase domain, but the long form also contains a histone acetyltransferase (HAT) – like domain. The short form of OGA is targeted to lipid droplets where it activates the proteasome and has the potential to regulate lipid metabolism by regulating lipid droplet surface remodeling [119]. The overexpression of OGA in the livers of diabetic mice is sufficient to return blood glucose to insulin responsive levels and restore hepatic insulin sensitivity [120]. Rat OGA has been mapped close to the diabetes susceptibility locus, *Niddm1*, for Goto-Kakizaki (GK) rats, a model of non-obese T2DM [121, 122]. A SNP in the gene encoding OGA is associated with increased diabetes risk in Mexican Americans [123]. In addition, increased OGA expression in erythrocytes is associated with diabetes in humans [124].

Many transcription factors and cofactors are modified with O-GlcNAc [87, 125]. Recently, we used proteomics to identify 254 proteins that were immunoprecipitated using O-GlcNAc specific antibodies. Thirty percent of the identified proteins were associated with gene expression and transcription [126]. Several of the known O-glycosylated transcription factors and cofactors are involved in insulin resistance, such as FoxO1, Pdx-1, CRTC2, and Sp1 [90]. Sp1 has been associated with the regulation of adipocytokine transcription in response to glucose flux, which is also known to increase the level of O-GlcNAc modification on Sp1 [48, 127-129]. The role of the O-GlcNAc modification of transcription factors is varied and has been shown to alter protein stability, protein-protein interaction, chromatin remodeling, transcriptional initiation and elongation, DNA binding, and localization [130]. The role of O-GlcNAc modification of eukaryotic transcription factors as well as methods to identify O-GlcNAc modification will be discussed in detail in Chapter 2.

The secretion of several adipocytokines is regulated at the level of transcription, and the O-GlcNAc modification appears to be intricately involved with transcriptional control [44, 91]. A proteomic experiment by our lab identified murine adipocytokines whose levels were modulated by both classical insulin resistance (hyperinsulinemia and hyperglycemia) and insulin resistance induced by elevation of O-GlcNAc levels [131]. Surprisingly, the role of O-GlcNAc in the regulation of adipocytokine transcription has not been well-defined. Therefore, the aim of this study was to examine whether O-GlcNAc modified transcription factors are modulating the transcriptional regulation of multiple adipocytokines identified by our lab, further advancing our goal of understanding the link between insulin resistance, elevated O-GlcNAc levels, and adipocytokine secretion (Figure 1.3). A brief description of the adipocytokines we focused on is given below.

SPARC

Secreted protein acidic and rich in cysteine (SPARC), also known as osteonectin and BM-40, is an extracellular matrix (ECM) - associated protein that is highly conserved. SPARC has diverse roles in osteogenesis, angiogenesis, fibrosis, tumerogenesis, and adipogenesis. SPARC is a modulator of cell – ECM interactions [132]. Sparc knockout mice are viable but show several phenotypes that support SPARC's role as an ECM regulator. The mice have a defect in collagen structure, accelerated wound healing, increased neovascularization, early cataract formation, increased susceptibility to the growth of pancreatic and lung cancers, and increased adipose tissue mass [133-135]. SPARC can be either pro- or anti-tumorigenic or pro- or anti- cell survival depending on the cell type [136]. SPARC expression can induce autophagy and upregulation of Cathepsin B expression which leads to apoptosis in neuroblastomas [137]. Many studies point to SPARC as a marker of poor prognosis in cancer [138, 139].

SPARC interacts with a diverse set of proteins such as plasminogen activator inhibitor 1, fibronectin, collagen, and matrix metalloproteinases (MMPs). SPARC can be cleaved by MMPs but also regulates their activity [140]. SPARC binds to the integrin receptors and regulates the signaling of many growth factors such as VEGF, bFGF, and TGF [141, 142].

SPARC is expressed in many human tissues, but the highest expression is observed in adipocytes [143]. SPARC expression is higher in larger adipocytes. Correspondingly, SPARC levels are increased in patients with T2DM and patients with cardiovascular disease [143-145]. Circulating levels of SPARC positively correlate with fat mass, insulin levels, and leptin levels in humans [143-147]. In cultured adipocytes, large doses of glucose can lower SPARC expression. SPARC null mice have more subcutaneous fat without an overall increase in body weight, larger adipocytes, more adipocytes, elevated leptin levels, and are protected from renal fibrosis. The decreased collagen levels and osteopenia in the null mice might compensate for the increased fat mass in maintaining normal body weight [133, 148, 149].

SPARC is thought to negatively regulate cellular differentiation by disrupting the ECM. During adipogenesis, adipocytes switch from a fibronectin-rich matrix to a laminin-rich matrix. SPARC enhances fibronectin and inhibits laminin deposition [150]. SPARC transcript and protein levels increase upon the initiation of preadipocyte differentiation then return to basal levels and finally increase again in mature adipocytes [151]. Increased SPARC levels activate integrin-linked kinase (ILK) which inhibits β-catenin degradation resulting in adipogenesis inhibition. The Wnt/β-catenin pathway is known to inhibit adipogenesis by inhibiting the major adipogenic transcription factors [150]. In addition, SPARC has been shown to interact with AMPK [152]. SPARC treatment increases Akt phosphorylation and this activity is needed for

SPARC promoted cell survival in glioma cells [153]. The functional role of the SPARC/AMPK interaction and whether SPARC activates Akt have not been investigated in adipocytes.

SPARC transcript and protein levels have been shown to correlate in several studies [143, 151, 154, 155]. SPARC has a single major transcriptional start site but no TATA or CAAT box [156]. There are several GGAGG repeats in the proximal promoter. These motifs are modified GC-boxes that may potentially be bound by Sp1/3 [156]. Transcriptional regulation seems to be dependent on the proximal promoter. Several studies have shown that Sp1 and/or Sp3 are required for SPARC transcriptional activation in chickens, mice, and humans [154, 155, 157]. In chick embryonic fibroblasts, v-Jun represses SPARC promoter activation and initiates cell transformation by targeting the minimal (-124/+16) promoter region. It was shown that v-Jun does not bind this DNA region directly but binds Sp1 or Sp3 to target promoter activation [157]. c-Jun has been shown to activate SPARC transcription in human MCF7 cells and repress SPARC transcription in rat and chick embryonic fibroblasts [158-160]. In mammary carcinoma, Brg-1, a SWI/SNF chromatin remodeling complex ATPase, was shown to interact with Sp1 to activate SPARC transcription [155]. Many reports have shown aberrant methylation of the SPARC gene in human tumors [161-164]. The mechanism of SPARC transcriptional regulation has not been investigated in adipocytes.

LPL

Lipoprotein lipase (LPL) hydrolyzes triacylglycerol from very low density lipoproteins (VLDLs) and chylomicrons into non-esterified fatty acids (NEFAs) and 2-monoacylglycerol. In addition to hydrolysis, LPL interacts with many lipoproteins and lipoprotein receptors to achieve a variety of functions including mediating the uptake of lipids, lipoproteins, and vitamins. LPL is secreted and attaches to the cell matrix via heparin sulfate proteoglycans. The cofactor apoC-

II and homodimerization are necessary for LPL activity [165]. LPL is expressed in many tissues. The highest expression includes tissues such as the heart, skeletal muscle, and adipose tissue that use and/or store fatty acids. LPL is a highly important enzyme in lipid metabolism and is regulated on many levels in a tissue-specific manner. Around one hundred mutations have been reported for human LPL [166] Mutations may increase or decrease LPL activity. Various mutations in LPL have been associated with familial combined hyperlipidemia, familial chylomicronemia syndrome, atherosclerosis, Alzheimer's disease, and obesity [166].

In adipose tissue, the first rate-limiting step for lipid metabolism is LPL. LPL activity increases during the fed state and decreases during the fasting state. Insulin regulates LPL at the transcriptional, post-translational, and post-transcriptional levels. Glucose increases LPL activity but not LPL transcript levels. LPL activity in adipocytes also depends on the levels of catecholamines, sex hormones, and thyroid hormones. LPL expression increases in human and rodent obesity, but LPL activity generally decreases [167-173]. Several LPL promoter SNPs have been positively correlated with human obesity and one has been associated with protection against obesity [174-176].

There are two major LPL splice forms in humans and mice. The human LPL promoter contains a CCAAT box and a TATA-like box. LPL contains a PPAR response element (PPRE) and its expression is upregulated by PPARγ in response to fatty acids levels and thiazolidinediones. Oct-1 and NF-Y are reported to be important for basal transcription. Estrogen regulates LPL through a distant AP-1 site. TNFα decreases LPL transcription in adipocytes by blocking NF-Y stimulated promoter activation. LPL transcription is also induced during adipocyte differentiation [163, 164, 175]. Glucose-dependent insulinotropic polypeptide (GIP), a gastrointestinal hormone, increases LPL expression and activity at the level of

transcription in human adipocytes. It was found the GIP and insulin treatment worked through the PI3K, Akt, AMPK pathway to promote the nuclear localization of TORC2 and the activation of CREB. CREB and TORC2 interact to bind a CRE element on the LPL promoter and activate transcription [177, 178].

Several studies have associated Sp1 and Sp3 with LPL transcriptional activation in macrophages. Interferon-γ (IFNγ) decreases macrophage LPL transcription by decreasing Sp3 protein levels and Sp1 DNA binding to sites in the 5' UTR [179]. It was later found that downregulation of LPL transcription by IFNγ was mediated by casein kinase 2 (CK2) and Akt [180]. Transforming growth factor-β (TGF-β) also represses LPL transcription through Sp1/Sp3 sites in the 5'-UTR [181]. Sp1/Sp3 binds an evolutionarily conserved CT element in the proximal promoter. A T(-93)G SNP that is close to the CT element has been associated with a predisposition to obesity and familial combined hyperlipidemia in some studies in humans. The minor allelic frequency is highly variable for different ethnic populations and the SNP effect may be influenced by the synergistic effects of a Asp9Asn and T(-93)G haplotype that is present in some populations [175, 182-184]. People with both the Asp9Asn and T(-93)G mutations have been shown to have an increased risk of cardiac disease and decreased LPL activity in some studies [176, 185, 186]. In the South African black population, the SNP was associated with mildly lower triglyceride levels and was associated with higher promoter activation in smooth muscle cells [184, 187]. This is in contrast to other studies which show that the mutation decreases Sp1 and/or Sp3 DNA binding leading to lowered transcriptional activation [166, 175, 182, 183]. Sterol regulatory element-binding protein (SREBP) was found to act synergistically with Sp1 to activate the promoter in macrophages. Mutation of the CT element is also reported to decrease promoter reporter activity in 3T3-F442a pre-adipocytes [188]. Sterols regulate LPL

through a SRE site that is close to the CT element [166, 189]. SREBP acts synergistically with Sp1 to activate the promoter. The –93 T-G mutation was found to decrease Sp1/Sp3 DNA binding leading to lowered transcriptional activation [182]. The importance of these Sp1/Sp3 binding sites has not been explored in adipocytes.

Cathepsin B

Cathepsin B is generally thought of as a lysosomal cysteine protease, but it can be found both intercellularly and extracellularly. Cathepsin B is associated with ECM degradation, apoptosis, and inflammation.

Cathepsin B has been implicated in acute pancreatitis. The exocrine pancreas secretes proteases that are necessary for protein digestion in the duodenum. The proteases are secreted as zymogens to protect the pancreas. The zymogens are activated by trypsin, which itself is secreted as a zymogen. The increased activation of trypsin is associated with pancreatitis. Cathepsin B is thought to help to produce the active form of trypsin [190]. Cathepsin B knockout mice are resistant to the induction of acute pancreatitis and diet-induced hepatic steatosis. TNFα is associated with the breakdown of lysosomal membranes, leading to Cathepsin B release into the cytosol [191]. In patients with non-alcoholic fatty liver disease (NAFLD), Cathepsin B was also found to be released into the cytosol from the lysosome. It is thought that the increase in FFA's leads to the destabilization of the lysosomal membrane, followed by Cathepsin B release into the cytosol, which leads to the activation of TNFα and the promotion of hepatic steatosis [192].

Cathepsin B expression is upregulated in atherosclerotic plaques. Inhibition of Cathepsin B inhibits low density lipoprotein degradation in endothelial cells [193]. Cathepsin B can degrade several types of collagen and aggrecan as well as activate proteolytic cascades.

Cathepsin B activity is increased in synovial cells and chondrocytes in rheumatioid and osteo-arthritis, respectively. The inflammatory cytokines, such as TNFα, present during arthritis inflammation are thought to upregulate Cathepsin B expression [194]. Many studies have shown that Cathepsin B also mediates apoptosis [137].

Interestingly, cathepsin B knockout mice females have been found to display depression-like behavior. Cathepsin B was identified as an important locus for anxiety and depression-like behaviors in mice. The mechanism is unclear but it could have something to do with Cathepsin B production of β-amyloid peptides [195].

Cathepsin B has a TATA-less promoter. Sp1 binding sites, Ets binding sites, and an E-box are important for basal transcriptional activation. Cathepsin B is transcriptionally upregulated in many carcinomas. The elevation in transcript level is reflected at the protein level [194]. Sp1 has been associated with high Cathepsin B promoter activation in glioblastoma [196]. Many Cathepsin B transcript variants have been found in human tumors [194].

Quiescin Q6

Quiescin Q6 (QSOX1) was identified by profiling for a protein whose level of expression increased in quiescent fibroblast cells [197]. It contains a thioredoxin domain and a domain homologous to yeast ERV1 and has been shown to function as a sulfhydryl oxidase, where it catalyzes the oxidation of thiols to disulfides by reducing oxygen to hydrogen peroxide [198, 199] [200]. There are homologs of Quiescin Q6 in most metazoans; however, it seems there is some discrepancy between the expression patterns based on the stage of development, rodent, and antibody specificity. Rat Quiescin Q6 has been shown to be widely expressed throughout neurons in the brain, with some staining in the choroid plexus. Some of the highest staining was in the neurosecretory neurons of the hypothalamus [201]. One report showed Quiescin Q6 was

expressed in heart, placenta, lung, liver, skeletal muscle, and pancreas but was barely detectable in brain and kidney in human tissues [202]. Another study showed Quiescin Q6 was widely expressed in fetal and P1 newborn mice [203].

The biological function of Quiescin Q6 is unclear. Quiescin Q6 might be an estrogen responsive gene [204]. Another study suggested Quiescin Q6 has an antioxidative effect and possibly helps to maintain the mitochondrial membrane potential [205]. Quiescin Q6 has also been shown to inhibit endothelial growth and sprouting, and it was suggested that it negatively regulates angiogenesis [206].

At least two splice variants exist; the long form has a transmembrane domain and is supposed to have more tissue-specific expression [207, 208]. However, several groups have predicted that Quiescin Q6 is secreted and involved in extracellular matrix remodeling [198, 202, 209-213]. Quiescin Q6 expression has been reported to be a marker for acutely decompensated heart failure [214]. It is also upregulated in pancreatic cancer and may promote tumor cell invasion by upregulating MMP-2 and MMP-9 [215, 216]. The role of Quiescin Q6 in insulin resistance is not known.

SerpinA

Serpina3N is a murine serine protease inhibitor. It is a homolog of human α1-antichymotrypsin (SERPINA3). The serpin family in rodents has many members that were created by gene duplication and diversification. Serpina3 is widely expressed. Its expression is upregulated during inflammation and in the brains of patients with schizophrenia and Alzheimer's disease [217-219]. It is known as an acute phase response protein. It expression is needed for wound healing [220]. Polymorphisms in Serpina3 have been associated with stroke,

prostrate cancer, and Alzheimer's disease [221-223]. The role of SerpinA in insulin resistance is not known.

Chitinase-3-like protein 1 (CHI3L1)

CHI3L1 is also known as YKL-40 and is part of a family of Chitinase-like proteins. It is expressed in several different cell types. Because it is highly expressed in late-stage macrophages, it is known as a macrophage marker. CHI3L1 induces M2 macrophage activation and prevents the apoptosis of inflammatory cells. It is highly associated with inflammation and tissue remodeling. CHI3L1 is regulated by many cytokines, including TNFα. CHI3L1 is associated with a myriad of diseases, including asthma, osteoarthritis, diabetes, artherosclerosis, cancer, liver fibrosis, etc [224]. Serum levels of CHI3L1 correlate with insulin resistance in diabetic patients [225, 226]. A Sp1 site in the proximal promoter has been shown to be important for promoter activation in macrophages [227].

Model systems

Several models have been used to study adipogenesis and adipocytokines. Mouse preadipocyte cell lines, such as 3T3-L1 and 3T3-F442a, can be differentiated into mature adipocytes in culture and are a widely accepted model to study adipocyte biology *in vitro*. The advantages of using 3T3 mouse preadipocyte cell lines are: 1) they are a well-characterized model system, 2) they are a pure population of adipocytes that mimic the structure and metabolism of adipocytes isolated *in vivo*, and 3) their culture conditions can be carefully controlled to elicit a variety of biological responses [21, 228]. However, adipocytes grown *in vitro* are not exposed to the wide range of endocrine signals present in an intact biological system, which may explain why they fail to secrete some proteins at the high levels measured *in vivo* [228, 229]. Primary preadipocytes isolated from adipose tissue better recapitulate *in vivo*

conditions, but they generally contain a proportion of stromal-vascular cells, which also secrete a wide array of cytokines, leading to potentially confounding results in the identification of adipocytokines [29, 228, 230]. Mature primary adipocytes can be isolated from fat tissue; however, they cannot be maintained for long periods in culture without significant alteration of metabolism [228, 231]. Rodent models of insulin resistance can be used to study adipocytokine expression and secretion in the context of complex endocrine and paracrine signaling [28-30]. In the following studies we will use a combination of mouse preadipocyte cell lines, human primary preadipocytes, and mouse adipose tissues. Each model system presents disadvantages and advantages, which will also be discussed in the text.

Figure. 1.1. The hexosamine biosynthesis pathway. Once glucose enters the cell, its by-products can be directed to several different pathways, including the HBP. Flux through the HBP generates the end product, UDP-GlcNAc, which is a substrate for the synthesis of other nucleotide sugars and multiple types of glycosylation, including the intracellular O-GlcNAc modification. Although the HBP requires several enzymatic steps, the two most well-studied enzymes (depicted in bold) in terms of insulin resistance are GFAT, the rate-limiting enzyme, and Emeg32. The HBP is posed to act as a "glucose sensor" since the synthesis of UDP-GlcNAc relies on the incorporation of products from glucose, amino acid (glutamine), fatty acid (acetyl-CoA), and nucleotide (uridine) metabolism. Modified from: Chin Fen Teo, Edith E. Wollaston-Hayden, Lance Wells. *Molecular and Cellular Endocrinology*. 318 (2010) 44–53.

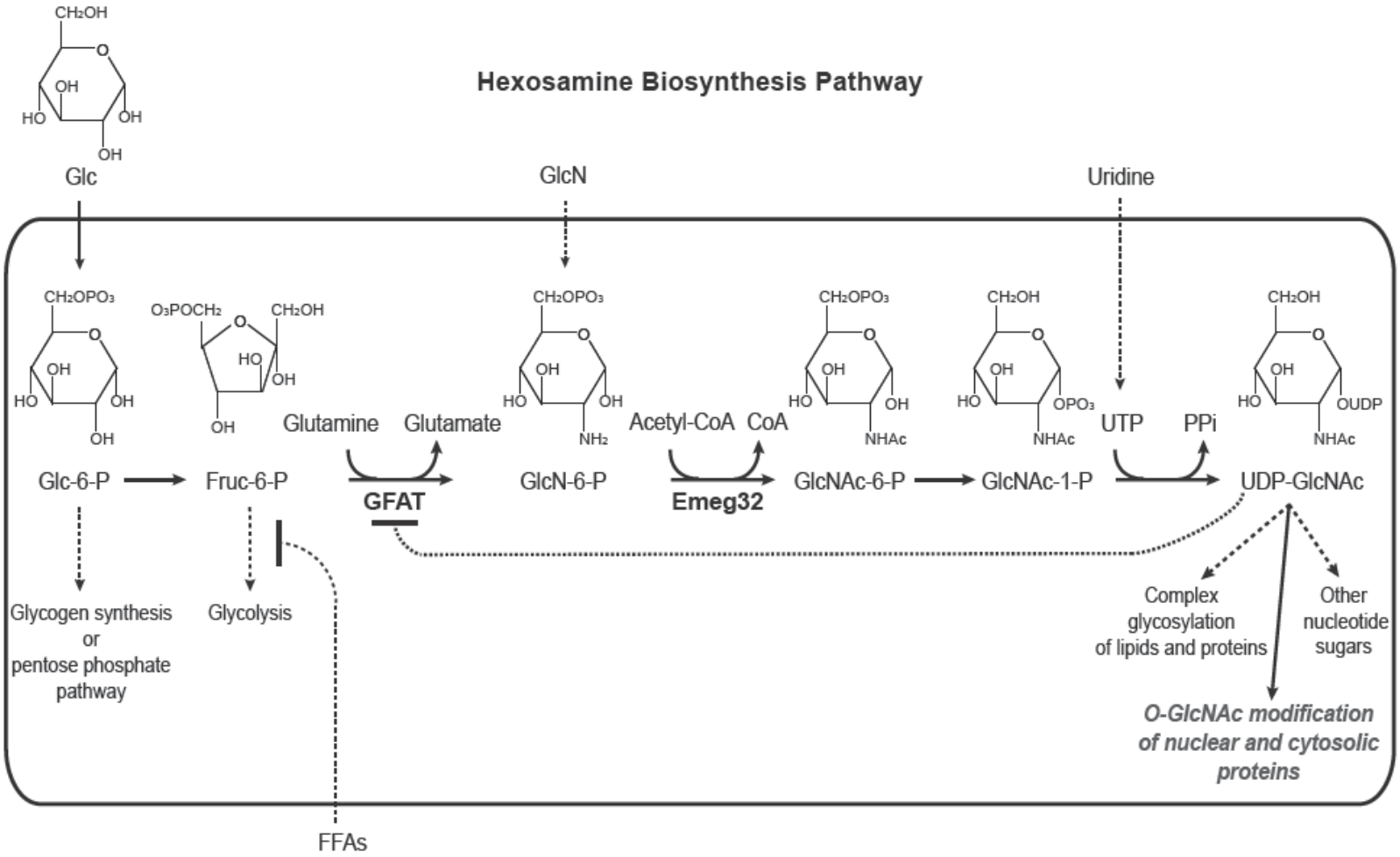
Hexosamine Biosynthesis Pathway
Glc
GlcN
Uridine
Glc-6-P
Fruc-6-P
Glutamine
Glutamate
GFAT
GlcN-6-P
Acetyl-CoA
CoA
Emeg32
GlcNAc-6-P
GlcNAc-1-P
UTP
PPi
UDP-GlcNAc
Glycogen synthesis or pentose phosphate pathway
Glycolysis
FFAs
Complex glycosylation of lipids and proteins
Other nucleotide sugars
O-GlcNAc modification of nuclear and cytosolic proteins

Figure. 1.2. The O-GlcNAc cycling enzymes. The dynamic and inducible post-translational modification, O-GlcNAc, is added to and removed from serine or threonine residues of polypeptides by OGT (in green) and OGA (in red), respectively. Modified from: Chin Fen Teo, Edith E. Wollaston-Hayden, Lance Wells. *Molecular and Cellular Endocrinology*. 318 (2010) 44–53.

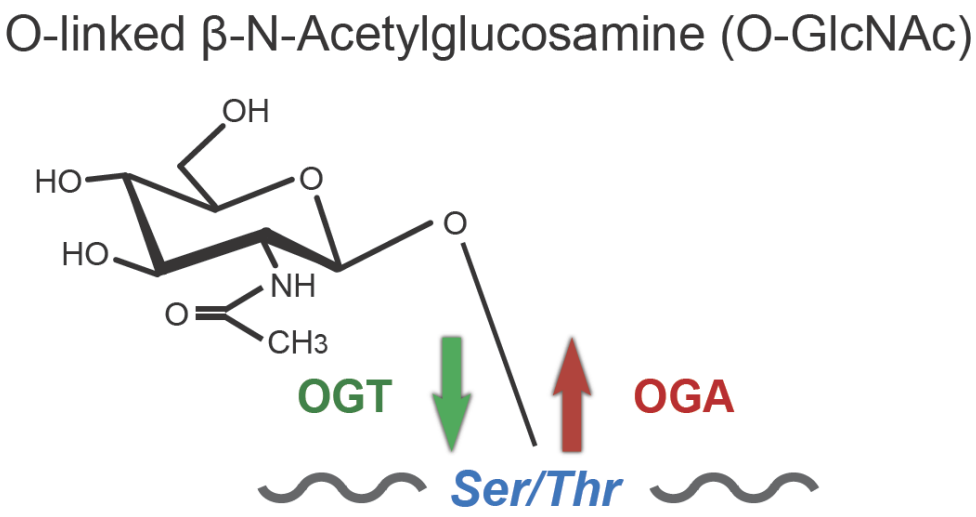

Figure 1.3. O-GlcNAc and Insulin Resistance in Adipocytes. Increased insulin-stimulated glucose flux increases the concentration of the end product of the HBP, UDP-GlcNAc, which is the sugar donor for OGT. Elevation of global O-GlcNAc levels is sufficient to induce IR and alter adipocytokine secretion. We hypothesize that O-GlcNAc modified transcription factors or cofactors are regulating the transcription of multiple adipocytokines.

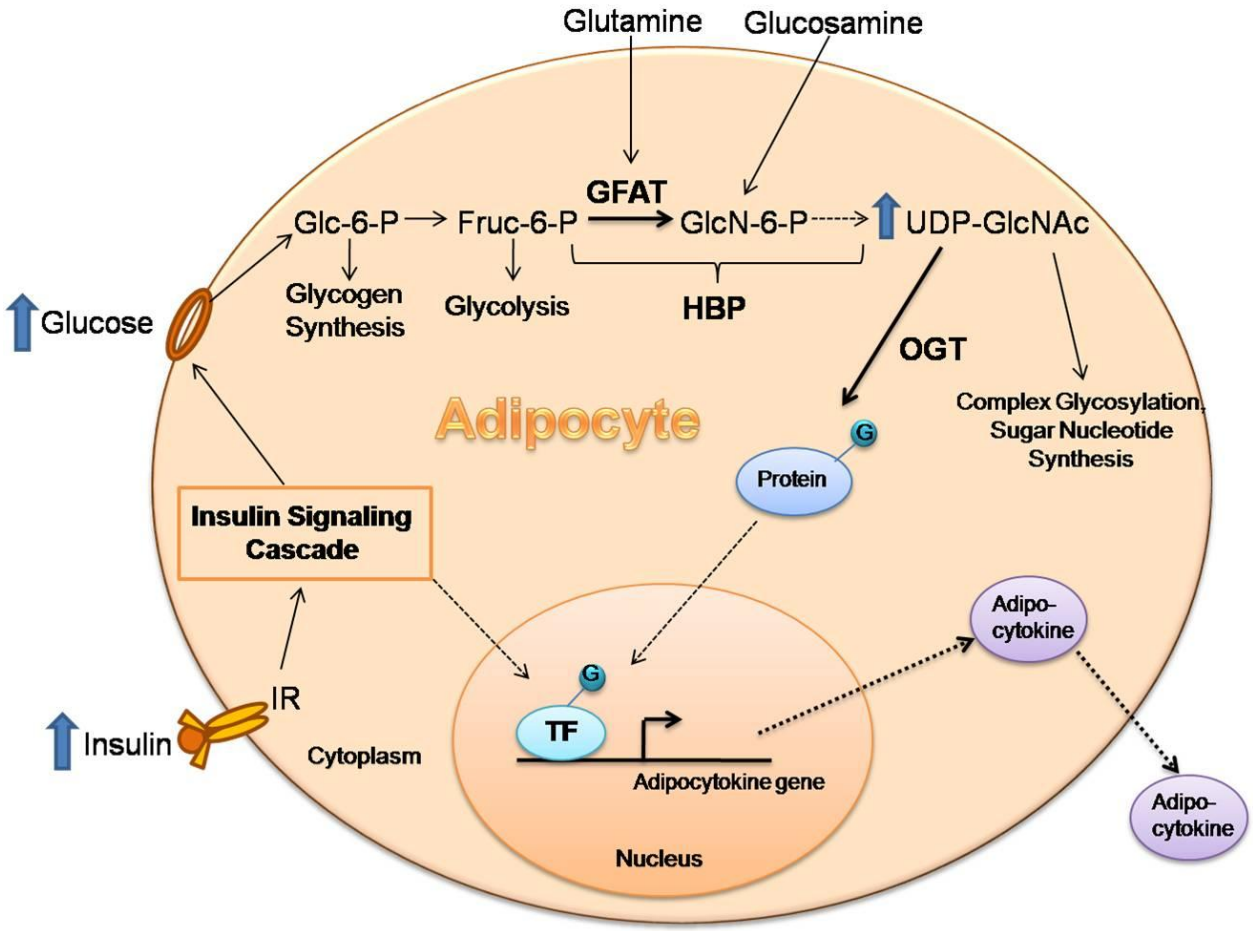

CHAPTER 2

THE ROLE OF THE O-GLCNAC MODIFICATION IN REGULATING EUKARYOTIC GENE EXPRESSION[1]

[1] Wollaston-Hayden, E.E.*; Brimble, S.*; Teo, C.F.; Morris, A.C. and L. Wells. 2010, *Current Signal Transduction Therapies*, 5(1):12-24.
Reprinted here with permission of publisher.

Abstract

O-linked β-N-acetylglucosamine (O-GlcNAc) modification of proteins has been shown to be involved in many different cellular processes, such as cell cycle control, nutrient sensing, signal transduction, stress response and transcriptional regulation. Cells have developed complex regulatory systems in order to regulate gene expression appropriately in response to environmental and intracellular cues. Control of eukaryotic gene transcription often involves post-translational modification of a multitude of proteins including transcription factors, basal transcription machinery, and chromatin remodeling complexes to modulate their functions in a variety of manners. In this review we describe the emerging functional roles for and techniques to detect and modulate the O-GlcNAc modification and illustrate that the O-GlcNAc modification is intricately involved in at least seven different general mechanisms for the control of gene transcription.

Introduction

Cells have developed a highly regulated system to respond to environmental and intracellular signals to specifically and coordinately express gene products [232, 233]. Surprisingly, the number of protein-coding genes in a genome does not reflect organism complexity, thus it has been hypothesized that increased complexity in gene regulation leads to increased organism complexity [234]. Indeed, the regulation of eukaryotic gene transcription involves a multitude of proteins including transcription factors, basal transcription machinery, and chromatin remodeling complexes [235]. An additional layer of complexity results from a wide variety of post-translational modifications on regulatory proteins [236]. Herein, we describe the emerging role of the O-GlcNAc post-translational modification of nuclear/cytosolic proteins in the regulation of transcription.

In the 1980's, Hart and coworkers reported a nucleocytoplasmic, post-translational sugar modification on serine and/or threonine residues of polypeptides, O-GlcNAc [237-239]. All metazoans currently studied contain the O-GlcNAc modification on proteins involved in many different cell processes, such as cell cycle control [240-242], nutrient sensing [81], signal transduction [98, 100, 243, 244], stress response [245, 246], and transcriptional regulation (the focus of this review) [88, 91, 247-249]. Furthermore, O-GlcNAc transferase (OGT) [92, 250, 251], the enzyme required for O-GlcNAc addition, is required for mouse embryonic stem cell viability, emphasizing the importance of this modification [113]. O-GlcNAc is more akin to phosphorylation than complex glycosylation in that it is not elongated, its cycling enzymes, OGT and O-GlcNAcase (OGA) [93, 252], are nucleocytoplasmic, it is dynamic and inducible, and it can regulate intracellular protein activity, localization, stability, and molecular interactions. O-GlcNAc is often found on the same residues as known phosphorylation sites, suggesting

reciprocity between the modifications in some cases, Fig. (2.1) [243, 253, 254]. However, unlike phosphorylation, which is modulated by hundreds of kinases and phosphatases, the cycling of the O-GlcNAc modification is accomplished by the gene products of single genes for OGT and OGA in most metazoans.

O-GlcNAc modification of transcription regulatory proteins could fine tune their regulation in response to nutrient levels in the cell because the synthesis of its sugar donor, UDP-GlcNAc, via the hexosamine biosynthetic pathway (HBP), responds to amino acid, fatty acid, nucleotide and glucose metabolism [81, 88]. There are several ways to modulate O-GlcNAc levels on proteins (for review see [90]) Figure (2.1). OGT is responsive to physiological levels of UDP-GlcNAc, so increased HBP flux by hyperglycemia or by the addition of glucosamine results in globally elevated levels of O-GlcNAc modification [82]. Decreased O-GlcNAc levels can be achieved by blocking glutamine-fructose-6-phosphate transaminase (GFAT), the rate limiting enzyme of the HBP, using the pharmacological inhibitors azaserine or 6-diazo-5-oxo-L-norleucine (DON) or by decreasing glucose levels. However, the alteration of HBP flux may lead to off-target effects as azaserine and DON are general amidotransferase inhibitors. A more specific way to alter global O-GlcNAc levels is by the use of pharmacological OGA inhibitors such as the widely used O-(2-acetamido-2-deoxy-D-glucopyrano-sylidene)amino-N-phenylcarbamate (PUGNAc) [255], or the more specific inhibitors 1,2-dideoxy-2'-propyl-α- D -glucopyranoso-[2,1- D] -Δ2'-thiazoline (NButGT) [256] and GlcNAcstatin [257, 258]. Several OGT inhibitors have also been recently characterized [259] although their specificity and *in vivo* utility has not been adequately explored. Alternatively, O-GlcNAc steady state levels can be modulated genetically by over expression or knockdown of OGT and/or OGA.

O-GlcNAc Detection and Site Mapping

Over the last 20 years more than 400 proteins have been shown to be modified by O-GlcNAc using a variety of detection methods [88, 260-263]. Interestingly, most RNA Polymerase II transcription factors are glycosylated; many of which respond to nutrient abundance [91, 264]. There are several methods to identify O-GlcNAc modification of proteins [265] and the relevant methods will be briefly discussed here. The first step in identifying O-GlcNAc modified proteins generally involves modification-specific enrichment. Detection or enrichment of O-GlcNAc modified proteins can be achieved using O-GlcNAc specific antibodies, such as RL2 [266, 267] and CTD110.6 [268], and by lectin-blotting or chromatography using succinylated Wheat Germ Agglutinin, a terminal GlcNAc-binding lectin. The presence of O-GlcNAc on proteins can also be determined by labeling with radiolabeled galactose using purified β-1,4-galactosyltransferase (GalT), a galactosyltransferase that transfers galactose onto terminal GlcNAc moieties [237]. Click-iT™ chemistry available from Invitrogen offers two different approaches for *in vitro* and *in vivo* labeling of O-GlcNAc residues. *In vitro* labeling takes advantage of a mutant form of GalT that transfers ketone-modified galactose onto the GlcNAc residues of proteins [269]. The ketone group introduces a chemically reactive group that can be tagged with biotin and then enriched with streptavidin [269]. Using an *in vivo* approach, introduction of N-azidoacetylglucosamine (GlcNAz) into the cells allows this azidosugar to be converted via the salvage pathway to UDP-GlcNAz and transferred onto proteins by OGT [270]. The azido group of GlcNAz acts as a bio-orthogonal handle for enrichment by the addition of functional groups using the Staudinger ligation [271]. However, there are limitations to using the *in vivo* approach, since it requires the UDP-GlcNAz to compete with the existing UDP-GlcNAc in the cell. These O-GlcNAc enrichment techniques can be

combined with mass spectrometry to identify the actual residues of modification [54-56]. Proteomic efforts in this area have identified hundreds of modified polypeptides with proteins involved in transcriptional regulation being a major class [45, 48, 54-56]; however, only about 75 proteins have had their sites of modification mapped. The modification is extremely labile, small, uncharged, and usually substoichiometric [90, 272] making detection difficult using standard mass spectrometry techniques.

Recently, several methods have been developed to make O-GlcNAc site-mapping by mass spectrometry (MS) feasible in biologically relevant tissues. O-GlcNAc enrichment techniques can be combined with mass spectrometry to identify the actual residues of modification [262, 273]. Collision-induced dissociation (CID) mass spectrometry tends to cleave PTMs, so a non-labile tag added to the site of O-GlcNAc modification facilitates identification. Site-mapping studies using β-elimination followed by Michael addition with dithiothreitol attach a non-labile tag to the site of O-GlcNAc modification so it can be identified by CID MS [263]. In addition, enrichment of O-GlcNAc containing peptides by chemoenzymatic labeling assists in detection [260, 269, 270, 272]. An advantage of these methods is that more O-GlcNAc peptides, which are generally substoichiometric in a total peptide pool, can be detected leading to a more prolific site mapping experiment. The development of electron transfer dissociation fragmentation and related dissociation techniques that often retain CID-labile PTMs have allowed for the identification of O-GlcNAc modified fragments directly [274, 275]. In Fig. (**2.2**), we show an example of an electron dissociation technique (electron capture dissociation) for definitively mapping a site of O-GlcNAc on UL32, a synthetic glycosylated peptide, to one particular residue on a peptide containing three potential sites of attachment. Unlike CID, the fragmented peptides containing the modified amino acid

retain the mass of the sugar. Electron dissociation techniques are an emerging technology for O-GlcNAc site-mapping that show great promise [272, 275-278].

O-GlcNAc Regulation of Eukaryotic Gene Expression

Specialized transcription factor regulation occurs through the actions of multiple post-translational modifications (PTMs) (reviewed in [236, 279]) such as phosphorylation [280, 281], SUMOylation [282], acetylation [283], and the focus of this review, O-GlcNAc modification. Transcriptional control can occur via at least seven different general mechanisms, Fig. (2.3), and examples of O-GlcNAc modification participation in each of these regulatory steps are explored below.

Chromatin Remodeling

Chromatin not only provides compact packaging for DNA, it also regulates transcription. For transcription to occur, nucleosomes, the histone proteins/DNA subunits of chromatin, must be positioned to allow transcriptional machinery to access both the promoter and upstream regulatory elements and to allow transcriptional elongation [284]. Access to DNA is regulated by chromatin remodeling enzymes, which recognize PTM's on histones [284, 285]. Acetylation, the most well studied histone PTM, is added by histone acetyltransferases and removed by histone deacetylases (HDACs) [284, 285]. Transcriptional regulation is associated with altered histone acetylation and movement, restructuring, and ejection of nucleosomes [284]. Methylation of certain histone lysines by histone methyltransferases also plays a role in both gene silencing and activation [286]. The actual chromatin remodeling enzymes are thought to be regulated by PTM's such as phosphorylation and acetylation [284]. Several studies have found glycosylation affects the regulation of chromatin remodeling [287, 288].

The first evidence for O-GlcNAc's role in transcriptional regulation was the observation that *Drosophila melanogaster* polytene chromosomes contain more O-GlcNAc modified proteins at the transcriptionally repressed condensed regions than at the active puff regions of the chromatin [289]. Further studies implicated OGT in transcriptional repression through the identification of an interaction between mSin3a and OGT [287]. mSin3a is a corepression scaffolding protein that forms a multi-protein complex with HDAC and can be recruited by transcription factors to modify histones and repress transcription [290]. Several transcription factors involved in cell survival and apoptosis, such as p53, an O-GlcNAc modified protein [291, 292], recruit mSin3a [293]. The paired amphipathic helix domain 4 of mSin3A was shown to bind to the tetracopeptide repeat (TPR) domain of OGT, suggesting a mechanism where mSin3a recruits OGT for gene silencing [287]. Although both the TPR and catalytic domain of OGT promote transcriptional repression, catalytically active OGT is required for full transcriptional repression [287]. The other proteins in the repression complex, mSin3A and HDAC1, were also found to be O-GlcNAc modified [287] and, although the functional significance is still to be elucidated, may explain why the catalytic activity of OGT is necessary. In agreement with the data seen in *Drosophila melanogaster* polytene chromosomes, a chromatin immunoprecipitation assay showed an increase in both O-GlcNAc modified proteins and mSin3a presence on the promoters of silenced genes [287]. In another study, OGT was found to interact with both mSin3A and Sp3 and was associated with the prevention of transcriptional repression of angiopoietin-2 during hyperglycemic conditions [294]. However, it is unclear whether the association of mSin3A with Sp3 or the direct O-GlcNAc modification of Sp3 was responsible for the transcriptional activation of angiopoietin-2 [294].

A landmark study recently identified a key role for O-GlcNAc in modulating the activity of MLL5, a histone lysine methyltransferase [288]. MLL5 was found to co-activate RARα (retinoic acid receptor α) induction of promyelocyte-like differentiation into granulocyte-like HL60 cells. OGT forms a complex with MLL5. Elevation of O-GlcNAc levels in undifferentiated HL60 cells increase retinoic acid (RA) stimulated differentiation. Upon RA stimulation, RARα activates the expression of C/EBPε, a major differentiation facilitating transcription factor. Expression of a T440A, the major site of O-GlcNAc modification, mutant of MLL5 failed to activate C/EBPε expression and enhancement of the RA effect on differentiation. Further experiments established that OGT is necessary for MLL5 methylation of H3K4, which allows the transcriptional activation of pro-differentiation genes [288]. Thus, this manuscript clearly illustrates a causal relationship between O-GlcNAc modification of a protein and its enzymatic activity, which is directly involved in chromatin remodeling.

Transcriptional Initiation and Elongation

O-GlcNAc modification has also been implicated in regulating transcriptional initiation via RNA Polymerase II (RNAP II). Transcriptional initiation is achieved in part by several general transcription factors that recruit hypophosphorylated RNAP II to the core promoter and form a pre-initiation complex [295]. RNAP II has a carboxyl terminal domain (CTD) that consists of several tandem consensus sequence repeats that are modified by phosphate and O-GlcNAc [268, 295]. The phosphorylation of the CTD is involved in promoter clearance, passage through promoter proximal pause sites, stabilization of the elongation complex, and recruitment of mRNA processing machinery [233]. The CTD exists in two states with regards to its phosphorylation status; IIO is the phosphorylated form and is found predominantly in the

elongation complex, while IIA is the unphosphorylated form generally found in the initiation complex [295].

When purified fractions of RNAP II were labeled with GalT, it was shown that only the IIA form, the unphosphorylated form, of CTD was modified with O-GlcNAc [296]. In an additional study, OGT failed to label a CTD consensus sequence that had been phosphorylated in vitro by CTD kinase, and CTD kinase would not label a CTD consensus sequence that had been synthetically glycosylated on the Thr 4 of each repeat, suggesting mutual exclusivity between the modifications [268]. This yin-yang relationship between phosphorylation and O-GlcNAc on the CTD suggests that the O-GlcNAc modification may prevent elongation from occurring by blocking phosphorylation or may help to recycle RNAP II after elongation has occurred to allow the complex to reattach to the promoter [268]. Further *in vivo* investigation is needed to clarify the function of glycosylation on the CTD of RNAP II; however, the suggestion that glycosylation regulates transcription initiation is not unprecedented.

Degradation

The proper maintenance of transcription factor levels in cells is often accomplished by degradation via the ubiquitin-proteasome system [297]. Degradation is achieved by two steps: first, ubiquitin is added by an E3 ubiquitin ligase to lysine residues on proteins targeted for destruction, and second, the polyubiquitinylated proteins are degraded by the 26S proteasome [298]. The 26S proteasome is comprised of two major subcomplexes: two 19S regulatory particle caps and the 20S catalytic core [298]. The 20S core catalyzes the proteolysis of protein substrates. The 19S particle caps contain six ATPases that work to recognize and unfold substrates for entry into the 20S core [298, 299]. Glycosylation and phosphorylation have been

suggested to regulate both the activity of the proteasome and the targeting of proteins to the proteasome [249, 300].

The most well-studied O-GlcNAc modified transcription factor is Sp1, a ubiquitous transcription factor for TATA-less genes. Sp1 target genes are involved in many different processes including metabolism, cell proliferation and oncogenesis [301]. In 1988, Jackson and Tjian determined that Sp1 is O-GlcNAc modified [129]. Since then, glycosylation has been described to affect Sp1 function by modulating its stability, protein-protein interactions, DNA binding, and localization [129, 249]. An initial study found that glucose starvation plus adenylate cyclase activation in normal rat kidney cells resulted in decreased Sp1 protein levels and Sp1 hypoglycosylation [302]. The authors suggested that hypoglycosylation of Sp1 promotes degradation through a proteasome-like mechanism [302]. However, it was subsequently shown that the degree of Sp1 glycosylation was independent of its degradation, and instead it was discovered that OGT inhibits and OGA activates the ATPase activity of the 19S regulatory particle caps of the proteasome [300]. OGT catalytic activity is necessary for this inhibition of the proteasome [300]. O-GlcNAc modification of Rpt2, one of the six ATPases present in the 19S cap, blocks the ATPase activity that provides the energy for hydrophobic proteins to unfold and be translocated inside the catalytic core of the proteasome for degradation [300]. Subsequently, in the 26S proteasome of *Drosophila melanogaster*, five out of nineteen regulatory subunits of the 19S cap and nine out of fourteen subunits of the 20S catalytic core were shown to be O-GlcNAc modified by immunoblotting with monoclonal antibodies and wheat germ agglutinin [303]. O-GlcNAc modification of the proteasome may function to regulate protein degradation in response to nutrient availability, which could potentially regulate

transcription by altering transcription factor steady-state levels of transcription factors, such as in the case of Sp1.

Besides its global effect on proteasome function, O-GlcNAc modification is also associated with altered stability of individual transcription factors such as c-Myc, estrogen receptor β (ER-β), and p53. These transcription factors have been shown to be regulated by the ubiquitin proteasome pathway via phosphorylation [292, 304, 305]. A reciprocal relationship between phosphorylation and O-GlcNAc modification is observed for both c-Myc and ER-β [304-307].

c-Myc, a proto-oncogene, was one of the earliest proteins to be site-mapped for O-GlcNAc modification. c-Myc is O-glycosylated on Thr 58 in the N-terminal transcriptional activation domain region [307, 308]. Thr 58 is in the major region of mutation seen in Burkitt's lymphomas [309], and phosphorylation at this site leads to c-Myc polyubiquitinylation and degradation [310]. T58A mutants have increased stability, suggesting that glycosylation via blocking of phosphorylation on this residue may result in increased stability, although the specific mechanism is not known [305]. c-Myc is targeted by several signaling pathways and regulates a plethora of target genes involved in cell proliferation, differentiation, and apoptosis [311]. Thus, PTM's on c-Myc including phosphorylation and glycosylation appear to influence the specificity and stability of c-Myc [310].

ER-β, an ER-α homologue, is important in many processes such as growth and development, response to stress, and control of energy balance [312, 313]. Phosphorylation of ER-α by GSK-3 (glycogen synthase kinase-3) promotes its stability and full transcriptional activation, and this regulation of ER-α has emerged as an important theme in estrogen signaling [314, 315]. Although this theme is not as well-studied for ER-β, phosphorylation of the ER-β

AF-1 domain has been shown to affect its proteasome-dependent degradation [316]. Glycosylation may also play a role in regulating ER-β stability. Ser 16 of ER-β is reciprocally glycosylated and phosphorylated [306]. S16A and S16E mutants were generated to mimic no modification and constitutive phosphorylation, respectively. The S16A mutant had a longer half-life (15-16 hours) and the S16E mutant had a shorter half-life (4-5 hours) than the wild type ER-β (7-8 hours), which suggests that glycosylation may promote ER-β stability by blocking phosphorylation and subsequent targeting for degradation [304].

p53 is a tumor suppressor gene required for cell cycle arrest and apoptosis. Normally, cellular p53 levels, which are highly regulated, are kept very low via degradation by the ubiquitin-dependent proteosome system [317]. Factors such as DNA damage or the activation of oncogenes induce increased p53 stability and activation [317]. p53 is found to be mutated and dysfunctional in many human cancers [317]. An early study determined p53 is O-GlcNAc modified and the presence of the modification was suggested to increase p53's ability to bind DNA [291]. A later study determined a role for O-GlcNAc modification in p53 stability [292]. p53 is O-GlcNAc modified on Ser 149, which is located on the DNA binding domain. Mutation of Ser 149 to alanine increases Thr 155 phosphorylation. Since elevated Thr 155 phosphorylation is associated with increased degradation of p53, Ser 149 glycosylation has been hypothesized to play an important role in p53 stabilization [292].

Localization

Several papers have been published showing a functional relationship between O-GlcNAc modification and nuclear or cytoplasmic localization [120, 318-320]. Transcription factors must localize to the nucleus to activate transcription, so sequestering latent transcription factors to the cytoplasm provides an additional mechanism of transcriptional regulation. In

response to signals, latent cytoplasmic transcription factors are activated by several mechanisms, many of which depend on phosphorylation or other PTM's, such as glycosylation [232].

The transducer of regulated cyclic adenosine 3'-5' monophosphate response element (CREB) protein (CRTC2) associates with CREB to regulate gluconeogenic genes, including glucose-6-phosphatase (G6Pase), in response to insulin and glucagon [321]. Gluconeogenic genes fail to be inactivated during chronic hyperglycemic conditions, leading to gluconeogenesis during energy prevalent conditions. CRTC2 associates with CREB to bind the cAMP response element on the G6Pase promoter. When insulin is present, SIK2 (salt-induced kinase 2) is activated by Akt and phosphorylates Ser 171 of CRTC2, which allows it to be sequestered in the cytoplasm by 14-3-3 proteins and targeted for degradation [322]. Glucagon signaling prevents SIK2 from phosphorylating CRTC2 [323]. The dephosphorylated form of CRTC2 is no longer sequestered in the cytosol by 14-3-3 proteins and is free to translocate to the nucleus and activate transcription of target genes. CRTC2 is reciprocally modified by O-GlcNAc and phosphate on Ser 171 and Ser 70, suggesting alternative roles for the modifications. Hyperglycemia or elevating O-GlcNAc levels via genetic or pharmacological methods decreases CRTC2 phosphorylation and increases its O-GlcNAc modification, nuclear localization, and G6Pase promoter activation [120]. Mutation of these sites to aspartate, which simulates phosphorylation, prevents hyperglycemic stimulation of G6Pase promoter activation. Overexpression of OGA in the liver of diabetic *db/db* mice restores their gluconeogenic profiles to nearly normal levels, suggesting that elevated O-GlcNAc levels contribute to the nuclear localization of CRTC2 and the subsequent deregulation of gluconeogenesis during hyperglycemic conditions [120].

O-GlcNAc modification appears to be required for the nuclear localization of NeuroD1 (neurogenic differentiation 1). NeuroD1 is required for the terminal differentiation of neurons

and for the development and insulin production of pancreatic β-cells [324]. Hyperglycemia results in increased phosphorylation of NeuroD1 on Ser 274, nuclear translocation, and increased NeuroD1 binding to the insulin promoter. Mutation to S274A results in the cytoplasmic accumulation of NeuroD1 even in hyperglycemic conditions [318]. Elevation of global O-GlcNAc levels using PUGNAc increased NeuroD1 nuclear localization, binding to the insulin promoter, and insulin expression even in normoglycemic conditions, suggesting that phosphorylation and O-GlcNAc modification are acting cooperatively. This result may be due to a similar increase in NeuroD1 glycosylation in both hyperglycemic and PUGNAc-treated conditions. OGT was found to associate with NeuroD1 in hyperglycemic conditions and OGA was found to associate in normoglycemic conditions [319]. Identifying the NeuroD1 glycosylation sites would help to distinguish whether the effect on localization and subsequent insulin transcriptional activation results from the specific glycosylation of NeuroD1, the interplay between glycosylation and phosphorylation, or from the alteration of global O-GlcNAc levels [319].

β-catenin glycosylation has been shown to regulate its cellular localization [320]. β-catenin plays two major roles in the cell: first, it associates with E-cadherin to form cellular adhesions, and secondly, it is the major downstream signaling molecule for the canonical arm of the Wnt signaling pathway. Wnt signaling pathways are involved in cell growth, movement, and cell survival and are associated with several types of cancer [325]. GSK-3 phosphorylation of β-catenin on its N-terminus targets it for ubiquitination and degradation. Wnt-activated signaling regulates β-catenin by inactivating GSK-3, allowing for the accumulation of β-catenin and its translocation to the nucleus. Here it can activate transcription of target genes by activating TCF (T-cell factor) and recruiting chromatin remodeling proteins [325]. β-catenin has been shown to

be O-GlcNAc modified [326]. PUGNAc treatment of several cancer cell lines resulted in the redistribution of glycosylated β-catenin from the nucleus to the cytoplasm without affecting total protein levels [320]. The increase in cytoplasmic localization was associated with decreased expression of two downstream targets genes, cyclin D and vascular endothelial growth factor A, and decreased promoter activation [320]. More work is needed to determine how the glycosylation of β-catenin influences its interaction with many regulatory binding partners, such as GSK-3 and TCF, and in turn the role of O-GlcNAc in regulating its degradation and transcriptional activation [320].

DNA Binding and Transcriptional Activation

All classical transcription factors share two features: a DNA binding domain for binding to a specific sequence of DNA and a transactivation domain for response to regulatory factors. Sequence-specific transcription factors recruit coactivators to initiate transcription. These coactivators include chromatin remodeling enzymes that are needed to allow the basal transcription machinery to access the DNA and form the pre-initiation complex with the help of additional regulatory proteins [235]. PTM's, such as glycosylation, can affect the ability of transcription factors to bind DNA and activate transcription [236].

The transcription factors PDX-1 (pancreatic/duodenal homeobox-1) protein, NeuroD1, and V-maf musculoaponeurotic fibrosarcoma oncogene homologue A co-regulate insulin transcription. The exact mechanisms of regulation are not clear, which is probably due to the number and complexity of post-translational modifications and cofactor interactions. PDX-1 is necessary for pancreatic development, and it activates several β-cell specific genes, such as insulin [324]. In response to changing glucose concentrations, PDX-1 recruits chromatin remodeling enzymes and other cofactors and regulates transcriptional elongation. PDX-1

phosphorylation is associated with its translocation to the nucleoplasm and its transactivation potential [324]. PDX-1 is also O-GlcNAc modified on at least two sites [327]. Hyperglycemia or PUGNAc treatment of MIN6 mouse insulinoma cells increases global O-GlcNAc protein levels, enhances PDX-1 binding to the insulin promoter, and is associated with an increase in insulin secretion [327]. The addition of azaserine, which inhibits GFAT and results in lower UDP-GlcNAc levels, decreases global O-GlcNAc levels and glucose-stimulated insulin secretion [327]. Treatment with siRNA against OGT also results in decreased glucose-stimulated insulin secretion, suggesting that the O-GlcNAc modification modulates insulin secretion, perhaps by activating PDX-1 binding to the insulin promoter [106, 327]. O-GlcNAc seems to be extensively involved in β-cell transcription factor regulation and may play an important role in controlling gene expression in response to glucose levels.

Like CRTC2, the forkhead transcription factor family, of which FoxO1 is a member, plays a major role in regulating energy homeostasis [328]. In the liver, FoxO1 and its coactivator, peroxisome proliferator activated receptor γ co-activator 1α (PGC1α), participate in the regulation of gluconeogenesis by activating the expression of G6Pase and phosphoenolpyruvate carboxykinase [329, 330]. Insulin signaling induces Akt to phosphorylate FoxO1 on residues Thr 24, Ser 256, and Ser 319, which results in FoxO1 cytoplasmic localization [331]. FoxO1 is subject to many PTM's, including glycosylation [332]. Increasing global O-GlcNAc levels by hyperglycemia, PUGNAc, or overexpression of OGT in HEK293 or rat hepatoma cells increases FoxO1 activation of a G6Pase promoter reporter construct [333, 334]. A triple alanine mutant of the Akt phosphorylation sites on FoxO1 is still able to be glycosylated, suggesting that the FoxO1 O-GlcNAc sites are not directly reciprocal with the Akt phosphorylation sites [333]. Consistent with this result, O-GlcNAc modification does not seem

to be required for FoxO1 translocation to the nucleus [333, 334]. FoxO1 has been shown to be O-GlcNAc modified on the following residues: Ser 550, Thr 648, Ser 654, and either Thr 317 or Ser 318 [333]. These sites were mutated to alanine and tested for activation of the G6Pase promoter. Only the T317A mutant had a small decrease in promoter activation under hyperglycemic conditions [333]. A follow-up study found that PGC1α interacts with OGT and enhances both OGT interaction and modification of FoxO1 [335]. Coexpression of PGC1α and FoxO1 in HEK293 cells cooperatively increases promoter activation in response to hyperglycemia [335].

Protein/Protein Interactions

Modification of proteins by O-GlcNAc has been shown to modulate protein-protein interactions that regulate nuclear localization [120, 336], stability [292], chromatin remodeling [287, 288], and transcriptional activation [320, 337, 338].

O-GlcNAc modification of Sp1 and β-catenin has been shown to decrease transcriptional activity possibly through inhibition of binding to co-activators [320, 338]. In addition, O-GlcNAc modification of a small peptide segment of Sp1 has been shown *in vitro* to prevent binding to the general transcription factor TAF110 (TATA-binding-protein-associated factor) [339].

Glycosylation of STAT5a (signal transducer and activator of transcription 5a) was found to be important for its interaction with CREB-binding protein (CBP) [337]. STAT proteins are activated by tyrosine phosphorylation in response to various cytokines and growth factors [340]. They initiate downstream transcriptional activation by dimerizing, translocating to the nucleus and activating transcription partly through the binding to co-activator molecules, such as CBP, that have histone acetyltransferase activity [341]. Mass spectrometry analysis and mutational

studies of STAT5a showed that Thr 92 and potentially Thr 97 are O-GlcNAc modified [337]. The mutant T92A prevented STAT5a interaction with CBP and transactivation without affecting DNA binding [337].

NFκB (Nuclear factor κB) signaling has been implicated in a wide range of cellular processes, such as cell immune response, survival, differentiation, and proliferation. In the canonical NFκB signaling pathway, NFκB is normally bound to IκB and sequestered in the cytoplasm [342]. Phosphorylation of IκB by IκB kinase (IKK) leads to IκB degradation via the ubiquitin-proteasome pathway and this allows NFκB to translocate to the nucleus where it can activate transcription [342]. PTM of NFκB subunits can alter transcriptional activation by affecting interactions with transcriptional coactivators and corepressors. NFκB is activated by many pathways, so differential PTMs may specify the particular targets of NFκB. IKK is also regulated by PTMs [342].

Manipulation of the HBP in mesangial cells showed that hyperglycemia increases glycosylation of the p65 subunit of NFκB and promoter activation of a target gene, VCAM-1 (vascular cell adhesion molecule 1) [343]. Hyperglycemia or OGT overexpression decreased the association of the p65 subunit of NFκB with IκB and increased NFκB nuclear localization. Overexpression of OGA in rat vascular smooth muscle cells resulted in lower global O-GlcNAc levels and the reversal of NFκB activation by hyperglycemia. OGT overexpression resulted in the same effects as NFκB activation by hyperglycemia. Mutation of an NFκB O-GlcNAc modification site, Thr 352, to an alanine was found to abrogate promoter activation, DNA binding affinity, association with IκB, nuclear localization, and the expression of VCAM-1 induced by PUGNAc or OGT overexpression [336]. The primary effect of NFκB O-GlcNAc modification may be to prevent p65/IκB interaction, which would lead to nuclear localization

and downstream target activation; however, more investigation is needed to target the exact mechanism.

A recent paper tied p53 repression of NFκB activation to the O-GlcNAc modification of IKKβ [344]. p53 inactivation leads to an increase in glycolysis through enhanced NFκB activation and results in a positive feedback loop where glycolysis further activates NFκB signaling [345]. The authors proposed that O-GlcNAc modification of IKKβ could be acting as a glucose-sensor to potentiate the feedback loop. In a hepatic cancer cell line, hyperglycemia enhanced IKKβ O-GlcNAc modification and TNFα (tumor necrosis factor α) -stimulated NFκB promoter activation and prolonged NFκB DNA binding and IKKβ activity. Since phosphorylation of IKKβ at Ser 733 is known to inhibit its activation [346], O-GlcNAc modification of Ser 733 is suggested to prevent phosphorylation-stimulated inactivation leading to an increased in activation of NFκB in transformed cells [344]. These studies establish a clear role for O-GlcNAc in the activation of NFκB.

OGT/OGA Targeting to Substrates – A Special Case of Protein/Protein Interactions

O-GlcNAc modification regulates the function of many target proteins, so aberrant modification by OGT needs to be avoided for proper cellular function. However, the mechanism by which OGT selects its targets is not currently known. No consensus sequence for O-GlcNAc attachment has been found, so it has been proposed that interaction with OGT's TPR domain may determine which proteins it modifies [83, 251, 347]. OGT may also use adaptor proteins that help to modulate its specificity and increase the complexity of its regulation [254, 348]. Cheung *et al.* used a yeast two-hybrid screen to identify proteins that interact with OGT from a human fetal brain cDNA library [348]. Two of the twenty-seven putative OGT-interacting proteins identified, MYPT1 (myosin phosphatase target subunit 1) and CARM1 (coactivating

arginine methyltransferase), were shown to interact with OGT and be O-GlcNAc modified by independent methods [348]. Knockdown of MYPT1 using siRNA in Neuro-2a cells reduced the O-GlcNAc levels of several proteins, suggesting that MYPT1 might target OGT to substrates *in vivo* [348]. CARM1 is a histone methyltransferase and functions as part of the p160 coactivator complex, which contributes to chromatin remodeling and transcriptional activation [349]. CARM1 may help to target OGT to substrates that are involved in transcriptional activation [348]. Trak1 (also known as OIP106) was identified by another yeast two-hybrid screen of OGT interacting proteins [347]. Trak1 associates with RNAP II, so it has been proposed that Trak1 targets OGT to the transcriptional machinery [347, 350]. Finally, as mentioned above, PGC-1α may act as an adaptor protein for OGT recruitment to FoxO1 [335].

Although little is known about targeting of OGT to its substrates, even less is known about the regulation of OGA [351]. In some cases, OGT and OGA are found in the same complex [352]. As described above, NeuroD1 can associate with either OGT or OGA depending on glucose concentration [319]. The identification of more OGA-interacting proteins might provide insight into the mechanism of deglycosylation. Using a similar strategy as the OGT experiments, we used a yeast two-hybrid assay obtained from Proquest to identify human OGA binding partners using a cDNA library from human skeletal muscle. Proteins not in frame, proteins identified only once, and proteins known to commonly give false positives were removed from the results. A total of ten proteins were identified by this screen as shown in Table (2.1). Several of these proteins, including Fragile X mental retardation-related protein 1 (FXR1), Interferon-related developmental regulator 1 (IFRD1), and TANK-Binding Kinase 1 (TBK1)-binding protein 1 (TBKBP1), are relevant to eukaryotic gene expression.

The leading cause of inherited mental retardation is Fragile X syndrome, which is caused by the reduction in an RNA binding protein, Fragile X Mental Retardation protein (FMRP) [353]. FMRP binds polyribosomes and suppresses translation [354]. FMRP has two homologs, FXR1 and FXR2, which share about 60% sequence homology to FMRP and have been shown to repress TNF translation [355]. Several other RNA-binding proteins, including Ewing-sarcoma RNA-binding protein, eukaryotic initiation factor 4A1, elongation factor 1, and the small and large ribosomal subunits, have been shown to be O-GlcNAc modified, suggesting a possible functional role for O-GlcNAc in post-transcriptional regulation as well [88, 245, 263].

IFRD1 has been shown to play a role in development by induction of differentiation by repression of a specific set of genes through interactions with the co-repressor complex mSin3B/HDAC1 [356, 357]. IFRD1 is implicated in the prevention of Sp1 binding to a common DNA element in IFRD1 regulated genes. It has also been implicated in recruiting HDAC to β-catenin in order to repress its transcriptional activity on downstream targets, such as osteopontin [358, 359]. Since IFRD1 interacts with already known O-GlcNAc targets, it will be interesting to see if the interaction with OGA is required to modify these targets for their function or for interaction with IFRD1.

TBKBP1 was found to interact with TBK1 and inducible IκB kinase (IKKi), which are members of the IKK family that regulate interferon regulatory factor (IRF) [360]. IRF and NFκB coordinate to regulate innate antiviral immunity [361]. TBK1 and IKKi phosphorylate and activate IRF in response to TLR3 (Toll-like receptor 3) activation. Like NFκB, upon activation, IRF dimerizes and translocates to the nucleus to initiate transcriptional activation. TBKBP1, which is also named Similar to NAP1 TBK1 adaptor (SINTBAD), along with two other cofactors, TANK and NAP1, are needed for full activation of IRF3 in response to the

Sendai virus [360]. These cofactors might serve as a link between downstream signaling from TLR3 and activation of TBK1 and IKKi [360]. Since OGA interacts with TBKBP1 and the O-GlcNAc modification is intricately involved in NFκB signaling that is similar to the IRF pathway, it is plausible that the IRF pathway is also regulated by O-GlcNAc modification. Future work will need to establish the relevance of this hypothesis.

Summary

The O-GlcNAc modification of nuclear and cytoplasmic proteins plays a variety of roles in transcription factor regulation including recruiting chromatin remodeling factors, affecting protein stability, changing nuclear localization, and altering DNA binding and transcriptional activation. O-GlcNAc modification can either exert its effects directly on the modified transcription factor or indirectly by altering protein-protein interactions with other modified co-factors. It is becoming increasingly clear that transcription factors do not function in a solely "on" or "off" state but are subject to a number of modifications, such as O-GlcNAc, that fine-tune their regulation [89]. This is advantageous to the cell because transcription factors must interpret a wide range of signals, including nutrient/metabolic signals, and specifically respond to regulate a subset of target genes.

A key feature of the O-GlcNAc modification is that the levels of its sugar donor, UDP-GlcNAc, are directly responsive to the changes in cellular glucose flux. A nutrient sensing ability is valuable for the cell because it prevents it from being a slave to its extracellular environment [81]. Because altering glucose flux readily modulates global protein O-GlcNAc levels and not just the O-GlcNAc modification on specific proteins, many O-GlcNAc studies to date are correlative. Specific mechanistic and functional studies that show O-GlcNAc modification is indispensable for protein function are beginning to appear in the literature,

primarily in relationship to transcriptional control (illustrated above). Advances in the O-GlcNAc site-mapping technology along with the initial experiments for understanding targeting mechanisms for OGT and OGA substrate recognition and the highlighted recent "smoking gun" experiments should facilitate increased interest in understanding functional mechanisms for O-GlcNAc on a wider range of proteins in an increasing number of systems.

Acknowledgments

Thanks to the members of the Wells group for the critical reading of this manuscript. This work was supported in part by a grant from NIH/NIDDK (1RO1DK075069 to LW). CFT is an American Heart Association predoctoral fellow (Southeast affiliate, 0715377B). LW is a Georgia Cancer Coalition Distinguished Scholar.

Figure 2.1

Modulation of cellular O-GlcNAc levels using HBP flux and specific enzyme inhibitors.

The end product of the HBP, UDP-GlcNAc, is sensitive to changes in nutrient levels. Glucosamine enters the HBP downstream of the rate-limiting enzyme GFAT to elevate UDP-GlcNAc levels. The use of the amidotransferase inhibitors azaserine or DON decreases UDP-GlcNAc levels. Proteins can be reciprocally modified by glycosylation and phosphorylation. However, unlike phosphorylation, which is regulated by hundreds of kinases and phosphatases, O-GlcNAc modification is cycled by the result of gene products from only two genes, *ogt* and *oga*. OGT transfers the GlcNAc onto serine and threonine residues of nuclear and cytosolic proteins and is responsive to changes in UDP-GlcNAc concentrations. Global O-GlcNAc levels can also be raised by the use of OGA inhibitors PUGNAc, NButGT and GlcNAcstatin. Enzymes are depicted in bold and biological pathways are in italics.

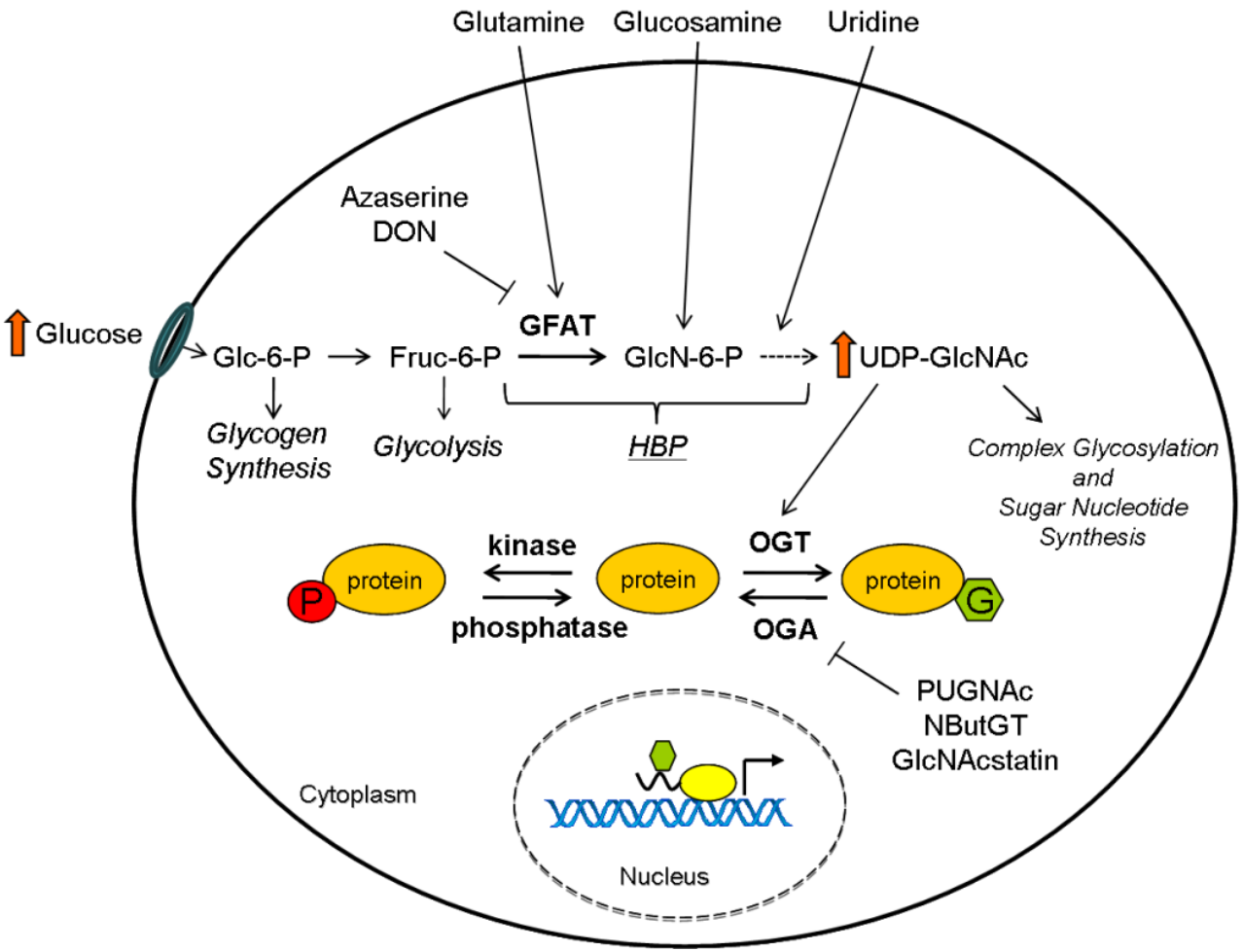
Glutamine
Glucosamine
Uridine
Azaserine
DON
GFAT
Glucose
Glc-6-P
Fruc-6-P
GlcN-6-P
UDP-GlcNAc
Glycogen
Synthesis
Glycolysis
HBP
Complex Glycosylation
and
Sugar Nucleotide
Synthesis
kinase
phosphatase
OGT
OGA
protein
protein
protein
P
G
PUGNAc
NButGT
GlcNAcstatin
Cytoplasm
Nucleus

Figure 2.2

Site-mapping of O-GlcNAc sites is facilitated by electron dissociation techniques.

UL32, a synthetic O-GlcNAc modified protein, is efficiently fragmented and the site of modification (from three possible sites) is easily assigned via electron capture dissociation. When comparing the spectra from unglycosylated (top) and glycosylated peptide (bottom), singly charged fragments retaining the O-GlcNAc modified serine (shown in BLUE) show an increase in mass to charge of 203 daltons, the weight of a single GlcNAc residue.

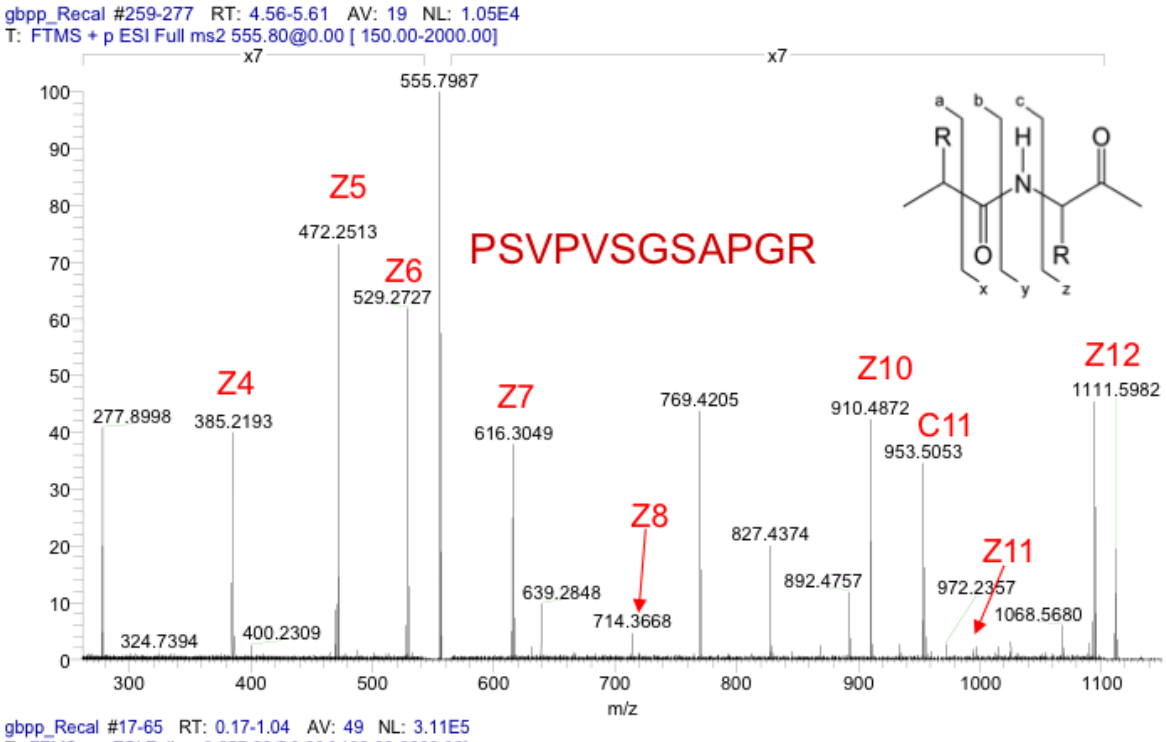
gbpp_Recal #259-277 RT: 4.56-5.61 AV: 19 NL: 1.05E4
T: FTMS + p ESI Full ms2 555.80@0.00 [150.00-2000.00]
x7
x7
555.7987
Z5
472.2513
Z6
529.2727
PSVPVSGSAPGR
Z4
277.8998
385.2193
Z7
616.3049
769.4205
Z10
910.4872
C11
953.5053
Z12
1111.5982
Z8
827.4374
Z11
892.4757
972.2357
639.2848
714.3668
1068.5680
324.7394
400.2309
m/z

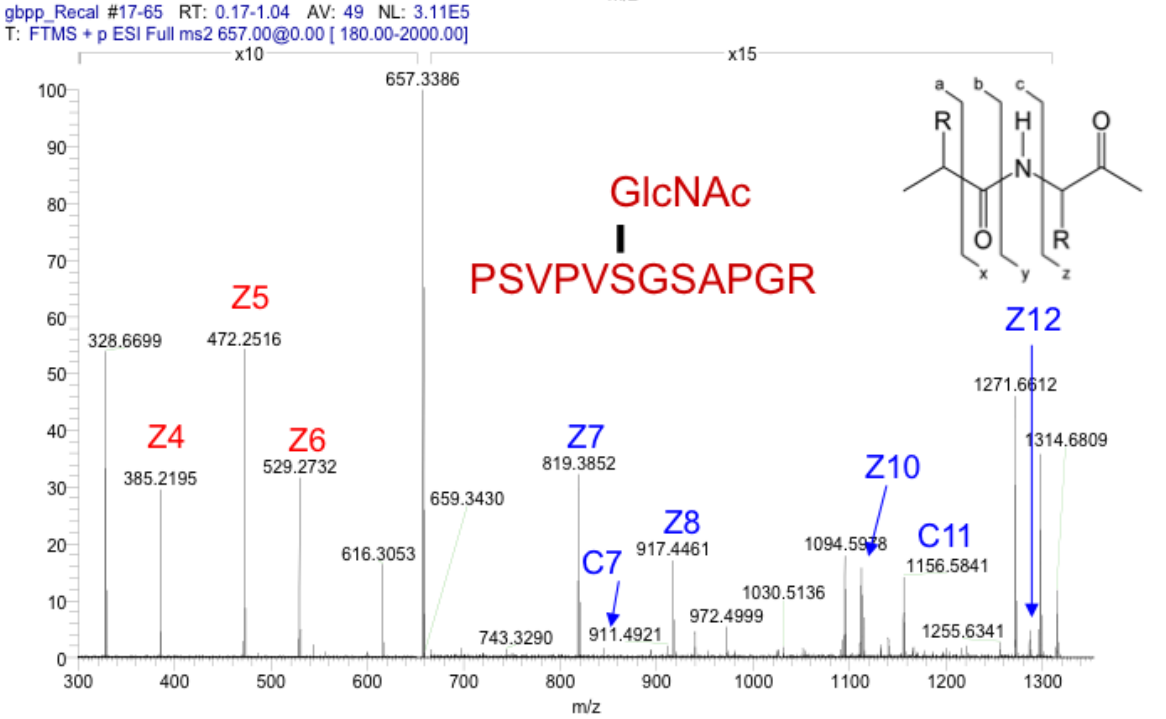
gbpp_Recal #17-65 RT: 0.17-1.04 AV: 49 NL: 3.11E5
T: FTMS + p ESI Full ms2 657.00@0.00 [180.00-2000.00]
x10
x15
657.3386
GlcNAc
PSVPVSGSAPGR
Z5
328.6699
472.2516
Z12
1271.6612
1314.6809
Z4
385.2195
Z6
529.2732
Z7
819.3852
Z10
659.3430
Z8
917.4461
1094.5938
C11
1156.5841
C7
616.3053
1030.5136
972.4999
743.3290
911.4921
1255.6341
m/z

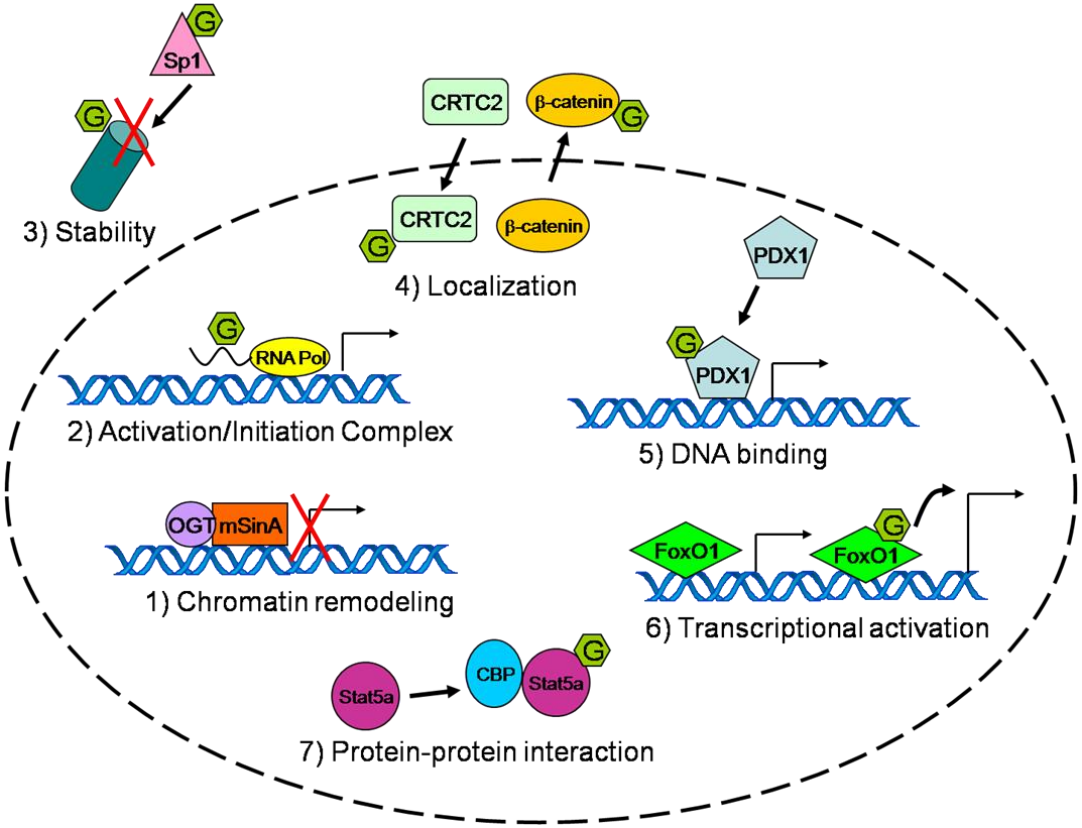

Figure 2.3

Transcriptional regulation by O-GlcNAc can occur via seven different mechanisms.

The O-GlcNAc modification has been demonstrated to regulate transcription by modulating proteins involved in chromatin remodeling and transcriptional initiation, as well as protein-protein associations, localization, stability, DNA binding, and transactivation capacity of individual transcription factors.

Table 2.1 Putative OGA-interacting proteins identified by yeast two-hybrid screen

gene ID	Symbol	Full Name	Description
12654856	IFRD1	Interferon-related developmental regulator 1	Interacts with corepressor complex
7662301	TBKBP1	ProSAPiP2 protein; TBK1-binding protein 1	NFκB Signaling
33504653	FXR1	Fragile X mental retardation-related protein 1	RNA binding protein, RNA transport
6288762	REV1L	Rev1-like protein	Scaffold for translesion synthesis (TLS) of damaged DNA
18426896	GNAS	GNAS complex locus	G-protein signaling
1730283	COPS8	COP9 signalosome subunit 8	Vesicular transport
34190677	KCNS3	Shab-related delayed-rectifier K+ channel alpha subunit 3	Voltage-gated potassium channel
13528788	MYOZ2	myozenin 2; calcineurin-binding protein calsarcin-1	Interacts with calcineurin: a phosphatase (S/T) calcium/calmodulin dependent
50345685	ATP5B	ATP synthase, H+ transporting, mitochondrial F1 complex	Membrane spanning component
33440538	CAPN7	Calpain 7	Calcium-dependent, cysteine protease

CHAPTER 3

GLOBAL O-GLCNAC LEVELS MODULATE ADIPOKINE TRANSCRIPTION DURING CHRONIC INSULIN RESISTANCE[2]

[2] Wollaston-Hayden, E.E.; Harris, R.B.S.; Liu, B.; Xu, Y. and L. Wells.
To be submitted to *Endocrinology*

Abstract:

Increased flux through the hexosamine biosynthetic pathway and the corresponding increase in intracellular glycosylation of proteins via O-linked β-N-acetylglucosamine (O-GlcNAc) is sufficient to induce insulin resistance (IR) in multiple systems. Previously, our group used shotgun proteomics to identify multiple secreted proteins from rodent adipocytes, refered to as adipokines, whose levels are modulated upon the induction of IR by indirectly and directly modulating O-GlcNAc levels. We have validated the relative levels of several of these adipokines using immunoblotting. Since adipokines levels are regulated primarily at the level of transcription and O-GlcNAc alters the function of many transcription factors, we hypothesized that elevated O-GlcNAc levels on key transcription factors are modulating adipokine expression. Here, we show that upon the elevation of O-GlcNAc levels and the induction of IR in mature 3T3-F442a adipocytes, the steady-state transcript levels of multiple adipokines, including LPL, SPARC, Cathepsin B, QuiescinQ6, and SerpinA, reflect the modulation observed at the protein level. We validate the adipokine transcript levels in male mouse models of diabetes. Using inguinal fat pads from the severely IR *db/db* mouse model and the mildly IR diet-induced mouse model, we have confirmed that the adipokines regulated by O-GlcNAc modulation in cell culture are likewise modulated in the whole animal upon a shift to IR. By comparing the promoters of similarly regulated adipokines, we determine that Sp1 is a common *cis*-acting element. Furthermore, we show that the LPL and SPARC promoters are enriched for Sp1 and O-GlcNAc modified proteins during insulin resistance in adipocytes. Thus, the O-GlcNAc modification of proteins bound to promoters, including Sp1, is linked to adipokine transcription during insulin resistance.

Introduction:

It is estimated that diabetes affects 8.3% of the United States population [362]. Type 2 diabetes mellitus (T2DM) is characterized by both hyperinsulemia and hyperglycemia, which result from a combination of whole-body insulin resistance and pancreatic beta-cell dysfunction that eventually leads to insulin insufficiency [1]. T2DM can lead to a wide-range of severe and costly complications such as blindness, kidney failure, stroke, and cardiovascular disease [9]. The abundance of complications associated with T2DM reflects the number of interrelated systems involved in T2DM pathogenesis [10].

White adipose tissue is an important mediator of energy homeostasis. In addition to its role as an energy storage depot, it acts as an endocrine organ by secreting adipokines, such as leptin and adiponectin. Adipokines, the secreted proteins from adipose tissue, can affect diverse processes that may include both local and distant tissue insulin sensitivity and energy homeostasis [19, 39]. Obesity alters the ability of adipose tissue to properly express and secrete adipokines. Obesity, which affects more than 10% of adults world-wide, is the leading environmental risk factor for the development insulin resistance and T2DM [6-8]. Importantly, several adipokines have been implicated in the development of insulin resistance and the pathogenesis of T2DM [363]. The mechanism by which adipocytes respond to insulin resistance and alter the secretion of adipokines is not completely understood.

One way for cells to sense nutrient abundance and thereby alter their metabolism and gene expression is through the hexosamine biosynthetic pathway (HBP). In 1991, Marshall et al. first implicated the HBP in the development of insulin resistance [61]. The HBP has been proposed to be a nutrient flux sensor, since it utilizes 2-5% of intracellular glucose, and acts to limit the amount of glucose uptake by inducing insulin resistance [61]. The end product of the HBP,

uridine 5'-diphospho-N-acetylglucosamine (UDP-GlcNAc), is the sugar donor for the enzyme O-GlcNAc transferase (OGT), which transfers the O-GlcNAc post-translational modification onto serine or threonine residues of nuclear and cytoplasmic proteins [80, 81]. It has been demonstrated by many groups, including our own, that in multiple systems the elevation of O-GlcNAc levels is sufficient to induce insulin resistance [98, 100, 103-105, 120].

The expression of several adipokines has been shown to be regulated at the level of transcription [43, 45-47, 364]. Additionally, the transcription and secretion of several adipokines, including leptin and adiponectin, is modulated by altered HBP flux [47, 58-60]. Transgenic mice overexpressing OGT in peripheral tissues have hyperinsulinemia, glucose disposal defects, and hyperleptinemia, suggesting that the O-GlcNAc modification is intricately tied to the development of insulin resistance and the regulation of adipokines [104].

We have recently used shotgun proteomics to identify multiple murine adipokines whose levels are modulated upon the induction of insulin resistance by indirectly and directly modulating O-GlcNAc levels [131]. In this study, we investigate the transcriptional regulation of several of the adipokines identified by proteomics. We explore whether O-GlcNAc modified transcription factors are regulating these adipokines, since several adipokines are known to be regulated at the level of transcription and O-GlcNAc has been demonstrated to modify and alter the function of many transcription factors [87, 91]. Here we show that these adipokines are co-regulated in a mouse adipocyte cell line and two mouse models of insulin resistance. The promoters of these adipokines contain a common *cis*-acting motif for Sp1. We determine that Sp1 is more heavily O-GlcNAc modified during insulin resistant conditions. Finally, we determine that Sp1 and O-GlcNAc modified proteins are enriched on the LPL and SPARC

promoters. Our findings suggest that the O-GlcNAc modification of proteins regulates adipokine transcription during chronic insulin resistance.

Materials and methods:

Materials and reagents:

Tissue culture media, serum, and antibiotics were purchased from Gibco (Grand Island, NY). 3-isobutyl-1-methyxanthine and dexamethasone were from Sigma (St. Louis, MO). Recombinant insulin, human, was from Roche Diagnostics (Indianapolis, IN). O-(2-acetamido-2-deoxy-D-glucopyranosylidene) amino N-phenyl carbamate (PUGNAc) was from Toronto Research Chemicals Inc. (North York, Ontario). GlcNAcstatin was a kind gift from Dr. Daan van Aalten (University of Dundee, Dundee, Scotland). Anti-Sp1 (PEP 2), anti-LPL (H-53), anti-Angiotensin I/II (N-10), anti-ERK-2 (C-14), normal sera, and agarose conjugated beads were from Santa Cruz Biotechnology (Santa Cruz, CA). Anti-PEBP1 was from Novus Biologicals (Littleton, CO). Anti-SPARC was from Abcam (Cambridge, MA). Anti-O-GlcNAc (RL2) was from Enzo Life Sciences (Farmingdale, NY). Anti-O-GlcNAC (CTD110.6) was previously generated in Dr. Gerald W. Hart's Laboratory (Johns Hopkins University, Baltimore, MD). Dynabead Protein G was from Life Technologies (Carlsbad, CA).

Cell culture and treatments:

3T3-F442a preadipocytes were maintained and differentiated as previously described [131, 365]. On day 6 after the induction of differentiation, the adipocytes were maintained in the appropriate low (1.0g/L; 5.5mM) or high glucose (4.5g/L; 25mM) DMEM media containing 10% FBS, antibiotics, and vitamins with or without 100µM PUGNAc, 20nM GlcNAcstatin, or 100nM insulin. After 24 hours incubation, cells were washed either three times or five times (for media immunoblotting) with low or high glucose serum-free media without antibiotics or vitamins.

Following the rinses, cells were incubated for 16 hrs in the appropriate low or high glucose media without serum, antibiotics, or vitamins and with or without 100μM PUGNAc, 20nM GlcNAcstatin, or 1nM insulin. After the incubation, the conditioned media was carefully collected, filtered, and buffer exchanged as previously described [131]. The cells were washed two times with ice cold PBS and then harvested by scraping and stored at -80°C until further analysis.

Animals:

Animal procedures were approved by the Institutional Animal Care and Use Committee of the University of Georgia. Animals were group housed with a 12-hr light, 12-hr dark cycle. Inguinal fat tissues from 12 week old male C57BL/6J wt (wt), C57BL/6J db^{Lepr}/db^{Lepr} (6J), and C57BL/6J $Lepr^{db3J}$ (3J) mice were used. Mice were fed *ad libitum* normal rodent chow (mouse diet 5015, PM1 Nutrition International, Brentwood, MO). After sacrifice by decapitation, the inguinal fat was weighed, snap frozen and stored at -80°C until transcript analysis. For the diet-induced insulin resistance experiment, young C57BL/6 male mice were purchased from The Jackson Laboratory (Bar Harbor, ME). Both treatment groups were fed *ad libitum* normal rodent chow and water. The mice in the high fat high sucrose (HFHS) treatment group were given free access to a 30% sucrose solution and lard in addition to their normal chow and water. After week 1, 2, and 3 of treatment, an insulin sensitivity test (ITT) was performed on a pair of mice closest to the average weight of each treatment group. The insulin sensitivity test was performed as previously described [366]. Body weights were recorded every week. After 3 weeks of treatment, 6 mice from each treatment group were sacrificed by decapitation. Trunk blood was collected for the measurement of serum insulin using a LINCO rat insulin RIA kit (EMD Millipore Corporation, Billerica, MA). The liver and four fat pads (inguinal, epididymal,

mesenteric, and retroperitoneal) were weighed, snap frozen, and stored at -80°C until transcript analysis.

Cell Lysates, Western blotting and immunoprecipitation:

For immunoprecipitations and anti-O-GlcNAc Western blots, 3T3-F442a cell pellets were lysed in 20mM Tris pH 7.5, 150mM NaCl, 1mM EDTA, 1% NP-40, 1:100 protease inhibitor cocktail set V, EDTA-free (Calbiochem), and 1uM PUGNAc. Protein concentration was determined using the Pierce BCA Protein Assay Kit (Thermo Scientific, Rockford, IL). The CTD110.6 Western blots were performed essentially as described [367]. Immunoprecipitations were carried out at 4°C overnight using anti-Sp1 or normal rabbit IgG with 750ug of precleared protein lysate. Immunocomplexes were collected using Protein A/G-PLUS agarose beads for 2 hours. Beads were washed 4 times with a modified RIPA buffer (20mM Tris pH 7.5, 150mM NaCl, 1mM EDTA, 1% NP-40, 0.1% SDS) and one time with a high salt modified RIPA buffer (same as above except 500mM NaCl). Proteins were eluted by boiling beads in 1x laemli buffer and then transferred to a fresh tube for Western blotting. For the concentrated media western blots, the protein concentration of the concentrated 3T3-F442a media was determined using the Bradford method and verified by Coomassie staining. Equal amounts of protein were separated by SDS-PAGE with Tris-HCl precast minigels (Bio-Rad, Hercules, CA) and transferred to poly(vinylidene difluoride) (PVDF) membranes (for concentrated media) or nitrocellulose membranes (for immunoprecipitations) for Western blot analysis. After blocking for at least 1 hour, membranes were incubated with the appropriate primary antibody overnight at 4°C. Membranes were incubated with the appropriate horseradish peroxidase-coupled secondary antibodies for 1 hour, followed by extensive washing and Pierce ECL detection. ImageJ was used for densitometry [368].

Chromatin immunoprecipitation:

Chromatin Immunoprecipitations were performed as described in the Millipore EZ-ChIP kit with some modifications. Day 8 adipocytes were washed once with room temperature PBS and then crosslinked by adding 1% formaldehyde in PBS and incubating for 10 minutes. The adipocytes were washed 3 times with cold PBS and then harvested by scraping. The adipocytes were resuspended in hypotonic lysis buffer (20mM Tris-HCl, pH 7.5, 10mM NaCl, 3mM $MgCl_2$, 1:100 Calbiochem protease inhibitor) and incubated on ice then dounce homogenized. The nuclei were collected by centrifugation and then resuspended in SDS lysis buffer. DNA was sheared to between 200 and 1000 base pair fragments using a Misonix S-4000 sonicator. Protein concentration was quantified using the Pierce BCA Protein Assay Kit. 100ug of chromatin was used per immunoprecipitation. Sonicated chromatin was diluted 1:10 with dilution buffer and precleared using Protein A/G-PLUS agarose, normal goat IgG, and sheared salmon sperm DNA (ssDNA) (Ambion). 3% of the sample was saved as Input. 1ug of anti-Sp1, anti-O-GlcNAc (RL2), or normal IgG was used for the immunoprecipitation. Immunocomplexes were collected for one hour using Protein G Dynabeads that were blocked with ssDNA and BSA (New England Biolabs). The Dynabeads were washed five times and then eluted with 1% SDS and 0.1M $NaHCO_3$. The elutions were decrosslinked at 65°C overnight with NaCl and RNase A (Ambion). After Proteinase K treatment (New England Biolabs), samples were purified by a Phenol-Chloroform extraction followed by ethanol precipitation overnight at -20°C using glycogen as a carrier. Precipitated DNA was resuspended in 3mM Tris-HCl pH 8.0, 0.1mM EDTA. qPCR was performed using primers for the proximal mouse SPARC and LPL promoter Sp1 binding sites. Sequences of primers were SPARC primers 5′-AGGCAAGTTCACTCGCTGGCT-3′ (forward) and 5′-AGACACCCTGGCCCCACCTG-3′

(reverse) and LPL primers 5′-CCTTCTTCTCGCTGGCACCGTT -3′ (forward) and 5′-GGGCAGAACAGTTACAAGGGGCA -3′ (reverse). The fold enrichment was calculated for each primer/antibody/treatment combination. First the normalized ChIP C_t values were calculated: $\Delta Ct_{\text{[normalized ChIP]}} = (C_{t\text{ [ChIP]}} - (C_{t\text{ [Input]}} - \text{Log}_2\text{ (Input Dilution Factor)}))$. The % Input was calculated: % Input = $2^{(-\Delta Ct\text{ [normalized ChIP]})}$. Lastly, fold enrichment was calculated: Fold Enrichment = (% Input of antibody / % Input of IgG).

Gene expression analysis:

RNA was isolated from 3T3-F442a cell pellets and inguinal fat pads using the Invitrogen PureLink Micro-to-Midi RNA Total RNA Purification System with Trizol reagent and on column DNase I treatment. The Invitrogen Superscript III First-Strand Synthesis System for RT-PCR was used to synthesize cDNA (Life Technologies, Carlsbad, CA). All RT-qPCR primers were obtained from Qiagen QuantiTect Primer Assays and used with Qiagen QuantiTect SYBR Green PCR Kits (Qiagen, Valencia, CA). ChIP-qPCR primers were used with iQ SYBR Green Supermix (Bio-Rad, Hercules, CA). Amplifications were performed in a Bio-Rad 96-well iCycler or myIQ real time detection system using the appropriate QuantiTect or iQ SYBR Green cycling protocol. Changes in target gene expression were normalized to TATA box binding protein (Tbp) and ribosomal protein L4 expression (Rpl4). Relative transcript levels were calculated using the ΔΔCt method [369]. Normoglycemic transcript levels were set to 100.

Motif analysis:

Promoter sequences containing 500 bp upstream of the transcriptional start site were collected for human, mouse, and rat using the UCSC Genome Browser [370]. No rat ortholog was found for Quiescin Q6. The human set was used as the main set and was supported by the mouse and rat ortholog sets. Three genes that were identified in the rodent adipocyte secretome but did not

change in expression during insulin resistance were used as the negative set for human, mouse, and rat [131]. Seven motif finding tools were used for primary motif finding : AlignACE [371], Bioprospecter [372], CONSENSUS[373], CUBIC [374], MDscan [375], MEME [376], and BOBRO [377]. For each candidate, a position weight matrix and scoring matrix were generated (Supplementary Table S3.1). Corresponding transcription factor binding motifs were determined by analyzing the position weight matrix with TOMTOM [378]. Conserved transcription factor binding motifs were confirmed using human and mouse sequences in rVISTA 2.0 [379].

Statistical analysis:

Statistics were performed using General Linear Models procedure of Statistix (Statistix 9, 2010, Tallahassee, FL). Error bars represent the SEM of independent experiments. *P* values under 0.05 were considered significant and represented using an * in all figures. The experiments shown are representative of two to five experiments with similar results.

Results:

The induction of insulin resistance in 3T3-F442a adipocytes modulates adipokine steady-state protein levels and transcript levels in the same manner.

3T3-F442a preadipocytes were differentiated into mature adipocytes before experimental treatments. Mature adipocytes were either maintained in insulin sensitive conditions (low glucose, LG) or shifted to insulin resistant conditions by the classical treatment of high glucose and chronic insulin (HG + INS) to generate hyperglycemia and hyperinsulemia or by treatment with low glucose and the OGA inhibitors PUGNAc (LG + PUGNAc) or GlcNAcstatin (LG + GlcNAcstatin) to more specifically elevate global O-GlcNAc levels. Figure 3.1A shows that all insulin resistant conditions generated elevated global O-GlcNAc levels as evaluated by immunoblotting with an O-GlcNAc specific antibody. Previously, our group used shotgun

proteomics to characterize the secreted proteome of rodent adipocytes and to identify multiple adipokines whose levels are modulated upon the induction of insulin resistance by indirectly and directly modulating O-GlcNAc levels in rodent adipocytes as described above [131]. Figure 3.1B shows a shortened list of adipokines whose protein expression was found to be positively regulated by the induction of insulin resistance using quantitative proteomics. We validated the relative levels of angiotensinogen, PEBP1, LPL, and SPARC using immunoblotting as an orthogonal method. 3T3-F442a adipocyte conditioned media from each treatment group was concentrated and buffer exchanged before immunoblotting with selected antibodies. Figure 3.1C shows that the regulation observed by quantitative proteomics is recapitulated by immunoblotting as an independent method. Since adipocyte insulin resistance was induced by either indirectly (HG + INS) or directly (LG + PUGNAc) altering O-GlcNAc levels, it is likely that O-GlcNAc is modulating the secretion of these adipokines. Since the secretion of many of the adipokines, including leptin and adiponectin, is regulated at the level of transcription [43, 45-47, 364] and O-GlcNAc has been shown to modify and alter the function of many transcription factors [130], we hypothesized that the elevation of O-GlcNAc levels was regulating many of the identified adipokines at the level of transcription. Figure 3.1D shows that upon the elevation of O-GlcNAc levels and the induction of insulin resistance in 3T3-F442a adipocytes, the steady-state transcript levels of the tested adipokines, as measured by qPCR, reflect the modulation observed at the protein level.

The induction of insulin resistance modulates adipokine steady-state transcript levels in a genetic insulin resistant mouse model.

The mouse preadipocyte cell lines are a very useful system for studying adipocyte biology; however, their ability to secrete proteins at the high levels measured *in vivo* is impaired

in many cases [228]. Additionally, the complex paracrine interactions between adipocytes and the stromal-vascular cell fraction that comprises adipose tissue as well as the signaling between tissues in a whole animal are lost in adipocyte cell line culture [229]. Therefore, the regulation of adipokine transcript levels upon the induction of insulin resistance was examined in a biologically relevant mouse model. The inguinal fat pads from severely insulin resistant 12 week-old male leptin receptor mutant (*db/db*) mice were used for transcript analysis. *db/db* mice produce leptin but fail to respond to it. The C57BL/6J db^{Lepr}/db^{Lepr} (6J) mice produce only the short-form leptin receptors (Ob-Ra, Ob-Rc, Ob-Rd) and the circulating form leptin receptor (Ob-Re) but not the long signaling form of the receptor (Ob-Rb). The C57BL/6J $Lepr^{db3J}$ (3J) mice produce only the circulating form leptin receptor (Ob-Re) [380]. Figure 3.2 shows the inguinal fat pad adipokine transcript levels in the *db/db* mouse models vary significantly from the *wt* mice and reflect the modulation shown at the transcript and protein levels in the 3T3-F442a adipocytes. All of the transcripts were elevated with the exception of the control gene, adipsin. Adipsin transcript levels have been shown to be downregulated in many models of rodent obesity [381].

The induction of insulin resistance modulates adipokine steady-state transcript levels in a diet-induced IR mouse model.

Evidence suggests that T2DM develops from a combination of genetic and environmental factors, but the relative contribution of each is unclear [2]. A monogenic genetic mouse model (*db/db*) does not represent the true genetic heterogeneity that is present in most cases of human T2DM [382]. In addition, the genetic defect is in an adipokine pathway, which could lead to potentially confounding effects for this experiment [383]. To address these concerns, a diet-induced insulin resistant mouse model was developed by feeding *ad libitum* sucrose solution and

lard (HFHS) to young C57BL/6 mice as described in *Materials and Methods*. After three weeks of treatment, the live weight of the mice as well as the wet weight of the inguinal, epididymal, mesenteric, and retroperitoneal fat pads was significantly increased in the HFHS mice compared to the mice on the normal chow diet (*Supplementary Figure 3.1A*). The mice on the HFHS diet had elevated glucose levels and an attenuated response to insulin (*Supplementary Figure 3.1B*). In addition the mice displayed significantly elevated insulin levels (*Supplementary Figure 3.1C*). After three weeks on the HFHS diet, these data suggest that the mice display mild insulin resistance, indicated by hyperglycemia and hyperinsulinemia, and mild obesity, so the inguinal fat pads were used for transcript analysis. Since the diet-induced insulin resistant mice were mildly obese and insulin resistant, we would expect the adipsin levels to only change slightly in contrast to the *db/db* mice, which were extremely obese. Figure 3.3 shows the transcript levels were significantly elevated in the HFHS mice inguinal fat pads for all genes excluding adipsin. The diet-induced insulin resistant mice transcript levels reflect the modulation shown at the transcript level in the *db/db* mouse fat pads and at the transcript and protein levels in the 3T3-F442a adipocytes.

Adipokine transcript levels correlate with mouse model obesity severity

Furthermore, the transcript levels were more severely modulated in the severely insulin resistant *db/db* mouse model than the mildly obese diet-induced mouse model suggesting that the adipokine transcript levels are proportional to the degree of obesity and insulin resistance. Table 3.1 shows the relative increase in transcript levels in the insulin resistant mice (HFHS and 6J) compared to the transcript levels of the insulin sensitive mice (N and wt), which are set to 100%. Given that transcript level regulation is consistent for both obese and insulin resistant mouse models, the transcript regulation observed in cell culture during insulin resistance is validated.

Sp1 is a common cis-acting element for the adipokine promoters and the O-GlcNAc modification of Sp1 is altered during insulin resistance.

We hypothesized that a common transcription factor or cofactor was responding to the elevation of O-GlcNAc levels and altering the transcription of the adipokines. Multiple complementary motif finding programs were used to analyze the same set of orthologous proximal adipokine promoters in order to find a more accurate set of regulatory motifs. Human, mouse, and rat promoters were used to identify conserved motifs, with the hope that the most important regulatory motifs would be under stronger evolutionary pressure (Figure 3.4A) [384]. Twenty-four common putative regulatory motifs were identified using motif analysis programs as described in *Materials and Methods* (Supplementary Table S3.1). The putative regulatory motifs were compared to known transcription factor binding motifs. The Sp1 binding motif was found to match putative regulatory motif 3 (Figure 3.4B). The conservation of the Sp1 sites between human and mouse promoters was verified using rVista 2.0. Sp1 is relevant to adipokine transcription since it is a target of the insulin signaling cascade and many promoters of genes regulated by insulin have Sp1 motifs [48, 57, 385-388]. In addition, Sp1 is known to be dynamically modified by O-GlcNAc [130]. Sp1 O-glycosylation is reported to be elevated in the liver, kidney, and adipose tissue of *db/db* mice [389]. Many studies have associated the altered O-GlcNAc modification of Sp1 with altered transcriptional activation of target genes [127, 338, 390-393]. Figure 3.4C shows that immunoprecipitated Sp1 has greater O-GlcNAc modification during insulin resistance in 3T3-F442a adipocytes. Both direct (LG + GlcNAcstatin) and indirect (HG + INS) modulation of O-GlcNAc levels resulted in elevated Sp1 O-GlcNAc modification. The more modest O-GlcNAc modification seen in the HG + INS condition was most likely due to the more modest increase in global O-GlcNAc levels (Figure 3.1A).

Sp1 and O-GlcNAc modified proteins are enriched on the proximal SPARC and LPL promoters during insulin resistance.

We noticed that two of the identified motif 3 positions on the promoters corresponded with known biologically relevant Sp1 binding sites for LPL and SPARC. Since these sites are reported to be important for transcriptional activation, we wanted to determine whether Sp1 and O-GlcNAc modified proteins were enriched at these sites during insulin resistance in 3T3-F442a adipocytes. ChIP was performed with Sp1 and O-GlcNAc specific antibodies. Enrichment on the promoters was determined by analyzing purified DNA using qPCR with primers designed to amplify the region containing the Sp1 binding motif on either the LPL or SPARC promoter. Figure 3.5 shows both of the promoter regions showed significant enrichment of both Sp1 and O-GlcNAc modified proteins during insulin resistant conditions. These results suggest that the elevation of global O-GlcNAc levels, either directly or indirectly, leads to increased O-GlcNAc modification of Sp1 and increased Sp1 enrichment on the SPARC and LPL proximal promoters. Since the O-GlcNAc antibody will bind any protein modified with O-GlcNAc, the enrichment of O-GlcNAc on the LPL and SPARC promoters could be due to O-GlcNAc modified Sp1 or potentially other O-GlcNAc modified proteins.

Discussion

White adipose tissue plays an important role in maintaining energy homeostatis by mediating lipid flux and altering the secretion of adipokines. Adipokines can act in an autocrine, paracrine, or endocrine manner to regulate a variety of processes, including energy homeostasis [19]. Genetic mouse models showing that the induction of insulin resistance in white adipose tissue induces whole body insulin resistance have highlighted the importance of adipokines during insulin resistance [16-18]. In addition, adipokines are implicated in many of the

complications leading to and resulting from T2DM, especially the tissue remodeling during nephropathy, cardiovascular disease, and obesity [394].

Many of the adipokines we studied are extracellular matrix (ECM) modulators and associated with inflammatory states. SPARC is a modulator of cell – ECM interactions and has diverse roles in osteogenesis, angiogenesis, fibrosis, tumorigenesis, and adipogenesis [132]. Cathepsin B is associated with ECM degradation, apoptosis, and inflammation [190]. SerpinA is an acute phase response protein that is involved in inflammation [218]. Quiescin Q6 is upregulated in pancreatic cancer and may promote tumor cell invasion by upregulating matrix metalloproteinases [215, 216]. Involvement in tumorigenesis is another common theme for these adipokines. During obesity, extensive remodeling is required for the expansion of fat pads [24]. These ECM modulators may play an important role in local tissue remodeling. Obese adipose tissue is associated with an inflammatory response, which may also be mediated in part by these adipokines [20-25].

In this study, we have attempted to better define the relationship between O-GlcNAc modification and adipokine transcription during insulin resistance. Several studies have suggested that leptin and adiponectin are regulated primarily at the level of transcription in adipocytes [43, 45-47, 395]. We investigated whether the adipokines we identified by quantitative proteomics were similarly regulated after confirming the elevation via an orthogonal method, Western blotting, for several of these secreted proteins. We found that the induction of insulin resistance in mouse adipocytes elevated transcript levels in the same manner as protein levels for several of the adipokines identified by proteomics (*Figure 3.1*). Although a role for the transcriptional regulation of adipokine secretion has been established for SPARC [151], there are conflicting reports for LPL [167, 169, 177, 189], and it was not known whether Cathepsin B,

Quiescin Q6, and SerpinA were transcriptionally regulated in adipocytes. In addition, the *in vivo* relevance of the transcriptional upregulation of the adipokines during insulin resistance was verified using both a genetic and diet-induced mouse model of obesity and insulin resistance (*Figures 3.2 and 3.3*).

Several studies have suggested that adipokine expression is regulated by the HBP and O-GlcNAc. Infusions of metabolites that increased HBP flux into rats increased leptin expression [47, 396]. Both GFAT and OGT transgenic mice displayed hyperleptinemia [58, 59, 104]. GFAT transgenic mice also displayed decreased adiponectin levels [58]. In primary human adipocytes and 3T3-L1 mouse adipocytes, HBP flux was shown to correlate with leptin expression [60, 397]. Although many studies have manipulated the HBP, studies that manipulate O-GlcNAc levels more directly and examine adipokine expression have been lacking. We found that both the direct modulation of O-GlcNAc levels by the addition of OGA inhibitors and the indirect modulation of O-GlcNAc levels by hyperglycemia and chronic hyperinsulinemia in mouse adipocytes elevated adipokine transcript levels in the same manner as protein levels (*Figure 3.1*). It was not known whether inducing insulin resistance solely by raising global O-GlcNAc levels would regulate these adipokines at the level of transcription.

It is reasonable to assume that co-regulated genes have a similar upstream regulator. Since we found that the expression of these adipocytokes was similarly regulated by both classical insulin resistance and by solely raising global O-GlcNAc levels, we hypothesized that O-GlcNAc was a regulator. O-GlcNAc has been proposed to be a "nutrient sensor" because the levels of the end product of the HBP, UDP-GlcNAc, are regulated by the flux of glucose, uridine, glutamine, and FFA's [62, 63]. OGT is responsive to physiological levels of UDP-GlcNAc, so increased HBP flux results in globally elevated levels of O-GlcNAc modification

[82]. The regulation of OGT is complex and still being elucidated, but it is clear that it has a preference for certain proteins and sites and does not universally add O-GlcNAc to all proteins [83, 84, 348]. A large body of literature has shown that the O-GlcNAc modification plays an important role in transcriptional regulation. O-GlcNAc modifies transcription factors and cofactors, RNA Pol II, chromatin remodelers, and has even been identified as part of the histone code. O-GlcNAc modification of proteins can affect protein stability, protein-protein interactions, chromatin remodeling, transcriptional initiation and elongation, DNA binding, and localization [112, 130]

The adipokines were regulated at the level of transcription, so we looked for common transcription factor binding motifs. After determining that Sp1 was a common *cis*-acting motif for the adipokines, we found that the O-GlcNAc modification of Sp1 increased during insulin resistance in mouse adipocytes (*Figure 3.4*). Sp1 has been implicated in the transcriptional regulation of LPL, SPARC, Cathepsin B, and SerpinA.

A role for Sp1 as a regulator of SPARC transcription has been established in transformed cells. The proximal promoter of SPARC contains several modified GC-boxes that are binding sites for Sp1 and/or Sp3. Sp1 and/or Sp3 are required for SPARC transcriptional activation in chickens, mice, and humans [154, 155, 157]. In chick embryonic fibroblasts, v-Jun represses SPARC promoter activation and initiates cell transformation by targeting the minimal promoter region. It was shown that v-Jun does not bind this DNA region directly but binds Sp1 and/or Sp3 to target promoter activation [157]. c-Jun activates SPARC transcription in human MCF7 cells through the activation of Sp1 [154]. In mammary carcinoma, Brg-1, a SWI/SNF chromatin remodeling complex ATPase, was shown to interact with Sp1 to activate SPARC transcription

[155]. Sp1's involvement in SPARC transcription in adipocytes has not previously been described.

Several studies have associated Sp1 and/or Sp3 with LPL transcriptional regulation. Interferon-γ (IFNγ) decreases macrophage LPL transcription by decreasing Sp3 protein levels and Sp1 DNA binding to sites in the 5' UTR, which is mediate by casein kinase 2 (CK2) and Akt [179, 180]. Transforming growth factor-β (TGF-β) represses macrophage LPL transcription through Sp1 and/or Sp3 sites in the 5'-UTR [181]. Sp1 and/or Sp3 also bind an evolutionarily conserved CT element (-91 to -83), also known as a GA box, in the proximal promoter. Sterols regulate LPL through a SRE site that is close to the CT element [166, 189]. A T(-93)G SNP that is close to the CT element has been associated with a predisposition to obesity and familial combined hyperlipidemia in some studies in humans. The minor allelic frequency is highly variable for difference ethnic populations and the SNP effect may be influenced by the synergistic effects of a Asp9Asn and T(-93)G haplotype that is present in some populations [175, 182-184]. People with both the Asp9Asn and T(-93)G mutations have been shown to have an increased risk of cardiac disease and decreased LPL activity in some studies [176, 185, 186]. In the South African black population, the SNP was associated with mildly lower triglyceride levels and was associated with higher promoter activation in smooth muscle cells [184, 187]. This is in contrast to other studies which show that the mutation decreases Sp1 and/or Sp3 DNA binding leading to lowered transcriptional activation [166, 175, 182, 183]. Sterol regulatory element-binding protein (SREBP) was found to act synergistically with Sp1 to activate the promoter in macrophages. Mutation of the CT element is also reported to decrease promoter reporter activity in 3T3-F442a pre-adipocytes [188]. The importance of these Sp1/Sp3 binding sites has not been previously explored in mature adipocytes.

Both Sp1 and O-GlcNAc modified proteins were found to be significantly enriched in the region of the conserved Sp1 site on both the LPL and SPARC promoters (*Figure 3.5*). In our experiments in mature mouse adipocytes, Sp1 is most likely facilitating transcriptional activation. The studies described above have begun to shed light on the role of O-GlcNAc in modulating adipokine transcription through the modification of Sp1; however, it is unclear why O-GlcNAc enrichment of the promoters in increased more in the HG+INS condition than the LG+GlcNAcstatin condition since global O-GlcNAc levels as measured in whole-cell extracts are much higher in the latter. Perhaps the level of O-GlcNAc modification is higher in the nucleas for the HG+INS condition than for the LG+GlcNAcstatin condition. Another possibility is that insulin stimulates the activation or stability of a cofactor that enhances O-GlcNAc modification of chromatin or chromatin-associated proteins.

Although Sp1 in ubiquitously expressed and often thought of as a housekeeping transcription factor, the diversity of Sp1 post-translational modifications and the wide-range of interaction partners can fine tune Sp1 activity in a context specific manner [398]. Sp1 is subject to many forms of post-translational modification including phosphorylation, acetylation, sumoylation, ubiquitylation, and glycosylation. The sites of phosphorylation on Sp1 can either increase or decrease Sp1 DNA binding and transcriptional activation [399]. Glycosylation can affect Sp1 stability, protein-protein interactions, DNA binding, degree of phosphorylation, and localization [130]. Sp1 has at least eight sites of O-GlcNAc modification, but the specific roles of each site is still being elucidated [129]. Five sites of modification have been mapped to the DNA binding domain, and the mutation of these sites can disrupt Sp1 transcriptional activation in hepatocytes [389, 391]. O-GlcNAc modification of the Sp1 activation domain inhibits Sp1 transactivation [338, 339]. Since O-GlcNAc acts as a nutrient-flux sensor, many studies

manipulate the glycosylation of Sp1 by manipulating nutrient flux. Studies using glycosylation site-specific Sp1 mutants would help to clarify the specific role of O-GlcNAc modification; however, determining the action of a specific glycosylation site could be complicated by the complex interplay between phosphorylation and O-GlcNAc modification as well as the presence of several other O-GlcNAc sites. In addition, site-specific Sp1 studies in adipocytes would be challenging since adipocytes are notoriously difficult to transfect. Other O-GlcNAc modified proteins could also be modulating the adipokine transcription since the O-GlcNAc enrichment on the promoters could be due to proteins other than Sp1. ChIP-reChIP would help to determine which proteins are in complex on the promoters.

In conclusion, these experiments serve to identify a possible mechanism by which adipocytes respond to insulin resistance and regulate the expression of adipokines. Future work is aimed at identifying the specific function of the O-GlcNAc modification on Sp1 during insulin resistance in adipocytes. In addition, the mechanism of adipokine transcriptional upregulation in animal models should be investigated. Understanding the transcriptional regulation of adipokines by O-GlcNAc may provide therapeutic targets for normalizing the expression of adipokines during obesity and T2DM.

Acknowledgements

We thank members of the Wells' lab for their helpful discussions and review of this manuscript. We thank Dr. Paul M. Cline for his assistance with statistical analysis. We thank Dr, Daan van Aalten for supplying us with GlcNAcstatin. This work is supported by an American Heart Association National Scientific Development Grant (L.W.) and the NIDDK/NIH (R01, LW).

Figure 3.1: Insulin resistant 3T3-F442a adipocytes display altered adipokine expression. A, 3T3-F442a adipocytes were grown under insulin responsive (LG) or insulin resistant (LG with PUGNAc, LG with GlcNAcstatin, or HG with insulin) conditions as described in *Materials and Methods*. Equal amounts of protein from whole cell lysates were separated by SDS-PAGE and Western blotting was performed using anti-O-GlcNAc (CTD110.6). Equal loading was confirmed by Western blotting with ERK2. B) A partial list of rodent adipokines found to be regulated by insulin resistance based on proteomic quantification. + indicates that the protein expression is upregulated upon the induction of insulin resistance. C) Proteomic quantification of protein expression was confirmed by Western blotting in 3T3-F442a adipocytes. Equal amounts of concentrated media were separated by SDS-PAGE and Western blotting was performed with the designated antibodies. D) The steady-state transcript levels were evaluated using qPCR in 3T3-F442a adipocytes. Data are presented so that 100% represents the transcript level in the insulin responsive condition (LG). *, $P < 0.05$.

A

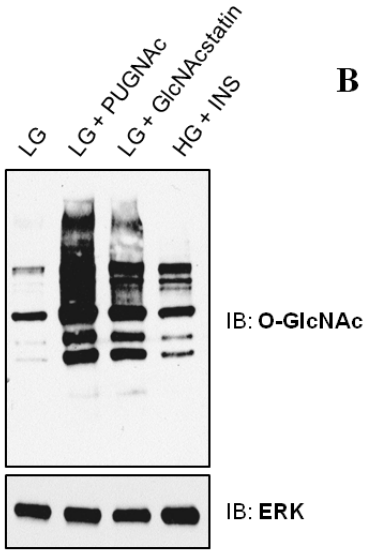

B

Identified Protein	Regulation
Angiotensinogen	+
HCNP (PEBP1)	+
LPL	+
SPARC	+
Cathepsin B	+
Serine protease inhibitor 2c (SerpinA)	+
Quiescin Q6	+

C

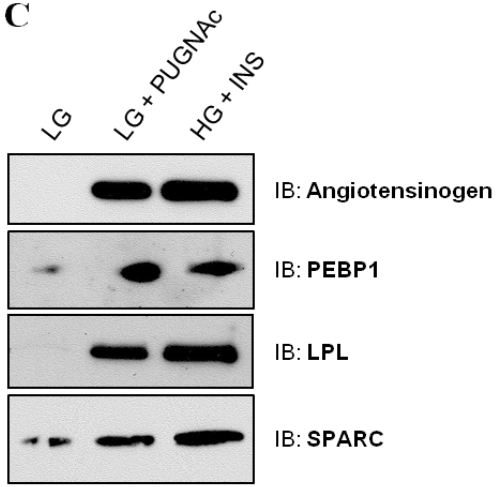

D

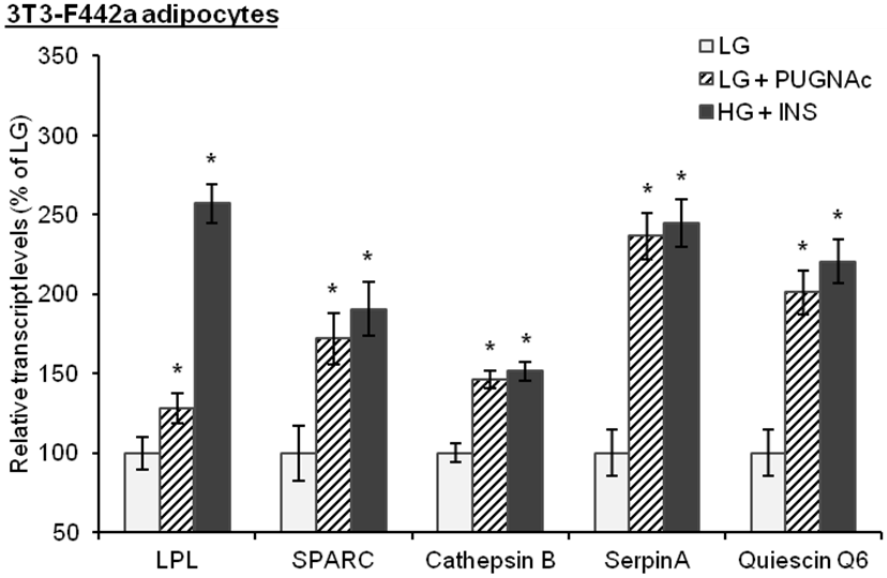

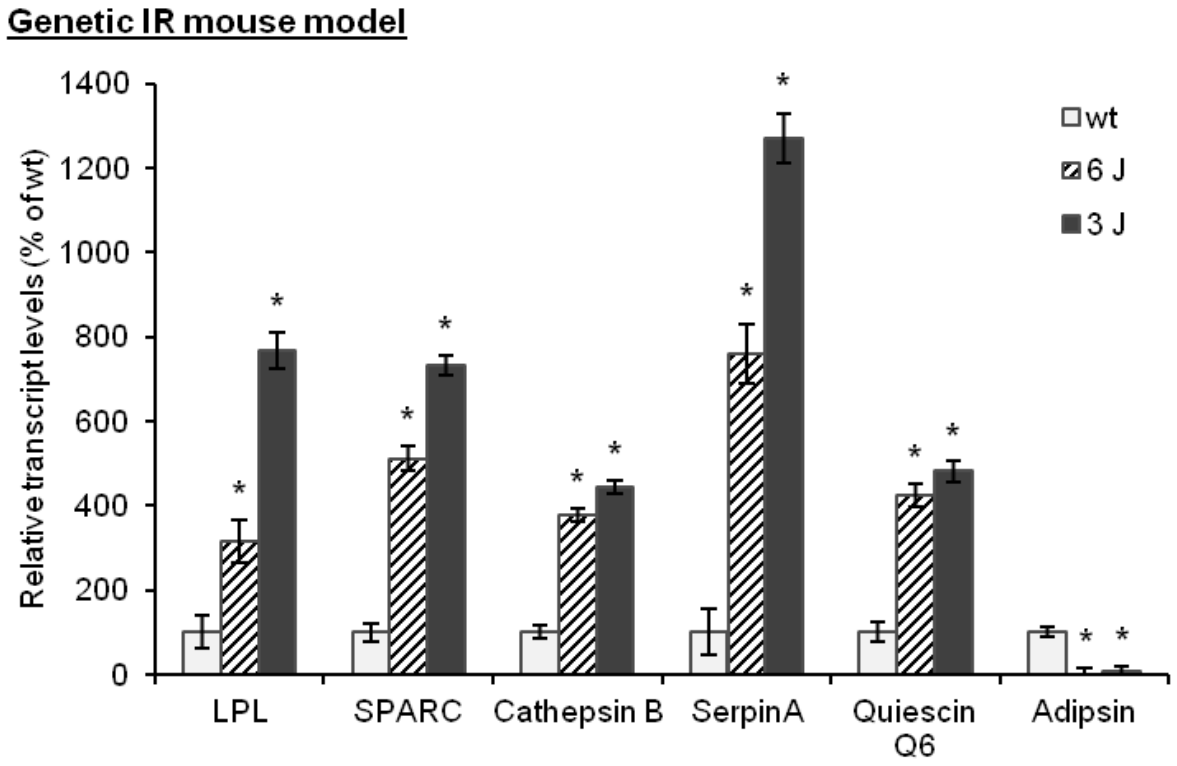

Figure 3.2: Genetic insulin resistant mice display altered adipokine steady-state transcript levels. Inguinal fat pads from 12-week old male *wt*, *6J*, and *3J* (n=6) mice were used for transcript analysis by qPCR. Data are presented so that 100% represents the transcript level in the insulin responsive condition (*wt*). *, $P < 0.03$.

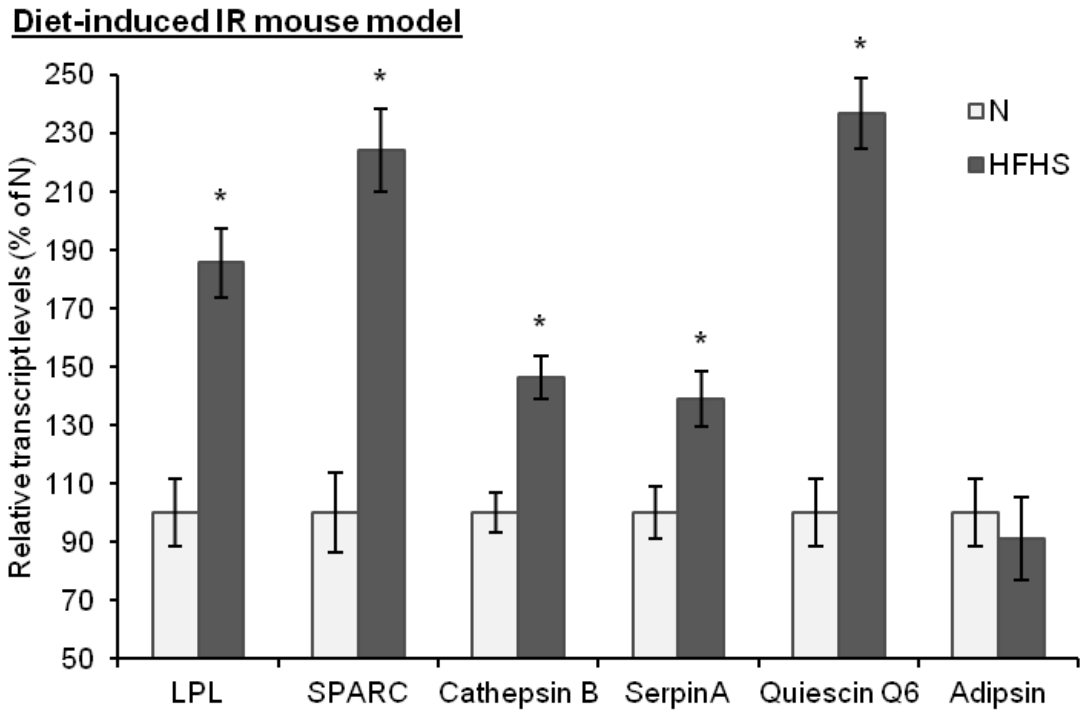

Figure 3.3. Diet-induced insulin resistant mice display altered adipokine steady-state transcript levels. Inguinal fat pads from C57BL/6 mice fed normal chow (N) (n=4) or a high fat, high sucrose (HFHS) (n=3) diet for three weeks were used for transcript analysis by qPCR. Data are presented so that 100% represents the transcript level in the insulin responsive condition (N). *, $P < 0.05$.

Table 3.1: Adipokine transcript levels are proportional to obesity severity

Mouse Model	LPL	SPARC	Cathepsin B	SerpinA	Quiescin Q6
Insulin sensitive	100	100	100	100	100
Diet- induced	224	185	146	139	237
Genetic	511	316	379	760	425

Figure 3.4. An O-GlcNAc modified protein is identified as a common regulatory element. A) The promoters of target co-regulated genes for human, mouse, and rat were analyzed for common regulatory motifs as described in *Materials and Methods*. Three genes that were not co-regulated were used as a negative set to avoid identifying non-regulatory motifs. *, denotes no orthologous gene in rat. B) TOMTOM was used to assign identified regulatory motifs to known transcription factor binding motifs. Regulatory motif 3 matches the Sp1 DNA binding motif with a p – value of 1.3×10^{-6}. C) Whole cell lysates from insulin responsive and insulin resistant 3T3-F442a adipocytes were subjected to immunoprecipitation with anti-Sp1 or normal rabbit IgG followed by immunoblotting with anti-Sp1 or anti-O-GlcNAc (RL2). A representative immunoblot is shown. (*right panel*) The ratio of O-GlcNAc modified Sp1 to total Sp1 was quantified using densitometry of independent experiments.

A

Species:	human	mouse	rat
Target genes	LPL	LPL	LPL
	Serpina3	Serpina3n	Spin2c
	CtsB	Ctsb	Ctsb
	Qscn6	Qscn6	*
	SPARC	SPARC	SPARC
Negative set	LUM	LUM	LUM
	MFAP4	MFAP4	*
	DCN	DCN	DCN

B

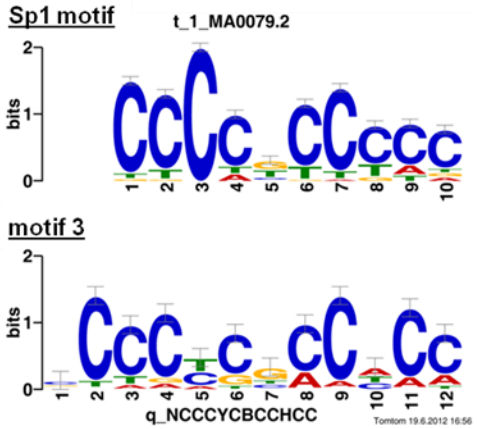

C

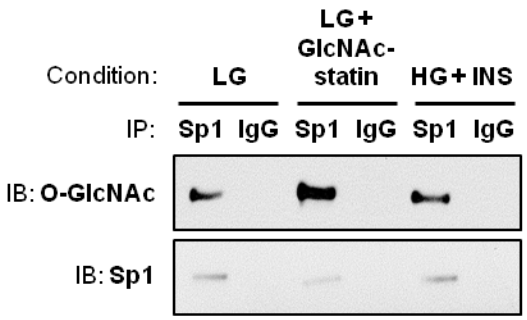

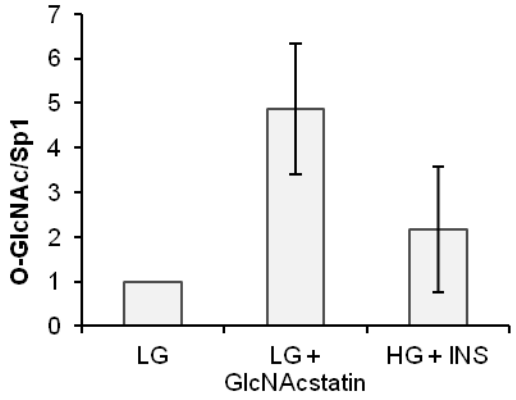

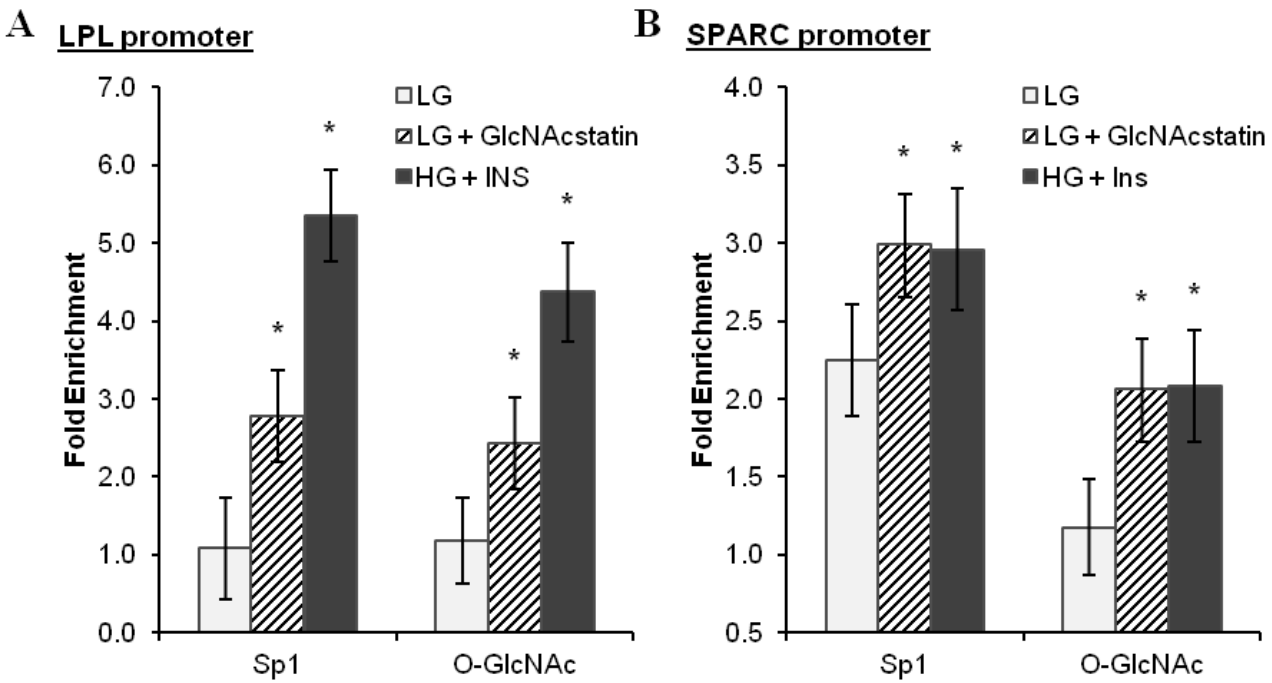

Figure 3.5. ChIP analysis of conserved Sp1 sites on the SPARC and LPL promoters. Insulin responsive and insulin resistant 3T3-F442a adipocytes were subjected to chromatin immunoprecipitation with anti-Sp1, anti-O-GlcNAc (RL2), or normal IgG. Quantitative PCR was performed with primers designed to amplify the conserved Sp1 binding site motif on the LPL (*left panel*) or SPARC (*right panel*) promoter. Fold enrichment was calculated using % Input as described in *Materials and Methods*. *, $P < 0.05$.

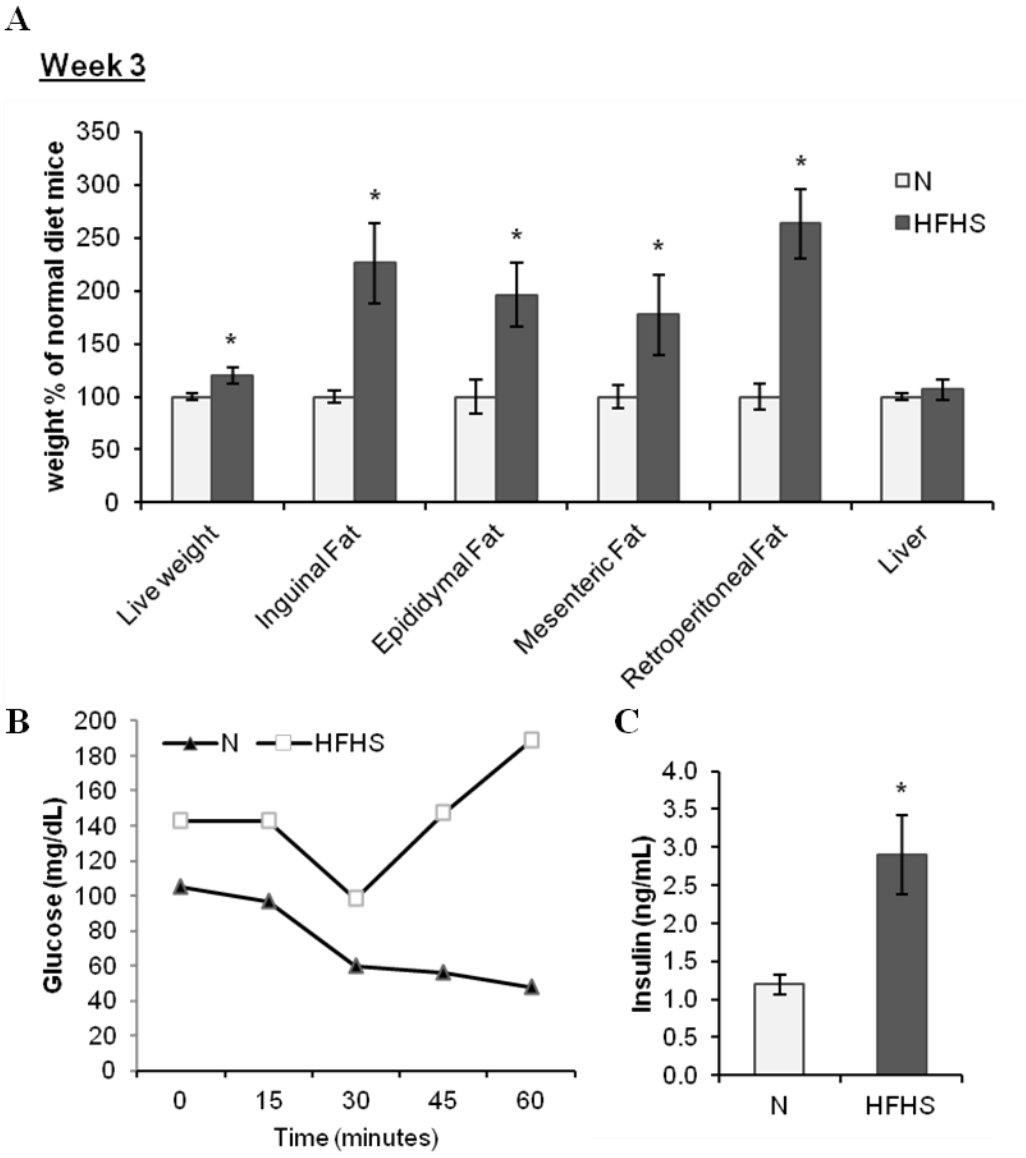

Supplementary Figure S3.1. Characterization of the diet-induced obesity mouse model. A) After three weeks on either the HFHS diet (n=6) or normal diet (n=6), mice were weighed, sacrificed, and the liver and four fat pads were dissected and weighed. Data are presented so that 100% represents the weight of the normal diet mice. B) Insulin sensitivity test was performed as in *Materials and Methods*. C) Trunk blood was used for an Insulin RIA. *, $P < 0.05$.

Supplementary Table 3S.1. Common motifs for adipokine promoters

Motif Candidate 1

Motif length: 12; Motif number: 16; Consensus: AGAGGCCGGGAG

The profile matrix:

A	8	1	13	2	3	3	0	5	1	1	11	2
G	4	14	2	14	11	0	2	9	15	15	3	12
C	0	0	1	0	1	12	8	0	0	0	1	0
T	4	1	0	0	1	1	6	2	0	0	1	2

Motif Candidate 2

Motif length: 12; Motif number: 16; Consensus: CTGCCCTTTCCC

The profile matrix:

A	2	0	0	5	0	2	2	1	0	1	0	5
G	1	0	11	3	0	0	1	3	3	0	0	0
C	12	1	2	7	14	11	3	0	0	14	14	9
T	1	15	3	1	2	3	10	12	13	1	2	2

Motif Candidate 3

Motif length: 12; Motif number: 16; Consensus: CCCCCCGCCACC

The profile matrix:

A	2	0	1	1	2	0	1	4	1	6	2	3
G	4	0	0	1	0	3	9	0	0	0	0	0
C	7	15	13	14	7	12	3	12	15	5	14	12
T	3	1	2	0	7	1	3	0	0	5	0	1

Motif Candidate 4

Motif length: 12; Motif number: 16; Consensus: CCCTTCCAGCCA

The profile matrix:

A	0	5	1	1	0	0	0	14	1	3	0	9
G	2	2	0	0	0	0	1	0	12	0	2	0
C	12	8	9	4	2	14	15	2	3	10	13	6
T	2	1	6	11	14	2	0	0	0	3	1	1

Motif Candidate 5

Motif length: 12; Motif number: 4; Consensus: GGGGGGGTGGGG

The profile matrix:

A	1	0	0	0	0	0	0	0	0	0	0	0
G	3	2	4	4	4	4	4	0	4	4	4	4
C	0	2	0	0	0	0	0	0	0	0	0	0
T	0	0	0	0	0	0	0	4	0	0	0	0

Motif Candidate 6

Motif length: 12; Motif number: 16; Consensus: CCTTTCCAGCCC

The profile matrix:

A	1	3	1	0	0	0	1	12	0	2	0	3
G	5	0	1	3	0	0	0	0	14	0	0	0
C	10	13	4	0	6	16	15	1	0	13	11	7
T	0	0	10	13	10	0	0	3	2	1	5	6

Supplementary Table 3S.1. Continued.

Motif Candidate 7

Motif length: 12; Motif number: 16; Consensus: ACCCTGCCAGCT

The profile matrix:

A	7	0	1	1	0	0	1	1	11	5	1	2
G	5	0	1	2	0	14	1	2	0	8	0	2
C	0	15	8	12	0	0	9	13	0	2	15	2
T	4	1	6	1	16	2	5	0	5	1	0	10

Motif Candidate 8

Motif length: 12; Motif number: 16; Consensus: CAGGAACCCCAG

The profile matrix:

A	4	11	0	7	9	8	5	1	3	0	8	1
G	1	1	16	9	7	0	0	5	1	0	0	11
C	10	0	0	0	0	7	8	10	12	16	0	4
T	1	4	0	0	0	1	3	0	0	0	8	0

Motif Candidate 9

Motif length: 12; Motif number: 6; Consensus: GCGGGGGTGGGG

The profile matrix:

A	1	0	0	2	0	0	0	0	0	2	0	1
G	4	2	5	4	6	6	3	0	6	4	6	4
C	0	3	0	0	0	0	3	0	0	0	0	0
T	1	1	1	0	0	0	0	6	0	0	0	1

Motif Candidate 10

Motif length: 12; Motif number: 2; Consensus: ATGAGTATTTAA

The profile matrix:

A	1	0	0	2	0	0	2	0	0	0	2	2
G	0	0	2	0	2	0	0	0	0	0	0	0
C	0	0	0	0	0	0	0	0	0	0	0	0
T	1	2	0	0	0	2	0	2	2	2	0	0

Motif Candidate 11

Motif length: 12; Motif number: 5; Consensus: GGGTGGGGCAGA

The profile matrix:

A	1	0	0	0	0	2	0	0	2	3	0	4
G	4	5	3	0	5	3	5	5	0	0	5	1
C	0	0	2	0	0	0	0	0	3	0	0	0
T	0	0	0	5	0	0	0	0	0	2	0	0

Motif Candidate 12

Motif length: 12; Motif number: 6; Consensus: GGGAGACTGAGG

The profile matrix:

A	0	0	0	2	1	2	0	0	0	6	0	1
G	6	5	6	2	4	2	2	0	6	0	6	4
C	0	0	0	1	0	1	4	0	0	0	0	1
T	0	1	0	1	1	1	0	6	0	0	0	0

Supplementary Table 3S.1. Continued.

Motif Candidate 13

Motif length: 12; Motif number: 6; Consensus: GGATGAGGCAGA

The profile matrix:

A	2	0	2	1	1	3	0	0	1	5	0	5
G	4	6	2	0	5	3	6	6	0	0	6	1
C	0	0	2	0	0	0	0	0	5	0	0	0
T	0	0	0	5	0	0	0	0	0	1	0	0

Motif Candidate 14

Motif length: 12; Motif number: 5; Consensus: AGGCAGGGAGAG

The profile matrix:

A	4	0	0	0	2	0	2	0	4	2	5	1
G	1	5	5	0	1	5	3	5	0	3	0	4
C	0	0	0	5	1	0	0	0	0	0	0	0
T	0	0	0	0	1	0	0	0	1	0	0	0

Motif Candidate 15

Motif length: 12; Motif number: 6; Consensus: AGGCAGAGAAAG

The profile matrix:

A	5	2	0	0	3	1	3	0	5	3	6	0
G	0	4	6	0	0	4	3	6	0	3	0	4
C	1	0	0	6	2	0	0	0	0	0	0	0
T	0	0	0	0	1	1	0	0	1	0	0	2

Motif Candidate 16

Motif length: 12; Motif number: 4; Consensus: AGGAAGAAGAAG

The profile matrix:

A	4	0	0	3	3	0	4	2	0	3	4	0
G	0	4	2	1	1	4	0	1	2	0	0	4
C	0	0	2	0	0	0	0	1	2	1	0	0
T	0	0	0	0	0	0	0	0	0	0	0	0

Motif Candidate 17

Motif length: 12; Motif number: 4; Consensus: AGGAGGACAGGA

The profile matrix:

A	4	0	0	4	0	0	3	1	3	0	1	2
G	0	3	4	0	4	4	0	0	0	3	3	1
C	0	0	0	0	0	0	0	3	0	1	0	1
T	0	1	0	0	0	0	1	0	1	0	0	0

Motif Candidate 18

Motif length: 12; Motif number: 4; Consensus: AGGACAGGAGGT

The profile matrix:

A	3	0	0	3	0	4	0	0	3	0	0	0
G	0	3	3	1	0	0	4	4	0	3	2	1
C	0	0	0	0	4	0	0	0	1	0	2	1
T	1	1	1	0	0	0	0	0	0	1	0	2

Supplementary Table 3S.1. Continued.

Motif Candidate 19

Motif length: 12; Motif number: 4; Consensus: GAGGACAGGAGG

The profile matrix:

A	0	4	0	0	2	0	3	0	0	2	0	0
G	4	0	4	3	0	0	1	4	4	1	2	2
C	0	0	0	0	2	4	0	0	0	1	0	2
T	0	0	0	1	0	0	0	0	0	0	2	0

Motif Candidate 20

Motif length: 12; Motif number: 4; Consensus: AGCAAGAAGAAG

The profile matrix:

A	4	0	0	3	2	0	4	2	0	3	4	0
G	0	4	1	1	2	4	0	1	2	0	0	4
C	0	0	3	0	0	0	0	1	2	1	0	0
T	0	0	0	0	0	0	0	0	0	0	0	0

Motif Candidate 21

Motif length: 12; Motif number: 4; Consensus: CCCAGAGACCCC

The profile matrix:

A	1	0	1	4	0	2	0	2	0	0	0	0
G	0	0	0	0	4	2	4	0	0	0	0	0
C	2	4	3	0	0	0	0	2	2	3	4	4
T	1	0	0	0	0	0	0	0	2	1	0	0

Motif Candidate 22

Motif length: 12; Motif number: 4; Consensus: CCTGCCCCCAAC

The profile matrix:

A	0	0	0	0	0	1	0	0	0	4	4	0
G	0	0	0	2	0	0	0	0	0	0	0	1
C	4	2	1	2	4	3	4	4	4	0	0	3
T	0	2	3	0	0	0	0	0	0	0	0	0

Motif Candidate 23

Motif length: 12; Motif number: 4; Consensus: TGGGGTCTCTGG

The profile matrix:

A	1	0	0	0	1	0	0	0	0	0	1	0
G	0	4	4	4	3	1	0	0	0	1	2	4
C	0	0	0	0	0	0	4	1	4	0	0	0
T	3	0	0	0	0	3	0	3	0	3	1	0

Motif Candidate 24

Motif length: 12; Motif number: 4; Consensus: AGGACAGGAGGG

The profile matrix:

A	4	0	0	2	0	4	1	0	2	0	1	1
G	0	4	4	2	1	0	3	4	1	4	3	3
C	0	0	0	0	3	0	0	0	0	0	0	0
T	0	0	0	0	0	0	0	0	1	0	0	0

CHAPTER 4

QUANTITATIVE SECRETOME AND GLYCOME OF PRIMARY HUMAN ADIPOCYTES DURING INSULIN RESISTANCE[3]

[3] Edith E. Wollaston-Hayden*, Jae-min Lim*, Chin Fen Teo, Dorothy Hausman, and Lance Wells.
To be submitted to *Molecular and Cellular Proteomics.*

Abstract

Adipose tissue is both an energy storage depot and an endocrine organ. The impaired regulation of the secreted proteins of adipose tissue, known as adipocytokines, observed during obesity contributes to the onset of whole-body insulin resistance and the pathobiology of type 2 diabetes mellitus (T2DM). In addition, the global elevation of the intracellular glycosylation of proteins by O-linked β-N-acetylglucosamine (O-GlcNAc) via either genetic or pharmacological methods is sufficient to induce insulin resistance in both cultured adipocytes and animal models. The elevation of global O-GlcNAc levels is associated with the altered expression of many adipocytokines. We have previously characterized the rodent adipocyte secretome during insulin sensitive and insulin resistant conditions. Here, we characterize and quantify the secretome and glycome of primary human adipocytes during insulin responsive and insulin resistant conditions generated by the classical method of hyperglycemia and hyperinsulinemia or by the pharmacological manipulation of O-GlcNAc levels. Using a proteomic approach, we identify 190 secreted proteins and report a total of 20 up-regulated and 6 down-regulated proteins that are detected in both insulin resistant conditions. Moreover, we apply glycomic techniques to examine (1) the sites of N-glycosylation on secreted proteins, (2) the structures of complex N- and O-glycans, and (3) the relative abundance of complex N- and O-glycans structures in insulin responsive and insulin resistant conditions. We identify 91 N-glycosylation sites derived from 51 secreted proteins, as well as 155 and 29 released N- and O-glycans respectively. We go on to quantify many of the N- and O-glycan structures between insulin responsive and insulin resistance conditions demonstrating no significant changes in complex glycosylation in the time frame for the induction of insulin resistance. Thus, our data support that the O-GlcNAc

modification is involved in the regulation of adipocytokine secretion upon the induction of insulin resistance in human adipocytes.

Introduction

Type 2 diabetes mellitus (T2DM) is a rapidly growing problem in the industrialized world. In the United States, it is estimated that 8.3% of the population has diabetes [362]. T2DM results from a combination of insulin resistance and pancreatic beta-cell dysfunction [9]. The development of T2DM depends on both genetic and environmental risk factors [400]. The major environmental risk factor for the development of insulin resistance and T2DM is obesity. Increased white adipose tissue (WAT) mass during obesity causes of variety of problems related to the development of insulin resistance. It is now established that WAT acts as a lipid metabolism modulator as well as an endocrine organ [23].

The secreted proteins of adipose tissue, known as adipocytokines, can act in a paracrine or endocrine manner to modulate a variety of processes such as inflammation and whole-body energy homeostasis. During obesity, adipocytokine secretion is altered, which can lead to the development of whole-body insulin resistance and T2DM [38, 401]. Although many adipocytokines have been identified using methods such as mass spectrometry-based proteomics, the alteration in the adipose tissue secretome for normal vs. insulin resistant human adipose tissue has not been well-defined [402]. Several adipocytokines identified in rodents have different expression patterns in humans highlighting the need for quantitative proteomic studies in human adipose tissue [403, 404]

Adipose tissue is comprised of many cell types including adipocytes, pre-adipocytes, mesenchymal stem cells, immune cells, and vascular cells. It is clear that these cells have complex paracrine interactions that influence the secretome. To achieve a more physiological representation of the adipose tissue secretome, we use primary human pre-adipocytes derived from human adipose tissue rather than an adipocyte cell line [228].

The regulation of adipocytokine expression during insulin resistance is still unclear in many cases. One possible way for cells to sense nutrient abundance and modulate insulin sensitivity and adipocytokine expression is through the hexosamine biosynthetic pathway (HBP). Flux through the HBP is affected by the levels of glucose, uridine, glutamine, and free fatty acids (FFAs). Excessive flux through the HBP results in insulin resistance, thereby limiting the amount of glucose that enters the cell and the resulting toxicity [61, 96]. Flux through the HBP also modulates the expression of several adipocytokines [47, 58-60]. The final product of the HBP is UDP-GlcNAc, which is the sugar donor for the enzyme O-GlcNAc transferase (OGT) that adds the O-linked β-N-acetylglucosamine (O-GlcNAc) modification onto the serine and threonine residues of nucleocytosolic proteins [80, 81]. It has been shown in multiple systems that the elevation of O-GlcNAc levels is sufficient to cause insulin resistance [98, 100, 103-105, 120]. Furthermore, the overexpression of OGT in the peripheral tissues of mice results in both glucose disposal defects and hyperleptinemia providing further evidence that the O-GlcNAc modification causes insulin resistance and the dysregulation of adipocytokine expression [104].

The role of the O-GlcNAc modification of proteins during insulin resistance on the secretome of human adipose tissue has not been explored. We have previously characterized and quantified the secretome of rodent adipocytes during insulin resistance generated by either directly or indirectly modulating O-GlcNAc levels [131]. We use a similar approach in this study. Insulin resistance is induced in primary human adipocytes by either the classical method of chronic hyperinsulinemia and hyperglycemia or by directly elevating O-GlcNAc levels using O-GlcNAcase (OGA) pharmacological inhibitors.

To identify and quantify the secretome we use a proteomic approach with reverse phase (RP) liquid chromatography-nanospray-tandem mass spectrometry (LC-NS-MS/MS). We

identify a total of 190 secreted proteins from primary human adipocytes. We compare the relative abundance of the adipocytokines during insulin responsive versus insulin resistant conditions using spectral counts. We report that 20 proteins are upregulated and 4 are downregulated when primary human adipocytes are shifted from insulin sensitive to insulin resistant conditions.

Glycosylation is one of the most common post-translational modifications (PTMs) of proteins. It is essential for the regulation of many physiological events such as cell-cell recognition, signal transduction, and inflammation during development, differentiation, and disease progression [405-413]. There are a wide-array of glycan structures in mammals, which are synthesized in a multi-step process by highly specific glycosyltransferases and glycosidases located in the endoplasmic reticulum and Golgi apparatus. In certain disease states, the expression of these enzymes is altered leading to changes in the glycome [414, 415]. It has been suggested that the increased pool of UDP-GlcNAc during excessive nutrient flux alters glycosyltransferase activity and the degree of N-glycan branching [416]; however, another study reported no change in complex glycosylation during elevated HBP flux [78]. Determining the glycome in different disease states is important for the future identification of structure-function relationships and to discover targets for diagnostic biomarkers [131, 417, 418]. The glycome of human adipose tissue has not been previously described. Glycan analysis is challenging due to the diversity of possible structures and their low abundance [414, 419-427]. We use several strategies to identify, site-map, and quantify glycans from adipose tissue using mass spectrometry (MS).

We characterize a total of 155 N-linked glycans and 29 O-linked glycans using MS/MS spectra by total ion mapping (TIM) scan. Predominant N-linked and O-linked glycans are

quantified by ^{13}C isotopic labeling by permethylation using heavy or light iodomethane ($^{13}CH_3I$ and $^{12}CH_3I$) and isobaric pairs of iodomethane ($^{13}CH_3I$ or $^{12}CH_2DI$) (48, 49). A total of 48 N-linked glycans and 12 O-linked glycans are compared between the insulin responsive condition and both insulin resistance conditions by calculating the $^{13}C/^{12}C$ ratios from the sum of peak areas and from non-labeled prevalence rates. We identify 91 N-glycosylation sites derived from 51 secreted proteins using the PNGase F digestion in ^{18}O water using a parent mass list method.

Thus, we describe the secretome and glycome of primary human adipocytes during insulin sensitive and insulin resistant condition. Given the important physiological roles of adipocytokines in maintaining whole-body energy homeostasis, the characterization of the primary human adipocyte secretome during insulin resistace could provide novel markers and/or therapeutic targets for the onset of insulin resistance.

Experimental Procedures

Tissue Culture and Conditioned Cell Treatments.

Cryopreserved human subcutaneous preadipocytes (number of donors: 6-7, gender of donors: female, average age: 39, and average BMI: 27.32) were purchased from Zen-Bio, Inc. (Research Triangle Park, NC). The adipose tissue culture protocols of the maintenance and differentiation from preadipocytes to adipocytes were based on Zen-Bio instruction manual (ZBM0001.01). Briefly approximately 6.7×10^5 cells were cultured in a T-75 cm^2 culture flask using preadipocyte medium (PM-1, Zen-Bio, Inc.), under a humidified atmosphere containing 5% CO_2 in air at 37 °C until they were 85-90% confluent, and then were trypsinized for 5 minutes at 37 °C. After neutralization and centrifugation steps, the cell pellet was resuspended in PM-1 and seeded at an average density of 2.67×10^4 cells/cm^2 in 10-cm cell culture dishes for differentiation. 2 days after the cells reached confluence (referred to as day 0), the medium was

replaced with adipocyte differentiation medium (DM-2, Zen-Bio, Inc.). On day 7, the DM-2 was removed and the cells were maintained in adipocyte maintenance medium (AM-1, Zen-Bio, Inc.). The medium was changed every 3 days. On day 15, at which the majority of the cells contained large lipid droplets, the AM-1 medium was replaced with low glucose DMEM (Cellgro, Mediatech, Inc.) containing 10% FBS (GIBCO, Invitrogen) and antibiotics (100 units/mL penicillin and 100 μg/mL streptomycin (P/S), Cellgro, Mediatech, Inc.). The medium was changed every 2 days until treatments were applied. On day 20, adipocytes were treated with different conditions, either (1) low glucose (LG) (LG, DMEM containing 10% FBS and P/S), (2) insulin (100 nM, human, Roche) in high glucose (HG + INS) (HG, DMEM containing 10% FBS and P/S), (3) PUGNAc (100 μM, TRC, Inc.) in low glucose (LG + PUGNAc) (LG, DMEM containing 10% FBS and P/S), or (4) GlcNAcstatin (20 nM, kind gift from Dr. Daan van Aalten) in low glucose (LG + PUGNAc) (LG, DMEM containing 10% FBS and P/S). After the first 24 h of incubation, the cells were washed five times (for mass spectrometry analysis) or 3 times (for immunoblotting) with low or high glucose serum-free DMEM without antibiotics and incubated for 15 min during the last rinse. After the final wash, the treatment conditions were added as above except no serum was added and the HG + INS treatment was changed to 1nM Insulin. The cells and media were harvested after 16 h of incubation.

Secreted Protein Sample Preparation.

The conditioned media was harvested with extreme care and then centrifuged once at 1800 rpm, at 4 °C for 7 min. The supernatant was filtered using 1 μm syringe filters (PALL). The samples were then centrifuged again at 30000 × g, at 4 °C for 30 min. The samples were then transferred to equilibrated spin columns (Centriprep YM-3, Amicon, Millipore) and buffer-exchanged at 2800 × g, at 4 °C into 40 mM ammonium bicarbonate (NH_4HCO_3) in the presence

of 1 mM dithiothreitol (DTT, Fisher Scientific) and concentrated. The samples were either quantified and prepared for immunoblotting or were denatured with 1 M urea (Sigma), reduced with 10 mM DTT for 1 h at 56 °C, carboxyamidomethylated with 55 mM iodoacetamide (ICH_2CONH_2, Sigma) in the dark for 45 min, and then digested with 4 μg of trypsin (Promega) in 40 mM NH_4HCO_3 overnight at 37 °C. After digestion, the peptides were acidified with 200 μL of 1% trifluoroacetic acid (TFA). Desalting was subsequently performed with C18 spin columns (Vydac Silica C18, The Nest Group, Inc.) and the resulting peptides were dried down in a Speed Vac and stored at -20 °C until analysis. For the subset of samples to be analyzed for N-linked glycosylation, peptides were resuspended in 19 μL of ^{18}O water ($H_2{}^{18}O$, 95%, Cambridge Isotope Laboratories, Inc.) and 1 μL of N-Glycosidase F (PNGase F, Prozyme) and allowed to incubate for 18 h at 37 °C. Peptides were dried back down and resuspended in 50 μL of 40 mM NH_4HCO_3, with 1 μg of trypsin for 4 hr, to remove any possible C-terminal incorporation of ^{18}O from residual trypsin activity, and then dried down and stored at -20 °C until analysis.

Whole Cell Extracts and Western Blots.

After culture medium was removed for secreted proteins analysis, the cell monolayer was washed twice with 10 ml of ice-cold PBS and scraped in the presence of 1 ml PBS plus protease inhibitors. After removing PBS by centrifugation at 6,000 x *g* for 5 min at 4 °C, the pellet was snap frozen and stored at -80 °C. To prepare lysate for immunoblotting, the pellets were lysed in 20mM Tris pH 7.5, 150mM NaCl, 1mM EDTA, 1% NP-40, 1:100 protease inhibitor cocktail set V, EDTA-free (Calbiochem), and 1uM PUGNAc. Protein concentration was determined using the Pierce BCA Protein Assay Kit (Thermo Scientific) and samples were boiled in Laemli sample buffer. The immunoblots were performed essentially as described [367] using CTD 110.6 (for O-GlcNAc modified proteins) and ERK-2 (as a positive control for loading)

antibodies. For secreted protein immunoblotting, the media concentration was quantified using the Bradford method and verified by Coomassie staining. Equal amounts of protein were separated by SDS-PAGE with Tris-HCl precast minigels (Bio-Rad) and transferred to nitrocellulose membranes for Western blot analysis. After blocking for at least 1 hour, membranes were incubated with the appropriate primary antibody, anti-SPARC (Abcam) or anti-Chitinase-3-like protein 1 (R&D Systems) overnight at 4°C. Membranes were incubated with the appropriate horseradish peroxidase-coupled secondary antibodies for 1 hour, followed by extensive washing and Pierce ECL detection.

Protein Extracts for Glycan Analysis.

After the conditioned media was collected, the adipocytes were immediately washed twice with ice-cold PBS and harvested by scraping for glycan analysis. The cells were centrifuged at 12,000 x g, at 4 °C for 15 min to remove the supernatant and debris, then snap frozen and stored at -80 °C until analysis. After the cell pellets thawed on ice, the samples were subjected to Dounce homogenization in ice-cold 100% methanol. The homogenized samples were delipidated by two solvent extractions using a mixture of chloroform/methanol/water (4:8:3, v/v/v) and rocking for 3 h at room temperature as described previously [414, 418]. The emulsion was centrifuged at 2800 × g for 15 min at 4 °C to remove the supernatant. The pellets were resuspended in an acetone/water (10:1, v/v) mixture and incubated on ice for 15 min for washing. The protein pellets were collected by centrifugation and dried on a heating module at 45 °C under a mild nitrogen stream (Reacti-Therm™ and Reacti-Vap™, Pierce). The dried protein powder was weighed and stored at -20 °C until analysis.

Preparation of N-linked Glycans.

Three mg of the protein powder was resuspended in 200 µL of 40 mM NH_4HCO_3 by sonication followed by boiling at 100 °C for 5 min. After cooling to room temperature, 25 µL of trypsin (2 mg/mL in 40 mM NH_4HCO_3, Sigma) and chymotrypsin (2 mg/mL in 40 mM NH_4HCO_3, Sigma) were added. The samples were denatured with 250 µL of 2 M urea in 40 mM NH_4HCO_3, leading to a final concentration of 1 M urea, and incubated overnight (18 h) at 37 °C. After digestion, the peptide samples were centrifuged and 10 µL of the supernatant was collected for protein quantification. The peptide concentrations were measured using a Pierce BCA Protein Assay Kit (Thermo Scientific). The samples were boiled at 100 °C for 5 min and then acidified by adding 500 µL of 10% acetic acid (AcOH) to deactivate proteases. The samples were loaded onto an equilibrated C18 extraction column (BakerBond™, J.T.Baker), washed with 1 mL of 5% AcOH three times, and then eluted stepwise using 1 mL of 20% isopropanol in 5% AcOH, 40% isopropanol in 5% AcOH, and 100% isopropanol. The resulting glycopeptides were dried in a Speed Vac, resuspended in 48 µL 1× PNGase F reaction buffer and 2 µL PNGase F and incubated for 18 h at 37 °C. Following PNGase F digestion, released oligosaccharides were separated by the C18 extraction column. The mixture was reconstituted in 5% AcOH and loaded onto an equilibrated C18 extraction column. The N-linked oligosaccharides were eluted using 1 mL of 5% AcOH three times and then collected and dried using a Speed Vac for subsequent permethylation.

Preparation of O-linked Glycans.

O-linked oligosaccharides were released by reductive *β*-elimination then purified by a cation exchange resin. Three mg of delipidated protein powder was weighed and transferred into a clean glass tube. 500 µL of 50 mM sodium hydroxide (NaOH) and 500 µL of alkaline

borohydride solution (a mixture of 2 M sodium borohydride ($NaBH_4$, Sigma-Aldrich) in 50 mM NaOH leading to a final concentration of 1 M $NaBH_4$) were added to the tube. The mixture was incubated for 16 h at 45 °C on the heating block and the reaction was stopped by the addition of 10% AcOH with vortexing. The acidified mixture was loaded onto an equilibrated cation exchange resin cartridge (AG 50W-X8, Bio-Rad) with 5% AcOH. O-linked glycans were eluted with 6 mL of 5% AcOH and then dried in a Speed Vac. The sample was resuspended in 1 mL methanol/glacial acetic acid (9:1, v/v) solution and dried on the heating module at 45 °C under a mild nitrogen stream to remove borates for subsequent permethylation.

Permethylation of Glycans.

To facilitate analysis of oligosaccharides by mass spectrometry, the released oligosaccharide mixtures were permethylated as described previously [414, 417, 428]. Briefly, glycans were resuspended in 200 µL of anhydrous dimethyl sulfoxide (DMSO, Sigma-Aldrich) and 250 µL of fresh dehydrated NaOH/DMSO reagent (mixture of 50 mg NaOH in 2 mL of anhydrous DMSO). After sonication and vortexing under nitrogen gas, 100 µL of ^{12}C or ^{13}C-iodomethane ($^{12}CH_3I$ and $^{13}CH_3I$, 99% of ^{13}C, Sigma-Aldrich) was added and the mixtures were vortexed vigorously for 5 min. 2 mL of distilled water was added to the samples and the excess iodomethane was removed by bubbling with a nitrogen stream. Two mL of dichloromethane (CH_2Cl_2, Sigma-Aldrich) was added. After vigorous mixing and phase separation by centrifugation, the upper aqueous layer was removed and discarded. The nonpolar organic phase was then extracted 4 times with distilled water. Dichloromethane was evaporated on the heating module at 45 °C with a mild nitrogen stream. The permethylated glycans were dissolved in adjusted volumes (15-30 µL) of 100% methanol according to the results of the protein assay.

The ^{12}C and ^{13}C-labeled permethylated glycans were mixed in the same proportion for each experimental condition before analysis.

Analysis Using Mass Spectrometry.

For proteome analysis of secreted proteins by liquid chromatography tandem mass spectrometry (LC-MS/MS), the peptides were resuspended with 19.5 μL of mobile phase A (0.1% formic acid, FA, in water) and 0.5 μL of mobile phase B (80% acetonitrile, ACN, and 0.1% formic acid in water) and filtered with 0.2 μm filters (Nanosep, PALL). The samples were loaded off-line onto a nanospray tapered capillary column/emitter (360 × 75 × 15 μm, PicoFrit®, New Objective) that was self-packed with C18 reverse phase (RP) resin (8.5 cm, Waters) in a nitrogen pressure bomb for 10 min at 1000 psi (~5 μL load). The samples were then separated via a 160 min linear gradient of increasing mobile phase B at a flow rate of ~200 nL/min directly into the mass spectrometer. One-dimensional LC-MS/MS analysis was performed using a linear ion trap and an Orbitrap mass spectrometer (LTQ and LTQ Orbitrap XL, Thermo Fisher Scientific Inc., San Jose, CA) equipped with a nanoelectrospray ion source at 2.0 kV capillary voltage and 200 °C capillary temperature. For secretome analysis, a full ITMS (Ion trap mass spectrometry) spectrum in positive ion and profile mode was collected at 300-2000 m/z followed by 8 MS/MS events on the 8 most intense peaks with enabled dynamic exclusion using a repeat count of 2, a maximum exclusion list size of 100, and an exclusion duration of 30 s. Each MS/MS scan event was followed by CID (34% normalized collision energy), 0.25 activation Q, and 30.0 ms activation time. For N-liked glycosylation site mapping, a full FTMS (Fourier transform mass spectrometry) spectrum, typically recorded at 60000 resolution in positive ion and profile mode, was acquired at 300-2000 m/z followed by 5 data dependent MS/MS spectra

of ITMS on the most intense ion peaks from parent mass list following CID (36 % normalized collision energy), 0.25 activation Q, and 30.0 ms activation time. Dynamic exclusion was set at a repeat count of 2, a maximum exclusion list of 100, and an exclusion duration of 60 s.

For glycome analysis by direct infusion nanospray MS, permethylated glycans were dissolved by combining 15 µL of the isotopically mixed sample in 100% methanol plus 35 µL 1 mM NaOH in 50% methanol. They were infused directly into a linear ion trap and an Orbitrap mass spectrometer using a nanospray ion source with a fused-silica emitter (360 × 75 × 30 µm, SilicaTip™, New Objective) at 2.0 kV capillary voltage, 200 °C capillary temperature, and a syringe flow rate of 0.4 µL/min. The full ITMS spectra and FTMS spectra, typically recorded at 60000 resolution in positive ion and profile mode, were collected at 400-2000 m/z for 30 s with 5 microscans and 150 maximum injection times (ms). The centroid MS/MS spectra following collision-induced dissociation (CID) were obtained from 400 to 2000 m/z at 34% and 28% normalized collision energy for N- and O-linked glycans, respectively, 0.25 activation Q, and 30.0 ms activation time by total ion mapping (TIM). Parent mass step size and isolation width were set at 2.0 m/z and 2.8 m/z, respectively, for automated MS/MS spectra with TIM scans.

Data Analysis.

The resulting data was searched against a target nonredundant human (*Homo sapiens*, 5-2-07) database including the common contaminants database obtained from the human International Protein Index (IPI) protein sequence database (European Bioinformatics Institute, www.ebi.ac.uk/IPI/) using the TurboSequest algorithm (BioWorks 3.3.1 SP1, Thermo Fisher Scientific Inc.) [429, 430]. It was also searched against a decoy human database to determine statistically relevant peptide identification. DTA files were generated for spectra with a threshold of 15 ions and a TIC of $2e^3$ over a range of $[MH]^+$ = 600-4000 for only IT data. The SEQUEST

parameters were set to allow 2.0 Da (20 ppm for FT) of precursor ion mass tolerance and 0.5 Da of fragment ion tolerance with monoisotopic mass. Only strict tryptic peptides were allowed with up to two missed internal cleavage sites. Dynamic mass increases of 15.99 and 57.02 Da (15.9949 and 57.0215 Da for FT) were allowed for oxidized methionine and alkylated cysteine, respectively. In the cases where sites of N-linked glycosylation were investigated with PNGase F and ^{18}O water, a dynamic mass increase of 3.0 Da (2.9883 Da for FT) was allowed for Asn residues [431]. The masses were selected between 300-2000 m/z at each charge state and 7352 total masses were obtained for parent mass list. Each sample was analyzed by four of LC-MS/MS run with different parent mass list up to 2000 because of maximum number of parent masses for FTMS and mass complexity. The results from shotgun method and parent mass list method were combined and filtered at $\geq$ 0.60 Final Score (Sf). For relative protein quantification, the identified peptides and proteins were statistically validated between the target and decoy database search results, and protein ratios were determined by normalized spectral counts using ProteoIQ 1.1 (BIOINQUIRE, GA). Proteins identified by two peptides were only considered to be statistically significant at less than 1% protein false discovery rate (FDR) using the ProValT algorithm as implemented in ProteoIQ [432, 433]. From the results, the subcellular location of secreted proteins was manually determined for each protein from the Human Protein Reference Database (http://www.hprd.org/), Bioinformatic Harvester III (http://harvester.fzk.de/harvester/) and the UniProtKB/Swiss-Prot (http://www.ebi.ac.uk/swissprot/) databases. The functional categories of secretome were annotated by the Ingenuity Pathways Analysis (IPA, Ingenuity Systems, Inc.).

The N- and O-linked glycans released from the protein power of adipocytes were analyzed by full MS following permethylation and subsequent MS/MS fragmentations for

specific glycan structures. We used GlycoWorkbench (http://www.dkfz-heidelberg.de/spec/EUROCarbDB/GlycoWorkbench/) to facilitate manually interpretation of the glycan structures from the MS/MS spectra by TIM scan. The areas of each isotopic peak were calculated by their Gaussian distribution and then averaged to compare the relative abundance of each glycan between different samples. The ratio of peak areas from isotopic permethylation defined the relative abundance of each glycan.

Results

Insulin Resistance and Global O-GlcNAc Levels in Primary Human Adipocytes.

Treatment with hyperglycemia and chronic insulin or normoglycemia and the pharmacological OGA inhibitor, PUGNAc, result in the global elevation of *O*-GlcNAc modified nucleocytosolic proteins and insulin resistance in rodent adipocytes [98, 99]. We tested these conditions as well as treatment with a more specific OGA inhibitor, GlcNAcstatin, in primary human adipocytes [257]. Cryopreserved human preadipocytes were expanded and differentiated into mature adipocytes before treatment as described in *Materials and Methods*. Figure 4.1 shows that when compared to normoglycemia (LG), treatment with OGA inhibitors (LG + PUGNAc or LG + GlcNAcstatin) or treatment with hyperglycemia and hyperinsulinemia (HG + INS) raises global O-GlcNAc levels as measure by immunoblotting with an O-GlcNAc specific antibody. In a previous study using rodent adipocytes, we characterized and quantified the secretome and glycome during insulin sensitive and insulin resistant conditions induced by indirectly (HG + INS) or directly (LG + PUGNAc) modulating O-GlcNAc levels. We found that many secreted proteins were up or down-regulated upon the induction of insulin resistance. Here we took a parallel approach to ask the same question using primary human adipocytes. As shown in Figure 4.2, after treatment both the cells and conditioned media were harvested.

Before the final 16 hour serum-free treatment incubation, the cells were washed five times with serum-free media to remove any traces of serum. This greatly reduced the complexity of the conditioned media. The conditioned media was buffer exchanged and concentrated before being processed for analysis by LC-MS/MS. Cells were collected and delipidated as in *Materials and Methods*. Protein was digested and prepared for either N-glycan or O-glycan analysis (Figure 4.2).

Characterization of the Primary Human Adipose Tissue Secretome by LC-MS/MS.

The mass spectra from 24 mass spectrometric analyses were searched against a target nonredundant human database as well as a decoy human database using SEQUEST. Proteins identified by at least two non-redundant peptides with less than a 1% FDR were identified using ProteoIQ. Secreted proteins were manually determined by a reference search as described in *Materials and Methods*. Using these criteria, a total of 190 secreted proteins were identified. Table 4.1 shows the complete list of the 173 secreted proteins identified by at least 2 unique peptides. 17 of the secreted proteins identified based on a single peptide are presented in Supplemental Table 4.1 (Table S4.1). Figure 4.3 shows the proportion of the secretome in each of the 9 main functional categories assigned by Ingenuity Pathways Analysis. The most highly represented categories are enzyme, peptidase, and other protein.

Quantification of the Primary Human Adipocyte Secretome.

Several mass spectrometry techniques can be used for quantitative analysis. Both isotopic and non-isotopic labeling are commonly used to provide quantitative analysis of proteins in complex protein samples [434-442]. For non-isotopic or label-free MS-based quantitative analysis, ion chromatogram intensity or observed peptide spectral counts are compared using quantitative software tools [443-451]. Peptide spectral counts quantification relies on the

association between protein abundance and the number of MS/MS spectra identifying each protein. For this study, we used three biological replicates of conditioned media samples, which differed in complex proteome profiles and relative number of normalized spectral counts. For each of the biological replicates, prepared conditioned media from three treatment groups (LG, LG + PUG, HG + INS) was subjected to two technical replicates of reverse phase LC-MS/MS. All together, a total of 18 LC-MS/MS experiments were performed. SEQUEST was used to search MS data files from each LC-MS/MS run against a forward and reversed human database to calculate a FDR. ProteoIQ was used to cluster the peptides to their assigned proteins and to gather normalized spectral counts for proteins identified at less than a 1% FDR and assigned by at least two non-redundant peptides. Spectral counts were normalized for each technical replicate. For each biological replicate the normalized spectral counts were averaged followed and then the comparative ratios between the two insulin resistant conditions and the insulin responsive condition were calculated. Finally, the comparative ratios were averaged between all of the biological replicates. We set the threshold for reporting statistically significant differences at ≥150% (1.5-fold), an average of ≥5 total spectral counts, and an average of ≥3 normalized spectral counts for each treatment group. We identified 20 human adipocytokines whose secretion levels were upregulated and 4 proteins that were downregulated by at least 1.5-fold by the transition from the insulin sensitive condition to both insulin resistant conditions (Table 4.2). We also identified 28 and 8 proteins that were upregulated or downregulated, respectively, in the transition from insulin sensitive to one of the insulin resistant conditions (Supplementary Table 4.S2).

To confirm the validity of the ratio that we used for statistical significance, we used the orthogonal method of immunoblotting. We confirmed that the regulation we observed in the

proteomic experiment with immunoblotting for two proteins whose levels changed by only 1.5-fold in at least one of the insulin resistant conditions as determined by proteomics. In addition, we used cells where insulin resistance was induced using a more specific OGA inhibitor, GlcNAcstatin, to confirm the regulation we observed by using the less specific OGA inhibitor, PUGNAc [257, 258]. Figure 4.4 shows that both SPARC and Chitinase-3-like protein 1 are upregulated in both insulin resistant conditions as determined by immunoblotting, which confirms our proteomic experiment.

N-Glycan Site-mapping of the Human Adipocyte Secretome.

Many secreted proteins are modified by N-glycans. During disease states, the glycoforms of these proteins may change and have the potential to be used as disease biomarkers. Since the glycome of adipocytes is not well-defined, we determine sites of N-linked glycosylation on secreted adipocytokines as an initial step in biomarker discovery. The tryptic peptides generated from conditioned media were digested with PNGase F in the presence of ^{18}O water to convert any N-glycan-modified Asp to an ^{18}O-Asp residue. The resulting peptides were analyzed by LC-MS/MS using the previously described method for ITMS and the parent mass list method for FTMS as described in *Materials and Methods*. To obtain the parent mass list, the protein sequences of the 190 identified secreted proteins from Table 4.1 and Table 4.S1 were extracted from the database. From these sequences, tryptic peptides, with allowance for two internal missed cleavage sites, that contained the consensus sequence, N-X-S/T, were obtained for theoretical mass calculations. Table 4.3 shows a total of 91 N-linked glycosylation sites that were indentified on 52 proteins. These sites covered 10.3% of the theoretical 882 N-linked glycosylation site sequences generated from the secreted protein list.

Characterization of the Human Adipocyte Glycome.

To better define the glycome of human adipocytes, we performed N-linked and O-linked glycan analysis using mass spectrometry. Glycans were released from whole-cell human adipocyte extracts by PNGase F for N-linked glycans and by β-elimination for O-linked glycans as shown in Figure 4.2C. Figure 4.5A shows that the permethylated N-linked glycans were characterized by full FTMS spectrum using a LTQ Orbitrap XL *(left panel, top)* followed by MS/MS fragmentation by TIM analysis in the ion trap *(left panel, bottom)*. The fragmentation of a biantennary N-linked glycan is shown as an example. We used the GlycoWorkbench to manually interpret a total of 155 N-linked glycan structures from MS/MS spectra at different charge states as shown in Table 4.S3. In Figure 4.5A *(right panel)*, we show that 28 of the predominant N-linked glycans are assigned to a full FTMS and a MS/MS spectrum.

Figure 4.5B *(left panel)* shows a full FTMS spectrum from an O-linked glycan mixture. 10 of the predominant O-linked glycans were assigned from the full FTMS spectra (Figure 4.5B, *bottom panel*). A representative fragmentation spectrum is shown for one of the core 2 O-linked glycans (Figure 4.5B, *right panel*). A total of 29 O-linked glycans were characterized from MS/MS spectra at singly and doubly charged states as shown in Table 4.S4.

Relative Quantification of the Human Adipocyte Glycome upon the Induction of Insulin Resistance using ^{13}C Labeling and Prevalence.

For the comparative quantification of glycans, we performed isotopic labeling using heavy/light iodomethane ($^{13}CH_3I$ and $^{12}CH_3I$) and isobaric pairs of iodomethane ($^{13}CH_3I$ or $^{12}CH_2DI$) during the permethylation step [452, 453]. The $^{13}C/^{12}C$ ratio from the sum of the peak areas and the prevalence ratio between the different treatment conditions were used for relative quantification. Permethylated glycans were mixed in a 1:1 protein ratio and analyzed in

quadruplicate using an LTQ Orbitrap XL. Figure 4.6A (*left panel*) shows the isotopic pairs of N-linked glycans on a full FTMS spectrum. Figure 4.6A (*right panel*) shows an example of a calculated $^{13}C/^{12}C$ ratio from sum of peak area between LG + PUGNAc (LGPUG) and LG conditions. Table S4.5 shows a total of 48 N-linked glycans that were relatively quantified between the insulin resistant conditions (LGPUG and HGINS) and insulin responsive condition (LG) by the average $^{13}C/^{12}C$ ratio and the average prevalence ratio. This approach simultaneously quantified a broad range of N-glycan structures in a complex mixture; however we did not observe highly significant changes in N-glycan $^{13}C/^{12}C$ ratios or prevalence ratios. Figure 4.6B (*left panel*) shows the isotopic pairs of O-linked glycans on a full FTMS spectrum. Figure 4.6B (*right panel*) shows an example of the calculated $^{13}C/^{12}C$ ratio from the sum of peak areas between LGPUG and LG conditions. Table S4.6 shows a total of 12 O-linked glycans that were relatively quantified between insulin resistant and insulin sensitive conditions. We did not observe highly significant changes in O-glycan $^{13}C/^{12}C$ ratios or prevalence ratios.

Discussion

Adipose tissue plays an important role in the maintenance of energy homeostasis. The disregulation of lipid metabolism and the alteration in adipocytokine secretion observed during insulin resistance contributes to the development of whole-body insulin resistance and T2DM [23]. Determining the complete profile of adipocytokines differentially expressed during insulin resistance may provide therapeutic targets for identifying and treating insulin resistance.

Several groups have reported the rodent adipocyte secretome during insulin resistance, but there have been fewer such studies performed with human adipocytes [131, 454-456]. It is advantageous to investigate the secretome of human adipose tissue because there are bound to be

differences between the rodent and human secretome [403]. The differences in the secretome of human adipose tissue have been investigated during adipogenesis and between different fat pad depots [457-460]. Other studies have characterized the secretome without quantification [461, 462]. Another approach has been to study a limited list of known adipocytokines during insulin sensitivity and insulin resistance [463, 464]. Therefore, our study fills an important gap in the literature by taking a discovery approach to characterizing and quantifying the human adipocyte secretome in both insulin sensitive and two different insulin resistance conditions. In addition, we characterize and quantify the glycome of human adipocytes, which has not been described to our knowledge.

We report a total of 193 secreted proteins from human adipocytes (Table 4.1 and Table 4.S1). Using Ingenuity Pathways Analysis we determined that many of the secreted proteins were enzymes, peptidases, or other functions (Figure 4.3). The largest pool of identified proteins from the other category corresponds to extracellular matrix proteins. A common theme among the adipose tissue secretome studies is that extracellular matrix (ECM) proteins, ECM remodelers, inflammatory, and angiogenesis proteins are highly represented [402, 455, 461, 465]. The accumulation of fat mass during obesity requires extensive tissue remodeling that is accomplished by ECM remodelers. The remodeling can generate an inflammatory response during obesity and insulin resistance due to limited angiogenesis, localized hypoxia, adipocyte necrosis, increased fibrosis, altered adipocytokine secretion, and M1-stage macrophage and other immune cell infiltration [20-25]. Many of the adipocytokines we identified, such as SPARC and Chitinase-3-like protein 1, have been implicated in inflammation [132, 224]. In addition, tissue remodeling requires extensive crosstalk between the different cell types that comprise adipose tissue. Several of the adipocytokines we identified, such as Gelsolin, Calreticulin, and Cathepsin

D, may be expressed in cell types other than adipocytes [461, 466]. By using primary adipocytes instead of a cell line, the secretome we identified better represents the physiological status of adipose tissue. In the future, these identified adipocytokines may potentially be used as prognostic/diagnostic biomarkers for metabolic syndrome, T2DM, and other complications.

We generated insulin resistance in the human adipocytes by both directly and indirectly modulating O-GlcNAc levels. The elevation of O-GlcNAc levels has been shown to be sufficient to induce insulin resistance in many systems [98, 100, 103-105, 120]. We have previously demonstrated that the induction of insulin resistance in this way in rodent adipocytes alters the secretion of several adipocytokines [131]. Here, we showed that 20 and 4 adipocytokines were upregulated or downregulated, respectively, upon the transition to insulin resistance by both directly and indirectly modulating O-GlcNAc levels (Table 4.2). We also identified 28 and 8 adipocytokines that were upregulated or downregulated, respectively, upon the induction of insulin resistance by one of the two methods (Table 4.S2). In this study, we find that Sulfhydryl oxidase 1 (Quiescin Q6), laminin B1, and Chitinase-3-like protein 1 are upregulated during both insulin resistant conditions, which was also observed in the rodent study. SPARC was upregulated in both insulin resistant conditions in human adipocytes and was found to be upregulated in HG + INS in rodent adipocytes by proteomics. It was subsequently confirmed by immunoblotting that SPARC was upregulated in both insulin resistant conditions in rodent adipocytes, so this protein is similarly regulated in both rodent and human adipocytes (unpublished results). Four other proteins were observed to be regulated by insulin resistance in both rodent and human adipocytes; however, the regulation was slightly different between species. Thioredoxin was downregulated in both insulin resistant conditions in rodent adipocytes and during HG + INS in human adipocytes but was upregulated during LG + PUG in human

adipocytes. Gelsolin was upregulated in both insulin resistant conditions in rodent adipocytes and during HG + INS in human adipocytes but was not regulated by LG + PUG. Fibulin 2 was downregulated in both insulin resistant conditions in rodent adipocytes but was not regulated or upregulated in LG + PUG and HG + INS, respectively, in human adipocytes. From these examples, it is clear that there are differences in adipocytokine secretion between rodents and humans. Because the proteome sample is extremely complex, we may not have achieved sufficient resolution to quantify some of the proteins that were observed in both rodent and human adipocyte secretomes, such as Angiotensinogen, Cathepsin B, and Spondin 1 [131, 467]. Because we assigned significance to a relatively small fold change (1.5 fold) for quantification, we verified the regulation of two adipocytokines that changed by 1.5 fold by an independent, orthogonal method. Both SPARC and Chitinase-3-like protein 1 protein levels were altered in a similar manner as measured by both quantitative proteomics and immunoblotting (Figure 4.4). In addition, the regulation of these proteins by O-GlcNAc was verified using a more OGA-specific N-acetyglucosaminidase inhibitor, GlcNAcstatin.

The inclusion of an insulin resistance condition generated by directly modulating O-GlcNAc levels in our proteomic study helped us to better define the proteins regulated by O-GlcNAc in human adipocytes. The O-GlcNAc modification is found on hundreds in nucleocytosolic proteins and can affect protein function in diverse ways, such as protein-protein interactions, protein degradation, interplay with phosphorylation, localization, and transcriptional activation [130]. Compiling a list of proteins modulated by O-GlcNAc is the first step in understanding the mechanism of how O-GlcNAc affects adipocytokine expression. We have used the data generated by our previous rodent proteomic study to investigate the transcriptional regulation of adipocytokines by global O-GlcNAc levels (unpublished data). Although several

studies have associated elevated O-GlcNAc levels with adipocytokine expression, no specific molecular mechanism has been reported [47, 58-60, 104, 396, 397].

We also characterize the N-linked and O-linked glycome for human adipocytes. Glycosylation and other PTM's provide an additional layer of regulatory complexity to expressed proteins. To understand the full functionality of a protein, one must know the state of the PTM's. Since secretory proteins, such as adipocytokines, are exposed to the glycosylation machinery that reside in the ER and Golgi apparatus as they make their way through the secretory pathway, they often have a high degree of complex glycosylation. The subset of glycans expressed by cells depends on multiple factors, such as developmental stage, tissue type, and the genetic and physiological state of the cell. It is not known whether adipocytes change glycan expression patterns in response to insulin resistance. Since glycosylation can affect diverse processes that are relevant to adipose tissue remodeling in obesity, such as cell-cell interactions, growth factor sequestration, cytokine activation, and cell migration, there is a need to define the adipocyte glycome [413, 468, 469].

Characterizing the glycome poses many challenges because there is no template for modification, as in DNA, and there is an incredible diversity of glycoforms. Mass spectrometry can provide both structural and abundance information using a small amount of material from a relatively complex mixture [470]. However, it is still difficult to assign specific glycoforms to specific protein residues in a complex mixture. To determine sites of N-glycosylation on the secreted proteins, we used PNGase F and ^{18}O water to convert the glycan-modified Asn to an ^{18}O-Asp residue, thereby leaving a chemical marker of the glycosylation site. We identified 91 sites on 51 proteins of N-linked glycosylation by Orbitrap mass spectrometer using the parent mass list obtained from theoretical consensus sequence in the secretome list (Table 4.3). For

relative glycan quantification, we permethylated using heavy or light iodomethane ($^{13}CH_3I$ and $^{12}CH_3I$) and used prevalence data. The use of isotopic labels allows for mixing of the samples to be compared before analysis, thus providing an internal standard and preventing run to run technical variation [427, 452]. In addition, we used the quantitation by isobaric labeling (QUIBL) method, which uses isobaric pairs of iodomethane ($^{13}CH_3I$ or $^{12}CH_2DI$) to distinguish between structurally distinct isomeric glycans [453]. These techniques allow us to determine the full diversity and changes in major and minor adipocyte glycans during insulin sensitive and resistant conditions. We characterized a total of 155 N-linked glycans and 29 of O-linked glycans (Figure 4.5, Table 4.S3, Table 4.S4). The results presented here demonstrate that the human adipocytes are expressing extended hybrid and complex N-linked glycans, in addition to the expected family of predominant high mannose glycans. Adipose tissues possess the biosynthetic ability to generate diverse O-linked glycans such as core structure, O-glucose glycans, and O-fucose glycans.

Following characterization, we determined the change in glycan prevalence during insulin resistance using isotopic and prevalence ratios. We quantified 48 N-linked glycans and 12 O-linked glycans (Figure 4.6, Table S4.5, Table S4.6). Our results showed that changes of glycan prevalence were not statistically different between the insulin sensitive and insulin resistant conditions. It has been suggested that altering the intracellular UDP-GlcNAc pool, such as during increased glucose flux, changes the degree of N-glycan branching in an ultrasensitive manner [416]. While it is clear that the induction of insulin resistance in adipocytes massively upregulates intracellular glycosylation (Figure 4.1), we did not observe significant changes in complex glycosylation. This suggests that changes in complex glycosylation are not necessary for the induction of insulin resistance; although we cannot rule out that they play a role in insulin

resistance that occurs over a long period of time. Since insulin resistance was generated by treatment for 40 hours, it is possible that the changes in glycan structure had not had time to fully change.

In conclusion, we have characterized the secretome and glycome of primary human adipocytes during insulin resistance using a proteomic approach. We generated insulin resistance by either directly or indirectly modulating O-GlcNAc levels, which provides a list of adipocytokines that are modulated by O-GlcNAc levels. Adipocytokine and glycan levels were quantified between insulin sensitive and insulin resistant conditions and sites of N-glycosylation were identified. This study helps to define the secretome of primary human adipocytes during insulin resistance and helps to characterize and quantify the previously unknown primary adipocyte glycome.

Acknowledgements

We thank all members of the Wells' laboratory, Ruth Harris, Ron Orlando, and James A. Atwood for helpful discussions. We thank Dr. Daan van Aalten for supplying us with GlcNAcstatin. This work was supported by an American Heart Association National Scientific Development Grant (L.W.).

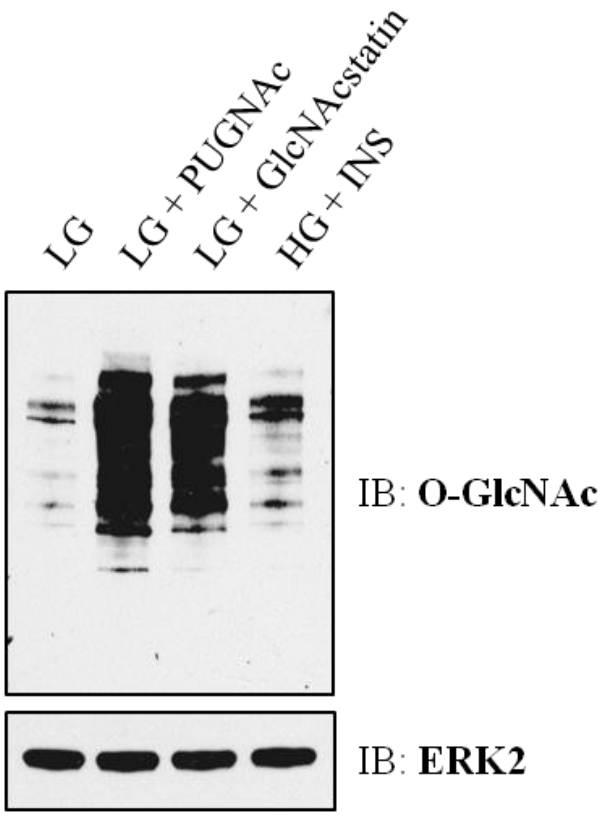

Figure 4.1. Detection of O-GlcNAc levels in primary human adipocytes. Global O-GlcNAc levels are elevated in three insulin resistant conditions generated by low glucose plus PUGNAc (LG + PUGNAc), low glucose plus GlcNAcstatin (LG + GlcNAcstatin), or high glucose plus chronic insulin exposure (HG+INS).

Figure 4.2. Schematic flow diagram of the experimental procedure. (A) Primary human adipocytes are treated with insulin responsive (LG, normoglycemic) or two insulin resistance generating conditions (HG + INS and LG + PUGNAc). (B) Identification and quantification of the secretory proteome and N-linked glycosylation site-mapping from the conditioned media of treated primary human adipocytes (C) Characterization and quantification of N- and O-linked glycans from a whole protein extract of treated primary human adipocytes.

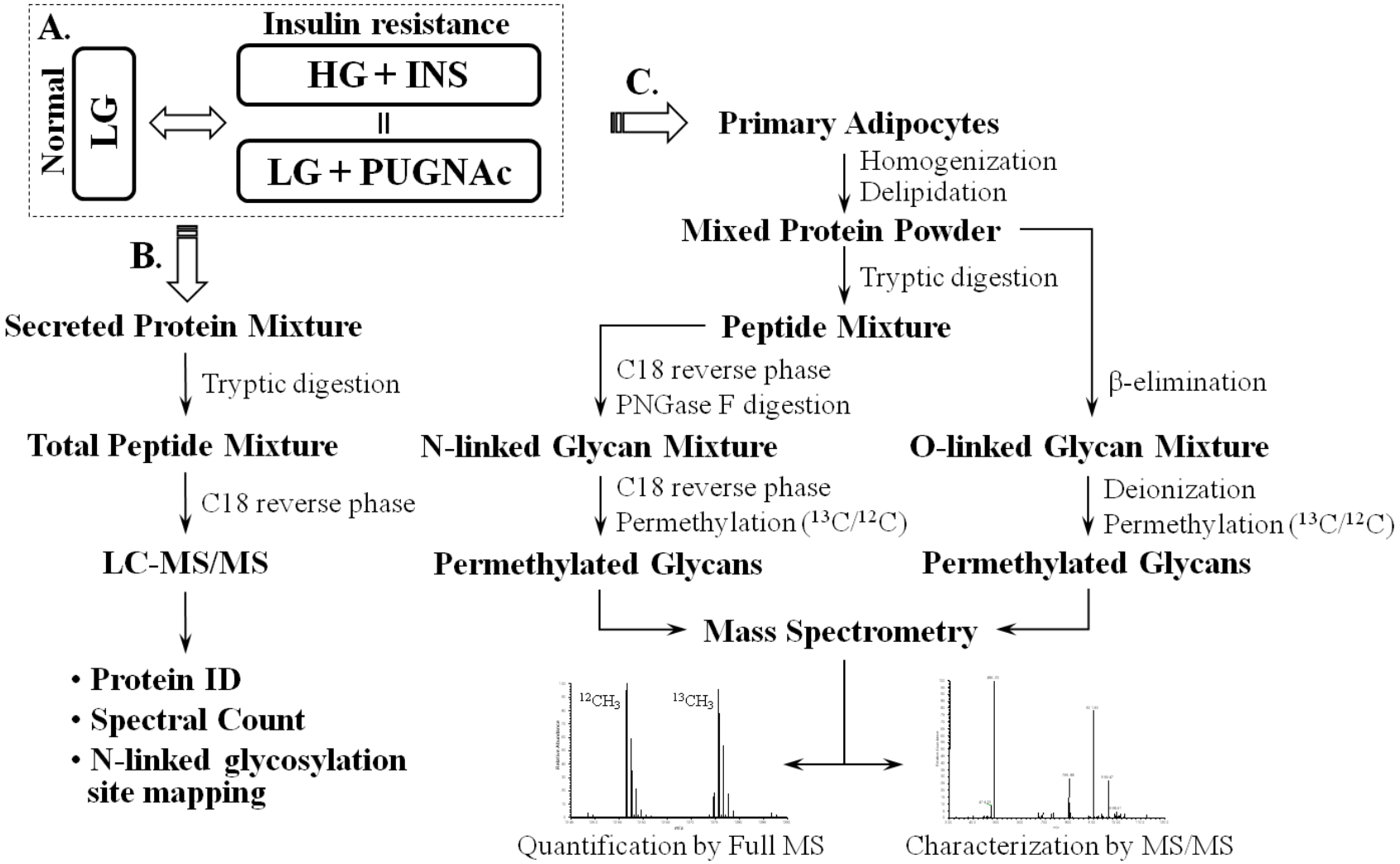
A.
Insulin resistance
Normal
LG
HG + INS
=
LG + PUGNAc
B.
Secreted Protein Mixture
Tryptic digestion
Total Peptide Mixture
C18 reverse phase
LC-MS/MS
• Protein ID
• Spectral Count
• N-linked glycosylation site mapping
C.
Primary Adipocytes
Homogenization
Delipidation
Mixed Protein Powder
Tryptic digestion
Peptide Mixture
C18 reverse phase
PNGase F digestion
β-elimination
N-linked Glycan Mixture
O-linked Glycan Mixture
C18 reverse phase
Permethylation (13C/12C)
Deionization
Permethylation (13C/12C)
Permethylated Glycans
Permethylated Glycans
Mass Spectrometry
12CH3
13CH3
Quantification by Full MS
Characterization by MS/MS

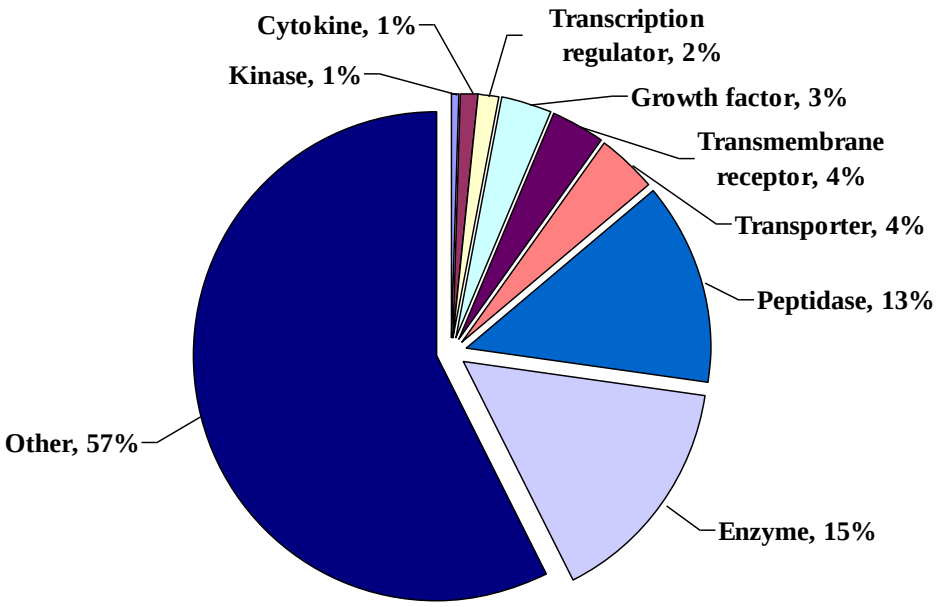

Figure 4.3. The functional categories of the primary human adipocyte secretome. The biological function analysis was determined for each protein based on the Ingenuity Pathway Analysis software (Ingenuity Systems).

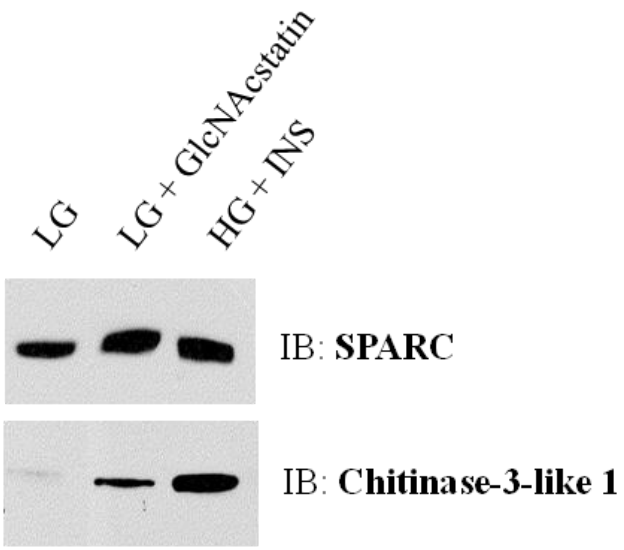

Figure 4.4. Orthogonal validation of proteomic quantification. Equal amounts of conditioned media from primary human adipocytes was immunoblotted with antibodies against SPARC or Chitinase-3-like protein 1.

Figure 4.5. Characterization of the primary human adipocyte glycome by MS/MS and TIM scan. (A) Upper left panel: a full FTMS spectrum of the N-linked glycan mixture, lower left panel: the characterization of a biantennary complex N-linked glycan structure by MS/MS fragmentation, right panel: a list of predominant N-linked glycans. (B) Upper left panel: a full FTMS spectrum of the O-linked glycan mixture, upper right panel: the characterization of a core 2 O-linked glycan structure by MS/MS fragmentation, lower panel: a list of predominant O-linked glycans. ☆: Xyl, ▼: Fuc, ●: Glc, ●: Man, ○: Gal, ■: GlcNAc, □: GalNAc, and ◆: NeuAc

A

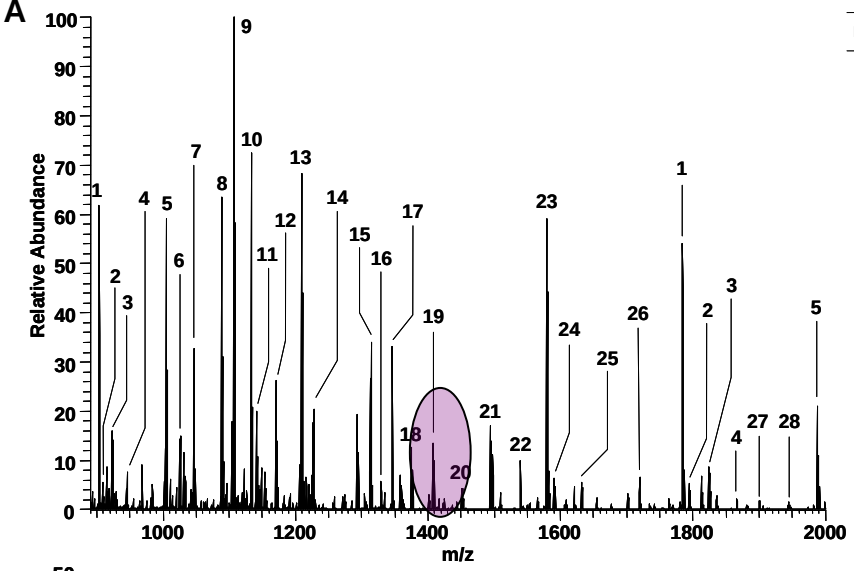

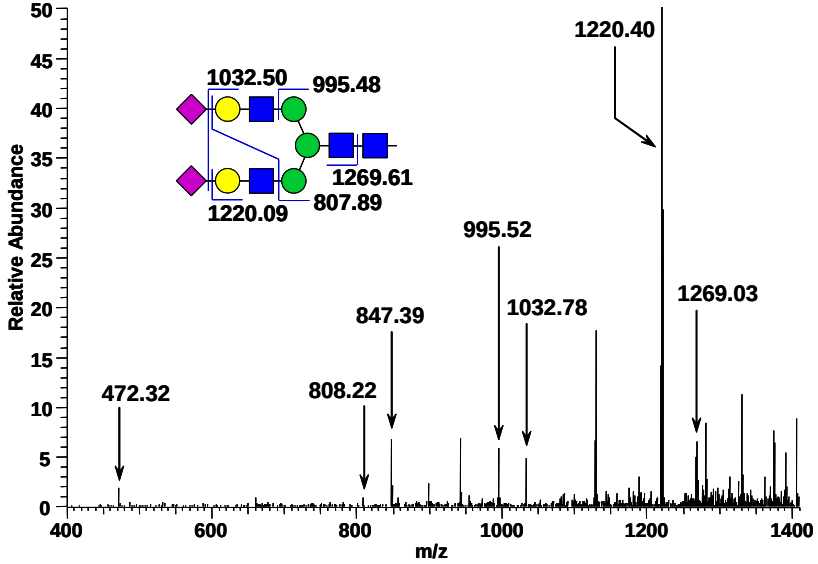

No.	N-linked oligosaccharide composition	Structure	Z	[M+zNa]$^{z+}$ (mono) Measured	[M+zNa]$^{z+}$ (mono) Theoretical
1	(Man)6(GlcNAc)2		2	903.427	903.436
			1	1783.865	1783.883
2	(Gal)1(GlcNAc)1(Man)3(GlcNAc)2(Fuc)1		2	908.935	908.944
			1	1794.881	1794.899
3	(GlcNAc)1(Man)5(GlcNAc)2		2	923.940	923.950
			1	1824.892	1824.909
4	(Gal)1(GlcNAc)2(Man)3(GlcNAc)2		2	944.453	944.463
			1	1865.918	1865.936
5	(Man)7(GlcNAc)2		2	1005.476	1005.486
			1	1987.962	1987.983
6	(Gal)1(GlcNAc)1(Man)5(GlcNAc)2		2	1025.989	1025.999
7	(Gal)2(GlcNAc)2(Man)3(GlcNAc)2		2	1046.513	1046.513
8	(NeuAc)1(Gal)1(GlcNAc)1(Man)3(GlcNAc)2(Fuc)1		2	1089.520	1089.531
9	(Man)8(GlcNAc)2		2	1107.525	1107.536
10	(Gal)2(GlcNAc)2(Man)3(GlcNAc)2(Fuc)1		2	1133.546	1133.557
11	(Man)2(GlcNAc)2(Fuc)1		1	1141.562	1141.573
12	(Man)3(GlcNAc)2		1	1171.572	1171.583
13	(Man)9(GlcNAc)2		2	1209.573	1209.586
14	(NeuAc)1(Gal)2(GlcNAc)2(Man)3(GlcNAc)2		2	1227.087	1227.100
15	(NeuAc)1(Gal)2(GlcNAc)2(Man)3(GlcNAc)2(Fuc)1		2	1314.131	1314.144
16	(NeuAc)1(Gal)1(GlcNAc)2(Man)5(GlcNAc)2		2	1329.136	1329.150
17	(Man)3(GlcNAc)2(Fuc)1		1	1345.660	1345.673
18	(Man)4(GlcNAc)2		1	1375.670	1375.683
19	(NeuAc)2(Gal)2(GlcNAc)2(Man)3(GlcNAc)2		2	1407.672	1407.687
20	(NeuAc)1(Gal)3(GlcNAc)3(Man)3(GlcNAc)2		2	1451.698	1451.713
21	(NeuAc)2(Gal)2(GlcNAc)2(Man)3(GlcNAc)2(Fuc)1		2	1494.716	1494.731
22	(NeuAc)1(Gal)3(GlcNAc)3(Man)3(GlcNAc)2(Fuc)1		2	1538.742	1538.757
23	(Man)5(GlcNAc)2		1	1579.768	1579.783
24	(GlcNAc)1(Man)3(GlcNAc)2(Fuc)1		1	1590.784	1590.799
25	(NeuAc)2(Gal)3(GlcNAc)3(Man)3(GlcNAc)2		2	1632.284	1632.300
26	(NeuAc)2(Gal)3(GlcNAc)3(Man)3(GlcNAc)2(Fuc)1		2	1719.327	1719.344
27	(NeuAc)3(Gal)3(GlcNAc)3(Man)3(GlcNAc)2(Fuc)1		2	1899.911	1899.9311
28	(NeuAc)2(Gal)4(GlcNAc)4(Man)3(GlcNAc)2(Fuc)1		2	1943.938	1943.957

B

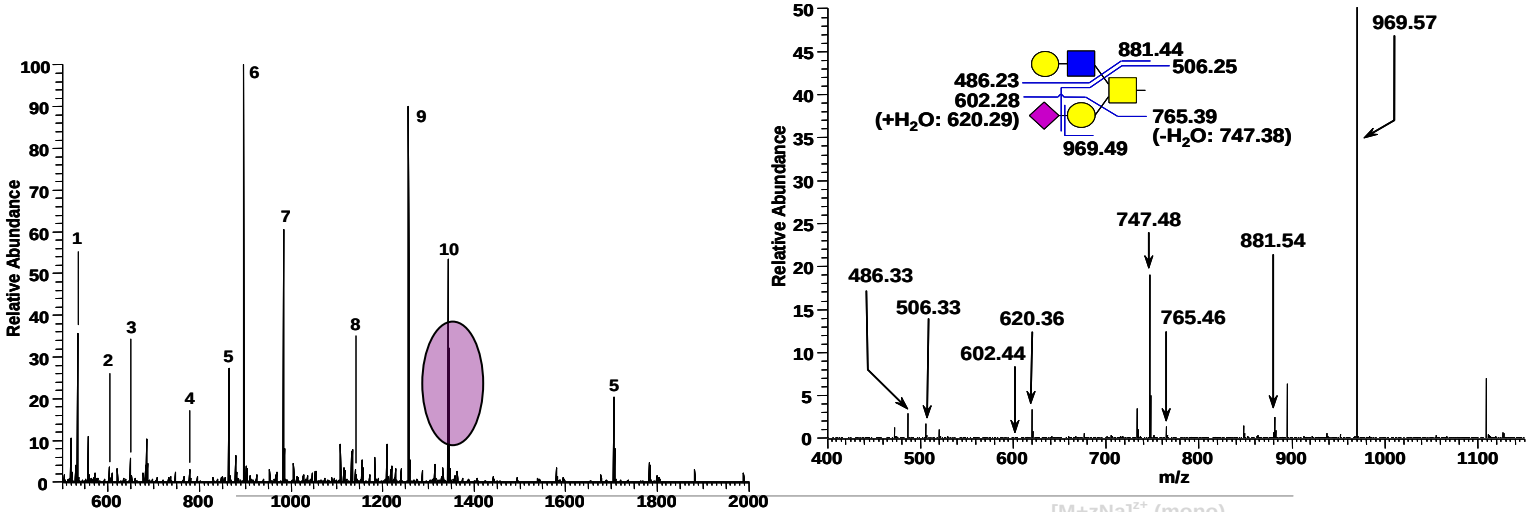

No.	O-linked oligosaccharide composition	Structure	Z	[M+zNa]$^{z+}$ (mono) Measured	Theoretical
1	(Hex)1(HexNAc)1 (HexNAc)1(Hex)1	/	1	534.284	534.289
2	(Xyl)2(Glc)1		1	609.304	609.310
3	(NeuAc)1(Hex)1		1	650.331	650.337
4	(HexNAc)2(Hex)1 (Hex)1(HexNAc)2	/	1	779.409	779.415
5	(NeuAc)2(Hex)2(HexNAc)2		2 1	864.419 1705.848	864.426 1705.862
6	(NeuAc)1(Hex)1(HexNAc)1		1	895.455	895.463
7	(Hex)2(HexNAc)2		1	983.507	983.515
8	(NeuAc)1(Hex)1(HexNAc)2		1	1140.579	1140.589
9	(NeuAc)2(Hex)1(HexNAc)1		1	1256.627	1256.636
10	(NeuAc)1(Hex)2(HexNAc)2		1	1344.678	1344.689

Figure 4.6. Relative quantification of the primary human adipocytes glycome during insulin resistance using $^{13}C/^{12}C$ labeling. (A) left panel: a full FTMS spectrum of $^{13}C/^{12}C$ labeled N-linked glycans in HGINS and LG, right panel: a FTMS spectrum to calculate $^{13}C/^{12}C$ ratios from the sum of isotopic peak areas between the isotopic pairs, (B) left panel: a full FTMS spectrum of $^{13}C/^{12}C$ labeled O-linked glycans in LGPUG and LG, right panel: a FTMS spectrum to calculate $^{13}C/^{12}C$ ratios from the sum of isotopic peak areas between the isotopic pairs.

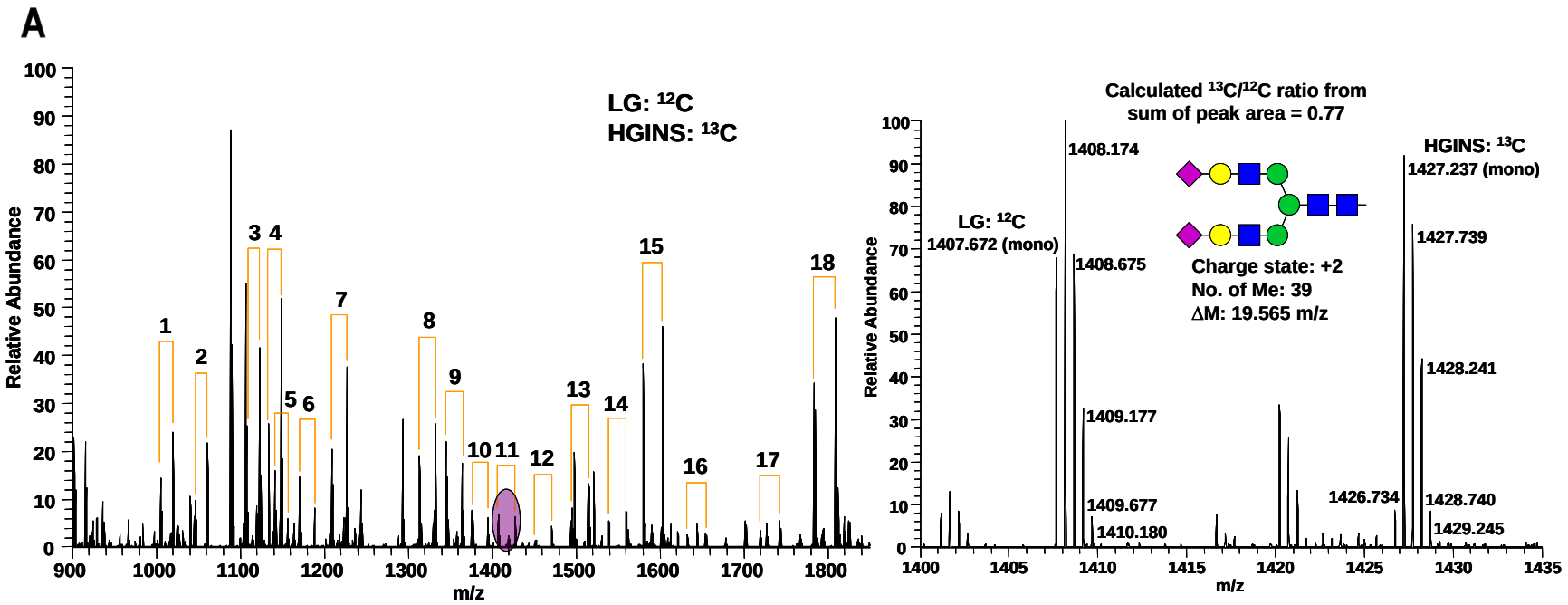
A
LG: 12C
HGINS: 13C
Relative Abundance
m/z
1
2
3 4
5 6
7
8
9
10 11
12
13
14
15
16
17
18
Calculated 13C/12C ratio from
sum of peak area = 0.77
LG: 12C
1407.672 (mono)
1408.174
1408.675
1409.177
1409.677
1410.180
HGINS: 13C
1427.237 (mono)
1427.739
1428.241
1426.734
1428.740
1429.245
Charge state: +2
No. of Me: 39
ΔM: 19.565 m/z

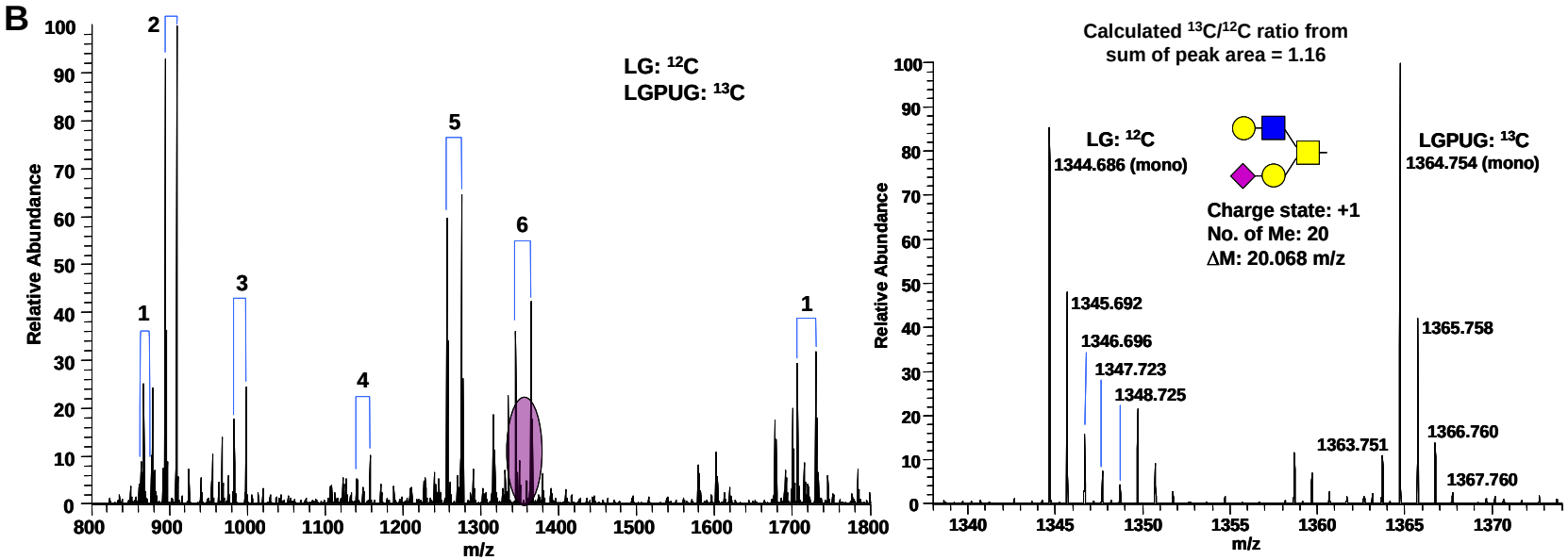
B
Relative Abundance
m/z
LG: 12C
LGPUG: 13C
1
2
3
4
5
6
1
Calculated 13C/12C ratio from
sum of peak area = 1.16
LG: 12C
1344.686 (mono)
LGPUG: 13C
1364.754 (mono)
Charge state: +1
No. of Me: 20
ΔM: 20.068 m/z
1345.692
1346.696
1347.723
1348.725
1363.751
1365.758
1366.760
1367.760

Table 4.1. Total secreted proteins from human adipose tissues by LC-MS/MS.

No.	Protein ID	Identifed Proteins	Subcellular Location[a]
1	Q92484	Acid sphingomyelinase-like phosphodiesterase 3a	Extracellular
2	P07108	Acyl-CoA-binding protein	Cytoplasm
3	Q8IUX7	Adipocyte enhancer-binding protein 1	Membrane
4	P01023	Alpha-2-macroglobulin	Nucleus
5	P06733	Alpha-enolase	Extracellular
6	P15144	Aminopeptidase N	Cytoplasm
7	P01019	Angiotensinogen	Membrane
8	P07355	Annexin A2	Extracellular
9	P08758	Annexin A5	Membrane
10	Q8NCW5	Apolipoprotein A-I binding protein	Extracellular
11	P05090	Apolipoprotein D	Extracellular
12	P02649	Apolipoprotein E	Extracellular
13	P15289	Arylsulfatase A	Cytoplasm
14	P61769	Beta-2-microglobulin	Membrane
15	P21810	Biglycan	Extracellular
16	P43251	Biotinidase	Extracellular
17	P55290	Cadherin-13	Membrane
18	P27797	Calreticulin	Cytoplasm
19	O43852	Calumenin	Cytoplasm
20	P16870	Carboxypeptidase E	Membrane
21	P49747	Cartilage oligomeric matrix protein	Extracellular
22	P07858	Cathepsin B	Cytoplasm
23	P07339	Cathepsin D	Cytoplasm
24	P43235	Cathepsin K	Cytoplasm
25	P07711	Cathepsin L	Cytoplasm
26	Q9UBR2	Cathepsin Z	Cytoplasm
27	P36222	Chitinase-3-like protein 1	Extracellular
28	Q15782	Chitinase-3-like protein 2	Extracellular
29	Q59FG9	Chondroitin sulfate proteoglycan 2 (versican) variant	Extracellular
30	P10909	Clusterin	Extracellular

Table 4.1. continued

31	P02452	Collagen alpha-1(I) chain	Extracellular
32	P02458	Collagen alpha-1(II) chain	Extracellular
33	P02461	Collagen alpha-1(III) chain	Extracellular
34	P02462	Collagen alpha-1(IV) chain	Extracellular
35	P20908	Collagen alpha-1(V) chain	Extracellular
36	P12109	Collagen alpha-1(VI) chain	Extracellular
37	Q02388	Collagen alpha-1(VII) chain	Extracellular
38	P12107	Collagen alpha-1(XI) chain	Extracellular
39	Q99715	Collagen alpha-1(XII) chain	Extracellular
40	P39059	Collagen alpha-1(XV) chain [Contains: Endostatin]	Extracellular
41	P39060	Collagen alpha-1(XVIII) chain [Contains: Endostatin]	Extracellular
42	P08123	Collagen alpha-2(I) chain	Extracellular
43	P08572	Collagen alpha-2(IV) chain [Contains: Canstatin]	Extracellular
44	P05997	Collagen alpha-2(V) chain	Extracellular
45	P12110	Collagen alpha-2(VI) chain	Extracellular
46	P25940	Collagen alpha-3(V) chain	Extracellular
47	P12111	Collagen alpha-3(VI) chain	Extracellular
48	P08253	Collagenase (72 kDa type IV)	Extracellular
49	P00736	Complement C1r subcomponent	Extracellular
50	P09871	Complement C1s subcomponent	Extracellular
51	P01024	Complement C3	Extracellular
52	P29279	Connective tissue growth factor	Extracellular
53	Q9Y240	C-type lectin domain family 11 member A	Extracellular
54	O75462	Cytokine receptor-like factor 1	Extracellular
55	P07585	Decorin	Extracellular
56	Q07507	Dermatopontin	Extracellular
57	Q4VWZ6	Diazepam binding inhibitor, splice form 1c	Cytoplasm
58	Q9UBP4	Dickkopf-related protein 3	Extracellular
59	Q14118	Dystroglycan	Membrane
60	Q13822	Ectonucleotide pyrophosphatase/phosphodiesterase 2	Membrane

Table 4.1. continued

61	Q12805	EGF-containing fibulin-like extracellular matrix protein 1	Extracellular
62	O95967	EGF-containing fibulin-like extracellular matrix protein 2	Extracellular
63	Q9Y6C2	EMILIN-1	Extracellular
64	Q9BXX0	EMILIN-2	Extracellular
65	P61916	Epididymal secretory protein E1	Extracellular
66	Q9Y2E5	Epididymis-specific alpha-mannosidase	Cytoplasm
67	Q16610	Extracellular matrix protein 1	Extracellular
68	P08294	Extracellular superoxide dismutase [Cu-Zn]	Extracellular
69	P35555	Fibrillin-1	Extracellular
70	Q53TP5	Fibroblast activation protein, alpha subunit	Cytoplasm
71	Q06828	Fibromodulin	Extracellular
72	P02751	Fibronectin	Membrane
73	P23142	Fibulin-1	Extracellular
74	P98095	Fibulin-2	Extracellular
75	Q9UBX5	Fibulin-5	Extracellular
76	Q12841	Follistatin-related protein 1	Extracellular
77	P16930	Fumarylacetoacetase	Cytoplasm
78	P09382	Galectin-1	Extracellular
79	Q08380	Galectin-3-binding protein	Membrane
80	Q92820	Gamma-glutamyl hydrolase	Cytoplasm
81	P06396	Gelsolin	Extracellular
82	Q9UJJ9	GlcNAc-1-phosphotransferase subunit gamma	Cytoplasm
83	P07093	Glia-derived nexin	Extracellular
84	P04406	Glyceraldehyde-3-phosphate dehydrogenase	Cytoplasm
85	P35052	Glypican-1	Membrane
86	P28799	Granulins	Extracellular
87	Q14393	Growth-arrest-specific protein 6	Extracellular
88	P00738	Haptoglobin	Extracellular
89	P00739	Haptoglobin-related protein	Extracellular
90	O75629	Human Protein CREG1	Nucleus

Table 4.1. continued

91	P17936	Insulin-like growth factor-binding protein 3	Extracellular
92	P22692	Insulin-like growth factor-binding protein 4	Extracellular
93	P24592	Insulin-like growth factor-binding protein 6	Extracellular
94	Q16270	Insulin-like growth factor-binding protein 7	Extracellular
95	O95965	Integrin beta-like protein 1	Unknown
96	P19823	Inter-alpha-trypsin inhibitor heavy chain H2	Extracellular
97	O14498	ISLR	Extracellular
98	Q08431	Lactadherin	Extracellular
99	Q8NHP8	LAMA-like protein 2	Extracellular
100	Q59H37	Laminin alpha 2 subunit isoform b	Extracellular
101	Q16363	Laminin subunit alpha-4	Extracellular
102	P07942	Laminin subunit beta-1	Extracellular
103	P55268	Laminin subunit beta-2	Extracellular
104	P11047	Laminin subunit gamma-1	Extracellular
105	Q14767	Latent-transforming growth factor beta-binding protein 2	Extracellular
106	Q99538	Legumain	Cytoplasm
107	Q07954	Low-density lipoprotein receptor-related protein 1	Membrane
108	P51884	Lumican	Extracellular
109	P10619	Lysosomal protective protein	Cytoplasm
110	P13473	Lysosome-associated membrane glycoprotein 2	Membrane
111	Q9Y4K0	Lysyl oxidase homolog 2	Extracellular
112	P09603	Macrophage colony-stimulating factor 1	Extracellular
113	Q9UM22	Mammalian ependymin-related protein 1	Nucleus
114	P48740	Mannan-binding lectin serine protease 1	Extracellular
115	P50281	Matrix metalloproteinase-14	Extracellular
116	P01033	Metalloproteinase inhibitor 1	Extracellular
117	P16035	Metalloproteinase inhibitor 2	Extracellular
118	Q71SW6	Muscle type neuropilin 1	Membrane
119	P14543	Nidogen-1	Extracellular
120	Q14112	Nidogen-2	Extracellular

Table 4.1. continued

121	Q02818	Nucleobindin-1	Cytoplasm
122	Q9NRN5	Olfactomedin-like protein 3	Extracellular
123	Q86UD1	Out at first protein homolog	Unknown
124	P26022	Pentraxin-related protein PTX3	Extracellular
125	P62937	Peptidyl-prolyl cis-trans isomerase A	Cytoplasm
126	P23284	Peptidylprolyl isomerase B	Cytoplasm
127	Q15063	Periostin	Extracellular
128	P98160	Perlecan	Membrane
129	Q92626	Peroxidasin homolog	Unknown
130	P30086	Phosphatidylethanolamine-binding protein 1	Cytoplasm
131	P55058	Phospholipid transfer protein	Extracellular
132	P36955	Pigment epithelium-derived factor	Extracellular
133	Q9BTY2	Plasma alpha-L-fucosidase	Extracellular
134	Q9Y646	Plasma glutamate carboxypeptidase	Extracellular
135	P05155	Plasma protease C1 inhibitor	Extracellular
136	P05121	Plasminogen activator inhibitor 1	Extracellular
137	Q9GZP0	Platelet-derived growth factor D	Extracellular
138	P07602	Proactivator polypeptide [Contains: Saposin-A]	Extracellular
139	Q15113	Procollagen C-endopeptidase enhancer 1	Extracellular
140	Q02809	Procollagen-lysine,2-oxoglutarate 5-dioxygenase 1	Cytoplasm
141	P07737	Profilin-1	Cytoplasm
142	P41222	Prostaglandin-H2 D-isomerase	Cytoplasm
143	Q6UXB8	Protease inhibitor 16	Membrane
144	P07237	Protein disulfide-isomerase	Cytoplasm
145	Q15084	Protein disulfide-isomerase A6	Cytoplasm
146	P14618	Pyruvate kinase isozymes M1/M2	Cytoplasm
147	Q96D15	Reticulocalbin-3	Cytoplasm
148	Q99969	Retinoic acid receptor responder protein 2	Membrane
149	O75326	Semaphorin-7A	Membrane
150	Q12884	Seprase	Cytoplasm

Table 4.1. continued

151	Q92743	Serine protease HTRA1	Extracellular
152	P02787	Serotransferrin	Extracellular
153	P09486	SPARC	Extracellular
154	Q9BUD6	Spondin-2	Extracellular
155	Q9BRK5	Stromal cell-derived factor 4	Cytoplasm
156	O00391	Sulfhydryl oxidase 1	Cytoplasm
157	P00441	Superoxide dismutase [Cu-Zn]	Cytoplasm
158	Q9Y490	Talin-1	Membrane
159	P24821	Tenascin	Extracellular
160	P22105	Tenascin-X	Extracellular
161	Q08629	Testican-1	Extracellular
162	P10599	Thioredoxin	Cytoplasm
163	Q16881	Thioredoxin reductase 1	Cytoplasm
164	P07996	Thrombospondin-1	Extracellular
165	P35442	Thrombospondin-2	Extracellular
166	Q6FGX5	TIMP1 protein	Extracellular
167	Q15582	Transforming growth factor-beta-induced protein ig-h3	Extracellular
168	O14773	Tripeptidyl-peptidase 1	Cytoplasm
169	Q6EMK4	Vasorin	Membrane
170	P13611	Versican core protein	Extracellular
171	P08670	Vimentin	Cytoplasm
172	P04004	Vitronectin	Extracellular
173	O76076	WNT1-inducible-signaling pathway protein 2	Extracellular

[a] The subcellular location was determined for each protein based on the Ingenuity Pathway Analysis software (Ingenuity Systems).

Table 4.2. Human adipocytokines regulated a minimum of 150% under both insulin resistant conditions.[a]

No.	Protein ID	Identified Proteins	LGPUG/LG	HGINS/LG	Ave. SC	SD	Ave. Peptides	SD
1	Q96D15	Reticulocalbin-3	9.00	8.52	11.50	2.89	3.00	1.15
2	Q9NRN5	Olfactomedin-like protein 3	5.40	7.57	13.60	6.31	3.00	0.00
3	P09603	Macrophage colony-stimulating factor 1	2.98	5.02	5.00	1.87	1.60	0.55
4	Q59H37	Laminin alpha 2 subunit isoform b	1.73	4.60	11.50	6.45	4.50	1.91
5	Q15113	Procollagen C-endopeptidase enhancer 1	1.53	4.11	14.00	3.56	3.75	0.50
6	Q07507	Dermatopontin	2.01	2.93	10.40	2.88	2.00	0.00
7	Q02809	Procollagen-lysine,2-oxoglutarate 5-dioxygenase 1	2.70	2.80	11.17	4.83	3.83	0.98
8	P36222	Chitinase-3-like protein 1	1.49	2.68	26.00	8.05	6.33	0.52
9	P05997	Collagen alpha-2(V) chain	1.55	2.44	9.33	2.89	2.67	0.58
10	Q9Y240	C-type lectin domain family 11 member A	2.07	2.44	11.00	2.00	3.00	0.00
11	Q06828	Fibromodulin	1.76	2.38	15.75	2.06	2.00	1.15
12	O00391	Sulfhydryl oxidase 1	2.20	2.27	8.17	3.06	2.67	0.52
13	P15144	Aminopeptidase N	2.19	2.03	22.00	13.34	4.33	1.86
14	Q99538	Legumain	1.60	1.92	11.67	4.18	1.83	0.98
15	Q6UXB8	Protease inhibitor 16	1.97	1.75	15.75	1.50	2.50	0.58
16	P09486	SPARC	1.48	1.74	263.00	169.53	10.33	1.37
17	P07942	Laminin subunit beta-1	1.48	1.69	63.67	13.34	16.83	1.72
18	O75326	Semaphorin-7A	1.95	1.66	21.17	8.89	3.67	1.03
19	P10909	Clusterin	1.77	1.63	17.00	6.39	3.17	0.75
20	P24821	Tenascin	1.61	1.54	37.33	4.76	9.83	1.72
No.	Protein ID	Identified Proteins	LG/LGPUG	LG/HGINS	Ave. SC	SD	Ave. Peptides	SD
1	P61769	Beta-2-microglobulin	2.40	1.90	68.17	35.76	3.17	0.98
2	P00739	Haptoglobin-related protein	1.87	1.66	5.67	0.58	2.00	0.00
3	Q16270	Insulin-like growth factor-binding protein 7	1.75	1.59	19.00	9.76	4.33	1.03
4	O95965	Integrin beta-like protein 1	1.68	1.57	9.00	1.41	3.00	0.00

[a] LGPUG: low glucose pluse PUGNAc; HGINS: high glucose pluse insulin as two insulin resistant conditions; Ave. SC: average total spectral count and SD: standard deviation.

Table 4.3. Identification of N-linked glycosylation sites using PNGase F with the incorporation of ^{18}O water in human adipocytokines.

No.	Protein ID	Identifed Proteins	N-linked Peptides[a]
1	P15144	Aminopeptidase N	KLN@YTLSQGHR
2	P21810	Biglycan	LLQVVYLHSNN@ITK
3	P16870	Carboxypeptidase E	GN@ETIVNLIHSTR
4	P07339	Cathepsin D	GSLSYLN@VTR
5	P43235	Cathepsin K	SN@DTLYIPEWEGR
6	P07711	Cathepsin L	YSVAN@DTGFVDIPK
7	P07711	Cathepsin L	YSVAN@DTGFVDIPKQEK
8	P10909	Clusterin	LAN@LTQGEDQYYLR
9	P02461	Collagen alpha-1(III) chain	ASQN@ITYHCK
10	P02461	Collagen alpha-1(III) chain	DGSPGGKGDRGEN@GSPGAPGAPGHPGPPGPVGPAGK
11	P20908	Collagen alpha-1(V) chain	VYCN@FTAGGSTCVFPDKK
12	P12109	Collagen alpha-1(VI) chain	ENYAELLEDAFLKN@VTAQICIDKK
13	P12109	Collagen alpha-1(VI) chain	GEDGPAGN@GTEGFPGFPGYPGNR
14	P12109	Collagen alpha-1(VI) chain	N@FTAADWGQSR
15	P12109	Collagen alpha-1(VI) chain	RN@FTAADWGQSR
16	Q02388	Collagen alpha-1(VII) chain	TAPEPVGRVSRLQILN@ASSDVLR
17	Q99715	Collagen alpha-1(XII) chain	EAGN@ITTDGYEILGK
18	P08123	Collagen alpha-2(I) chain	LLANYASQN@ITYHCK
19	P05997	Collagen alpha-2(V) chain	EASQN@ITYICK
20	P12111	Collagen alpha-3(VI) chain	GNPGEPGLN@GTTGPKGIR
21	P12111	Collagen alpha-3(VI) chain	GPPGVN@GTQGFQGCPGQR
22	P12111	Collagen alpha-3(VI) chain	GYPGDEGGPGERGPPGVN@GTQGFQGCPGQR
23	P09871	Complement C1s subcomponent	NCGVN@CSGDVFTALIGEIASPNYPKPYPENSR
24	O75462	Cytokine receptor-like factor 1	VLN@ASTLALALANLN@GSR
25	O75462	Cytokine receptor-like factor 1	VVDDVSN@QTSCR
26	P07585	Decorin	IADTN@ITSIPQGLPPSLTELHLDGNK
27	P07585	Decorin	LGLSFNSISAVDN@GSLANTPHLR
28	Q9UBP4	Dickkopf-related protein 3	GSN@GTICDNQR
29	Q13822	Ectonucleotide pyrophosphatase/phosphodiesterase 2	AEGWEEGPPTVLSDSPWTN@ISGSCK

Table 4.3 Continued

30	Q13822	Ectonucleotide pyrophosphatase/phosphodiesterase 2	AIIAN@LTCK
31	Q9Y6C2	EMILIN-1	LGALN@SSLQLLEDR
32	P35555	Fibrillin-1	TAIFAFN@ISHVSNK
33	P02751	Fibronectin	DQCIVDDITYNVN@DTFHKR
34	P02751	Fibronectin	DQCIVDDITYNVN@DTFHK
35	P02751	Fibronectin	LDAPTNLQFVN@ETDSTVLVR
36	Q12841	Follistatin-related protein 1	GSN@YSEILDK
37	Q12841	Follistatin-related protein 1	GSN@YSEILDKYFK
38	P09382	Galectin-1	FNAHGDANTIVCNSK
39	Q08380	Galectin-3-binding protein	ALGFEN@ATQALGR
40	Q08380	Galectin-3-binding protein	DAGVVCTN@ETR
41	Q08380	Galectin-3-binding protein	TVIRPFYLTN@SSGVD
42	P00738	Haptoglobin	VVLHPN@YSQVDIGLIK
43	O75629	Human Protein CREG1	LN@ITNIWVLDYFGGPK
44	P17936	Insulin-like growth factor-binding protein 3	GLCVN@ASAVSR
45	O14498	ISLR	SLDLSHNLISDFAWSDLHN@LSALQLLK
46	Q8NHP8	LAMA-like protein 2	SDLNPAN@GSYPFKALR
47	Q16363	Laminin subunit alpha-4	DAVRN@LTEVVPQLLDQLR
48	Q16363	Laminin subunit alpha-4	FYFGGSPISAQYAN@FTGCISNAYFTR
49	Q16363	Laminin subunit alpha-4	LITEEAN@R
50	Q16363	Laminin subunit alpha-4	LTLSELDDIIKN@ASGIYAEIDGAK
51	Q16363	Laminin subunit alpha-4	RPASN@VSASIQR
52	P07942	Laminin subunit beta-1	LSDTTSQSN@STAK
53	P11047	Laminin subunit gamma-1	VN@NTLSSQISR
54	P11047	Laminin subunit gamma-1	KYEQAKN@ISQDLEK
55	P11047	Laminin subunit gamma-1	LLNN@LTSIK
56	P11047	Laminin subunit gamma-1	TAN@DTSTEAYNLLLR
57	P11047	Laminin subunit gamma-1	TLAGEN@QTAFEIEELNR
58	P11047	Laminin subunit gamma-1	VNDN@KTAAEEALR
59	Q14767	Latent-transforming growth factor beta-binding protein 2	DGTQQAVPLEHPSSPWGLN@LTEK

Table 4.3 Continued

60	P51884	Lumican	AFEN@VTDLQWLILDHNLLENSK
61	P51884	Lumican	LGSFEGLVN@LTFIHLQHNR
62	P51884	Lumican	LHINHNN@LTESVGPLPK
63	P13473	Lysosome-associated membrane glycoprotein 2	IAVQFGPGFSWIAN@FTK
64	P01033	Metalloproteinase inhibitor 1	AKFVGTPEVN@QTTLYQR
65	P01033	Metalloproteinase inhibitor 1	FVGTPEVN@QTTLYQR
66	P01033	Metalloproteinase inhibitor 1	SHN@RSEEFLIAGK
67	Q9NRN5	Olfactomedin-like protein 3	IYVLDGTQN@DTAFVFPR
68	P26022	Pentraxin-related protein PTX3	ATDVLN@K
69	Q15063	Periostin	EVN@DTLLVNELK
70	Q15063	Periostin	IFLKEVN@DTLLVNELK
71	P98160	Perlecan	SLTQGSLIVGDLAPVN@GTSQGK
72	P55058	Phospholipid transfer protein	VSN@VSCQASVSR
73	P36955	Pigment epithelium-derived factor	VTQN@LTLIEESLTSEFIHDIDR
74	P36955	Pigment epithelium-derived factor	VTQN@LTLIEESLTSEFIHDIDRELK
75	P05155	Plasma protease C1 inhibitor	VGQLQLSHN@LSLVILVPQNLK
76	P05155	Plasma protease C1 inhibitor	VLSN@NSDANLELINTWVAK
77	P07602	Proactivator polypeptide [Contains: Saposin-A]	TN@STFVQALVEHVK
78	P07602	Proactivator polypeptide [Contains: Saposin-A]	LIDNN@KTEK
79	P07602	Proactivator polypeptide [Contains: Saposin-A]	LIDNN@KTEKEILDAFDK
80	P07602	Proactivator polypeptide [Contains: Saposin-A]	NLEKN@STK
81	P07602	Proactivator polypeptide [Contains: Saposin-A]	NLEKN@STKQEILAALEK
82	P07602	Proactivator polypeptide [Contains: Saposin-A]	TN@STFVQALVEHVKEECDR
83	P09486	SPARC	VCSNDN@K
84	P09486	SPARC	VCSNDN@KTFDSSCHFFATK
85	P24821	Tenascin	N@TTSYVLR
86	P24821	Tenascin	LN@YSLPTGQWVGVQLPR
87	P07996	Thrombospondin-1	VVN@STTGPGEHLR
88	P35442	Thrombospondin-2	VVN@STTGTGEHLR
89	Q6FGX5	TIMP1 protein	FVGTPEVN@QTTLYQR

Table 4.3 Continued

90	Q6FGX5	TIMP1 protein	SHN@RSEEFLIAGK
91	Q6EMK4	Vasorin	LHEITN@ETFR

[a] An @ indicates the site of N-linked glycosylation.

.

Table S4.1. The list of secreted proteins for a single peptide detection from human adipose tissues.

No.	Protein ID	Identifed Proteins	Subcellular Location[a]
1	O75882	Attractin	Extracellular
2	P15291	Beta-1,4-galactosyltransferase 1	Cytoplasm
3	P01034	Cystatin-C	Extracellular
4	P15502	Elastin	Extracellular
5	P19883	Follistatin	Extracellular
6	P17900	Ganglioside GM2 activator	Cytoplasm
7	P02788	Growth-inhibiting protein 12	Extracellular
8	P03956	Interstitial collagenase	Extracellular
9	P25391	Laminin subunit alpha-1	Extracellular
10	Q5VUM2	Laminin, alpha 2	Extracellular
11	P14174	Macrophage migration inhibitory factor	Extracellular
12	Q13361	Microfibrillar-associated protein 5	Extracellular
13	Q99497	Oncogene DJ1	Unknown
14	P45877	Peptidyl-prolyl cis-trans isomerase C	Cytoplasm
15	Q92954	Proteoglycan-4	Extracellular
16	Q9HCB6	Spondin-1	Extracellular
17	Q9NPK8	Tenascin XB	Extracellular

[a] The subcellular location was determined for each protein based on the Ingenuity Pathway Analysis software (Ingenuity Systems).

Table S4.2. Human adipocytokines regulated a minimum of 150% under one of the insulin resistant conditions.

No.	Protein ID	Identified Proteins	LGPUG/LG	HGINS/LG	Ave. SC	SD	Ave. Peptides	SD
1	P17936	Insulin-like growth factor-binding protein 3	1.78	1.02	12.83	2.23	2.67	0.52
2	P41222	Prostaglandin-H2 D-isomerase	1.73	1.11	5.50	4.04	1.25	0.50
3	P04406	Glyceraldehyde-3-phosphate dehydrogenase	1.71	1.17	15.50	4.72	3.33	0.52
4	P10599	Thioredoxin	1.57	0.80	21.17	5.88	3.00	0.89
5	P26022	Pentraxin-related protein PTX3	1.46	1.30	74.67	16.37	8.00	1.67
6	Q07954	Low-density lipoprotein receptor-related protein 1	[3.84/0][a]	[2.11/0]	5.50	0.58	2.50	0.58
7	P02787	Serotransferrin	1.35	3.67	16.75	7.23	5.00	2.31
8	Q92743	Serine protease HTRA1	1.10	3.65	7.40	1.52	2.80	0.84
9	P02649	Apolipoprotein E	0.82	2.90	19.67	13.68	5.00	2.68
10	P05121	Plasminogen activator inhibitor 1	0.70	2.58	13.25	1.50	2.00	1.15
11	Q08629	Testican-1	1.22	2.52	12.83	4.67	3.50	0.55
12	P06396	Gelsolin	1.18	2.52	23.17	12.16	4.50	2.07
13	P12110	Collagen alpha-2(VI) chain	0.78	2.26	17.00	6.84	4.17	0.98
14	P15289	Arylsulfatase A	1.41	2.10	6.33	2.34	1.83	0.75
15	P13611	Versican core protein	1.33	2.03	51.00	7.38	9.33	1.51
16	P12111	Collagen alpha-3(VI) chain	1.37	1.99	38.33	20.47	10.83	6.01
17	Q16363	Laminin subunit alpha-4	1.20	1.98	41.33	29.37	8.67	3.67
18	P08758	Annexin A5	1.44	1.89	13.20	9.26	4.20	2.05
19	Q12841	Follistatin-related protein 1	1.27	1.85	82.83	15.22	11.00	1.67
20	Q14767	Latent-transforming growth factor beta-binding protein 2	1.12	1.81	40.67	6.68	10.00	1.55
21	Q08380	Galectin-3-binding protein	1.44	1.78	68.33	4.72	10.17	1.17
22	Q02818	Nucleobindin-1	1.01	1.60	33.33	1.97	6.83	1.47

Table S4.2. Continued. Human adipocytokines regulated a minimum of 150% under one of the insulin resistant conditions.

No.	Protein ID	Identified Proteins	LGPUG/LG	HGINS/LG	Ave. SC	SD	Ave. Peptides	SD
23	P27797	Calreticulin	0.92	1.59	44.50	28.59	4.83	1.17
24	P07355	Annexin A2	0.90	1.56	29.75	0.96	6.50	0.58
25	P35052	Glypican-1	0.84	1.54	5.75	0.50	2.25	0.50
26	Q99715	Collagen alpha-1(XII) chain	1.30	1.53	106.67	51.02	21.67	7.31
27	O95967	EGF-containing fibulin-like extracellular matrix protein 2	0.43	1.51	7.67	1.15	2.33	0.58
28	P98095	Fibulin-2	1.13	1.46	101.83	34.75	16.33	3.01
No.	Protein ID	Identified Proteins	LG/LGPUG	LG/HGINS	Ave. SC	SD	Ave. Peptides	SD
1	P07093	Glia-derived nexin	4.03	0.92	5.00	1.73	2.00	0.00
2	Q9Y4K0	Lysyl oxidase homolog 2	2.44	1.07	16.00	5.66	4.75	1.71
3	O95967	EGF-containing fibulin-like extracellular matrix protein 2	2.32	0.66	7.67	1.15	2.33	0.58
4	O14549	Osteoblast specific cysteine-rich protein	1.73	1.44	19.00	11.21	4.00	0.89
5	P20908	Collagen alpha-1(V) chain	1.62	1.30	35.17	18.49	7.17	2.04
6	Q9BRK5	Stromal cell derived factor 4	1.21	3.00	11.80	8.87	1.80	1.10
7	P23284	Peptidylprolyl isomerase B	0.96	1.83	25.33	12.89	3.00	1.55
8	P62937	Peptidyl-prolyl cis-trans isomerase A	0.75	1.64	18.00	6.98	2.50	0.58

[a] Brackets indicate the average number of normalized spectral counts assigned to the proteins when no peptides were detected under a given condition.

Table S4.3. Characterization of total N-linked glycans from human adipocytes by MS-MS and TIM scan.

No.	N-linked oligosaccharide composition	Z	$[M+zNa]^{z+}$ m/z (mono)	No.	N-linked oligosaccharide composition	Z	$[M+zNa]^{z+}$ m/z (mono)
1	(Man)1(GlcNAc)2	1	763.384	82	(Gal)2(GlcNAc)3(Fuc)1(Man)3(GlcNAc)2(Fuc)1	2	1343.165
2	(Man)1(GlcNAc)2(Fuc)1	1	937.473	83	(NeuAc)1(Gal)2(GlcNAc)3(Man)3(GlcNAc)2	2	1349.663
3	(Man)2(GlcNAc)2	1	967.484	84	(Gal)3(GlcNAc)3(Man)3(GlcNAc)2(Fuc)1	2	1358.171
4	(Man)2(GlcNAc)2(Fuc)1	1	1141.573	85	(Gal)1(GlcNAc)4(Fuc)1(Man)3(GlcNAc)2(Fuc)1	2	1363.679
5	(Man)3(GlcNAc)2	1	1171.583	86	(NeuAc)1(Gal)1(GlcNAc)4(Man)3(GlcNAc)2	2	1370.176
6	(Man)3(GlcNAc)2(Fuc)1	1	1345.673	87	(Gal)4(GlcNAc)3(Man)3(GlcNAc)2	2	1373.176
7	(Man)4(GlcNAc)2	1	1375.683	88	(Gal)2(GlcNAc)4(Man)3(GlcNAc)2(Fuc)1	2	1378.684
8	(GlcNAc)1(Man)2(GlcNAc)2(Fuc)1	1	1386.699	89	(NeuAc)2(Gal)1(GlcNAc)2(Man)3(GlcNAc)2(Fuc)1	2	1392.681
9	(GlcNAc)1(Man)3(GlcNAc)2	1	1416.710	90	(Gal)3(GlcNAc)4(Man)3(GlcNAc)2	2	1393.689
		2	719.850	91	(Gal)1(GlcNAc)5(Man)3(GlcNAc)2(Fuc)1	2	1399.197
10	(Man)4(GlcNAc)2(Fuc)1	1	1549.772	92	(NeuAc)1(Gal)2(GlcNAc)2(Fuc)1(Man)3(GlcNAc)2(Fuc)1	2	1401.189
11	(Man)5(GlcNAc)2	1	1579.783	93	(NeuAc)2(Gal)2(GlcNAc)2(Man)3(GlcNAc)2	2	1407.687
		2	801.386			3	946.121
12	(GlcNAc)1(Man)3(GlcNAc)2(Fuc)1	1	1590.799	94	(NeuAc)1(Gal)3(GlcNAc)2(Man)3(GlcNAc)2(Fuc)1	2	1416.194
		2	806.894	95	(Gal)1(GlcNAc)1(Man)8(GlcNAc)2(Fuc)1	2	1419.194
13	(Gal)1(GlcNAc)1(Man)3(GlcNAc)2	1	1620.810	96	(GlcNAc)6(Man)3(GlcNAc)2(Fuc)1	2	1419.710
		2	821.900	97	(NeuAc)1(Gal)1(GlcNAc)3(Fuc)1(Man)3(GlcNAc)2(Fuc)1	2	1421.702
14	(GlcNAc)2(Man)3(GlcNAc)2	1	1661.836	98	(Gal)2(GlcNAc)3(Fuc)2(Man)3(GlcNAc)2(Fuc)1	2	1430.210
15	(Man)5(GlcNAc)2(Fuc)1	1	1753.872	99	(NeuAc)1(Gal)2(GlcNAc)2(Man)2(Man)3(GlcNAc)2	2	1431.199
16	(Man)6(GlcNAc)2	1	1783.883	100	(NeuAc)1(Gal)2(GlcNAc)3(Man)3(GlcNAc)2(Fuc)1	2	1436.707
		2	903.436	101	(Gal)3(GlcNAc)3(Fuc)1(Man)3(GlcNAc)2(Fuc)1	2	1445.215
17	(Gal)1(GlcNAc)1(Man)3(GlcNAc)2(Fuc)1	1	1794.899	102	(NeuAc)1(Gal)3(GlcNAc)3(Man)3(GlcNAc)2	2	1451.713
		2	908.944			3	975.472

Table S4.3. Continued. Characterization of total N-linked glycans from human adipocytes by MS-MS and TIM scan.

18	(GlcNAc)1(Man)5(GlcNAc)2	1	1824.909	103	(NeuAc)1(Gal)1(GlcNAc)4(Man)3(GlcNAc)2(Fuc)1	2	1457.221
		2	923.950	104	(Gal)2(GlcNAc)3(Man)2(Man)3(GlcNAc)2(Fuc)1	2	1460.220
19	(GlcNAc)2(Man)3(GlcNAc)2(Fuc)1	1	1835.925	105	(Gal)4(GlcNAc)3(Man)3(GlcNAc)2(Fuc)1	2	1460.220
		2	929.458	106	(Gal)2(GlcNAc)4(Fuc)1(Man)3(GlcNAc)2(Fuc)1	2	1465.728
20	(Gal)1(GlcNAc)2(Man)3(GlcNAc)2	1	1865.936	107	(NeuAc)1(Gal)2(GlcNAc)4(Man)3(GlcNAc)2	2	1472.226
		2	944.463			3	989.147
21	(GlcNAc)3(Man)3(GlcNAc)2	1	1906.963	108	(Gal)3(GlcNAc)4(Man)3(GlcNAc)2(Fuc)1	2	1480.734
		2	964.976	109	(NeuAc)2(Gal)2(GlcNAc)2(Man)3(GlcNAc)2(Fuc)1	2	1494.731
22	(Man)6(GlcNAc)2(Fuc)1	1	1957.972	110	(Gal)4(GlcNAc)4(Man)3(GlcNAc)2	2	1495.739
		2	990.481	111	(NeuAc)1(Gal)1(GlcNAc)2(Fuc)1(Man)5(GlcNAc)2(Fuc)1	2	1503.239
23	(Gal)1(GlcNAc)1(Fuc)1(Man)3(GlcNAc)2(Fuc)1	1	1968.988	112	(NeuAc)2(Gal)3(GlcNAc)2(Man)3(GlcNAc)2	2	1509.736
		2	995.989			3	1014.154
24	(NeuAc)1(Gal)1(GlcNAc)1(Man)3(GlcNAc)2	1	1981.983	113	(NeuAc)2(Gal)1(GlcNAc)3(Man)3(GlcNAc)2(Fuc)1	2	1515.244
		2	1002.487			3	1017.826
25	(Man)7(GlcNAc)2	1	1987.983	114	(NeuAc)2(Gal)1(GalNAc)1(GlcNAc)2(Man)3(GlcNAc)2(Fuc)1	2	1515.244
		2	1005.486			3	1017.826
26	(GlcNAc)1(Man)5(GlcNAc)2(Fuc)1	1	1998.999	115	(Man)12(GlcNAc)2	2	1515.736
		2	1010.994	116	(Gal)3(GlcNAc)5(Man)3(GlcNAc)2	2	1516.252
27	(Gal)1(GlcNAc)1(Man)5(GlcNAc)2	2	1025.999	117	(NeuAc)1(Gal)2(GlcNAc)3(Fuc)1(Man)3(GlcNAc)2(Fuc)1	2	1523.752
28	(Gal)1(GlcNAc)2(Man)3(GlcNAc)2(Fuc)1	2	1031.507	118	(NeuAc)2(Gal)2(GlcNAc)3(Man)3(GlcNAc)2	2	1530.250
29	(Gal)2(GlcNAc)2(Man)3(GlcNAc)2	2	1046.513	119	(NeuAc)1(Gal)3(GlcNAc)3(Man)3(GlcNAc)2(Fuc)1	2	1538.757
30	(GlcNAc)3(Man)3(GlcNAc)2(Fuc)1	2	1052.021			3	1033.502
31	(Gal)1(GlcNAc)3(Man)3(GlcNAc)2	2	1067.026	120	(NeuAc)1(Gal)2(GlcNAc)4(Fuc)1(Man)3(GlcNAc)2	2	1559.271
32	(NeuAc)1(Gal)1(GlcNAc)1(Man)3(GlcNAc)2(Fuc)1	2	1089.531			3	1047.177

Table S4.3. Continued. Characterization of total N-linked glycans from human adipocytes by MS-MS and TIM scan.

33	(NeuAc)1(Gal)1(GlcNAc)1(Man)1(Man)3(GlcNAc)2	2	1104.536	121	(Gal)5(GlcNAc)3(Man)3(GlcNAc)2(Fuc)1	2	1562.270
34	(Man)8(GlcNAc)2	2	1107.536	122	(NeuAc)1(Gal)3(GlcNAc)4(Man)3(GlcNAc)2	2	1574.276
35	(Gal)1(GlcNAc)1(Man)5(GlcNAc)2(Fuc)1	2	1113.044			3	1057.181
36	(Gal)1(GlcNAc)2(Fuc)1(Man)3(GlcNAc)2(Fuc)1	2	1118.552	123	(NeuAc)2(Gal)2(GlcNAc)3(Man)3(GlcNAc)2(Fuc)1	2	1617.294
37	(NeuAc)1(Gal)1(GlcNAc)2(Man)3(GlcNAc)2	2	1125.050			3	1085.860
38	(Gal)1(GlcNAc)1(Man)3(Man)3(GlcNAc)2	2	1128.049	124	(Gal)4(GlcNAc)5(Man)3(GlcNAc)2	2	1618.302
39	(Gal)2(GlcNAc)2(Man)3(GlcNAc)2(Fuc)1	2	1133.557	125	(NeuAc)2(Gal)3(GlcNAc)3(Man)3(GlcNAc)2	2	1632.300
40	(Gal)3(GlcNAc)2(Man)3(GlcNAc)2	2	1148.563			3	1095.863
41	(Gal)1(GlcNAc)3(Man)3(GlcNAc)2(Fuc)1	2	1154.071	126	(NeuAc)1(Gal)3(GlcNAc)4(Man)3(GlcNAc)2(Fuc)1	2	1661.321
42	(Gal)2(GlcNAc)3(Man)3(GlcNAc)2	2	1169.076	127	(NeuAc)1(Gal)4(GlcNAc)4(Man)3(GlcNAc)2	2	1676.326
43	(Gal)1(GlcNAc)3(Man)4(GlcNAc)2	2	1169.076			3	1125.214
44	(GlcNAc)3(Man)5(GlcNAc)2	2	1169.076	128	(NeuAc)2(Gal)2(GlcNAc)3(Fuc)1(Man)3(GlcNAc)2(Fuc)1	2	1704.339
45	(GlcNAc)4(Man)3(GlcNAc)2(Fuc)1	2	1174.584	129	(NeuAc)1(Gal)3(GlcNAc)3(Fuc)2(Man)3(GlcNAc)2(Fuc)1	2	1712.847
46	(NeuAc)1(Gal)1(GlcNAc)1(Fuc)1(Man)3(GlcNAc)2(Fuc)1	2	1176.576			3	1149.561
47	(Gal)1(GlcNAc)4(Man)3(GlcNAc)2	2	1189.589	130	(NeuAc)2(Gal)3(GlcNAc)3(Man)3(GlcNAc)2(Fuc)1	2	1719.344
48	(NeuAc)1(Gal)2(GlcNAc1)(Man)3(GlcNAc)2(Fuc)1	2	1191.581			3	1153.893
49	(Man)8(GlcNAc)2(Fuc)1	2	1194.581	131	(NeuAc)1(Gal)2(GlcNAc)4(Fuc)2(Man)3(GlcNAc)2(Fuc)1	2	1733.360
50	(Gal)1(GlcNAc)1(Fuc)1(Man)2(Man)3(GlcNAc)2(Fuc)1	2	1200.089			3	1163.237
51	(Gal)1(GlcNAc)2(Fuc)2(Man)3(GlcNAc)2(Fuc)1	2	1205.597	132	(NeuAc)2(Gal)2(GlcNAc)4(Man)3(GlcNAc)2(Fuc)1	2	1739.858
52	(NeuAc)1(Gal)3(GlcNAc1)(Man)3(GlcNAc)2	2	1206.586			3	1167.568
53	(Man)9(GlcNAc)2	2	1209.586	133	(NeuAc)1(Gal)4(GlcNAc)4(Man)3(GlcNAc)2(Fuc)1	2	1763.370
54	(GlcNAc)5(Man)3(GlcNAc)2	2	1210.103			3	1183.244
55	(NeuAc)1(Gal)1(GlcNAc)2(Man)3(GlcNAc)2(Fuc)1	2	1212.094	134	(NeuAc)1(Gal)5(GlcNAc)4(Man)3(GlcNAc)2	2	1778.376

Table S4.3. Continued. Characterization of total N-linked glycans from human adipocytes by MS-MS and TIM scan.

57	(NeuAc)1(Gal)2(GlcNAc)2(Man)3(GlcNAc)2	2	1227.100	135	(NeuAc)1(Gal)4(GlcNAc)5(Man)3(GlcNAc)2	2	1798.889
58	(Gal)1(GlcNAc1)(Man)4(Man)3(GlcNAc)2	2	1230.099	136	(NeuAc)2(Gal)3(GlcNAc)3(Fuc)1(Man)3(GlcNAc)2(Fuc)1	2	1806.389
59	(Gal)3(GlcNAc)2(Man)3(GlcNAc)2(Fuc)1	2	1235.607	137	(NeuAc)3(Gal)3(GlcNAc)3(Man)3(GlcNAc)2	2	1812.887
60	(Gal)1(GlcNAc)3(Fuc)1(Man)3(GlcNAc)2(Fuc)1	2	1241.115			3	1216.254
61	(NeuAc)1(Gal)1(GlcNAc)3(Man)3(GlcNAc)2	2	1247.613	138	(NeuAc)2(Gal)3(GlcNAc)4(Man)3(GlcNAc)2(Fuc)1	3	1235.602
62	(Gal)4(GlcNAc)2(Man)3(GlcNAc)2	2	1250.613	139	(NeuAc)1(Gal)4(GlcNAc)4(Fuc)1(Man)3(GlcNAc)2(Fuc)1	2	1850.415
63	(Gal)2(GlcNAc)3(Man)3(GlcNAc)2(Fuc)1	2	1256.121			3	1241.273
64	(GlcNAc)4(Fuc)1(Man)3(GlcNAc)2(Fuc)1	2	1261.629	140	(NeuAc)2(Gal)4(GlcNAc)4(Man)3(GlcNAc)2	2	1856.913
65	(NeuAc)2(Gal)1(GlcNAc1)(Man)3(GlcNAc)2(Fuc)1	2	1270.118			3	1245.605
66	(Gal)3(GlcNAc)3(Man)3(GlcNAc)2	2	1271.126	141	(NeuAc)1(Gal)3(GlcNAc)5(Fuc)1(Man)3(GlcNAc)2(Fuc)1	3	1254.949
67	(Gal)1(GlcNAc)4(Man)3(GlcNAc)2(Fuc)1	2	1276.634	142	(NeuAc)1(Gal)6(GlcNAc)4(Man)3(GlcNAc)2	3	1261.280
68	(Gal)2(GlcNAc)4(Man)3(GlcNAc)2	2	1291.639	143	(NeuAc)2(Gal)3(GlcNAc)3(Fuc)2(Man)3(GlcNAc)2(Fuc)1	3	1269.952
69	(NeuAc)1(Gal)1(GlcNAc1)(Man)2(Man)3(GlcNAc)2(Fuc)1	2	1293.631	144	(NeuAc)3(Gal)3(GlcNAc)3(Man)3(GlcNAc)2(Fuc)1	2	1899.931
70	(GlcNAc)5(Man)3(GlcNAc)2(Fuc)1	2	1297.147			3	1274.284
71	(NeuAc)1(Gal)1(GlcNAc)2(Fuc)1(Man)3(GlcNAc)2(Fuc)1	2	1299.139	145	(NeuAc)3(Gal)4(GlcNAc)3(Man)3(GlcNAc)2	3	1284.288
72	(NeuAc)2(Gal)1(GlcNAc)2(Man)3(GlcNAc)2	2	1305.637	146	(Gal)4(GalNAc)1(GlcNAc)5(Fuc)1(Man)3(GlcNAc)2(Fuc)1	3	1284.300
73	(Gal)2(GlcNAc)2(Fuc)2(Man)3(GlcNAc)2(Fuc)1	2	1307.647	147	(NeuAc)2(Gal)5(GlcNAc)3(Man)3(GlcNAc)2(Fuc)1	3	1289.959
		3	879.428	148	(NeuAc)3(Gal)3(GlcNAc)4(Man)3(GlcNAc)2	2	1935.450
74	(Glc)1(Man)9(GlcNAc)2	2	1311.636			3	1297.963
75	(Gal)1(GlcNAc)5(Man)3(GlcNAc)2	2	1312.152	149	(NeuAc)2(Gal)4(GlcNAc)4(Man)3(GlcNAc)2(Fuc)1	2	1943.957
		3	882.431			3	1303.635

Table S4.3. Continued. Characterization of total N-linked glycans from human adipocytes by MS-MS and TIM scan.

76	(NeuAc)1(Gal)2(GlcNAc)2(Man)3(GlcNAc)2(Fuc)1	2	1314.144	150	(NeuAc)3(Gal)3(GlcNAc)3(Fuc)1(Man)3(GlcNAc)2(Fuc)1	3	1332.314
		3	883.759	151	(NeuAc)4(Gal)3(GlcNAc)3(Man)3(GlcNAc)2	2	1993.473
77	(Gal)1(GlcNAc)2(Fuc)1(Man)2(Man)3(GlcNAc)2(Fuc)1	2	1322.652	152	(NeuAc)3(Gal)4(GlcNAc)4(Man)3(GlcNAc)2	3	1365.996
78	(Gal)3(GlcNAc)2(Fuc)1(Man)3(GlcNAc)2(Fuc)1	2	1322.652	153	(NeuAc)3(Gal)4(GlcNAc)4(Man)3(GlcNAc)2(Fuc)1	3	1424.026
79	(NeuAc)1(Gal)3(GlcNAc)2(Man)3(GlcNAc)2	2	1329.150	154	(NeuAc)3(Gal)3(GlcNAc)5(Man)3(GlcNAc)2(Fuc)1	3	1437.702
80	(NeuAc)1(Gal)1(GlcNAc)3(Man)3(GlcNAc)2(Fuc)1	2	1334.658	155	(NeuAc)4(Gal)4(GlcNAc)4(Man)3(GlcNAc)2(Fuc)1	3	1544.417
81	(Gal)4(GlcNAc)2(Man)3(GlcNAc)2(Fuc)1	2	1337.657				

Table S4.4. Characterization of total O-linked glycans from human adipocytes by NS-MS and TIM scan.

No.	O-linked oligosaccharide composition	Z	$[M+zNa]^{z+}$ m/z (mono)
1	(Hex)1(HexNAc)1 (HexNAc)1(Hex)1	1	534.289
2	(Xyl)2(Glc)1	1	609.310
3	(NeuAc)1(Hex)1	1	650.337
4	(Hex)1(HexNAc)1(Hex)1	1	738.389
5	(HexNAc)2(Hex)1 (Hex)1(HexNAc)2	1	779.415
6	(NeuAc)1(Hex)1(HexNAc)1	1	895.463
7	(Hex)2(HexNAc)2	1	983.515
8	(NeuAc)1(Hex)1(HexNAc)1(Fuc)1	1	1069.552
9	(NeuAc)1(Hex)1(HexNAc)1(Hex)1	1	1099.563
10	(NeuAc)1(Hex)1(HexNAc)2	1	1140.589
11	(Hex)2(HexNAc)2(Hex)1 (Hex)3(HexNAc)2	1	1187.615
12	(NeuAc)2(Hex)1(HexNAc)1	1	1256.636
13	(NeuAc)1(Hex)1(Fuc)1(HexNAc)2	1	1314.678
14	(NeuAc)1(Hex)2(HexNAc)2	1	1344.689
15	(HexA)1(Hex)2(HexNAc)2(Hex)1	1	1405.694
16	(NeuAc)2(Hex)1(HexNAc)2	1	1501.763
17	(NeuAc)1(Hex)2(Fuc)1(HexNAc)2	1	1518.778
18	(NeuAc)1(Hex)2(HexNAc)3	1	1589.815
19	(NeuAc)2(Hex)1(Fuc)1(HexNAc)2	1	1675.852
20	(NeuAc)2(Hex)2(HexNAc)2	1 2	1705.862 864.426
21	(NeuAc)1(Hex)3(HexNAc)3	1	1793.915
22	(NeuAc)2(Hex)2(Fuc)1(HexNAc)2	1 2	1879.952 951.471
23	(NeuAc)2(Hex)2(Fuc)1(HexNAc)2(Hex)1	2	1053.521
24	(NeuAc)2(Hex)2(Fuc)1(HexNAc)2(HexNAc)1	2	1074.034
25	(NeuAc)2(Hex)3(HexNAc)3	2	1089.039
26	(NeuAc)1(Hex)4(HexNAc)4	2	1133.065
27	(NeuAc)2(Hex)4(Fuc)1(HexNAc)2	2	1155.570
28	(Hex)6(HexNAc)4	2	1156.578
29	(Hex)3(Fuc)1(HexNAc)6	2	1182.600

Table S4.5. Relative quantification of N-linked glycans from human adipocytes between insulin resistant conditions and insulin response condition by $^{13}C/^{12}C$ ratio and prevalence ratio.

No.	N-linked oligosaccharide composition	Z	$[M+zNa]^{z+}$ (mono)		DM (m/z)	LGPUG/LG		HGINS/LG	
			^{12}C	^{13}C		$^{13}C/^{12}C$ ratios	SD	$^{13}C/^{12}C$ ratios	SD
1	(Man)2(GlcNAc)2	1	967.484	981.531	14.047	0.49	0.31	0.58	0.34
2	(Man)2(GlcNAc)2(Fuc)1	1	1141.573	1157.626	16.054	0.30	0.14	0.39	0.15
3	(Man)3(GlcNAc)2	1	1171.583	1188.640	17.057	0.35	0.12	0.49	0.13
4	(Man)3(GlcNAc)2(Fuc)1	1	1345.673	1364.736	19.064	0.32	0.01	0.55	0.01
5	(Man)4(GlcNAc)2	1	1375.683	1395.750	20.067	0.52	0.06	0.59	0.10
6	(Man)5(GlcNAc)2	1	1579.783	1602.860	23.077	0.74	0.25	0.80	0.31
		2	801.386	812.925	11.539	0.64	0.33	0.79	0.33
7	(GlcNAc)1(Man)3(GlcNAc)2(Fuc)1	1	1590.799	1612.873	22.074	0.97	0.28	0.73	0.35
8	(Gal)1(GlcNAc)1(Man)3(GlcNAc)2	1	1620.810	1643.887	23.077	0.86	0.51	0.91	0.68
		2	821.900	833.438	11.539	1.92	1.65	1.82	1.32
9	(Man)6(GlcNAc)2	1	1783.883	1809.970	26.087	0.78	0.26	0.90	0.36
		2	903.436	916.480	13.044	0.75	0.29	0.88	0.40
10	(Gal)1(GlcNAc)1(Man)3(GlcNAc)2(Fuc)1	1	1794.899	1819.983	25.084	0.51	0.27	0.80	0.51
		2	908.944	921.486	12.542	0.92	0.51	1.75	1.79
11	(GlcNAc)1(Man)5(GlcNAc)2	1	1824.909	1850.997	26.087	1.13	0.83	1.37	1.10
		2	923.950	936.993	13.044	1.22	0.93	1.61	1.37
12	(GlcNAc)2(Man)3(GlcNAc)2(Fuc)1	1	1835.925	1861.009	25.084	2.14	0.25	0.66	0.22
		2	929.458	942.000	12.542	0.76	0.15	0.17	0.09
13	(Gal)1(GlcNAc)2(Man)3(GlcNAc)2	2	944.463	957.506	13.044	1.68	1.26	1.24	0.78
14	(NeuAc)1(Gal)1(GlcNAc)1(Man)3(GlcNAc)2	2	1002.487	1016.534	14.047	0.23	0.04	0.40	0.22
15	(Man)7(GlcNAc)2	2	1005.486	1020.035	14.549	0.83	0.36	0.97	0.50

Table S4.5. Relative quantification of N-linked glycans from human adipocytes between insulin resistant conditions and insulin response condition by $^{13}C/^{12}C$ ratio and prevalence ratio.

No.	N-linked oligosaccharide composition	Z	Ave. prevalence (%)			Prevalence ratios	
			LGPUG	HGINS	LG	LGPUG/LG	HGINS/LG
1	(Man)2(GlcNAc)2	1	0.20	0.23	0.46	0.45	0.50
2	(Man)2(GlcNAc)2(Fuc)1	1	0.52	0.66	1.81	0.29	0.37
3	(Man)3(GlcNAc)2	1	0.68	0.93	1.87	0.36	0.50
4	(Man)3(GlcNAc)2(Fuc)1	1	1.42	2.30	3.79	0.38	0.61
5	(Man)4(GlcNAc)2	1	0.71	0.78	1.15	0.61	0.68
6	(Man)5(GlcNAc)2	1	7.74	7.60	8.44	0.92	0.90
		2	0.85	0.85	1.05	0.82	0.81
7	(GlcNAc)1(Man)3(GlcNAc)2(Fuc)1	1	0.87	0.59	0.73	1.19	0.81
8	(Gal)1(GlcNAc)1(Man)3(GlcNAc)2	1	0.59	0.56	0.61	0.97	0.92
		2	0.12	0.11	0.06	1.93	1.85
9	(Man)6(GlcNAc)2	1	8.28	8.91	8.67	0.95	1.03
		2	3.26	3.29	3.47	0.94	0.95
10	(Gal)1(GlcNAc)1(Man)3(GlcNAc)2(Fuc)1	1	0.56	0.81	0.95	0.59	0.85
		2	0.20	0.21	0.17	1.16	1.24
11	(GlcNAc)1(Man)5(GlcNAc)2	1	2.14	2.30	1.80	1.19	1.28
		2	1.28	1.36	0.97	1.32	1.41
12	(GlcNAc)2(Man)3(GlcNAc)2(Fuc)1	1	0.77	0.22	0.30	2.58	0.75
		2	0.22	0.09	0.36	0.60	0.25
13	(Gal)1(GlcNAc)2(Man)3(GlcNAc)2	2	0.28	0.27	0.18	1.55	1.47
14	(NeuAc)1(Gal)1(GlcNAc)1(Man)3(GlcNAc)2	2	0.07	0.10	0.23	0.29	0.41
15	(Man)7(GlcNAc)2	2	4.01	4.10	3.94	1.02	1.04

Table S4.5 continued

No.	N-linked oligosaccharide composition	Z	$[M+zNa]^{z+}$ (mono)		DM (m/z)	LGPUG/LG		HGINS/LG	
			^{12}C	^{13}C		$^{13}C/^{12}C$ ratios	SD	$^{13}C/^{12}C$ ratios	SD
16	(GlcNAc)1(Man)5(GlcNAc)2(Fuc)1	2	1010.994	1025.041	14.047	0.98	0.63	1.08	0.81
17	(Gal)1(GlcNAc)1(Man)5(GlcNAc)2	2	1025.999	1040.548	14.549	1.20	0.80	1.31	1.05
18	(Gal)1(GlcNAc)2(Man)3(GlcNAc)2(Fuc)1	2	1031.507	1045.554	14.047	1.22	0.77	0.98	0.79
19	(Gal)2(GlcNAc)2(Man)3(GlcNAc)2	2	1046.513	1061.061	14.549	1.01	0.67	1.21	0.88
20	(GlcNAc)3(Man)3(GlcNAc)2(Fuc)1	2	1052.021	1066.068	14.047	3.63	4.08	2.19	2.20
21	(NeuAc)1(Gal)1(GlcNAc)1(Man)3(GlcNAc)2(Fuc)1	2	1089.531	1104.582	15.050	0.62	0.67	1.46	1.04
22	(NeuAc)1(Gal)1(GlcNAc)1(Man)1(Man)3(GlcNAc)2	2	1104.536	1120.088	15.552	0.92	0.64	1.16	0.89
23	(Man)8(GlcNAc)2	2	1107.536	1123.590	16.054	0.80	0.36	0.97	0.53
24	(Gal)1(GlcNAc)1(Man)5(GlcNAc)2(Fuc)1	2	1113.044	1128.596	15.552	1.18	0.90	1.17	1.06
25	(NeuAc)1(Gal)1(GlcNAc)2(Man)3(GlcNAc)2	2	1125.050	1140.602	15.552	1.45	0.72	2.45	2.40
26	(Gal)2(GlcNAc)2(Man)3(GlcNAc)2(Fuc)1	2	1133.557	1149.109	15.552	1.03	0.66	1.13	0.75
27	(NeuAc)1(Gal)2(GlcNAc)1(Man)3(GlcNAc)2(Fuc)1	2	1191.581	1208.136	16.555	1.73	1.80	2.26	2.45
28	(NeuAc)1(Gal)3(GlcNAc)1(Man)3(GlcNAc)2	2	1206.586	1223.643	17.057	0.95	0.59	0.94	0.71
29	(Man)9(GlcNAc)2	2	1209.586	1227.145	17.559	0.90	0.47	1.19	0.74
30	(Gal)2(GlcNAc)2(Fuc)1(Man)3(GlcNAc)2(Fuc)1	2	1220.602	1237.157	16.555	1.27	1.11	1.51	1.50
31	(NeuAc)1(Gal)2(GlcNAc)2(Man)3(GlcNAc)2	2	1227.100	1244.157	17.057	0.93	0.56	1.02	0.68
32	(Gal)2(GlcNAc)3(Man)3(GlcNAc)2(Fuc)1	2	1256.121	1273.178	17.057	1.43	1.51	2.15	2.50
33	(Gal)3(GlcNAc)3(Man)3(GlcNAc)2	2	1271.126	1288.685	17.559	3.01	3.65	2.33	2.67
34	(NeuAc)1(Gal)2(GlcNAc)2(Man)3(GlcNAc)2(Fuc)1	2	1314.144	1332.205	18.060	1.07	0.71	1.14	0.82
		3	883.759	895.800	12.040	1.32	1.32	1.32	1.27
35	(Gal)3(GlcNAc)3(Man)3(GlcNAc)2(Fuc)1	2	1358.171	1376.733	18.562	1.53	0.93	1.78	1.38
36	(NeuAc)1(Gal)2(GlcNAc)2(Fuc)1(Man)3(GlcNAc)2(Fuc)1	2	1401.189	1420.253	19.064	1.08	1.02	1.70	1.87

Table S4.5 continued

No.	N-linked oligosaccharide composition	Z	Ave. prevalence (%)			Prevalence ratios	
			LGPUG	HGINS	LG	LGPUG/LG	HGINS/LG
16	(GlcNAc)1(Man)5(GlcNAc)2(Fuc)1	2	0.56	0.51	0.49	1.15	1.04
17	(Gal)1(GlcNAc)1(Man)5(GlcNAc)2	2	2.05	1.94	1.54	1.33	1.26
18	(Gal)1(GlcNAc)2(Man)3(GlcNAc)2(Fuc)1	2	1.28	0.84	0.90	1.42	0.93
19	(Gal)2(GlcNAc)2(Man)3(GlcNAc)2	2	3.72	3.93	3.29	1.13	1.20
20	(GlcNAc)3(Man)3(GlcNAc)2(Fuc)1	2	0.03	0.02	0.01	2.99	2.13
21	(NeuAc)1(Gal)1(GlcNAc)1(Man)3(GlcNAc)2(Fuc)1	2	0.20	0.50	0.34	0.59	1.46
22	(NeuAc)1(Gal)1(GlcNAc)1(Man)1(Man)3(GlcNAc)2	2	1.59	1.63	1.51	1.06	1.08
23	(Man)8(GlcNAc)2	2	7.76	8.26	7.96	0.97	1.04
24	(Gal)1(GlcNAc)1(Man)5(GlcNAc)2(Fuc)1	2	0.27	0.20	0.20	1.31	0.99
25	(NeuAc)1(Gal)1(GlcNAc)2(Man)3(GlcNAc)2	2	0.27	0.23	0.14	1.95	1.70
26	(Gal)2(GlcNAc)2(Man)3(GlcNAc)2(Fuc)1	2	10.46	10.46	8.97	1.17	1.17
27	(NeuAc)1(Gal)2(GlcNAc)1(Man)3(GlcNAc)2(Fuc)1	2	0.22	0.21	0.15	1.45	1.44
28	(NeuAc)1(Gal)3(GlcNAc)1(Man)3(GlcNAc)2	2	1.05	0.92	0.98	1.07	0.94
29	(Man)9(GlcNAc)2	2	7.32	8.67	6.91	1.06	1.25
30	(Gal)2(GlcNAc)2(Fuc)1(Man)3(GlcNAc)2(Fuc)1	2	0.60	0.53	0.46	1.32	1.16
31	(NeuAc)1(Gal)2(GlcNAc)2(Man)3(GlcNAc)2	2	2.72	2.62	2.53	1.08	1.03
32	(Gal)2(GlcNAc)3(Man)3(GlcNAc)2(Fuc)1	2	0.13	0.11	0.09	1.42	1.22
33	(Gal)3(GlcNAc)3(Man)3(GlcNAc)2	2	0.28	0.33	0.19	1.47	1.75
34	(NeuAc)1(Gal)2(GlcNAc)2(Man)3(GlcNAc)2(Fuc)1	2	6.36	6.01	5.30	1.20	1.13
		3	0.58	0.49	0.46	1.27	1.06
35	(Gal)3(GlcNAc)3(Man)3(GlcNAc)2(Fuc)1	2	1.72	1.64	0.97	1.77	1.69
36	(NeuAc)1(Gal)2(GlcNAc)2(Fuc)1(Man)3(GlcNAc)2(Fuc)1	2	0.37	0.37	0.35	1.08	1.06

Table S4.5 continued

No.	N-linked oligosaccharide composition	Z	[M+zNa]$^{z+}$ (mono)		DM (m/z)	LGPUG/LG		HGINS/LG	
			^{12}C	^{13}C		^{13}C/^{12}C ratios	SD	^{13}C/^{12}C ratios	SD
36	(NeuAc)1(Gal)2(GlcNAc)2(Fuc)1(Man)3(GlcNAc)2(Fuc)1	2	1401.189	1420.253	19.064	1.08	1.02	1.70	1.87
37	(NeuAc)2(Gal)2(GlcNAc)2(Man)3(GlcNAc)2	2	1407.687	1427.252	19.565	0.67	0.28	0.54	0.33
		3	946.121	959.165	13.044	0.56	0.47	0.33	0.20
38	(NeuAc)1(Gal)3(GlcNAc)3(Man)3(GlcNAc)2	2	1451.713	1471.780	20.067	1.41	1.29	1.33	1.25
39	(NeuAc)2(Gal)2(GlcNAc)2(Man)3(GlcNAc)2(Fuc)1	2	1494.731	1515.300	20.569	0.99	0.69	1.07	0.83
		3	1004.151	1017.863	13.713	1.06	0.95	1.07	0.94
40	(NeuAc)2(Gal)3(GlcNAc)2(Man)3(GlcNAc)2	3	1509.736	1530.807	21.070	0.88	0.83	1.10	1.08
41	(NeuAc)1(Gal)3(GlcNAc)3(Man)3(GlcNAc)2(Fuc)1	2	1538.757	1559.828	21.070	0.91	0.61	0.96	0.66
42	(NeuAc)2(Gal)3(GlcNAc)3(Man)3(GlcNAc)2	2	1632.300	1654.875	22.575	0.81	0.55	0.63	0.59
		3	1095.863	1110.913	15.050	1.08	0.85	0.83	0.98
43	(NeuAc)2(Gal)3(GlcNAc)3(Man)3(GlcNAc)2(Fuc)1	2	1719.344	1742.923	23.579	1.22	1.01	0.99	0.82
		3	1153.893	1169.612	15.719	1.29	1.42	1.35	1.34
44	(NeuAc)1(Gal)4(GlcNAc)4(Man)3(GlcNAc)2(Fuc)1	2	1763.370	1787.451	24.081	1.92	1.70	2.11	2.06
		3	1183.244	1199.297	16.054	0.75	0.59	1.15	1.30
45	(NeuAc)3(Gal)3(GlcNAc)3(Man)3(GlcNAc)2	2	1812.887	1837.970	25.084	0.42	0.28	0.18	0.12
		3	1216.254	1232.977	16.723	0.70	0.36	0.68	0.38
46	(NeuAc)3(Gal)3(GlcNAc)3(Man)3(GlcNAc)2(Fuc)1	2	1899.931	1926.018	26.087	1.08	1.11	1.13	1.25
		3	1274.284	1291.675	17.391	1.72	1.91	1.86	2.09
47	(NeuAc)2(Gal)4(GlcNAc)4(Man)3(GlcNAc)2(Fuc)1	2	1943.957	1970.546	26.589	1.15	1.10	1.45	1.66
		3	1303.635	1321.361	17.726	1.65	1.93	1.19	1.33
48	(NeuAc)3(Gal)4(GlcNAc)4(Man)3(GlcNAc)2(Fuc)1	3	1424.026	1443.424	19.398	0.93	0.84	1.48	1.60

Table S4.5 continued

No.	N-linked oligosaccharide composition	Z	Ave. prevalence (%)			Prevalence ratios	
			LGPUG	HGINS	LG	LGPUG/LG	HGINS/LG
36	(NeuAc)1(Gal)2(GlcNAc)2(Fuc)1(Man)3(GlcNAc)2(Fuc)1	2	0.37	0.37	0.35	1.08	1.06
37	(NeuAc)2(Gal)2(GlcNAc)2(Man)3(GlcNAc)2	2	1.62	1.16	2.01	0.81	0.58
		3	0.11	0.05	0.17	0.63	0.32
38	(NeuAc)1(Gal)3(GlcNAc)3(Man)3(GlcNAc)2	2	0.74	0.65	0.57	1.30	1.15
39	(NeuAc)2(Gal)2(GlcNAc)2(Man)3(GlcNAc)2(Fuc)1	2	3.58	3.36	3.27	1.10	1.03
		3	0.60	0.54	0.55	1.09	0.97
40	(NeuAc)2(Gal)3(GlcNAc)2(Man)3(GlcNAc)2	3	0.40	0.39	0.46	0.86	0.84
41	(NeuAc)1(Gal)3(GlcNAc)3(Man)3(GlcNAc)2(Fuc)1	2	2.17	2.04	2.11	1.03	0.96
42	(NeuAc)2(Gal)3(GlcNAc)3(Man)3(GlcNAc)2	2	0.73	0.44	0.80	0.91	0.55
		3	0.14	0.06	0.11	1.21	0.55
43	(NeuAc)2(Gal)3(GlcNAc)3(Man)3(GlcNAc)2(Fuc)1	2	1.75	1.40	1.47	1.19	0.95
		3	0.38	0.33	0.34	1.14	0.98
44	(NeuAc)1(Gal)4(GlcNAc)4(Man)3(GlcNAc)2(Fuc)1	2	0.63	0.56	0.35	1.78	1.57
		3	0.06	0.05	0.07	0.96	0.74
45	(NeuAc)3(Gal)3(GlcNAc)3(Man)3(GlcNAc)2	2	0.48	0.19	1.01	0.47	0.19
		3	0.24	0.17	0.26	0.90	0.66
46	(NeuAc)3(Gal)3(GlcNAc)3(Man)3(GlcNAc)2(Fuc)1	2	0.43	0.39	0.51	0.85	0.78
		3	0.13	0.13	0.11	1.23	1.24
47	(NeuAc)2(Gal)4(GlcNAc)4(Man)3(GlcNAc)2(Fuc)1	2	0.36	0.34	0.37	0.98	0.93
		3	0.15	0.13	0.14	1.05	0.89
48	(NeuAc)3(Gal)4(GlcNAc)4(Man)3(GlcNAc)2(Fuc)1	3	0.13	0.12	0.13	1.04	0.90

Table S4.6. Relative quantification of O-linked glycans from human adipocytes between insulin resistant conditions and insulin responsive condition by $^{13}C/^{12}C$ ratio and prevalence ratio.

No.	O-linked oligosaccharide composition	Z	$[M+zNa]^{z+}$ (mono)		DM (m/z)	LGPUG/LG		HGINS/LG	
			^{12}C	^{13}C		$^{13}C/^{12}C$ ratios	SD	$^{13}C/^{12}C$ ratios	SD
1	(Hex)1(HexNAc)1	1	534.289	543.319	9.030	1.46	0.66	1.51	0.62
2	(Xyl)2(Glc)1	1	609.310	619.343	10.034	1.81	1.05	1.53	0.66
3	(NeuAc)1(Hex)1	1	650.337	661.374	11.037	1.34	0.42	1.43	0.40
4	(Hex)1(HexNAc)1(Hex)1	1	738.389	750.429	12.040	1.56	1.55	1.87	1.24
5	(Hex)1(HexNAc)2	1	779.415	791.455	12.040	2.28	0.51	1.26	0.37
6	(NeuAc)1(Hex)1(HexNAc)1	1	895.463	909.510	14.047	1.20	0.38	1.32	0.35
7	(Hex)2(HexNAc)2	1	983.515	998.565	15.050	1.25	0.48	1.32	0.38
8	(NeuAc)1(Hex)1(HexNAc)2	1	1140.589	1157.810	17.221	1.70	0.44	1.32	0.42
9	(NeuAc)2(Hex)1(HexNAc)1	1	1256.636	1275.700	19.064	1.10	0.19	1.32	0.16
10	(NeuAc)1(Hex)2(HexNAc)2	1	1344.689	1364.756	20.067	1.38	0.37	1.63	0.29
11	(NeuAc)2(Hex)2(HexNAc)2	1	1705.862	1730.946	25.084	1.10	0.29	1.40	0.27
		2	864.426	876.968	12.542	1.18	0.31	1.51	0.31
12	(NeuAc)1(Hex)4(HexNAc)4	2	1133.065	1149.119	16.054	1.31	0.56	1.31	0.28

Table S4.6. Continued. Relative quantification of O-linked glycans from human adipocytes between insulin resistant conditions and insulin responsive condition by $^{13}C/^{12}C$ ratio and prevalence ratio.

No.	O-linked oligosaccharide composition	Z	Ave. prevalence (%)			Prevalence ratios	
			LGPUG	HGINS	LG	LGPUG/LG	HGINS/LG
1	(Hex)1(HexNAc)1	1	4.95	3.94	3.52	1.41	1.12
2	(Xyl)2(Glc)1	1	0.89	0.63	0.51	1.75	1.24
3	(NeuAc)1(Hex)1	1	1.35	1.15	1.22	1.11	0.95
4	(Hex)1(HexNAc)1(Hex)1	1	0.18	0.14	0.11	1.60	1.22
5	(Hex)1(HexNAc)2	1	1.09	0.50	0.57	1.91	0.89
6	(NeuAc)1(Hex)1(HexNAc)1	1	27.95	27.68	27.90	1.00	0.99
7	(Hex)2(HexNAc)2	1	6.89	6.58	6.14	1.12	1.07
8	(NeuAc)1(Hex)1(HexNAc)2	1	3.53	2.28	3.02	1.17	0.75
9	(NeuAc)2(Hex)1(HexNAc)1	1	21.65	24.34	25.28	0.86	0.96
10	(NeuAc)1(Hex)2(HexNAc)2	1	13.32	13.49	12.28	1.08	1.10
11	(NeuAc)2(Hex)2(HexNAc)2	1	12.14	14.00	13.85	0.88	1.01
		2	4.53	4.15	4.33	1.05	0.96
12	(NeuAc)1(Hex)4(HexNAc)4	2	1.55	1.11	1.27	1.21	0.87

DISCUSSION

In these studies, we have investigated the regulation of adipocytokine expression during chronic insulin resistance. We showed the adipocytokines LPL, SPARC, Cathepsin B, SerpinA, and Quiescin Q6 are upregulated at both the protein level and the transcript level, as tested in the mouse 3T3-F442a adipocyte cell line as well as in a genetic insulin resistant mouse model and a diet-induced insulin resistant mouse model. We went on to explore common motifs on the promoters using bioinformatics, and we found that the Sp1 binding site is a common *cis*-acting element for the promoters. As Sp1 has been tied to the transcription of several of these genes in other cell types and since Sp1 is a well-studied O-GlcNAc modified protein, we investigated the role of Sp1 in adipocytokine transcription. We found that Sp1 is more heavily O-GlcNAc modified during insulin resistance, which is supported by the literature [48, 127-129, 156, 166, 388]. In addition, we showed that both Sp1 and O-GlcNAc modified proteins are enriched on the LPL and SPARC promoters during insulin resistance. Therefore, we have tied increase in global O-GlcNAc levels during insulin resistance to increased Sp1 O-GlcNAc modification and transcriptional activation of several adipocytokines.

Since not all adipocytokines are likely expressed similarly in mice and humans, we determined that several of the adipocytokines we identified in rodents by quantitative proteomics were also similarly regulated in primary human adipocytes. By generating insulin resistance in primary human adipocytes by either directly or indirectly modulating O-GlcNAc levels, we now have a list of human adipocytokines that are likely modulated by O-GlcNAc. Future studies to

investigate the role of O-GlcNAc in human adipocytokine expression would help to solidify the physiological role of O-GlcNAc in the generation of human insulin resistance.

In the future, we would like to determine the specific role of the O-GlcNAc modification on Sp1 with regards to adipocytokine transcription. Many roles have been assigned to the O-GlcNAc modification of Sp1 in the literature [130, 388]. It would be informative to investigate Sp1 localization, DNA binding, and protein-protein interactions during insulin resistance in adipocytes. Sp1 often interacts with other proteins, such as with SREBP to activate LPL transcription, so we would like to see which other proteins are interacting with Sp1 during insulin resistance and whether these interactions are altered by the presence of O-GlcNAc [188]. To identify potential interacting proteins, we could perform a bioinformatic analysis to see if other transcription factor binding sites cluster around the Sp1 sites on the co-regulated adipocytokine promoters. In addition, we would like to extend our ChIP analysis to see if Sp1 and O-GlcNAc modified proteins are enriched on some of the other adipocytokine promoters. Since we now have a list of human adipocytokines that are modulated by O-GlcNAc levels, we could extend this analysis to human adipocytes. Setting a precedent in mouse adipocytes was still advantageous, because mouse adipocytes are much easier and more cost effective to culture. In addition, we could extend our study to investigate the biological function of the less well-characterized adipocytokines, such as Quiescin Q6, by making transgenic mice.

The study of O-GlcNAc modification of proteins is relatively tedious due to the limited methods to manipulate O-GlcNAc levels, especially on specific protein sites. Manipulating global O-GlcNAc levels using altered HBP flux, pharmacological OGA inhibitors, or genetic manipulation of OGT or OGA all lead to the alteration of O-GlcNAc levels on many different proteins. This could potentially lead to confounding effects in the study of a single protein or

process. Since it is still not clear how OGT determines its substrates, it is difficult to manipulate O-GlcNAc levels on a single protein. Site-specific mutations on O-GlcNAc sites are currently the golden standard for assigning the functionality of O-GlcNAc on proteins. Although mass spectrometric methods for mapping sites of O-GlcNAc modification of proteins have improved, it is still not a trivial experiment, especially if there are multiple sites of O-GlcNAc modification that may also be reciprocal with phosphorylation [112, 130]. To solidify the role of the O-GlcNAc modification of Sp1 in adipocytokine transcription, we would like to perform experiments using genetic manipulation of the O-GlcNAc cycling enzymes to manipulate global O-GlcNAc levels and confirm the pharmocological inhibition. In addition, we would like to map the sites of O-GlcNAc modification on Sp1 and use site directed mutagenesis to further establish the functionality of the O-GlcNAc modification.

As far as adipocytokines, it would be helpful to have more specific nomenclature as not all adipocytokines are expressed solely by adipocytes and not all adipocytokines are cytokines. Since many adipocytokines are also expressed by other cell types, it is difficult to determine the relative contribution of the adipocyte-derived protein in whole-animal genetic knockouts. Some of the adipocytokines we studied, such as Cathepsin B, have had whole-animal genetic knockouts generated [471]. It would be interesting to challenge an adipose tissue-specific Cathepsin B knockout mouse with a high fat, high sucrose diet to determine the role Cathepsin B plays in insulin resistance. It is also possible that some of these adipocytokines play more of a role in the complications of T2DM than in the actual insulin resistance. To test for the influence of the adipocytokine on neuropathy, nephropathy, atherosclerosis, etc., it would be advantageous to perform a long-term study with adipocytokine adipose-tissue specific knockout or transgenic mice on a high fat, high sucrose diet.

Hopefully some of the newly identified adipocytokines from proteomic secretome studies will be investigated as prognostic/diagnostic markers for insulin resistance, obesity, metabolic syndrome, and/or T2DM. Developing therapies to normalize the secretion of adipocytokines during human T2DM may have major implications in the control of T2DM related complications, such as atherosclerosis. Already, TZDs, which are commonly used to treat T2DM, have been shown to normalize the expression of some adipocytokines [455, 472]. It is also clear that many adipocytokines have roles in tumorigenesis and inflammation [401]. It will be interesting to see how the cancer and diabetes stories intersect, since it may be possible to identify complementary therapies.

In conclusion, it is clear that adipocytokines play a major role in the maintenance of whole-body energy homeostasis and the pathogenesis of insulin resistance and T2DM. We have further solidified the link between insulin resistance, adipocytokine expression, and the O-GlcNAc modification of proteins.

REFERENCES

1. Kahn, S.E., R.L. Hull, and K.M. Utzschneider, *Mechanisms linking obesity to insulin resistance and type 2 diabetes.* Nature, 2006. **444**(7121): p. 840-6.
2. Doria, A., M.E. Patti, and C.R. Kahn, *The emerging genetic architecture of type 2 diabetes.* Cell Metab, 2008. **8**(3): p. 186-200.
3. Cho, Y.S., et al., *Meta-analysis of genome-wide association studies identifies eight new loci for type 2 diabetes in east Asians.* Nat Genet, 2012. **44**(1): p. 67-72.
4. Imamura, M. and S. Maeda, *Genetics of type 2 diabetes: the GWAS era and future perspectives [Review]*. Endocr J, 2011. **58**(9): p. 723-39.
5. Vimaleswaran, K.S. and R.J. Loos, *Progress in the genetics of common obesity and type 2 diabetes.* Expert Rev Mol Med, 2010. **12**: p. e7.
6. Kilmer, G., et al., *Surveillance of certain health behaviors and conditions among states and selected local areas--Behavioral Risk Factor Surveillance System (BRFSS), United States, 2006.* MMWR Surveill Summ, 2008. **57**(7): p. 1-188.
7. Ahima, R.S., *Digging deeper into obesity.* J Clin Invest, 2011. **121**(6): p. 2076-9.
8. Organization, W.H. *Obesity and overweight*. May 2012 June 11, 2012]; Available from: http://www.who.int/mediacentre/factsheets/fs311/en/index.html.
9. Brownlee, M., *The pathobiology of diabetic complications: a unifying mechanism.* Diabetes, 2005. **54**(6): p. 1615-25.
10. Hotamisligil, G.S., *Inflammation and metabolic disorders.* Nature, 2006. **444**(7121): p. 860-7.

11. Schwartz, M.W. and D. Porte, Jr., *Diabetes, obesity, and the brain.* Science, 2005. **307**(5708): p. 375-9.

12. Wu, C., et al., *Reduction of hepatic glucose production as a therapeutic target in the treatment of diabetes.* Curr Drug Targets Immune Endocr Metabol Disord, 2005. **5**(1): p. 51-9.

13. Abdul-Ghani, M.A. and R.A. DeFronzo, *Pathogenesis of insulin resistance in skeletal muscle.* J Biomed Biotechnol, 2010. **2010**: p. 476279.

14. Lafontan, M. and D. Langin, *Lipolysis and lipid mobilization in human adipose tissue.* Prog Lipid Res, 2009. **48**(5): p. 275-97.

15. Obici, S. and L. Rossetti, *Minireview: nutrient sensing and the regulation of insulin action and energy balance.* Endocrinology, 2003. **144**(12): p. 5172-8.

16. Abel, E.D., et al., *Adipose-selective targeting of the GLUT4 gene impairs insulin action in muscle and liver.* Nature, 2001. **409**(6821): p. 729-33.

17. Carvalho, E., et al., *Adipose-specific overexpression of GLUT4 reverses insulin resistance and diabetes in mice lacking GLUT4 selectively in muscle.* Am J Physiol Endocrinol Metab, 2005. **289**(4): p. E551-61.

18. Yang, Q., et al., *Serum retinol binding protein 4 contributes to insulin resistance in obesity and type 2 diabetes.* Nature, 2005. **436**(7049): p. 356-62.

19. Ahima, R.S. and M.A. Lazar, *Adipokines and the peripheral and neural control of energy balance.* Mol Endocrinol, 2008. **22**(5): p. 1023-31.

20. Trujillo, M.E. and P.E. Scherer, *Adipose tissue-derived factors: impact on health and disease.* Endocr Rev, 2006. **27**(7): p. 762-78.

21. MacDougald, O.A. and M.D. Lane, *Transcriptional regulation of gene expression during adipocyte differentiation.* Annu Rev Biochem, 1995. **64**: p. 345-73.

22. Hwang, C.S., et al., *Adipocyte differentiation and leptin expression.* Annu Rev Cell Dev Biol, 1997. **13**: p. 231-59.

23. Guilherme, A., et al., *Adipocyte dysfunctions linking obesity to insulin resistance and type 2 diabetes.* Nat Rev Mol Cell Biol, 2008. **9**(5): p. 367-77.

24. Sun, K., C.M. Kusminski, and P.E. Scherer, *Adipose tissue remodeling and obesity.* J Clin Invest, 2011. **121**(6): p. 2094-101.

25. Olefsky, J.M. and C.K. Glass, *Macrophages, inflammation, and insulin resistance.* Annu Rev Physiol, 2010. **72**: p. 219-46.

26. Lumeng, C.N. and A.R. Saltiel, *Inflammatory links between obesity and metabolic disease.* J Clin Invest, 2011. **121**(6): p. 2111-7.

27. Waki, H. and P. Tontonoz, *Endocrine functions of adipose tissue.* Annu Rev Pathol, 2007. **2**: p. 31-56.

28. Schwartz, M.W. and K.D. Niswender, *Adiposity signaling and biological defense against weight gain: absence of protection or central hormone resistance?* J Clin Endocrinol Metab, 2004. **89**(12): p. 5889-97.

29. Rajala, M.W. and P.E. Scherer, *Minireview: The adipocyte--at the crossroads of energy homeostasis, inflammation, and atherosclerosis.* Endocrinology, 2003. **144**(9): p. 3765-73.

30. Minokoshi, Y., C.R. Kahn, and B.B. Kahn, *Tissue-specific ablation of the GLUT4 glucose transporter or the insulin receptor challenges assumptions about insulin action and glucose homeostasis.* J Biol Chem, 2003. **278**(36): p. 33609-12.

31. Zhang, Y., et al., *Positional cloning of the mouse obese gene and its human homologue.* Nature, 1994. **372**(6505): p. 425-32.

32. Flier, J.S. and E. Maratos-Flier, *Lasker lauds leptin.* Cell Metab, 2010. **12**(4): p. 317-20.

33. Gautron, L. and J.K. Elmquist, *Sixteen years and counting: an update on leptin in energy balance.* J Clin Invest, 2011. **121**(6): p. 2087-93.

34. Gorska, E., et al., *Leptin receptors.* Eur J Med Res, 2010. **15 Suppl 2**: p. 50-4.

35. Morton, G.J. and M.W. Schwartz, *Leptin and the central nervous system control of glucose metabolism.* Physiol Rev, 2011. **91**(2): p. 389-411.

36. Sahu, A., *Intracellular leptin-signaling pathways in hypothalamic neurons: the emerging role of phosphatidylinositol-3 kinase-phosphodiesterase-3B-cAMP pathway.* Neuroendocrinology, 2011. **93**(4): p. 201-10.

37. Liu, M. and F. Liu, *Transcriptional and post-translational regulation of adiponectin.* Biochem J, 2010. **425**(1): p. 41-52.

38. Harwood, H.J., Jr., *The adipocyte as an endocrine organ in the regulation of metabolic homeostasis.* Neuropharmacology, 2011.

39. Maury, E. and S.M. Brichard, *Adipokine dysregulation, adipose tissue inflammation and metabolic syndrome.* Mol Cell Endocrinol, 2010. **314**(1): p. 1-16.

40. Berry, D.C., et al., *Cross-talk between signalling and vitamin A transport by the retinol-binding protein receptor STRA6.* Mol Cell Biol, 2012.

41. Kotnik, P., P. Fischer-Posovszky, and M. Wabitsch, *RBP4: a controversial adipokine.* Eur J Endocrinol, 2011. **165**(5): p. 703-11.

42. Keicho, N., et al., *Circulating levels of adiponectin, leptin, fetuin-a and retinol-binding protein in patients with tuberculosis: markers of metabolism and inflammation.* PLoS One, 2012. **7**(6): p. e38703.

43. Yuan, G., et al., *C-reactive protein inhibits adiponectin gene expression and secretion in 3T3-L1 adipocytes.* J Endocrinol, 2007. **194**(2): p. 275-81.

44. Moore, G.B., et al., *Differential regulation of adipocytokine mRNAs by rosiglitazone in db/db mice.* Biochem Biophys Res Commun, 2001. **286**(4): p. 735-41.

45. Nozaki, M., et al., *Nitric oxide dysregulates adipocytokine expression in 3T3-L1 adipocytes.* Biochem Biophys Res Commun, 2007. **364**(1): p. 33-9.

46. Kurata, A., et al., *Blockade of Angiotensin II type-1 receptor reduces oxidative stress in adipose tissue and ameliorates adipocytokine dysregulation.* Kidney Int, 2006. **70**(10): p. 1717-24.

47. Wang, J., et al., *A nutrient-sensing pathway regulates leptin gene expression in muscle and fat.* Nature, 1998. **393**(6686): p. 684-8.

48. Barth, N., et al., *Identification of regulatory elements in the human adipose most abundant gene transcript-1 (apM-1) promoter: role of SP1/SP3 and TNF-alpha as regulatory pathways.* Diabetologia, 2002. **45**(10): p. 1425-33.

49. Chevillotte, E., et al., *Uncoupling protein-2 controls adiponectin gene expression in adipose tissue through the modulation of reactive oxygen species production.* Diabetes, 2007. **56**(4): p. 1042-50.

50. Doran, A.C., et al., *The helix-loop-helix factors Id3 and E47 are novel regulators of adiponectin.* Circ Res, 2008. **103**(6): p. 624-34.

51. Kanatani, Y., et al., *Effects of pioglitazone on suppressor of cytokine signaling 3 expression: potential mechanisms for its effects on insulin sensitivity and adiponectin expression.* Diabetes, 2007. **56**(3): p. 795-803.

52. Kita, A., et al., *Identification of the promoter region required for human adiponectin gene transcription: Association with CCAAT/enhancer binding protein-beta and tumor necrosis factor-alpha.* Biochem Biophys Res Commun, 2005. **331**(2): p. 484-90.

53. Koshiishi, C., et al., *Regulation of expression of the mouse adiponectin gene by the C/EBP family via a novel enhancer region.* Gene, 2008.

54. Park, S.K., et al., *CCAAT/enhancer binding protein and nuclear factor-Y regulate adiponectin gene expression in adipose tissue.* Diabetes, 2004. **53**(11): p. 2757-66.

55. Rahmouni, K. and C.D. Sigmund, *Id3, E47, and SREBP-1c: fat factors controlling adiponectin expression.* Circ Res, 2008. **103**(6): p. 565-7.

56. Schaffler, A., et al., *Mutation analysis of the human adipocyte-specific apM-1 gene.* Eur J Clin Invest, 2000. **30**(10): p. 879-87.

57. Mason, M.M., et al., *Regulation of leptin promoter function by Sp1, C/EBP, and a novel factor.* Endocrinology, 1998. **139**(3): p. 1013-22.

58. Hazel, M., et al., *Activation of the hexosamine signaling pathway in adipose tissue results in decreased serum adiponectin and skeletal muscle insulin resistance.* Endocrinology, 2004. **145**(5): p. 2118-28.

59. McClain, D.A., et al., *Hexosamines stimulate leptin production in transgenic mice.* Endocrinology, 2000. **141**(6): p. 1999-2002.

60. Considine, R.V., et al., *Hexosamines regulate leptin production in human subcutaneous adipocytes.* J Clin Endocrinol Metab, 2000. **85**(10): p. 3551-6.

61. Marshall, S., V. Bacote, and R.R. Traxinger, *Discovery of a metabolic pathway mediating glucose-induced desensitization of the glucose transport system. Role of hexosamine biosynthesis in the induction of insulin resistance.* J Biol Chem, 1991. **266**(8): p. 4706-12.

62. Hawkins, M., et al., *Role of the glucosamine pathway in fat-induced insulin resistance.* J Clin Invest, 1997. **99**(9): p. 2173-82.

63. Donald A. McClain, R.P.T., Yudi Soesanto, and Bai Luo, *Metabolic Regulation by the Hexosamine Biosynthesis/O-Linked N-Acetylglucosamine Pathway*. Current Signal Transduction Therapy, 2010. **5**(1): p. 3-11.

64. Bhonagiri, P., et al., *Evidence coupling increased hexosamine biosynthesis pathway activity to membrane cholesterol toxicity and cortical filamentous actin derangement contributing to cellular insulin resistance.* Endocrinology, 2011. **152**(9): p. 3373-84.

65. Nelson, B.A., K.A. Robinson, and M.G. Buse, *Insulin acutely regulates Munc18-c subcellular trafficking: altered response in insulin-resistant 3T3-L1 adipocytes.* J Biol Chem, 2002. **277**(6): p. 3809-12.

66. Chen, G., et al., *Glucosamine-induced insulin resistance is coupled to O-linked glycosylation of Munc18c.* FEBS Lett, 2003. **534**(1-3): p. 54-60.

67. Heart, E., W.S. Choi, and C.K. Sung, *Glucosamine-induced insulin resistance in 3T3-L1 adipocytes.* Am J Physiol Endocrinol Metab, 2000. **278**(1): p. E103-12.

68. Nelson, B.A., K.A. Robinson, and M.G. Buse, *High glucose and glucosamine induce insulin resistance via different mechanisms in 3T3-L1 adipocytes.* Diabetes, 2000. **49**(6): p. 981-91.

69. Cooksey, R.C., et al., *Mechanism of hexosamine-induced insulin resistance in transgenic mice overexpressing glutamine:fructose-6-phosphate amidotransferase: decreased*

glucose transporter GLUT4 translocation and reversal by treatment with thiazolidinedione. Endocrinology, 1999. **140**(3): p. 1151-7.

70. Hebert, L.F., Jr., et al., *Overexpression of glutamine:fructose-6-phosphate amidotransferase in transgenic mice leads to insulin resistance.* J Clin Invest, 1996. **98**(4): p. 930-6.

71. Baron, A.D., et al., *Glucosamine induces insulin resistance in vivo by affecting GLUT 4 translocation in skeletal muscle. Implications for glucose toxicity.* J Clin Invest, 1995. **96**(6): p. 2792-801.

72. Giaccari, A., et al., *In vivo effects of glucosamine on insulin secretion and insulin sensitivity in the rat: possible relevance to the maladaptive responses to chronic hyperglycaemia.* Diabetologia, 1995. **38**(5): p. 518-24.

73. Robinson, K.A., D.A. Sens, and M.G. Buse, *Pre-exposure to glucosamine induces insulin resistance of glucose transport and glycogen synthesis in isolated rat skeletal muscles. Study of mechanisms in muscle and in rat-1 fibroblasts overexpressing the human insulin receptor.* Diabetes, 1993. **42**(9): p. 1333-46.

74. Hresko, R.C., et al., *Glucosamine-induced insulin resistance in 3T3-L1 adipocytes is caused by depletion of intracellular ATP.* J Biol Chem, 1998. **273**(32): p. 20658-68.

75. McClain, D.A., et al., *Adipocytes with increased hexosamine flux exhibit insulin resistance, increased glucose uptake, and increased synthesis and storage of lipid.* Am J Physiol Endocrinol Metab, 2005. **288**(5): p. E973-9.

76. Luo, B., et al., *Chronic hexosamine flux stimulates fatty acid oxidation by activating AMP-activated protein kinase in adipocytes.* J Biol Chem, 2007. **282**(10): p. 7172-80.

77. Zhang, H., et al., *Common variants in glutamine:fructose-6-phosphate amidotransferase 2 (GFPT2) gene are associated with type 2 diabetes, diabetic nephropathy, and increased GFPT2 mRNA levels.* J Clin Endocrinol Metab, 2004. **89**(2): p. 748-55.

78. Boehmelt, G., et al., *Decreased UDP-GlcNAc levels abrogate proliferation control in EMeg32-deficient cells.* EMBO J, 2000. **19**(19): p. 5092-104.

79. Robinson, K.A., L.E. Ball, and M.G. Buse, *Reduction of O-GlcNAc protein modification does not prevent insulin resistance in 3T3-L1 adipocytes.* Am J Physiol Endocrinol Metab, 2007. **292**(3): p. E884-90.

80. McClain, D.A., *Hexosamines as mediators of nutrient sensing and regulation in diabetes.* J Diabetes Complications, 2002. **16**(1): p. 72-80.

81. Wells, L., K. Vosseller, and G.W. Hart, *A role for N-acetylglucosamine as a nutrient sensor and mediator of insulin resistance.* Cell Mol Life Sci, 2003. **60**(2): p. 222-8.

82. Haltiwanger, R.S., M.A. Blomberg, and G.W. Hart, *Glycosylation of nuclear and cytoplasmic proteins. Purification and characterization of a uridine diphospho-N-acetylglucosamine:polypeptide beta-N-acetylglucosaminyltransferase.* J Biol Chem, 1992. **267**(13): p. 9005-13.

83. Kreppel, L.K. and G.W. Hart, *Regulation of a cytosolic and nuclear O-GlcNAc transferase. Role of the tetratricopeptide repeats.* J Biol Chem, 1999. **274**(45): p. 32015-22.

84. Shen, D.L., et al., *Insights into O-Linked N-Acetylglucosamine ([0-9]O-GlcNAc) Processing and Dynamics through Kinetic Analysis of O-GlcNAc Transferase and O-GlcNAcase Activity on Protein Substrates.* J Biol Chem, 2012. **287**(19): p. 15395-408.

85. Wells, L. and G.W. Hart, *O-GlcNAc turns twenty: functional implications for post-translational modification of nuclear and cytosolic proteins with a sugar.* FEBS Lett, 2003. **546**(1): p. 154-8.

86. Vosseller, K., L. Wells, and G.W. Hart, *Nucleocytoplasmic O-glycosylation: O-GlcNAc and functional proteomics.* Biochimie, 2001. **83**(7): p. 575-81.

87. Zachara, N.E. and G.W. Hart, *Cell signaling, the essential role of O-GlcNAc!* Biochim Biophys Acta, 2006. **1761**(5-6): p. 599-617.

88. Love, D.C. and J.A. Hanover, *The hexosamine signaling pathway: deciphering the "O-GlcNAc code".* Sci STKE, 2005. **2005**(312): p. re13.

89. Hart, G.W., M.P. Housley, and C. Slawson, *Cycling of O-linked beta-N-acetylglucosamine on nucleocytoplasmic proteins.* Nature, 2007. **446**(7139): p. 1017-22.

90. Copeland, R.J., J.W. Bullen, and G.W. Hart, *Cross-talk between GlcNAcylation and phosphorylation: roles in insulin resistance and glucose toxicity.* Am J Physiol Endocrinol Metab, 2008. **295**(1): p. E17-28.

91. Comer, F.I. and G.W. Hart, *O-GlcNAc and the control of gene expression.* Biochim Biophys Acta, 1999. **1473**(1): p. 161-71.

92. Haltiwanger, R.S., G.D. Holt, and G.W. Hart, *Enzymatic addition of O-GlcNAc to nuclear and cytoplasmic proteins. Identification of a uridine diphospho-N-acetylglucosamine:peptide beta-N-acetylglucosaminyltransferase.* J Biol Chem, 1990. **265**(5): p. 2563-8.

93. Gao, Y., et al., *Dynamic O-glycosylation of nuclear and cytosolic proteins: cloning and characterization of a neutral, cytosolic beta-N-acetylglucosaminidase from human brain.* J Biol Chem, 2001. **276**(13): p. 9838-45.

94. Wang, Z., M. Gucek, and G.W. Hart, *Cross-talk between GlcNAcylation and phosphorylation: site-specific phosphorylation dynamics in response to globally elevated O-GlcNAc.* Proc Natl Acad Sci U S A, 2008. **105**(37): p. 13793-8.

95. Dias, W.B., W.D. Cheung, and G.W. Hart, *O-GlcNAcylation of kinases.* Biochem Biophys Res Commun, 2012. **422**(2): p. 224-8.

96. Teo, C.F., E.E. Wollaston-Hayden, and L. Wells, *Hexosamine flux, the O-GlcNAc modification, and the development of insulin resistance in adipocytes.* Mol Cell Endocrinol, 2010. **318**(1-2): p. 44-53.

97. Wang, S., et al., *Extensive Crosstalk between O-GlcNAcylation and Phosphorylation Regulates Akt Signaling.* PLoS One, 2012. **7**(5): p. e37427.

98. Vosseller, K., et al., *Elevated nucleocytoplasmic glycosylation by O-GlcNAc results in insulin resistance associated with defects in Akt activation in 3T3-L1 adipocytes.* Proc Natl Acad Sci U S A, 2002. **99**(8): p. 5313-8.

99. Park, S.Y., J. Ryu, and W. Lee, *O-GlcNAc modification on IRS-1 and Akt2 by PUGNAc inhibits their phosphorylation and induces insulin resistance in rat primary adipocytes.* Exp Mol Med, 2005. **37**(3): p. 220-9.

100. Yang, X., et al., *Phosphoinositide signalling links O-GlcNAc transferase to insulin resistance.* Nature, 2008. **451**(7181): p. 964-9.

101. Walgren, J.L., et al., *High glucose and insulin promote O-GlcNAc modification of proteins, including alpha-tubulin.* Am J Physiol Endocrinol Metab, 2003. **284**(2): p. E424-34.

102. Yki-Jarvinen, H., et al., *Insulin and glucosamine infusions increase O-linked N-acetyl-glucosamine in skeletal muscle proteins in vivo.* Metabolism, 1998. **47**(4): p. 449-55.

103. Parker, G.J., et al., *Insulin resistance of glycogen synthase mediated by o-linked N-acetylglucosamine.* J Biol Chem, 2003. **278**(12): p. 10022-7.

104. McClain, D.A., et al., *Altered glycan-dependent signaling induces insulin resistance and hyperleptinemia.* Proc Natl Acad Sci U S A, 2002. **99**(16): p. 10695-9.

105. Arias, E.B., J. Kim, and G.D. Cartee, *Prolonged incubation in PUGNAc results in increased protein O-Linked glycosylation and insulin resistance in rat skeletal muscle.* Diabetes, 2004. **53**(4): p. 921-30.

106. Akimoto, Y., et al., *Elevation of the post-translational modification of proteins by O-linked N-acetylglucosamine leads to deterioration of the glucose-stimulated insulin secretion in the pancreas of diabetic Goto-Kakizaki rats.* Glycobiology, 2007. **17**(2): p. 127-40.

107. Parker, G., et al., *Hyperglycemia and inhibition of glycogen synthase in streptozotocin-treated mice: role of O-linked N-acetylglucosamine.* J Biol Chem, 2004. **279**(20): p. 20636-42.

108. Patti, M.E., et al., *Activation of the hexosamine pathway by glucosamine in vivo induces insulin resistance of early postreceptor insulin signaling events in skeletal muscle.* Diabetes, 1999. **48**(8): p. 1562-71.

109. Jinek, M., et al., *The superhelical TPR-repeat domain of O-linked GlcNAc transferase exhibits structural similarities to importin alpha.* Nat Struct Mol Biol, 2004. **11**(10): p. 1001-7.

110. Lazarus, M.B., et al., *Structure of human O-GlcNAc transferase and its complex with a peptide substrate.* Nature, 2011. **469**(7331): p. 564-7.

111. Capotosti, F., et al., *O-GlcNAc transferase catalyzes site-specific proteolysis of HCF-1*. Cell, 2011. **144**(3): p. 376-88.

112. Hart, G.W., et al., *Cross talk between O-GlcNAcylation and phosphorylation: roles in signaling, transcription, and chronic disease.* Annu Rev Biochem, 2011. **80**: p. 825-58.

113. Shafi, R., et al., *The O-GlcNAc transferase gene resides on the X chromosome and is essential for embryonic stem cell viability and mouse ontogeny.* Proc Natl Acad Sci U S A, 2000. **97**(11): p. 5735-9.

114. Hanover, J.A., et al., *A Caenorhabditis elegans model of insulin resistance: altered macronutrient storage and dauer formation in an OGT-1 knockout.* Proc Natl Acad Sci U S A, 2005. **102**(32): p. 11266-71.

115. Forsythe, M.E., et al., *Caenorhabditis elegans ortholog of a diabetes susceptibility locus: oga-1 (O-GlcNAcase) knockout impacts O-GlcNAc cycling, metabolism, and dauer.* Proc Natl Acad Sci U S A, 2006. **103**(32): p. 11952-7.

116. Mondoux, M.A., et al., *O-linked-N-acetylglucosamine cycling and insulin signaling are required for the glucose stress response in Caenorhabditis elegans.* Genetics, 2011. **188**(2): p. 369-82.

117. Rahman, M.M., et al., *Intracellular protein glycosylation modulates insulin mediated lifespan in C.elegans.* Aging (Albany NY), 2010. **2**(10): p. 678-90.

118. Gambetta, M.C., K. Oktaba, and J. Muller, *Essential role of the glycosyltransferase sxc/Ogt in polycomb repression.* Science, 2009. **325**(5936): p. 93-6.

119. Keembiyehetty, C.N., et al., *A lipid-droplet-targeted O-GlcNAcase isoform is a key regulator of the proteasome.* J Cell Sci, 2011. **124**(Pt 16): p. 2851-60.

120. Dentin, R., et al., *Hepatic glucose sensing via the CREB coactivator CRTC2.* Science, 2008. **319**(5868): p. 1402-5.

121. Galli, J., et al., *Genetic analysis of non-insulin dependent diabetes mellitus in the GK rat.* Nat Genet, 1996. **12**(1): p. 31-7.

122. Van Tine, B.A., A.J. Patterson, and J.E. Kudlow, *Assignment of N-acetyl-D-glucosaminidase (Mgea5) to rat chromosome 1q5 by tyramide fluorescence in situ hybridization (T-FISH): synteny between rat, mouse and human with Insulin Degradation Enzyme (IDE).* Cytogenet Genome Res, 2003. **103**(1-2): p. 202B.

123. Lehman, D.M., et al., *A single nucleotide polymorphism in MGEA5 encoding O-GlcNAc-selective N-acetyl-beta-D glucosaminidase is associated with type 2 diabetes in Mexican Americans.* Diabetes, 2005. **54**(4): p. 1214-21.

124. Park, K., C.D. Saudek, and G.W. Hart, *Increased expression of beta-N-acetylglucosaminidase in erythrocytes from individuals with pre-diabetes and diabetes.* Diabetes, 2010. **59**(7): p. 1845-50.

125. Issad, T. and M. Kuo, *O-GlcNAc modification of transcription factors, glucose sensing and glucotoxicity.* Trends Endocrinol Metab, 2008.

126. Teo, C.F., et al., *Glycopeptide-specific monoclonal antibodies suggest new roles for O-GlcNAc.* Nat Chem Biol, 2010. **6**(5): p. 338-43.

127. Du, X.L., et al., *Hyperglycemia-induced mitochondrial superoxide overproduction activates the hexosamine pathway and induces plasminogen activator inhibitor-1 expression by increasing Sp1 glycosylation.* Proc Natl Acad Sci U S A, 2000. **97**(22): p. 12222-6.

128. Moreno-Aliaga, M.J., et al., *Sp1-mediated transcription is involved in the induction of leptin by insulin-stimulated glucose metabolism.* J Mol Endocrinol, 2007. **38**(5): p. 537-46.

129. Jackson, S.P. and R. Tjian, *O-glycosylation of eukaryotic transcription factors: implications for mechanisms of transcriptional regulation.* Cell, 1988. **55**(1): p. 125-33.

130. Brimble, S.W.-H., E.E.; Teo, C.F.; Morris, A.C.; Wells, L., *The Role of the O-GlcNAc Modification in Regulating Eukaryotic Gene*

Expression. Curr Signal Transduct Ther, 2010. **5**(1): p. 12-24.

131. Lim, J.M., et al., *Defining the regulated secreted proteome of rodent adipocytes upon the induction of insulin resistance.* J Proteome Res, 2008. **7**(3): p. 1251-63.

132. Nagaraju, G.P. and D. Sharma, *Anti-cancer role of SPARC, an inhibitor of adipogenesis.* Cancer Treat Rev, 2011. **37**(7): p. 559-66.

133. Bradshaw, A.D., et al., *SPARC-null mice exhibit increased adiposity without significant differences in overall body weight.* Proc Natl Acad Sci U S A, 2003. **100**(10): p. 6045-50.

134. Bradshaw, A.D., et al., *SPARC-null mice display abnormalities in the dermis characterized by decreased collagen fibril diameter and reduced tensile strength.* J Invest Dermatol, 2003. **120**(6): p. 949-55.

135. Bradshaw, A.D., M.J. Reed, and E.H. Sage, *SPARC-null mice exhibit accelerated cutaneous wound closure.* J Histochem Cytochem, 2002. **50**(1): p. 1-10.

136. Bradshaw, A.D., *Diverse biological functions of the SPARC family of proteins.* Int J Biochem Cell Biol, 2012. **44**(3): p. 480-8.

137. Bhoopathi, P., et al., *Cathepsin B facilitates autophagy-mediated apoptosis in SPARC overexpressed primitive neuroectodermal tumor cells.* Cell Death Differ, 2010. **17**(10): p. 1529-39.

138. Fenouille, N., et al., *SPARC functions as an anti-stress factor by inactivating p53 through Akt-mediated MDM2 phosphorylation to promote melanoma cell survival.* Oncogene, 2011. **30**(49): p. 4887-900.

139. Gerson, K.D., et al., *Integrin beta4 regulates SPARC protein to promote invasion.* J Biol Chem, 2012. **287**(13): p. 9835-44.

140. Tremble, P.M., et al., *SPARC, a secreted protein associated with morphogenesis and tissue remodeling, induces expression of metalloproteinases in fibroblasts through a novel extracellular matrix-dependent pathway.* J Cell Biol, 1993. **121**(6): p. 1433-44.

141. Nie, J., et al., *IFATS collection: Combinatorial peptides identify alpha5beta1 integrin as a receptor for the matricellular protein SPARC on adipose stromal cells.* Stem Cells, 2008. **26**(10): p. 2735-45.

142. Rivera, L.B., A.D. Bradshaw, and R.A. Brekken, *The regulatory function of SPARC in vascular biology.* Cell Mol Life Sci, 2011. **68**(19): p. 3165-73.

143. Kos, K., et al., *Regulation of the fibrosis and angiogenesis promoter SPARC/osteonectin in human adipose tissue by weight change, leptin, insulin, and glucose.* Diabetes, 2009. **58**(8): p. 1780-8.

144. Takahashi, M., et al., *The expression of SPARC in adipose tissue and its increased plasma concentration in patients with coronary artery disease.* Obes Res, 2001. **9**(7): p. 388-93.

145. Wu, D., et al., *Elevated plasma levels of SPARC in patients with newly diagnosed type 2 diabetes mellitus.* Eur J Endocrinol, 2011. **165**(4): p. 597-601.

146. Tartare-Deckert, S., et al., *The matricellular protein SPARC/osteonectin as a newly identified factor up-regulated in obesity.* J Biol Chem, 2001. **276**(25): p. 22231-7.

147. Franck, N., et al., *Identification of adipocyte genes regulated by caloric intake.* J Clin Endocrinol Metab, 2011. **96**(2): p. E413-8.

148. Socha, M.J., et al., *Secreted protein acidic and rich in cysteine deficiency ameliorates renal inflammation and fibrosis in angiotensin hypertension.* Am J Pathol, 2007. **171**(4): p. 1104-12.

149. Taneda, S., et al., *Amelioration of diabetic nephropathy in SPARC-null mice.* J Am Soc Nephrol, 2003. **14**(4): p. 968-80.

150. Nie, J. and E.H. Sage, *SPARC inhibits adipogenesis by its enhancement of beta-catenin signaling.* J Biol Chem, 2009. **284**(2): p. 1279-90.

151. Chavey, C., et al., *Regulation of secreted protein acidic and rich in cysteine during adipose conversion and adipose tissue hyperplasia.* Obesity (Silver Spring), 2006. **14**(11): p. 1890-7.

152. Song, H., et al., *SPARC interacts with AMPK and regulates GLUT4 expression.* Biochem Biophys Res Commun, 2010. **396**(4): p. 961-6.

153. Shi, Q., et al., *Secreted protein acidic, rich in cysteine (SPARC), mediates cellular survival of gliomas through AKT activation.* J Biol Chem, 2004. **279**(50): p. 52200-9.

154. Briggs, J., et al., *Transcriptional upregulation of SPARC, in response to c-Jun overexpression, contributes to increased motility and invasion of MCF7 breast cancer cells.* Oncogene, 2002. **21**(46): p. 7077-91.

155. Xu, Y.Z., et al., *Brg-1 mediates the constitutive and fenretinide-induced expression of SPARC in mammary carcinoma cells via its interaction with transcription factor Sp1*. Mol Cancer, 2010. **9**: p. 210.

156. McVey, J.H., et al., *Characterization of the mouse SPARC/osteonectin gene. Intron/exon organization and an unusual promoter region.* J Biol Chem, 1988. **263**(23): p. 11111-6.

157. Chamboredon, S., et al., *v-Jun downregulates the SPARC target gene by binding to the proximal promoter indirectly through Sp1/3.* Oncogene, 2003. **22**(26): p. 4047-61.

158. Vial, E., S. Perez, and M. Castellazzi, *Transcriptional control of SPARC by v-Jun and other members of the AP1 family of transcription factors.* Oncogene, 2000. **19**(43): p. 5020-9.

159. Mettouchi, A., et al., *SPARC and thrombospondin genes are repressed by the c-jun oncogene in rat embryo fibroblasts.* EMBO J, 1994. **13**(23): p. 5668-78.

160. Kraemer, M., et al., *Rat embryo fibroblasts transformed by c-Jun display highly metastatic and angiogenic activities in vivo and deregulate gene expression of both angiogenic and antiangiogenic factors.* Cell Growth Differ, 1999. **10**(3): p. 193-200.

161. Zhang, Y., et al., *Aberrant methylation of SPARC in human hepatocellular carcinoma and its clinical implication.* World J Gastroenterol, 2012. **18**(17): p. 2043-52.

162. Suzuki, M., et al., *Aberrant methylation of SPARC in human lung cancers.* Br J Cancer, 2005. **92**(5): p. 942-8.

163. Socha, M.J., et al., *Aberrant promoter methylation of SPARC in ovarian cancer.* Neoplasia, 2009. **11**(2): p. 126-35.

164. Gao, J., et al., *Methylation of the SPARC gene promoter and its clinical implication in pancreatic cancer.* J Exp Clin Cancer Res, 2010. **29**: p. 28.

165. Wang, H. and R.H. Eckel, *Lipoprotein lipase: from gene to obesity.* Am J Physiol Endocrinol Metab, 2009. **297**(2): p. E271-88.

166. Merkel, M., R.H. Eckel, and I.J. Goldberg, *Lipoprotein lipase: genetics, lipid uptake, and regulation.* J Lipid Res, 2002. **43**(12): p. 1997-2006.

167. Bessesen, D.H., A.D. Robertson, and R.H. Eckel, *Weight reduction increases adipose but decreases cardiac LPL in reduced-obese Zucker rats.* Am J Physiol, 1991. **261**(2 Pt 1): p. E246-51.

168. Eckel, R.H. and T.J. Yost, *Weight reduction increases adipose tissue lipoprotein lipase responsiveness in obese women.* J Clin Invest, 1987. **80**(4): p. 992-7.

169. Terrettaz, J., et al., *In vivo regulation of adipose tissue lipoprotein lipase in normal rats made hyperinsulinemic and in hyperinsulinemic genetically-obese (fa/fa) rats.* Int J Obes Relat Metab Disord, 1994. **18**(1): p. 9-15.

170. Hartman, A.D., *Lipoprotein lipase activities in adipose tissues and muscle in the obese Zucker rat.* Am J Physiol, 1981. **241**(2): p. E108-15.

171. Yki-Jarvinen, H., et al., *Response of adipose tissue lipoprotein lipase activity and serum lipoproteins to acute hyperinsulinaemia in man.* Diabetologia, 1984. **27**(3): p. 364-9.

172. Farese, R.V., Jr., T.J. Yost, and R.H. Eckel, *Tissue-specific regulation of lipoprotein lipase activity by insulin/glucose in normal-weight humans.* Metabolism, 1991. **40**(2): p. 214-6.

173. Ruge, T., et al., *Effects of hyperinsulinemia on lipoprotein lipase, angiopoietin-like protein 4, and glycosylphosphatidylinositol-anchored high-density lipoprotein binding protein 1 in subjects with and without type 2 diabetes mellitus.* Metabolism, 2012. **61**(5): p. 652-60.

174. Jemaa, R., et al., *Lipoprotein lipase gene polymorphisms: associations with hypertriglyceridemia and body mass index in obese people.* Int J Obes Relat Metab Disord, 1995. **19**(4): p. 270-4.

175. Radha, V., et al., *Association of lipoprotein lipase gene polymorphisms with obesity and type 2 diabetes in an Asian Indian population.* Int J Obes (Lond), 2007. **31**(6): p. 913-8.

176. Kastelein, J.J., et al., *The Asn9 variant of lipoprotein lipase is associated with the -93G promoter mutation and an increased risk of coronary artery disease. The Regress Study Group.* Clin Genet, 1998. **53**(1): p. 27-33.

177. Kim, S.J., C. Nian, and C.H. McIntosh, *GIP increases human adipocyte LPL expression through CREB and TORC2-mediated trans-activation of the LPL gene.* J Lipid Res, 2010. **51**(11): p. 3145-57.

178. Kim, S.J., C. Nian, and C.H. McIntosh, *Activation of lipoprotein lipase by glucose-dependent insulinotropic polypeptide in adipocytes. A role for a protein kinase B, LKB1, and AMP-activated protein kinase cascade.* J Biol Chem, 2007. **282**(12): p. 8557-67.

179. Hughes, T.R., et al., *A novel role of Sp1 and Sp3 in the interferon-gamma -mediated suppression of macrophage lipoprotein lipase gene transcription.* J Biol Chem, 2002. **277**(13): p. 11097-106.

180. Harris, S.M., et al., *The interferon-gamma-mediated inhibition of lipoprotein lipase gene transcription in macrophages involves casein kinase 2- and phosphoinositide-3-kinase-mediated regulation of transcription factors Sp1 and Sp3.* Cell Signal, 2008. **20**(12): p. 2296-301.

181. Irvine, S.A., et al., *A critical role for the Sp1-binding sites in the transforming growth factor-beta-mediated inhibition of lipoprotein lipase gene expression in macrophages.* Nucleic Acids Res, 2005. **33**(5): p. 1423-34.

182. Yang, W.S., et al., *Regulatory mutations in the human lipoprotein lipase gene in patients with familial combined hyperlipidemia and coronary artery disease.* J Lipid Res, 1996. **37**(12): p. 2627-37.

183. Smith, C.E., et al., *Apolipoprotein A5 and lipoprotein lipase interact to modulate anthropometric measures in Hispanics of Caribbean origin.* Obesity (Silver Spring), 2010. **18**(2): p. 327-32.

184. Ehrenborg, E., et al., *Ethnic variation and in vivo effects of the -93t-->g promoter variant in the lipoprotein lipase gene.* Arterioscler Thromb Vasc Biol, 1997. **17**(11): p. 2672-8.

185. Wittrup, H.H., et al., *Combined analysis of six lipoprotein lipase genetic variants on triglycerides, high-density lipoprotein, and ischemic heart disease: cross-sectional, prospective, and case-control studies from the Copenhagen City Heart Study.* J Clin Endocrinol Metab, 2006. **91**(4): p. 1438-45.

186. Hokanson, J.E., *Functional variants in the lipoprotein lipase gene and risk cardiovascular disease.* Curr Opin Lipidol, 1999. **10**(5): p. 393-9.

187. Hall, S., et al., *A common mutation in the lipoprotein lipase gene promoter, -93T/G, is associated with lower plasma triglyceride levels and increased promoter activity in vitro.* Arterioscler Thromb Vasc Biol, 1997. **17**(10): p. 1969-76.

188. Yang, W.S. and S.S. Deeb, *Sp1 and Sp3 transactivate the human lipoprotein lipase gene promoter through binding to a CT element: synergy with the sterol regulatory element*

binding protein and reduced transactivation of a naturally occurring promoter variant. J Lipid Res, 1998. **39**(10): p. 2054-64.

189. Preiss-Landl, K., et al., *Lipoprotein lipase: the regulation of tissue specific expression and its role in lipid and energy metabolism.* Curr Opin Lipidol, 2002. **13**(5): p. 471-81.

190. Reiser, J., B. Adair, and T. Reinheckel, *Specialized roles for cysteine cathepsins in health and disease.* J Clin Invest, 2010. **120**(10): p. 3421-31.

191. Guicciardi, M.E., et al., *Cathepsin B contributes to TNF-alpha-mediated hepatocyte apoptosis by promoting mitochondrial release of cytochrome c.* J Clin Invest, 2000. **106**(9): p. 1127-37.

192. Feldstein, A.E., et al., *Free fatty acids promote hepatic lipotoxicity by stimulating TNF-alpha expression via a lysosomal pathway.* Hepatology, 2004. **40**(1): p. 185-94.

193. Lutgens, S.P., et al., *Cathepsin cysteine proteases in cardiovascular disease.* FASEB J, 2007. **21**(12): p. 3029-41.

194. Yan, S. and B.F. Sloane, *Molecular regulation of human cathepsin B: implication in pathologies.* Biol Chem, 2003. **384**(6): p. 845-54.

195. Czibere, L., et al., *Profiling trait anxiety: transcriptome analysis reveals cathepsin B (Ctsb) as a novel candidate gene for emotionality in mice.* PLoS One, 2011. **6**(8): p. e23604.

196. Konduri, S., et al., *Elevated levels of cathepsin B in human glioblastoma cell lines.* Int J Oncol, 2001. **19**(3): p. 519-24.

197. Coppock, D.L., et al., *Preferential gene expression in quiescent human lung fibroblasts.* Cell Growth Differ, 1993. **4**(6): p. 483-93.

198. Coppock, D.L., D. Cina-Poppe, and S. Gilleran, *The quiescin Q6 gene (QSCN6) is a fusion of two ancient gene families: thioredoxin and ERV1*. Genomics, 1998. **54**(3): p. 460-8.

199. Coppock, D.L. and C. Thorpe, *Multidomain flavin-dependent sulfhydryl oxidases.* Antioxid Redox Signal, 2006. **8**(3-4): p. 300-11.

200. Hoober, K.L., et al., *Homology between egg white sulfhydryl oxidase and quiescin Q6 defines a new class of flavin-linked sulfhydryl oxidases.* J Biol Chem, 1999. **274**(45): p. 31759-62.

201. Mairet-Coello, G., et al., *FAD-linked sulfhydryl oxidase QSOX: topographic, cellular, and subcellular immunolocalization in adult rat central nervous system.* J Comp Neurol, 2004. **473**(3): p. 334-63.

202. Coppock, D., et al., *Regulation of the quiescence-induced genes: quiescin Q6, decorin, and ribosomal protein S29.* Biochem Biophys Res Commun, 2000. **269**(2): p. 604-10.

203. Portes, K.F., et al., *Tissue distribution of quiescin Q6/sulfhydryl oxidase (QSOX) in developing mouse.* J Mol Histol, 2008. **39**(2): p. 217-25.

204. Inoue, A., et al., *Development of cDNA microarray for expression profiling of estrogen-responsive genes.* J Mol Endocrinol, 2002. **29**(2): p. 175-92.

205. Morel, C., et al., *Involvement of sulfhydryl oxidase QSOX1 in the protection of cells against oxidative stress-induced apoptosis.* Exp Cell Res, 2007. **313**(19): p. 3971-82.

206. Hellebrekers, D.M., et al., *Identification of epigenetically silenced genes in tumor endothelial cells.* Cancer Res, 2007. **67**(9): p. 4138-48.

207. Musard, J.F., et al., *Identification and expression of a new sulfhydryl oxidase SOx-3 during the cell cycle and the estrus cycle in uterine cells.* Biochem Biophys Res Commun, 2001. **287**(1): p. 83-91.

208. Radom, J., et al., *Identification and expression of a new splicing variant of FAD-sulfhydryl oxidase in adult rat brain.* Biochim Biophys Acta, 2006. **1759**(5): p. 225-33.

209. Amiot, C., et al., *Expression of the secreted FAD-dependent sulfydryl oxidase (QSOX) in the guinea pig central nervous system.* Brain Res Mol Brain Res, 2004. **125**(1-2): p. 13-21.

210. Chang, T.S. and B.R. Zirkin, *Distribution of sulfhydryl oxidase activity in the rat and hamster male reproductive tract.* Biol Reprod, 1978. **18**(5): p. 745-8.

211. Hoober, K.L., et al., *A sulfhydryl oxidase from chicken egg white.* J Biol Chem, 1996. **271**(48): p. 30510-6.

212. Matsuba, S., et al., *Sulfhydryl oxidase (SOx) from mouse epidermis: molecular cloning, nucleotide sequence, and expression of recombinant protein in the cultured cells.* J Dermatol Sci, 2002. **30**(1): p. 50-62.

213. Thorpe, C. and D.L. Coppock, *Generating disulfides in multicellular organisms: emerging roles for a new flavoprotein family.* J Biol Chem, 2007. **282**(19): p. 13929-33.

214. Mebazaa, A., et al., *Unbiased plasma proteomics for novel diagnostic biomarkers in cardiovascular disease: identification of quiescin Q6 as a candidate biomarker of acutely decompensated heart failure.* Eur Heart J, 2012.

215. Antwi, K., et al., *Analysis of the plasma peptidome from pancreas cancer patients connects a peptide in plasma to overexpression of the parent protein in tumors.* J Proteome Res, 2009. **8**(10): p. 4722-31.

216. Katchman, B.A., et al., *Quiescin sulfhydryl oxidase 1 promotes invasion of pancreatic tumor cells mediated by matrix metalloproteinases.* Mol Cancer Res, 2011. **9**(12): p. 1621-31.

217. Saetre, P., et al., *Inflammation-related genes up-regulated in schizophrenia brains.* BMC Psychiatry, 2007. **7**: p. 46.

218. Horvath, A.J., et al., *The murine orthologue of human antichymotrypsin: a structural paradigm for clade A3 serpins.* J Biol Chem, 2005. **280**(52): p. 43168-78.

219. Porcellini, E., et al., *Elevated plasma levels of alpha-1-anti-chymotrypsin in age-related cognitive decline and Alzheimer's disease: a potential therapeutic target.* Curr Pharm Des, 2008. **14**(26): p. 2659-64.

220. Hoffmann, D.C., et al., *Pivotal role for alpha1-antichymotrypsin in skin repair*. J Biol Chem, 2011. **286**(33): p. 28889-901.

221. Licastro, F., et al., *Alpha 1 antichymotrypsin genotype is associated with increased risk of prostate carcinoma and PSA levels.* Anticancer Res, 2008. **28**(1B): p. 395-9.

222. Peck, G., et al., *The genetics of primary haemorrhagic stroke, subarachnoid haemorrhage and ruptured intracranial aneurysms in adults.* PLoS One, 2008. **3**(11): p. e3691.

223. Licastro, F., et al., *A new promoter polymorphism in the alpha-1-antichymotrypsin gene is a disease modifier of Alzheimer's disease.* Neurobiol Aging, 2005. **26**(4): p. 449-53.

224. Lee, C.G., et al., *Role of chitin and chitinase/chitinase-like proteins in inflammation, tissue remodeling, and injury.* Annu Rev Physiol, 2011. **73**: p. 479-501.

225. Nielsen, A.R., et al., *Plasma YKL-40: a BMI-independent marker of type 2 diabetes.* Diabetes, 2008. **57**(11): p. 3078-82.

226. Rathcke, C.N., J.S. Johansen, and H. Vestergaard, *YKL-40, a biomarker of inflammation, is elevated in patients with type 2 diabetes and is related to insulin resistance.* Inflamm Res, 2006. **55**(2): p. 53-9.

227. Rehli, M., et al., *Transcriptional regulation of CHI3L1, a marker gene for late stages of macrophage differentiation.* J Biol Chem, 2003. **278**(45): p. 44058-67.

228. Poulos, S.P., M.V. Dodson, and G.J. Hausman, *Cell line models for differentiation: preadipocytes and adipocytes.* Exp Biol Med (Maywood), 2010. **235**(10): p. 1185-93.

229. MacDougald, O.A., et al., *Regulated expression of the obese gene product (leptin) in white adipose tissue and 3T3-L1 adipocytes.* Proc Natl Acad Sci U S A, 1995. **92**(20): p. 9034-7.

230. Hausman, D.B., H.J. Park, and G.J. Hausman, *Isolation and culture of preadipocytes from rodent white adipose tissue.* Methods Mol Biol, 2008. **456**: p. 201-19.

231. Moro, C., et al., *Atrial natriuretic peptide inhibits the production of adipokines and cytokines linked to inflammation and insulin resistance in human subcutaneous adipose tissue.* Diabetologia, 2007. **50**(5): p. 1038-47.

232. Brivanlou, A.H. and J.E. Darnell, Jr., *Signal transduction and the control of gene expression.* Science, 2002. **295**(5556): p. 813-8.

233. Orphanides, G. and D. Reinberg, *A unified theory of gene expression.* Cell, 2002. **108**(4): p. 439-51.

234. Levine, M. and R. Tjian, *Transcription regulation and animal diversity.* Nature, 2003. **424**(6945): p. 147-51.

235. Heintzman, N.D. and B. Ren, *The gateway to transcription: identifying, characterizing and understanding promoters in the eukaryotic genome.* Cell Mol Life Sci, 2007. **64**(4): p. 386-400.

236. Khidekel, N. and L.C. Hsieh-Wilson, *A 'molecular switchboard'--covalent modifications to proteins and their impact on transcription.* Org Biomol Chem, 2004. **2**(1): p. 1-7.

237. Torres, C.R. and G.W. Hart, *Topography and polypeptide distribution of terminal N-acetylglucosamine residues on the surfaces of intact lymphocytes. Evidence for O-linked GlcNAc.* J Biol Chem, 1984. **259**(5): p. 3308-17.

238. Holt, G.D. and G.W. Hart, *The subcellular distribution of terminal N-acetylglucosamine moieties. Localization of a novel protein-saccharide linkage, O-linked GlcNAc.* J Biol Chem, 1986. **261**(17): p. 8049-57.

239. Holt, G.D., et al., *Erythrocytes contain cytoplasmic glycoproteins. O-linked GlcNAc on Band 4.1.* J Biol Chem, 1987. **262**(31): p. 14847-50.

240. Dehennaut, V., et al., *O-linked N-acetylglucosaminyltransferase inhibition prevents G2/M transition in Xenopus laevis oocytes.* J Biol Chem, 2007. **282**(17): p. 12527-36.

241. Dehennaut, V., et al., *Microinjection of recombinant O-GlcNAc transferase potentiates Xenopus oocytes M-phase entry.* Biochem Biophys Res Commun, 2008. **369**(2): p. 539-46.

242. Slawson, C., et al., *Perturbations in O-linked beta-N-acetylglucosamine protein modification cause severe defects in mitotic progression and cytokinesis.* J Biol Chem, 2005. **280**(38): p. 32944-56.

243. Wells, L., K. Vosseller, and G.W. Hart, *Glycosylation of nucleocytoplasmic proteins: signal transduction and O-GlcNAc.* Science, 2001. **291**(5512): p. 2376-8.

244. Gandy, J.C., A.E. Rountree, and G.N. Bijur, *Akt1 is dynamically modified with O-GlcNAc following treatments with PUGNAc and insulin-like growth factor-1.* FEBS Lett, 2006. **580**(13): p. 3051-8.

245. Ohn, T., et al., *A functional RNAi screen links O-GlcNAc modification of ribosomal proteins to stress granule and processing body assembly.* Nat Cell Biol, 2008. **10**(10): p. 1224-31.

246. Zachara, N.E. and G.W. Hart, *O-GlcNAc a sensor of cellular state: the role of nucleocytoplasmic glycosylation in modulating cellular function in response to nutrition and stress.* Biochim Biophys Acta, 2004. **1673**(1-2): p. 13-28.

247. Dias, W.B. and G.W. Hart, *O-GlcNAc modification in diabetes and Alzheimer's disease.* Mol Biosyst, 2007. **3**(11): p. 766-72.

248. Vosseller, K., et al., *Diverse regulation of protein function by O-GlcNAc: a nuclear and cytoplasmic carbohydrate post-translational modification.* Curr Opin Chem Biol, 2002. **6**(6): p. 851-7.

249. Zachara, N.E. and G.W. Hart, *Cell signaling, the essential role of O-GlcNAc!* Biochimica et Biophysica Acta (BBA) - Molecular and Cell Biology of Lipids, 2006. **1761**(5-6): p. 599-617.

250. Kreppel, L.K., M.A. Blomberg, and G.W. Hart, *Dynamic glycosylation of nuclear and cytosolic proteins. Cloning and characterization of a unique O-GlcNAc transferase with multiple tetratricopeptide repeats.* J Biol Chem, 1997. **272**(14): p. 9308-15.

251. Lubas, W.A. and J.A. Hanover, *Functional expression of O-linked GlcNAc transferase. Domain structure and substrate specificity.* J Biol Chem, 2000. **275**(15): p. 10983-8.

252. Dong, D.L. and G.W. Hart, *Purification and characterization of an O-GlcNAc selective N-acetyl-beta-D-glucosaminidase from rat spleen cytosol.* J Biol Chem, 1994. **269**(30): p. 19321-30.

253. Comer, F.I. and G.W. Hart, *O-Glycosylation of nuclear and cytosolic proteins. Dynamic interplay between O-GlcNAc and O-phosphate.* J Biol Chem, 2000. **275**(38): p. 29179-82.

254. Wells, L., et al., *O-GlcNAc transferase is in a functional complex with protein phosphatase 1 catalytic subunits.* J Biol Chem, 2004. **279**(37): p. 38466-70.

255. Haltiwanger, R.S., K. Grove, and G.A. Philipsberg, *Modulation of O-linked N-acetylglucosamine levels on nuclear and cytoplasmic proteins in vivo using the peptide O-GlcNAc-beta-N-acetylglucosaminidase inhibitor O-(2-acetamido-2-deoxy-D-glucopyranosylidene)amino-N-phenylcarbamate.* J Biol Chem, 1998. **273**(6): p. 3611-7.

256. Macauley, M.S., et al., *O-GlcNAcase uses substrate-assisted catalysis: kinetic analysis and development of highly selective mechanism-inspired inhibitors.* J Biol Chem, 2005. **280**(27): p. 25313-22.

257. Dorfmueller, H.C., et al., *GlcNAcstatin: a picomolar, selective O-GlcNAcase inhibitor that modulates intracellular O-glcNAcylation levels.* J Am Chem Soc, 2006. **128**(51): p. 16484-5.

258. Dorfmueller, H.C., et al., *GlcNAcstatins are nanomolar inhibitors of human O-GlcNAcase inducing cellular hyper-O-GlcNAcylation.* Biochem J, 2009.

259. Gross, B.J., J.G. Swoboda, and S. Walker, *A strategy to discover inhibitors of O-linked glycosylation.* J Am Chem Soc, 2008. **130**(2): p. 440-1.

260. Vosseller, K., et al., *O-linked N-acetylglucosamine proteomics of postsynaptic density preparations using lectin weak affinity chromatography and mass spectrometry.* Mol Cell Proteomics, 2006. **5**(5): p. 923-34.

261. Khidekel, N., et al., *Exploring the O-GlcNAc proteome: direct identification of O-GlcNAc-modified proteins from the brain.* Proc Natl Acad Sci U S A, 2004. **101**(36): p. 13132-7.

262. Khidekel, N., et al., *Probing the dynamics of O-GlcNAc glycosylation in the brain using quantitative proteomics.* Nat Chem Biol, 2007. **3**(6): p. 339-48.

263. Wells, L., et al., *Mapping sites of O-GlcNAc modification using affinity tags for serine and threonine post-translational modifications.* Mol Cell Proteomics, 2002. **1**(10): p. 791-804.

264. Issad, T. and M. Kuo, *O-GlcNAc modification of transcription factors, glucose sensing and glucotoxicity.* Trends Endocrinol Metab, 2008. **19**(10): p. 380-9.

265. Zachara, N.E., *Detecting the "O-GlcNAc-ome"; detection, purification, and analysis of O-GlcNAc modified proteins.* Methods Mol Biol, 2009. **534**: p. 251-79.

266. Hanover, J.A., et al., *O-linked N-acetylglucosamine is attached to proteins of the nuclear pore. Evidence for cytoplasmic and nucleoplasmic glycoproteins.* J Biol Chem, 1987. **262**(20): p. 9887-94.

267. Snow, C.M., A. Senior, and L. Gerace, *Monoclonal antibodies identify a group of nuclear pore complex glycoproteins.* J Cell Biol, 1987. **104**(5): p. 1143-56.

268. Comer, F.I. and G.W. Hart, *Reciprocity between O-GlcNAc and O-phosphate on the carboxyl terminal domain of RNA polymerase II.* Biochemistry, 2001. **40**(26): p. 7845-52.

269. Khidekel, N., et al., *A chemoenzymatic approach toward the rapid and sensitive detection of O-GlcNAc posttranslational modifications.* J Am Chem Soc, 2003. **125**(52): p. 16162-3.

270. Vocadlo, D.J., et al., *A chemical approach for identifying O-GlcNAc-modified proteins in cells.* Proc Natl Acad Sci U S A, 2003. **100**(16): p. 9116-21.

271. Saxon, E. and C.R. Bertozzi, *Cell surface engineering by a modified Staudinger reaction.* Science, 2000. **287**(5460): p. 2007-10.

272. Whelan, S.A. and G.W. Hart, *Identification of O-GlcNAc sites on proteins.* Methods Enzymol, 2006. **415**: p. 113-33.

273. Nandi, A., et al., *Global identification of O-GlcNAc-modified proteins.* Anal Chem, 2006. **78**(2): p. 452-8.

274. Zubarev, R.A., N.L. Kelleher, and F.W. McLafferty, *Electron Capture Dissociation of Multiply Charged Protein Cations. A Nonergodic Process.* Journal of the American Chemical Society, 1998. **120**(13): p. 3265-3266.

275. Syka, J.E., et al., *Peptide and protein sequence analysis by electron transfer dissociation mass spectrometry.* Proc Natl Acad Sci U S A, 2004. **101**(26): p. 9528-33.

276. Mikesh, L.M., et al., *The utility of ETD mass spectrometry in proteomic analysis.* Biochim Biophys Acta, 2006. **1764**(12): p. 1811-22.

277. Wiesner, J., T. Premsler, and A. Sickmann, *Application of electron transfer dissociation (ETD) for the analysis of posttranslational modifications.* Proteomics, 2008. **8**(21): p. 4466-83.

278. Viner, R.I., et al., *Quantification of post-translationally modified peptides of bovine alpha-crystallin using tandem mass tags and electron transfer dissociation.* J Proteomics, 2009.

279. O'Malley, B.W., J. Qin, and R.B. Lanz, *Cracking the coregulator codes.* Curr Opin Cell Biol, 2008. **20**(3): p. 310-5.

280. Whitmarsh, A.J. and R.J. Davis, *Regulation of transcription factor function by phosphorylation.* Cell Mol Life Sci, 2000. **57**(8-9): p. 1172-83.

281. Holmberg, C.I., et al., *Multisite phosphorylation provides sophisticated regulation of transcription factors.* Trends Biochem Sci, 2002. **27**(12): p. 619-27.

282. Lyst, M.J. and I. Stancheva, *A role for SUMO modification in transcriptional repression and activation.* Biochem Soc Trans, 2007. **35**(Pt 6): p. 1389-92.

283. Spange, S., et al., *Acetylation of non-histone proteins modulates cellular signalling at multiple levels.* Int J Biochem Cell Biol, 2009. **41**(1): p. 185-98.

284. Clapier, C.R. and B.R. Cairns, *The Biology of Chromatin Remodeling Complexes.* Annu Rev Biochem, 2009.

285. Lee, T.I. and R.A. Young, *Transcription of eukaryotic protein-coding genes.* Annu Rev Genet, 2000. **34**: p. 77-137.

286. Zhang, Y. and D. Reinberg, *Transcription regulation by histone methylation: interplay between different covalent modifications of the core histone tails.* Genes Dev, 2001. **15**(18): p. 2343-60.

287. Yang, X., F. Zhang, and J.E. Kudlow, *Recruitment of O-GlcNAc transferase to promoters by corepressor mSin3A: coupling protein O-GlcNAcylation to transcriptional repression.* Cell, 2002. **110**(1): p. 69-80.

288. Fujiki, R., et al., *GlcNAcylation of a histone methyltransferase in retinoic-acid-induced granulopoiesis.* Nature, 2009.

289. Kelly, W.G. and G.W. Hart, *Glycosylation of chromosomal proteins: localization of O-linked N-acetylglucosamine in Drosophila chromatin.* Cell, 1989. **57**(2): p. 243-51.

290. Dannenberg, J.H., et al., *mSin3A corepressor regulates diverse transcriptional networks governing normal and neoplastic growth and survival.* Genes Dev, 2005. **19**(13): p. 1581-95.

291. Shaw, P., et al., *Regulation of specific DNA binding by p53: evidence for a role for O-glycosylation and charged residues at the carboxy-terminus.* Oncogene, 1996. **12**(4): p. 921-30.

292. Yang, W.H., et al., *Modification of p53 with O-linked N-acetylglucosamine regulates p53 activity and stability.* Nat Cell Biol, 2006. **8**(10): p. 1074-83.

293. Murphy, M., et al., *Transcriptional repression by wild-type p53 utilizes histone deacetylases, mediated by interaction with mSin3a.* Genes Dev, 1999. **13**(19): p. 2490-501.

294. Yao, D., et al., *High glucose increases angiopoietin-2 transcription in microvascular endothelial cells through methylglyoxal modification of mSin3A.* J Biol Chem, 2007. **282**(42): p. 31038-45.

295. Corden, J.L., *Tails of RNA polymerase II.* Trends Biochem Sci, 1990. **15**(10): p. 383-7.

296. Kelly, W.G., M.E. Dahmus, and G.W. Hart, *RNA polymerase II is a glycoprotein. Modification of the COOH-terminal domain by O-GlcNAc.* J Biol Chem, 1993. **268**(14): p. 10416-24.

297. Desterro, J.M., M.S. Rodriguez, and R.T. Hay, *Regulation of transcription factors by protein degradation.* Cell Mol Life Sci, 2000. **57**(8-9): p. 1207-19.

298. Ravid, T. and M. Hochstrasser, *Diversity of degradation signals in the ubiquitin-proteasome system.* Nat Rev Mol Cell Biol, 2008. **9**(9): p. 679-90.

299. Glickman, M.H. and A. Ciechanover, *The ubiquitin-proteasome proteolytic pathway: destruction for the sake of construction.* Physiol Rev, 2002. **82**(2): p. 373-428.

300. Zhang, F., et al., *O-GlcNAc modification is an endogenous inhibitor of the proteasome.* Cell, 2003. **115**(6): p. 715-25.

301. Wierstra, I., *Sp1: Emerging roles--Beyond constitutive activation of TATA-less housekeeping genes.* Biochemical and Biophysical Research Communications, 2008. **372**(1): p. 1-13.

302. Han, I. and J.E. Kudlow, *Reduced O glycosylation of Sp1 is associated with increased proteasome susceptibility.* Mol Cell Biol, 1997. **17**(5): p. 2550-8.

303. Sumegi, M., et al., *26S proteasome subunits are O-linked N-acetylglucosamine-modified in Drosophila melanogaster.* Biochem Biophys Res Commun, 2003. **312**(4): p. 1284-9.

304. Cheng, X. and G.W. Hart, *Alternative O-glycosylation/O-phosphorylation of serine-16 in murine estrogen receptor beta: post-translational regulation of turnover and transactivation activity.* J Biol Chem, 2001. **276**(13): p. 10570-5.

305. Sears, R., et al., *Multiple Ras-dependent phosphorylation pathways regulate Myc protein stability.* Genes Dev, 2000. **14**(19): p. 2501-14.

306. Cheng, X., et al., *Alternative O-glycosylation/O-phosphorylation of the murine estrogen receptor beta.* Biochemistry, 2000. **39**(38): p. 11609-20.

307. Chou, T.Y., C.V. Dang, and G.W. Hart, *Glycosylation of the c-Myc transactivation domain.* Proc Natl Acad Sci U S A, 1995. **92**(10): p. 4417-21.

308. Chou, T.Y., G.W. Hart, and C.V. Dang, *c-Myc is glycosylated at threonine 58, a known phosphorylation site and a mutational hot spot in lymphomas.* J Biol Chem, 1995. **270**(32): p. 18961-5.

309. Yustein, J.T. and C.V. Dang, *Biology and treatment of Burkitt's lymphoma.* Curr Opin Hematol, 2007. **14**(4): p. 375-81.

310. Vervoorts, J., J. Luscher-Firzlaff, and B. Luscher, *The ins and outs of MYC regulation by posttranslational mechanisms.* J Biol Chem, 2006. **281**(46): p. 34725-9.

311. Adhikary, S. and M. Eilers, *Transcriptional regulation and transformation by Myc proteins.* Nat Rev Mol Cell Biol, 2005. **6**(8): p. 635-645.

312. Kuiper, G.G. and J.A. Gustafsson, *The novel estrogen receptor-beta subtype: potential role in the cell- and promoter-specific actions of estrogens and anti-estrogens.* FEBS Lett, 1997. **410**(1): p. 87-90.

313. Zhao, C., K. Dahlman-Wright, and J.A. Gustafsson, *Estrogen receptor beta: an overview and update.* Nucl Recept Signal, 2008. **6**: p. e003.

314. Grisouard, J., et al., *Glycogen synthase kinase-3 protects estrogen receptor alpha from proteasomal degradation and is required for full transcriptional activity of the receptor.* Mol Endocrinol, 2007. **21**(10): p. 2427-39.

315. Reid, G., et al., *Cyclic, proteasome-mediated turnover of unliganded and liganded ERalpha on responsive promoters is an integral feature of estrogen signaling.* Mol Cell, 2003. **11**(3): p. 695-707.

316. Picard, N., et al., *Phosphorylation of activation function-1 regulates proteasome-dependent nuclear mobility and E6-associated protein ubiquitin ligase recruitment to the estrogen receptor beta.* Mol Endocrinol, 2008. **22**(2): p. 317-30.

317. Whibley, C., P.D. Pharoah, and M. Hollstein, *p53 polymorphisms: cancer implications.* Nat Rev Cancer, 2009. **9**(2): p. 95-107.

318. Petersen, H.V., et al., *Glucose induced MAPK signalling influences NeuroD1-mediated activation and nuclear localization.* FEBS Lett, 2002. **528**(1-3): p. 241-5.

319. Andrali, S.S., Q. Qian, and S. Ozcan, *Glucose mediates the translocation of NeuroD1 by O-linked glycosylation.* J Biol Chem, 2007. **282**(21): p. 15589-96.

320. Sayat, R., et al., *O-GlcNAc-glycosylation of beta-catenin regulates its nuclear localization and transcriptional activity.* Exp Cell Res, 2008. **314**(15): p. 2774-87.

321. Koo, S.H., et al., *The CREB coactivator TORC2 is a key regulator of fasting glucose metabolism.* Nature, 2005. **437**(7062): p. 1109-11.

322. Dentin, R., et al., *Insulin modulates gluconeogenesis by inhibition of the coactivator TORC2.* Nature, 2007. **449**(7160): p. 366-9.

323. Screaton, R.A., et al., *The CREB coactivator TORC2 functions as a calcium- and cAMP-sensitive coincidence detector.* Cell, 2004. **119**(1): p. 61-74.

324. Andrali, S.S., et al., *Glucose regulation of insulin gene expression in pancreatic beta-cells.* Biochem J, 2008. **415**(1): p. 1-10.

325. Barker, N., *The canonical Wnt/beta-catenin signalling pathway.* Methods Mol Biol, 2008. **468**: p. 5-15.

326. Zhu, W., B. Leber, and D.W. Andrews, *Cytoplasmic O-glycosylation prevents cell surface transport of E-cadherin during apoptosis.* EMBO J, 2001. **20**(21): p. 5999-6007.

327. Gao, Y., J. Miyazaki, and G.W. Hart, *The transcription factor PDX-1 is post-translationally modified by O-linked N-acetylglucosamine and this modification is correlated with its DNA binding activity and insulin secretion in min6 beta-cells.* Arch Biochem Biophys, 2003. **415**(2): p. 155-63.

328. Zhang, W., et al., *FoxO1 regulates multiple metabolic pathways in the liver: effects on gluconeogenic, glycolytic, and lipogenic gene expression.* J Biol Chem, 2006. **281**(15): p. 10105-17.

329. Finck, B.N. and D.P. Kelly, *PGC-1 coactivators: inducible regulators of energy metabolism in health and disease.* J Clin Invest, 2006. **116**(3): p. 615-22.

330. Puigserver, P., et al., *Insulin-regulated hepatic gluconeogenesis through FOXO1-PGC-1alpha interaction.* Nature, 2003. **423**(6939): p. 550-5.

331. Barthel, A., D. Schmoll, and T.G. Unterman, *FoxO proteins in insulin action and metabolism.* Trends Endocrinol Metab, 2005. **16**(4): p. 183-9.

332. Gross, D.N., A.P. van den Heuvel, and M.J. Birnbaum, *The role of FoxO in the regulation of metabolism.* Oncogene, 2008. **27**(16): p. 2320-36.

333. Housley, M.P., et al., *O-GlcNAc regulates FoxO activation in response to glucose.* J Biol Chem, 2008. **283**(24): p. 16283-92.

334. Kuo, M., et al., *O-glycosylation of FoxO1 increases its transcriptional activity towards the glucose 6-phosphatase gene.* FEBS Lett, 2008. **582**(5): p. 829-34.

335. Housley, M.P., et al., *A PGC-1{alpha}-O-GlcNAc Transferase Complex Regulates FoxO Transcription Factor Activity in Response to Glucose.* J Biol Chem, 2009. **284**(8): p. 5148-57.

336. Yang, W.H., et al., *NFkappaB activation is associated with its O-GlcNAcylation state under hyperglycemic conditions.* Proc Natl Acad Sci U S A, 2008. **105**(45): p. 17345-50.

337. Gewinner, C., et al., *The coactivator of transcription CREB-binding protein interacts preferentially with the glycosylated form of Stat5.* J Biol Chem, 2004. **279**(5): p. 3563-72.

338. Yang, X., et al., *O-linkage of N-acetylglucosamine to Sp1 activation domain inhibits its transcriptional capability.* Proc Natl Acad Sci U S A, 2001. **98**(12): p. 6611-6.

339. Roos, M.D., et al., *O glycosylation of an Sp1-derived peptide blocks known Sp1 protein interactions.* Mol Cell Biol, 1997. **17**(11): p. 6472-80.

340. Levy, D.E. and J.E. Darnell, Jr., *Stats: transcriptional control and biological impact.* Nat Rev Mol Cell Biol, 2002. **3**(9): p. 651-62.

341. Korzus, E., et al., *Transcription factor-specific requirements for coactivators and their acetyltransferase functions.* Science, 1998. **279**(5351): p. 703-7.

342. Hayden, M.S. and S. Ghosh, *Shared principles in NF-kappaB signaling.* Cell, 2008. **132**(3): p. 344-62.

343. James, L.R., et al., *Flux through the hexosamine pathway is a determinant of nuclear factor kappaB- dependent promoter activation.* Diabetes, 2002. **51**(4): p. 1146-56.

344. Kawauchi, K., et al., *Loss of p53 enhances catalytic activity of IKKbeta through O-linked beta-N-acetyl glucosamine modification.* Proc Natl Acad Sci U S A, 2009. **106**(9): p. 3431-6.

345. Kawauchi, K., et al., *p53 regulates glucose metabolism through an IKK-NF-kappaB pathway and inhibits cell transformation.* Nat Cell Biol, 2008. **10**(5): p. 611-8.

346. Schomer-Miller, B., et al., *Regulation of IkappaB kinase (IKK) complex by IKKgamma-dependent phosphorylation of the T-loop and C terminus of IKKbeta.* J Biol Chem, 2006. **281**(22): p. 15268-76.

347. Iyer, S.P., Y. Akimoto, and G.W. Hart, *Identification and cloning of a novel family of coiled-coil domain proteins that interact with O-GlcNAc transferase.* J Biol Chem, 2003. **278**(7): p. 5399-409.

348. Cheung, W.D., et al., *O-linked beta-N-acetylglucosaminyltransferase substrate specificity is regulated by myosin phosphatase targeting and other interacting proteins.* J Biol Chem, 2008. **283**(49): p. 33935-41.

349. Stallcup, M.R., et al., *The roles of protein-protein interactions and protein methylation in transcriptional activation by nuclear receptors and their coactivators.* J Steroid Biochem Mol Biol, 2003. **85**(2-5): p. 139-45.

350. Iyer, S.P. and G.W. Hart, *Roles of the tetratricopeptide repeat domain in O-GlcNAc transferase targeting and protein substrate specificity.* J Biol Chem, 2003. **278**(27): p. 24608-16.

351. Hurtado-Guerrero, R., H.C. Dorfmueller, and D.M. van Aalten, *Molecular mechanisms of O-GlcNAcylation.* Curr Opin Struct Biol, 2008. **18**(5): p. 551-7.

352. Whisenhunt, T.R., et al., *Disrupting the enzyme complex regulating O-GlcNAcylation blocks signaling and development.* Glycobiology, 2006. **16**(6): p. 551-63.

353. Verkerk, A.J., et al., *Identification of a gene (FMR-1) containing a CGG repeat coincident with a breakpoint cluster region exhibiting length variation in fragile X syndrome.* Cell, 1991. **65**(5): p. 905-14.

354. Garber, K., et al., *Transcription, translation and fragile X syndrome.* Curr Opin Genet Dev, 2006. **16**(3): p. 270-5.

355. Garnon, J., et al., *Fragile X-related protein FXR1P regulates proinflammatory cytokine tumor necrosis factor expression at the post-transcriptional level.* J Biol Chem, 2005. **280**(7): p. 5750-63.

356. Vietor, I. and L.A. Huber, *Role of TIS7 family of transcriptional regulators in differentiation and regeneration.* Differentiation, 2007. **75**(9): p. 891-7.

357. Vietor, I., et al., *TIS7 interacts with the mammalian SIN3 histone deacetylase complex in epithelial cells.* EMBO J, 2002. **21**(17): p. 4621-31.

358. Vietor, I., et al., *TIS7 regulation of the beta-catenin/Tcf-4 target gene osteopontin (OPN) is histone deacetylase-dependent.* J Biol Chem, 2005. **280**(48): p. 39795-801.

359. Wick, N., et al., *Inhibitory effect of TIS7 on Sp1-C/EBPalpha transcription factor module activity.* J Mol Biol, 2004. **336**(3): p. 589-95.

360. Ryzhakov, G. and F. Randow, *SINTBAD, a novel component of innate antiviral immunity, shares a TBK1-binding domain with NAP1 and TANK.* EMBO J, 2007. **26**(13): p. 3180-90.

361. Hiscott, J., et al., *Manipulation of the nuclear factor-kappaB pathway and the innate immune response by viruses.* Oncogene, 2006. **25**(51): p. 6844-67.

362. Prevention., C.f.D.C.a. *National diabetes fact sheet: national estimates and general information on diabetes and prediabetes in the United States*. 2011.

363. Havel, P.J., *Update on adipocyte hormones: regulation of energy balance and carbohydrate/lipid metabolism.* Diabetes, 2004. **53 Suppl 1**: p. S143-51.

364. Szalowska, E., et al., *Comparative analysis of the human hepatic and adipose tissue transcriptomes during LPS-induced inflammation leads to the identification of differential biological pathways and candidate biomarkers.* BMC Med Genomics, 2011. **4**: p. 71.

365. Student, A.K., R.Y. Hsu, and M.D. Lane, *Induction of fatty acid synthetase synthesis in differentiating 3T3-L1 preadipocytes.* J Biol Chem, 1980. **255**(10): p. 4745-50.

366. Harris, R.B., T.D. Mitchell, and S. Hebert, *Leptin-induced changes in body composition in high fat-fed mice.* Exp Biol Med (Maywood), 2003. **228**(1): p. 24-32.

367. Macauley, M.S., et al., *Elevation of global O-GlcNAc levels in 3T3-L1 adipocytes by selective inhibition of O-GlcNAcase does not induce insulin resistance.* J Biol Chem, 2008. **283**(50): p. 34687-95.

368. Abramoff, M.D., Magalhaes, P.J., Ram, S.J., *Image Processing with ImageJ.* Biophotonics International, 2004. **11**(7): p. 36-42.

369. Livak, K.J. and T.D. Schmittgen, *Analysis of relative gene expression data using real-time quantitative PCR and the 2(-Delta Delta C(T)) Method.* Methods, 2001. **25**(4): p. 402-8.

370. Kent, W.J., et al., *The human genome browser at UCSC.* Genome Res, 2002. **12**(6): p. 996-1006.

371. Hughes, J.D., et al., *Computational identification of cis-regulatory elements associated with groups of functionally related genes in Saccharomyces cerevisiae.* J Mol Biol, 2000. **296**(5): p. 1205-14.

372. Liu, X., D.L. Brutlag, and J.S. Liu, *BioProspector: discovering conserved DNA motifs in upstream regulatory regions of co-expressed genes.* Pac Symp Biocomput, 2001: p. 127-38.

373. Hertz, G.Z. and G.D. Stormo, *Identifying DNA and protein patterns with statistically significant alignments of multiple sequences.* Bioinformatics, 1999. **15**(7-8): p. 563-77.

374. Olman, V., D. Xu, and Y. Xu, *CUBIC: identification of regulatory binding sites through data clustering.* J Bioinform Comput Biol, 2003. **1**(1): p. 21-40.

375. Liu, X.S., D.L. Brutlag, and J.S. Liu, *An algorithm for finding protein-DNA binding sites with applications to chromatin-immunoprecipitation microarray experiments.* Nat Biotechnol, 2002. **20**(8): p. 835-9.

376. Bailey, T.L. and C. Elkan, *Fitting a mixture model by expectation maximization to discover motifs in biopolymers.* Proc Int Conf Intell Syst Mol Biol, 1994. **2**: p. 28-36.

377. Li, G., et al., *A new framework for identifying cis-regulatory motifs in prokaryotes.* Nucleic Acids Res, 2011. **39**(7): p. e42.

378. Gupta, S., et al., *Quantifying similarity between motifs.* Genome Biol, 2007. **8**(2): p. R24.

379. Loots, G.G. and I. Ovcharenko, *rVISTA 2.0: evolutionary analysis of transcription factor binding sites.* Nucleic Acids Res, 2004. **32**(Web Server issue): p. W217-21.

380. Madiehe, A.M., T.D. Mitchell, and R.B. Harris, *Hyperleptinemia and reduced TNF-alpha secretion cause resistance of db/db mice to endotoxin.* Am J Physiol Regul Integr Comp Physiol, 2003. **284**(3): p. R763-70.

381. Rosen, B.S., et al., *Adipsin and complement factor D activity: an immune-related defect in obesity.* Science, 1989. **244**(4911): p. 1483-7.

382. Stolerman, E.S. and J.C. Florez, *Genomics of type 2 diabetes mellitus: implications for the clinician.* Nat Rev Endocrinol, 2009. **5**(8): p. 429-36.

383. Muhlhausler, B.S., *Nutritional models of type 2 diabetes mellitus.* Methods Mol Biol, 2009. **560**: p. 19-36.

384. D'Haeseleer, P., *How does DNA sequence motif discovery work?* Nat Biotechnol, 2006. **24**(8): p. 959-61.

385. Samson, S.L. and N.C. Wong, *Role of Sp1 in insulin regulation of gene expression.* J Mol Endocrinol, 2002. **29**(3): p. 265-79.

386. Chung, S.S., et al., *Regulation of human resistin gene expression in cell systems: an important role of stimulatory protein 1 interaction with a common promoter polymorphic site.* Diabetologia, 2005. **48**(6): p. 1150-8.

387. Rohrwasser, A., et al., *Contribution of Sp1 to initiation of transcription of angiotensinogen.* J Hum Genet, 2002. **47**(5): p. 249-56.

388. Solomon, S.S., et al., *A critical role of Sp1 transcription factor in regulating gene expression in response to insulin and other hormones.* Life Sci, 2008. **83**(9-10): p. 305-12.

389. Chung, S.S., et al., *Activation of PPARgamma negatively regulates O-GlcNAcylation of Sp1.* Biochem Biophys Res Commun, 2008. **372**(4): p. 713-8.

390. Majumdar, G., et al., *O-glycosylation of Sp1 and transcriptional regulation of the calmodulin gene by insulin and glucagon.* Am J Physiol Endocrinol Metab, 2003. **285**(3): p. E584-91.

391. Majumdar, G., et al., *Insulin dynamically regulates calmodulin gene expression by sequential o-glycosylation and phosphorylation of sp1 and its subcellular compartmentalization in liver cells.* J Biol Chem, 2006. **281**(6): p. 3642-50.

392. Majumdar, G., et al., *Insulin stimulates and diabetes inhibits O-linked N-acetylglucosamine transferase and O-glycosylation of Sp1.* Diabetes, 2004. **53**(12): p. 3184-92.

393. Goldberg, H.J., et al., *Posttranslational, reversible O-glycosylation is stimulated by high glucose and mediates plasminogen activator inhibitor-1 gene expression and Sp1 transcriptional activity in glomerular mesangial cells.* Endocrinology, 2006. **147**(1): p. 222-31.

394. Rasouli, N. and P.A. Kern, *Adipocytokines and the metabolic complications of obesity.* J Clin Endocrinol Metab, 2008. **93**(11 Suppl 1): p. S64-73.

395. Moreno-Aliaga, M.a.J., et al., *Effects of inhibiting transcription and protein synthesis on basal and insulin-stimulated leptin gene expression and leptin secretion in cultured rat adipocytes.* Biochem Biophys Res Commun, 2003. **307**(4): p. 907-914.

396. Einstein, F.H., et al., *Enhanced activation of a "nutrient-sensing" pathway with age contributes to insulin resistance.* FASEB J, 2008. **22**(10): p. 3450-7.

397. Zhang, P., et al., *Hexosamines regulate leptin production in 3T3-L1 adipocytes through transcriptional mechanisms.* Endocrinology, 2002. **143**(1): p. 99-106.

398. Wierstra, I., *Sp1: emerging roles--beyond constitutive activation of TATA-less housekeeping genes.* Biochem Biophys Res Commun, 2008. **372**(1): p. 1-13.

399. Li, X., et al., *O-linked N-acetylglucosamine modification on CCAAT enhancer-binding protein beta: role during adipocyte differentiation.* J Biol Chem, 2009. **284**(29): p. 19248-54.

400. O'Rahilly, S., *Human genetics illuminates the paths to metabolic disease.* Nature, 2009. **462**(7271): p. 307-14.

401. Ouchi, N., et al., *Adipokines in inflammation and metabolic disease.* Nat Rev Immunol, 2011. **11**(2): p. 85-97.

402. Chen, X. and S. Hess, *Adipose proteome analysis: focus on mediators of insulin resistance.* Expert Rev Proteomics, 2008. **5**(6): p. 827-39.

403. Arner, P., *Resistin: yet another adipokine tells us that men are not mice.* Diabetologia, 2005. **48**(11): p. 2203-5.

404. Cianflone, K., Z. Xia, and L.Y. Chen, *Critical review of acylation-stimulating protein physiology in humans and rodents.* Biochim Biophys Acta, 2003. **1609**(2): p. 127-43.

405. Chui, D., et al., *Genetic remodeling of protein glycosylation in vivo induces autoimmune disease.* Proc Natl Acad Sci U S A, 2001. **98**(3): p. 1142-7.

406. Delves, P.J., *The role of glycosylation in autoimmune disease.* Autoimmunity, 1998. **27**(4): p. 239-53.

407. Dennis, J.W., M. Granovsky, and C.E. Warren, *Glycoprotein glycosylation and cancer progression.* Biochim Biophys Acta, 1999. **1473**(1): p. 21-34.

408. Gleeson, P.A., *Glycoconjugates in autoimmunity.* Biochim Biophys Acta, 1994. **1197**(3): p. 237-55.

409. Isaji, T., et al., *Introduction of bisecting GlcNAc into integrin alpha5beta1 reduces ligand binding and down-regulates cell adhesion and cell migration.* J Biol Chem, 2004. **279**(19): p. 19747-54.

410. Krueger, K.E. and S. Srivastava, *Posttranslational protein modifications: current implications for cancer detection, prevention, and therapeutics.* Mol Cell Proteomics, 2006. **5**(10): p. 1799-810.

411. Schachter, H., *Congenital disorders involving defective N-glycosylation of proteins.* Cell Mol Life Sci, 2001. **58**(8): p. 1085-104.

412. Stanley, P., *Biological consequences of overexpressing or eliminating N-acetylglucosaminyltransferase-TIII in the mouse.* Biochim Biophys Acta, 2002. **1573**(3): p. 363-8.

413. Varki, A., *Biological roles of oligosaccharides: all of the theories are correct.* Glycobiology, 1993. **3**(2): p. 97-130.

414. Aoki, K., et al., *Dynamic developmental elaboration of N-linked glycan complexity in the Drosophila melanogaster embryo.* J Biol Chem, 2007. **282**(12): p. 9127-42.

415. Kudo, T., et al., *N-glycan alterations are associated with drug resistance in human hepatocellular carcinoma.* Mol Cancer, 2007. **6**: p. 32.

416. Dennis, J.W., I.R. Nabi, and M. Demetriou, *Metabolism, cell surface organization, and disease.* Cell, 2009. **139**(7): p. 1229-41.

417. Koles, K., et al., *Identification of N-glycosylated proteins from the central nervous system of Drosophila melanogaster.* Glycobiology, 2007. **17**(12): p. 1388-403.

418. Lim, J.M., et al., *Mapping glycans onto specific N-linked glycosylation sites of Pyrus communis PGIP redefines the interface for EPG-PGIP interactions.* J Proteome Res, 2009. **8**(2): p. 673-80.

419. Dell, A., et al., *Mass spectrometry of carbohydrate-containing biopolymers.* Methods Enzymol, 1994. **230**: p. 108-32.

420. Morelle, W., V. Faid, and J.C. Michalski, *Structural analysis of permethylated oligosaccharides using electrospray ionization quadrupole time-of-flight tandem mass spectrometry and deutero-reduction.* Rapid Commun Mass Spectrom, 2004. **18**(20): p. 2451-64.

421. Prien, J.M., et al., *Differentiating N-linked glycan structural isomers in metastatic and nonmetastatic tumor cells using sequential mass spectrometry.* Glycobiology, 2008. **18**(5): p. 353-66.

422. Reinhold, V.N. and D.M. Sheeley, *Detailed characterization of carbohydrate linkage and sequence in an ion trap mass spectrometer: glycosphingolipids.* Anal Biochem, 1998. **259**(1): p. 28-33.

423. Sheeley, D.M. and V.N. Reinhold, *Structural characterization of carbohydrate sequence, linkage, and branching in a quadrupole Ion trap mass spectrometer: neutral oligosaccharides and N-linked glycans.* Anal Chem, 1998. **70**(14): p. 3053-9.

424. Viseux, N., E. de Hoffmann, and B. Domon, *Structural analysis of permethylated oligosaccharides by electrospray tandem mass spectrometry.* Anal Chem, 1997. **69**(16): p. 3193-8.

425. Wuhrer, M., A.M. Deelder, and C.H. Hokke, *Protein glycosylation analysis by liquid chromatography-mass spectrometry.* J Chromatogr B Analyt Technol Biomed Life Sci, 2005. **825**(2): p. 124-33.

426. Abbott, K.L., et al., *Targeted glycoproteomic identification of biomarkers for human breast carcinoma.* J Proteome Res, 2008. **7**(4): p. 1470-80.

427. Aoki, K., et al., *The diversity of O-linked glycans expressed during Drosophila melanogaster development reflects stage- and tissue-specific requirements for cell signaling.* J Biol Chem, 2008. **283**(44): p. 30385-400.

428. Ciucanu, I.K., F., *A simple and rapid method for the permethylation of carbohydrates.* Carbohydr Res, 1984. **131**: p. 209-217.

429. Yates, J.R., 3rd, A.L. McCormack, and J. Eng, *Mining genomes with MS.* Anal Chem, 1996. **68**(17): p. 534A-540A.

430. Peng, J., et al., *Evaluation of multidimensional chromatography coupled with tandem mass spectrometry (LC/LC-MS/MS) for large-scale protein analysis: the yeast proteome.* J Proteome Res, 2003. **2**(1): p. 43-50.

431. Kristiansen, T.Z., et al., *A proteomic analysis of human bile.* Mol Cell Proteomics, 2004. **3**(7): p. 715-28.

432. Weatherly, D.B., et al., *A Heuristic method for assigning a false-discovery rate for protein identifications from Mascot database search results.* Mol Cell Proteomics, 2005. **4**(6): p. 762-72.

433. Shah, P., et al., *A proteomic study of pectin-degrading enzymes secreted by Botrytis cinerea grown in liquid culture.* Proteomics, 2009. **9**(11): p. 3126-35.

434. Gygi, S.P., et al., *Quantitative analysis of complex protein mixtures using isotope-coded affinity tags.* Nat Biotechnol, 1999. **17**(10): p. 994-9.

435. Haqqani, A.S., et al., *Biomarkers and diagnosis; protein biomarkers in serum of pediatric patients with severe traumatic brain injury identified by ICAT-LC-MS/MS.* J Neurotrauma, 2007. **24**(1): p. 54-74.

436. Haqqani, A.S., et al., *Characterization of vascular protein expression patterns in cerebral ischemia/reperfusion using laser capture microdissection and ICAT-nanoLC-MS/MS.* FASEB J, 2005. **19**(13): p. 1809-21.

437. Ong, S.E., et al., *Stable isotope labeling by amino acids in cell culture, SILAC, as a simple and accurate approach to expression proteomics.* Mol Cell Proteomics, 2002. **1**(5): p. 376-86.

438. Ong, S.E., I. Kratchmarova, and M. Mann, *Properties of 13C-substituted arginine in stable isotope labeling by amino acids in cell culture (SILAC).* J Proteome Res, 2003. **2**(2): p. 173-81.

439. Ong, S.E. and M. Mann, *Mass spectrometry-based proteomics turns quantitative.* Nat Chem Biol, 2005. **1**(5): p. 252-62.

440. Schnolzer, M., P. Jedrzejewski, and W.D. Lehmann, *Protease-catalyzed incorporation of 18O into peptide fragments and its application for protein sequencing by electrospray and matrix-assisted laser desorption/ionization mass spectrometry.* Electrophoresis, 1996. **17**(5): p. 945-53.

441. Shevchenko, A., M. Wilm, and M. Mann, *Peptide sequencing by mass spectrometry for homology searches and cloning of genes.* J Protein Chem, 1997. **16**(5): p. 481-90.

442. Uttenweiler-Joseph, S., et al., *Automated de novo sequencing of proteins using the differential scanning technique.* Proteomics, 2001. **1**(5): p. 668-82.

443. Andreev, V.P., et al., *A new algorithm using cross-assignment for label-free quantitation with LC-LTQ-FT MS.* J Proteome Res, 2007. **6**(6): p. 2186-94.

444. Bondarenko, P.V., D. Chelius, and T.A. Shaler, *Identification and relative quantitation of protein mixtures by enzymatic digestion followed by capillary reversed-phase liquid chromatography-tandem mass spectrometry.* Anal Chem, 2002. **74**(18): p. 4741-9.

445. Chelius, D. and P.V. Bondarenko, *Quantitative profiling of proteins in complex mixtures using liquid chromatography and mass spectrometry.* J Proteome Res, 2002. **1**(4): p. 317-23.

446. Higgs, R.E., et al., *Comprehensive label-free method for the relative quantification of proteins from biological samples.* J Proteome Res, 2005. **4**(4): p. 1442-50.

447. Liu, H., R.G. Sadygov, and J.R. Yates, 3rd, *A model for random sampling and estimation of relative protein abundance in shotgun proteomics.* Anal Chem, 2004. **76**(14): p. 4193-201.

448. Mallick, P., et al., *Computational prediction of proteotypic peptides for quantitative proteomics.* Nat Biotechnol, 2007. **25**(1): p. 125-31.

449. Nesvizhskii, A.I., et al., *A statistical model for identifying proteins by tandem mass spectrometry.* Anal Chem, 2003. **75**(17): p. 4646-58.

450. Old, W.M., et al., *Comparison of label-free methods for quantifying human proteins by shotgun proteomics.* Mol Cell Proteomics, 2005. **4**(10): p. 1487-502.

451. Wiener, M.C., et al., *Differential mass spectrometry: a label-free LC-MS method for finding significant differences in complex peptide and protein mixtures.* Anal Chem, 2004. **76**(20): p. 6085-96.

452. Alvarez-Manilla, G., et al., *Tools for glycomics: relative quantitation of glycans by isotopic permethylation using 13CH3I.* Glycobiology, 2007. **17**(7): p. 677-87.

453. Atwood, J.A., 3rd, et al., *Quantitation by isobaric labeling: applications to glycomics.* J Proteome Res, 2008. **7**(1): p. 367-74.

454. Chen, X., et al., *Quantitative proteomic analysis of the secretory proteins from rat adipose cells using a 2D liquid chromatography-MS/MS approach.* J Proteome Res, 2005. **4**(2): p. 570-7.

455. Chen, X., et al., *Proteomic characterization of thiazolidinedione regulation of obese adipose secretome in Zucker obese rats.* Proteomics Clin Appl, 2009. **3**(9): p. 1099-111.

456. Zhou, H., et al., *Quantitative analysis of secretome from adipocytes regulated by insulin.* Acta Biochimica et Biophysica Sinica, 2009. **41**(11): p. 910-921.

457. Hocking, S.L., et al., *Intrinsic depot-specific differences in the secretome of adipose tissue, preadipocytes, and adipose tissue-derived microvascular endothelial cells.* Diabetes, 2010. **59**(12): p. 3008-16.

458. Kim, J., et al., *Comparative analysis of the secretory proteome of human adipose stromal vascular fraction cells during adipogenesis.* Proteomics, 2010. **10**(3): p. 394-405.

459. Zhong, J., et al., *Temporal profiling of the secretome during adipogenesis in humans.* J Proteome Res, 2010. **9**(10): p. 5228-38.

460. Zvonic, S., et al., *Secretome of primary cultures of human adipose-derived stem cells: modulation of serpins by adipogenesis.* Mol Cell Proteomics, 2007. **6**(1): p. 18-28.

461. Alvarez-Llamas, G., et al., *Characterization of the human visceral adipose tissue secretome.* Mol Cell Proteomics, 2007. **6**(4): p. 589-600.

462. Rosenow, A., et al., *Identification of novel human adipocyte secreted proteins by using SGBS cells.* J Proteome Res, 2010. **9**(10): p. 5389-401.

463. Fain, J.N., et al., *Comparison of the release of adipokines by adipose tissue, adipose tissue matrix, and adipocytes from visceral and subcutaneous abdominal adipose tissues of obese humans.* Endocrinology, 2004. **145**(5): p. 2273-82.

464. Sell, H., et al., *Cytokine secretion by human adipocytes is differentially regulated by adiponectin, AICAR, and troglitazone.* Biochem Biophys Res Commun, 2006. **343**(3): p. 700-6.

465. Roelofsen, H., et al., *Comparison of isotope-labeled amino acid incorporation rates (CILAIR) provides a quantitative method to study tissue secretomes.* Mol Cell Proteomics, 2009. **8**(2): p. 316-24.

466. Dupont, A., et al., *Two-dimensional maps and databases of the human macrophage proteome and secretome.* Proteomics, 2004. **4**(6): p. 1761-78.

467. Coombs, K.M., *Quantitative proteomics of complex mixtures.* Expert Rev Proteomics, 2011. **8**(5): p. 659-77.

468. Taniguchi, N. and H. Korekane, *Branched N-glycans and their implications for cell adhesion, signaling and clinical applications for cancer biomarkers and in therapeutics.* BMB Rep, 2011. **44**(12): p. 772-81.

469. Hart, G.W. and R.J. Copeland, *Glycomics hits the big time.* Cell, 2010. **143**(5): p. 672-6.

470. Zaia, J., *Mass spectrometry and glycomics.* OMICS, 2010. **14**(4): p. 401-18.

471. Deussing, J., et al., *Cathepsins B and D are dispensable for major histocompatibility complex class II-mediated antigen presentation.* Proc Natl Acad Sci U S A, 1998. **95**(8): p. 4516-21.

472. Sanchez, J.C., et al., *Effect of rosiglitazone on the differential expression of obesity and insulin resistance associated proteins in lep/lep mice.* Proteomics, 2003. **3**(8): p. 1500-20.